

**A STUDY OF SOME NON-COVALENT FUNCTIONAL  
GROUP  $\pi$  INTERACTIONS**

A Thesis Presented by

**Josephine Rose Theodora Arendorf**

In partial Fulfillment of the Requirements of the Award of the Degree of

**Doctor of Philosophy**

**Of**

**University College London**



**UCL**

## ABSTRACT

The present thesis is concerned with the quantification of weak non-covalent interactions between a simple  $\pi$  system and functional groups through dynamic NMR studies of conformational equilibria of specifically designed molecular balance systems.

The work begins with an introduction which provides a formal review of the current literature on various aspects of non-covalent  $\pi$ -interactions, starting with an examination of the physical properties of non-covalent arene interactions, including arene-arene interactions, the behaviour of aromatic rings as hydrogen bond acceptors and the interactions between aromatic rings and cationic species. The use of molecular balance systems for studying these weak interactions will then be discussed together with some other important methods used. The introduction concludes with an account of olefinic  $\pi$ -interactions and methods for their study as described in the current chemical literature.

The second section presents and discusses the results obtained in the present study and begins with the description of the synthetic routes employed to prepare two series of molecular balance systems, both of which feature a common bicyclo[3.2.2]nona-6,8-diene framework and a flexible three carbon atom bridge, whose central carbon atom can possess two different functional groups. The relative abundance of each of the two possible conformers in solution provides a measure of the relative interaction energies. Dynamic NMR studies in a range of solvents were employed to study each derivative. The results from these studies were then compared in order to gain insight into the relative strengths of both olefinic and aromatic  $\pi$ -interactions.

The thesis concludes with a formal description of the experimental procedures used in this study and appendices detailing the data obtained from dynamic NMR studies and crystal structure data.



## **DECLARATION**

The research described in this thesis is, to the best of my knowledge, original except where due reference is made to other authors.

## **ACKNOWLEDGEMENTS**

First and foremost I would like to thank my supervisor, Prof. Willie Motherwell, for the opportunity to study such an exciting area of chemistry and for his guidance, encouragement, help and witty anecdotes.

I am also very grateful to Dr Abil Aliev, whose help and advice has proved invaluable over the last few years. I would also like to thank him for the theoretical calculations he performed. I would also like to thank all the technical staff at the UCL Chemistry Department.

Special thanks to Robyn for all her practical help and advice and to Dr Tom Sheppard for his continued guidance and inspiration. I would especially like to thank all past, present and honorary members of the Motherwell group for their continued kindness and support, for making the lab an enjoyable place to work and for many happy memories. I am very grateful to my year buddy Matt for his constant support, encouragement and reassurance. I would also like to thank all my family and friends outside of the Motherwell group for their support and understanding.

---

## Table of Contents

<b>ABSTRACT.....</b>	<b>2</b>
<b>DECLARATION.....</b>	<b>3</b>
<b>ACKNOWLEDGEMENTS.....</b>	<b>4</b>
<b>ABBREVIATIONS.....</b>	<b>9</b>
 <b>CHAPTER 1 INTRODUCTION.....</b>	 <b>13</b>
<b>1.1 Introduction .....</b>	<b>14</b>
<b>1.2 Interactions between aromatic rings.....</b>	<b>14</b>
1.2.1 Evidence for arene-arene interactions .....	15
1.2.1.1 Biomolecules .....	15
1.2.1.2 Benzene dimer studies .....	16
1.2.2 The nature of $\pi$ - $\pi$ interactions.....	19
1.2.2.1 Van der Waals contribution .....	20
1.2.2.2 Contribution from induction .....	20
1.2.2.3 Charge transfer.....	21
1.2.2.4 Desolvation .....	21
1.2.2.5 Electrostatic contribution .....	22
<b>1.3 Interactions between an aromatic ring and a functional group.....</b>	<b>27</b>
1.3.1 C-H/ $\pi$ hydrogen bonds.....	27
1.3.1.1 Definition and physical properties.....	27
1.3.1.2 Intramolecular C-H/ $\pi$ interactions and the conformation of organic compounds .....	30
1.3.1.3 Interactions involving alkyne groups.....	33
1.3.2 X-H/ $\pi$ hydrogen bonds .....	35
1.3.2.1 Definition and physical properties.....	35
<b>1.4 Cation/<math>\pi</math> interactions .....</b>	<b>37</b>
1.4.1 Cation/ $\pi$ interactions in biological systems .....	37
1.4.2 Definition and physical properties.....	38
<b>1.5 Molecular balance systems .....</b>	<b>41</b>
1.5.1 Quantifying $\pi$ -interactions using molecular torsion balances .....	42
1.5.2 Wilcox molecular torsion balance .....	42
1.5.3 Other examples of molecular balance systems.....	50
1.5.3.1 $\pi$ - $\pi$ interactions .....	51
1.5.3.2 X-H/ $\pi$ interactions .....	59
1.5.3.3 Cation/ $\pi$ interactions.....	63

<b>1.6 Other methods for studying <math>\pi</math>-interactions</b>	<b>64</b>
1.6.1 Molecular recognition	64
1.6.2 Double mutant cycles	67
1.6.3 Organic reactions	68
<b>1.7 Non-covalent interactions involving alkene <math>\pi</math> systems</b>	<b>70</b>
1.7.1 Definition and physical properties	70
1.7.2 Olefinic $\pi$ -interactions in organic molecules	72
<b>1.8 Conclusions and perspectives</b>	<b>81</b>
<b>CHAPTER 2 RESULTS AND DISCUSSION</b>	<b>82</b>
<b>2.1 Previous studies within our group</b>	<b>83</b>
<b>2.2 Objectives</b>	<b>87</b>
<b>2.3 The synthesis of the “parent diene” system</b>	<b>90</b>
2.3.1 Synthesis of bicyclo[3.2.2]nona-6,8-dien-3-one <b>183</b>	90
2.3.2 Synthesis of alcohol derivatives	98
2.3.3 Attempted synthesis of ether derivatives	101
2.3.4 Synthesis of substrates with a spirocyclic unit on the flexible bridge	102
2.3.4.1 Attempted synthesis of epoxide derivative <b>218</b>	103
2.3.4.2 Synthesis of oxathiolane derivative <b>219</b>	103
2.3.5 Replacement of the hydroxyl group by a fluorine atom	104
<b>2.4 Synthesis of the “propanonaphthalene system”</b>	<b>105</b>
2.4.1 Synthesis of 6,7-benzobicyclo[3.2.2]nona-6,8-dien-3-one <b>184</b>	105
2.4.2 Synthesis of alcohol derivatives	107
2.4.3 Attempted synthesis of ether derivatives	110
2.4.4 Synthesis of cyanohydrin derivatives <b>241</b> and <b>242</b>	111
2.4.5 Synthesis of substrates with a spirocyclic unit on the flexible bridge	112
2.4.6 Replacement of the hydroxyl group by a fluorine atom	114
<b>2.5 Synthetic summary</b>	<b>115</b>
<b>2.6 NMR spectroscopy techniques used to study conformational equilibria</b>	<b>117</b>
2.6.1 Dihedral angle	117
2.6.2 Determination of the predominant conformer by NOE measurements	119
2.6.3 Determination of the conformational ratios using the coupling constants between the protons on the central bridge	120
2.6.4 Temperature dependence	123
<b>2.7 Results from parent diene system</b>	<b>124</b>
2.7.1 Relative strengths of functional group interactions in CDCl <sub>3</sub>	124
2.7.1.1 Alcohol derivatives – Importance of O-H/ $\pi$ interaction	126

2.7.1.2	Oxathiolane <b>219</b> and epoxide <b>218</b> derivatives .....	130
2.7.2	Effects of temperature on the parent diene system in CDCl <sub>3</sub> .....	132
2.7.2.1	Studies of the propargylic alcohol at low temperatures.....	133
2.7.3	Solvent dependence studies .....	135
2.7.3.1	Effects of the solvent nature on the conformational equilibria of alcohol derivatives.....	136
<b>2.8</b>	<b>Results from propanonaphthalene system .....</b>	<b>141</b>
2.8.1	Introduction .....	141
2.8.2	Relative strengths of functional group interactions in CDCl <sub>3</sub> .....	142
2.8.2.1	Alcohol derivatives – Importance of the O-H/ $\pi$ interaction .....	143
2.8.2.2	Cyanohydrin derivatives – The influence of a cyano group.....	147
2.8.2.3	Oxathiolane derivatives <b>243</b> and <b>244</b> .....	147
2.8.3	Effects of temperature on the propanonaphthalene system in CDCl <sub>3</sub> .....	148
2.8.3.1	Effects of temperature on the propargylic alcohols <b>236</b> and <b>237</b> .....	149
2.8.3.2	Effects of temperature on the cyanohydrins <b>241</b> and <b>242</b> .....	150
2.8.3.3	Some preliminary conclusions from the studies of the propanonaphthalene derivatives in CDCl <sub>3</sub> solution .....	152
2.8.4	Solvent dependence studies .....	153
2.8.4.1	Effects of the solvent nature on the conformational equilibria of alcohol derivatives.....	153
2.8.4.2	Effects of the solvent nature on the conformational equilibria of oxathiolane derivatives <b>243</b> and <b>244</b> .....	162
2.8.4.3	X-Ray Studies.....	163
2.8.4.4	Crystal structure of propargylic alcohol <b>237</b> .....	164
2.8.4.5	Crystal structure of the cyanohydrin <b>241</b> .....	166
<b>2.9</b>	<b>Comparison of the parent diene, propanonaphthalene and propanonanthracene molecular balance systems .....</b>	<b>168</b>
2.9.1	Introduction .....	168
2.9.2	Alcohol derivatives.....	171
2.9.3	Cyanohydrins.....	175
2.9.4	Oxathiolane derivatives .....	178
<b>CHAPTER 3</b>	<b>CONCLUSIONS AND PERSPECTIVES .....</b>	<b>180</b>
<b>3.1</b>	<b>Synthetic studies .....</b>	<b>181</b>
<b>3.2</b>	<b>Conformational equilibria of the molecular balance systems .....</b>	<b>183</b>
<b>3.3</b>	<b>Future scope for extending the types of non-covalent <math>\pi</math>-interactions investigated.....</b>	<b>184</b>

3.3.1 Investigation of other functional groups on the central carbon of the flexible bridge .....	184
3.3.2 Modification of the electron density of the $\pi$ system .....	187
<b>CHAPTER 4 EXPERIMENTAL.....</b>	<b>189</b>
4.1 General Information.....	190
4.2 Experimental Procedure .....	192
<b>CHAPTER 5 APPENDICES.....</b>	<b>233</b>
Appendix 1.....	233
Appendix 2.....	235
Appendix 3.....	241
Appendix 4.....	242
Appendix 5.....	243
Appendix 6.....	244
Appendix 7.....	245
Appendix 8.....	246
Appendix 9.....	247
Appendix 10.....	248
Appendix 11.....	249
Appendix 12.....	250
Appendix 13.....	260
<b>CHAPTER 6 REFERENCES.....</b>	<b>276</b>

---

**ABBREVIATIONS**

AcOH	Acetic acid
Arg	Arginine
BH <sub>3</sub>	Borane
b.p.	Boiling point
br	Broad
Bu	Butyl
cat.	Catalytic
C <sub>6</sub> D <sub>6</sub>	Deuterated benzene
CDCl <sub>3</sub>	Deuterated chloroform
CD <sub>3</sub> OD	Deuterated methanol
CH <sub>4</sub>	Methane
CH <sub>2</sub> Cl <sub>2</sub>	Dichloromethane
CI	Chemical ionisation
d	Doublet
DABCO	1,4-diazabicyclo[2.2.2]octane
DAST	Diethylaminosulphur trifluoride
DFT	Density functional theory
DNA	Deoxyribonucleic acid
DMSO	Dimethylsulfoxide
D <sub>2</sub> O	Deuterium oxide
EI	Electronic impact
eq.	Molar equivalent(s)

---

Et	Ethyl
Et <sub>2</sub> O	Diethyl ether
EtOAc	Ethyl acetate
EtOH	Ethanol
g	Gram(s)
h	Hour(s)
H <sub>Ar</sub>	Aromatic proton
HF	Hydrogen fluoride
His	Histidine
HMBC	Heteronuclear multiple bond correlation
Hz	Hertz
<i>i</i>	<i>iso</i>
IR	Infrared
<i>J</i>	Coupling constant
Lys	Lysine
m	Multiplet
M <sup>+</sup>	Molecular ion
Me	Methyl
MeOH	Methanol
min	Minute(s)
mL	Millilitre(s)
mol	Mole(s)



mmol	Millimole(s)
m.p.	Melting point
<i>n</i>	<i>neo</i>
NMR	Nuclear Magnetic Resonance
NH <sub>3</sub>	Ammonia
NOE	Nuclear Overhauser Effect
PCC	Pyridinium chlorochromate
P.E.	Petroleum ether
Ph	Phenyl
Phe	Phenylalanine
ppm	Parts per million
Py	Pyridine
R	Unspecified carbon substituent
R <sub>f</sub>	Retention factor
r.t.	Room temperature
s	Singlet
t	Triplet
TBDMS	Tert-butyldimethylsilyl
THF	Tetrahydrofuran
TLC	Thin layer chromatography
TMS	Trimethylsilyl
Trp	Tryptophan

Ts                    *para*-Toluenesulfonyl

Tyr                   Tyrosine

w                    Weak

---

# **CHAPTER 1**

## **INTRODUCTION**

## 1.1 Introduction

The present thesis is concerned with the synthesis and studies, through dynamic NMR measurements of two series of molecules which can function as conformational balances, in order to probe weak non-covalent interactions between  $\pi$  systems and functional groups.

It is therefore appropriate, in this introductory section, to discuss the nature of these non-covalent interactions and the significant role that they play in areas as diverse as drug-receptor interactions, protein folding, base pair stacking in DNA, crystal engineering, host-guest binding and many more molecular recognition processes.<sup>1-6</sup> However, to date, the chemical literature on olefinic  $\pi$ -interactions is limited. Consequently, the focus of this introduction will be on the more widely studied aromatic  $\pi$ -interactions. Such interactions can be divided into three main topics. These are; arene-arene interactions, the behaviour of aromatic rings as hydrogen bond acceptors, and the interactions between aromatic rings and cationic species. The fundamental aspects of these three main topics will be discussed in turn, followed by a review of molecular torsion balance systems and other important methods used to quantify these interactions. Finally, a review of the current literature on olefinic  $\pi$ -interactions will be presented.

## 1.2 Interactions between aromatic rings

The arene-arene interaction is the most commonly observed  $\pi$ -interaction and it is therefore considered a fundamental interaction. As a consequence, a large volume of research has been focused on investigating the  $\pi$ -stacking behaviour of aromatic rings.

## 1.2.1 Evidence for arene-arene interactions

### 1.2.1.1 Biomolecules

The early work of Burley and Petsko demonstrated that  $\pi$ - $\pi$  interactions play an important role in protein packing structures.<sup>1</sup> Whilst studying the crystal structures of 34 proteins at 2 Å (or higher) resolution, an abundance of intramolecular edge-to-face interactions between aromatic side chains, where the aromatic rings were arranged perpendicular to one another, was found. For each separation of less than 10 Å, the distance between the phenyl ring centroids was calculated. It was found that on average, 61% of Phe residues, 54% of Tyr residues and 59% of Trp residues were involved in  $\pi$ - $\pi$  interactions; two residues were considered to interact if their centroid separation was less than 7 Å. The preferential geometry of phenyl ring centroids was found to be with a separation of between 4.5 Å and 7.0 Å and a dihedral angle of 90°, indicating that an edge-to-face  $\pi$ - $\pi$  interaction was favoured. In later studies, Burley and Petsko used a model developed by Karlström, based on *ab initio* calculations of the benzene dimer to calculate the non-bonded potential energy of  $\pi$ - $\pi$  interactions in the previously studied aromatic pairs.<sup>7,8</sup> They reported that the frequency distribution of interaction geometries correlated well with that of the benzene dimer. Of the 225 aromatic side chain pairs with a centroid separation of 3.4 Å to 6.5 Å, 84% were found to make energetically favourable interactions. Edge-to-face interactions between two aromatic side chains make an enthalpic contribution of between -1 and -2 kcal per mol to the energy stabilisation of protein structures. The findings of this seminal study imply that protein packing can be attributed to the formation of a large number of favourable interactions between neighbouring aromatic side chains.

### 1.2.1.2 Benzene dimer studies

As it is the most simple example of an arene-arene interaction, the benzene dimer is a model system for studying  $\pi$ - $\pi$  interactions. As a consequence, a significant volume of research has been done in this area, ranging from early gas phase studies to more recent computational studies.<sup>9-13</sup> This vast amount of research has led to key insights into the fundamental properties of  $\pi$ - $\pi$  interactions. A detailed knowledge of the physical properties of  $\pi$ - $\pi$  interactions will help us to gain an understanding of the fundamental aspects of all  $\pi$ -interactions.

The quadrupole moment of aromatic systems provides a simple unifying theoretical basis for  $\pi$ - $\pi$  interactions. It is similar to the dipole moment and is a fundamental property which describes the molecular charge distribution of an aromatic system. Ritchie *et al.* determined the quadrupole moment of several different aromatic systems using electric field-gradient birefringence.<sup>14</sup> The quadrupole moment of benzene has a value of  $-33.3 \times 10^{-40} \text{ Cm}^2$ , and this can be visualised as having delocalized negative charge above and below the plane of the ring (Figure 1). Interestingly, in hexafluorobenzene the sign of the quadrupole moment is reversed and the quadrupole moment is  $+31. \times 10^{-40} \text{ Cm}^2$ , and with the positive charge now delocalized above and below the ring. This demonstrates the effect that the electronegativity of the ring substituents has on the aromaticity of the ring.

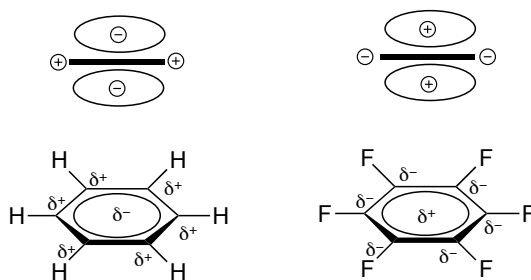


**Figure 1** Schematic representation of the quadrupole moments of benzene and hexafluorobenzene

Early gas phase studies by Klemperer *et al.*, showed that the benzene dimer is polar in its ground vibrational state, and this polarity can be attributed to the presence of a permanent dipole.<sup>11,12</sup> This eliminates the possibility of all geometries where the planes of the two benzene molecules are parallel as the preferred lowest energy geometry. Several important theoretical studies of the benzene dimer followed, notably those by Price and Stone<sup>15</sup>, Jorgenson and Severance<sup>16</sup>, Linse<sup>17</sup> and Jaffe and Smith.<sup>18</sup> From several *ab initio* studies, Schlag *et al.* found there to be two minima in the potential energy surface of the dimer, and these are the edge-to-face (T-shaped) and offset stacked (parallel displaced) geometries (Figure 2).<sup>19-21</sup>

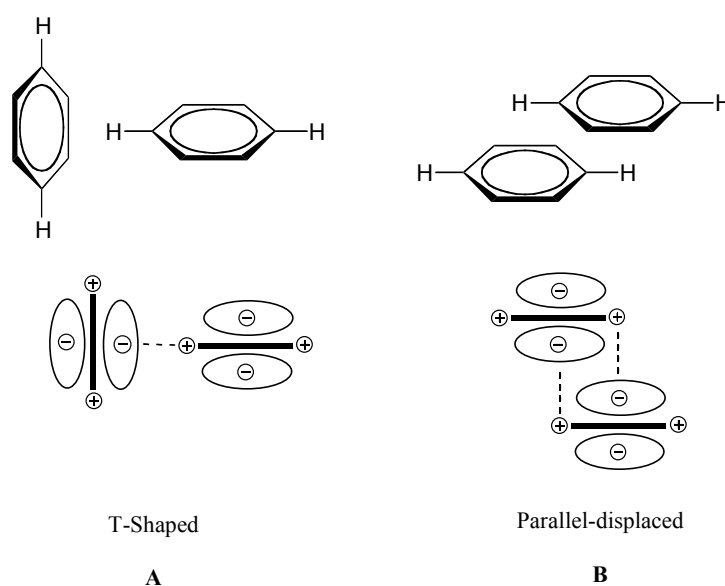


**Figure 2** T-Shaped and parallel-displaced stacking geometries of the benzene dimer indicated by the quadrupole moments of the benzene ring

This finding has been confirmed by more recent experimental work on benzene dimers.<sup>22, 10</sup> Studies have also been conducted on the dimers of other simple aromatic molecules, most notably by Tsuzuki and co-workers.<sup>23</sup> In 2002, the group published the results of extensive theoretical studies on the thiophene

dimer and it was concluded that the perpendicular dimers give rise to the largest total interaction energies, consequently **9** is the geometry with the lowest total interaction energy. Figure 3 shows the dimer geometries studied, which consist of parallel **1** to **3**, perpendicular **4** to **10** and co-planar geometries **11** to **17**. Tsuzuki also found that the interaction is dominated by dispersion forces, due to the large atomic polarisability of the sulphur atom. In contrast to the benzene dimer, parallel (stacked) geometries of the thiophene dimers are considerably stabilised. This can be explained by the large contribution from dispersion forces in the thiophene dimer.

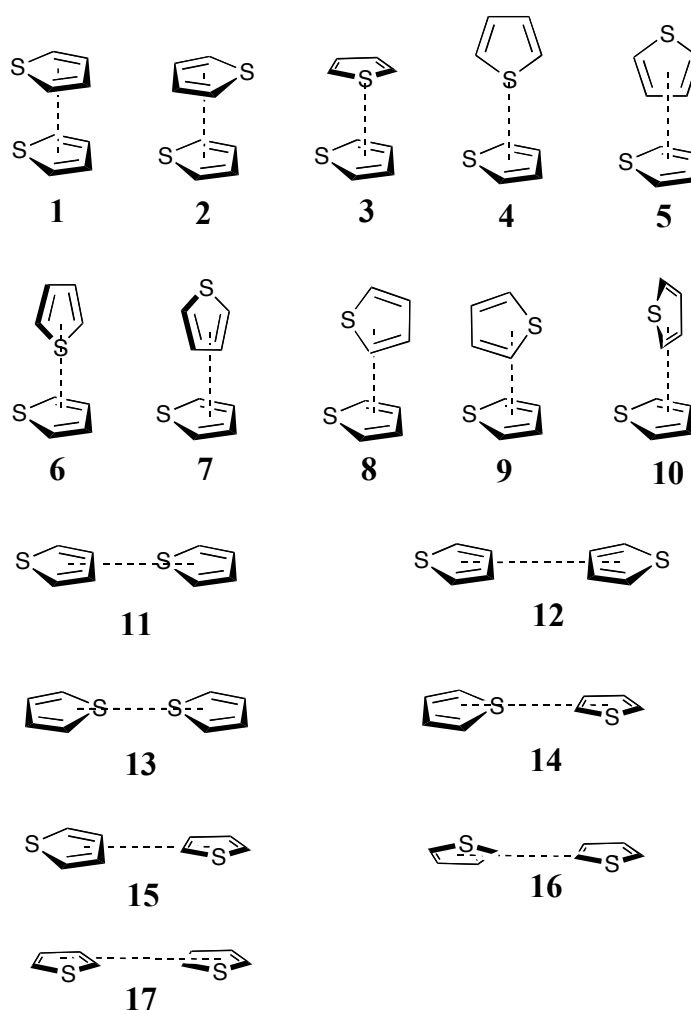


**Figure 3** Geometries of the thiophene dimer studied



### 1.2.2 The nature of $\pi$ - $\pi$ interactions

However, even after extensive studies, few unifying rules for understanding the fundamental aspects of  $\pi$ - $\pi$  interactions had appeared. As a consequence Hunter and Sanders in 1990 set out to describe a simple model to explain experimental observations of aromatic interactions.<sup>24</sup> Their work was inspired by observations of the strong attractive interactions between two porphyrin molecules in solution, whilst studying host-guest chemistry of flexible macromolecules.<sup>25-28</sup> An example of one of the macrocyclic porphyrin dimers studied is shown in Figure 4.

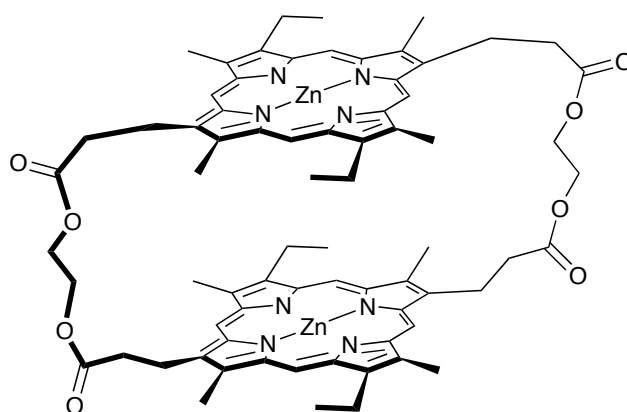


**Figure 4** Example of a porphyrin dimer studied by Hunter and Sanders

To gain information on the  $\pi$ - $\pi$  interactions occurring between the porphyrin rings of the dimer, they studied the effects of metallation and co-ordination of the central zinc ion and the kinetics and thermodynamics of binding with host molecules such as DABCO inside the cavity between the porphyrins. From these investigations they were able to estimate the strength of the  $\pi$ - $\pi$  interaction between the porphyrins. From their observations and calculations, a simple set of rules based on electrostatics for understanding  $\pi$ - $\pi$  interactions was developed. Critically, it was shown that  $\pi$ - $\pi$  interactions are not, as was widely accepted, due to attractive electronic interactions between two aromatic rings, but actually arise

when attractive interactions between  $\sigma$ -framework and  $\pi$ -electrons outweigh  $\pi$ - $\pi$  repulsion. These rules will be discussed in turn, with the contribution from electrostatics.

Rather than attributing the nature of  $\pi$ - $\pi$  interactions to a single force, such as solvophobic, charge transfer or electrostatics, it is important to take into account several contributions. With any non-covalent interaction between two molecules the total energy of the interaction can be calculated by taking into account the contributions from van der Waals interactions, electrostatic interactions, induction energy, charge transfer and desolvation.<sup>29</sup> The role of each of these when considering  $\pi$ - $\pi$  interactions will now be discussed in turn.

#### **1.2.2.1 Van der Waals contribution**

Van der Waals interactions clearly contribute to the energy of  $\pi$ - $\pi$  interactions, as, at the separations of interest, the van der Waals term is always attractive. However, the van der Waals interaction between aromatic rings is proportional to the area of  $\pi$  overlap, but this cannot explain the observed geometry as this would predict that a stacked geometry is preferred as it maximises  $\pi$  overlap.<sup>24</sup> Therefore other forces between the two molecules must be responsible for the observed geometries of  $\pi$ - $\pi$  interactions.

#### **1.2.2.2 Contribution from induction**

Induction energy arises when the induced dipole of one molecule interacts with the permanent dipole of another molecule. However, to date there has been no significant experimental or theoretical evidence to suggest that induction effects play an important role in  $\pi$ - $\pi$  interactions. Hunter and Sanders also concluded that induction effects can be ignored when considering these interactions.<sup>24</sup>

### 1.2.2.3 Charge transfer

Charge transfer complexes stabilise non-covalent interactions through the mixing of the ground state with an excited charge separated state. They are readily spotted by their characteristic bands in UV-Visible absorption spectra as they often lead to the formation of highly coloured solutions. Picric acid **18** (2,4,6-trinitrophenol) is known to form charge transfer complexes with various different organic molecules (Figure 5).<sup>30</sup>

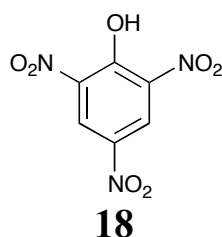


**Figure 5** Structure of picric acid (2,4,6-trinitrophenol)

These are often observed for aromatic complexes. However they are not observed for all aromatic interactions, so they cannot be attributed to the fundamentals of  $\pi$ - $\pi$  interactions.<sup>31</sup>

### 1.2.2.4 Desolvation

When studying non-covalent interactions in solution, desolvation becomes important as the interaction between substrate and solvent compete with the non-covalent interaction.<sup>32</sup> In order for an interaction to occur between two molecules in solution they must first be desolvated (Figure 6).

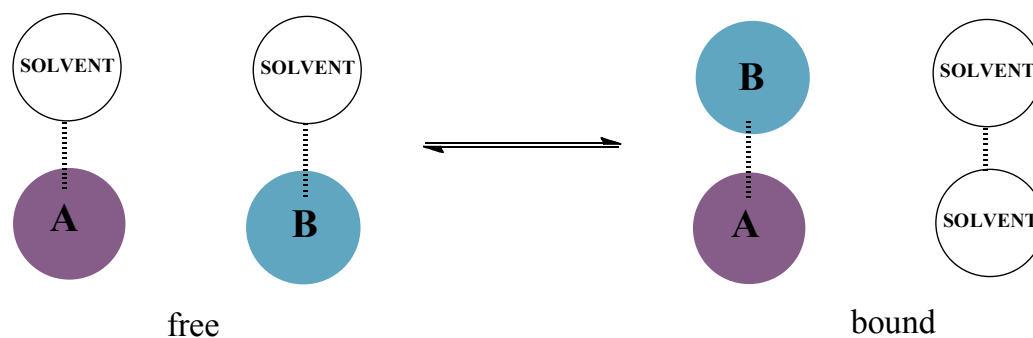


**Figure 6** Interactions between solute-solvent and solvent-solvent are in competition

If the solvent interacts strongly with the substrate the non-covalent interaction is destabilised. It is therefore important that  $\pi$ - $\pi$  interactions are studied in a range of polar and non-polar solvents to fully understand them. However, due to the flat  $\pi$ -electron surfaces of aromatic molecules, solvophobic forces favour  $\pi$ -stacking geometries which allow for maximum overlap and these are not commonly observed for  $\pi$ - $\pi$  interactions. As a consequence solvophobic forces do not determine the geometry of these interactions.

#### 1.2.2.5 Electrostatic contribution

The electrostatics of the interaction can be visualised by describing the aromatic ring as two regions of negatively charged  $\pi$ -electron density surrounding a positively charged  $\sigma$  framework, as this is a description of the quadrupole moment. The interaction between two such systems as a function of orientation is described in Figure 7.<sup>29</sup>

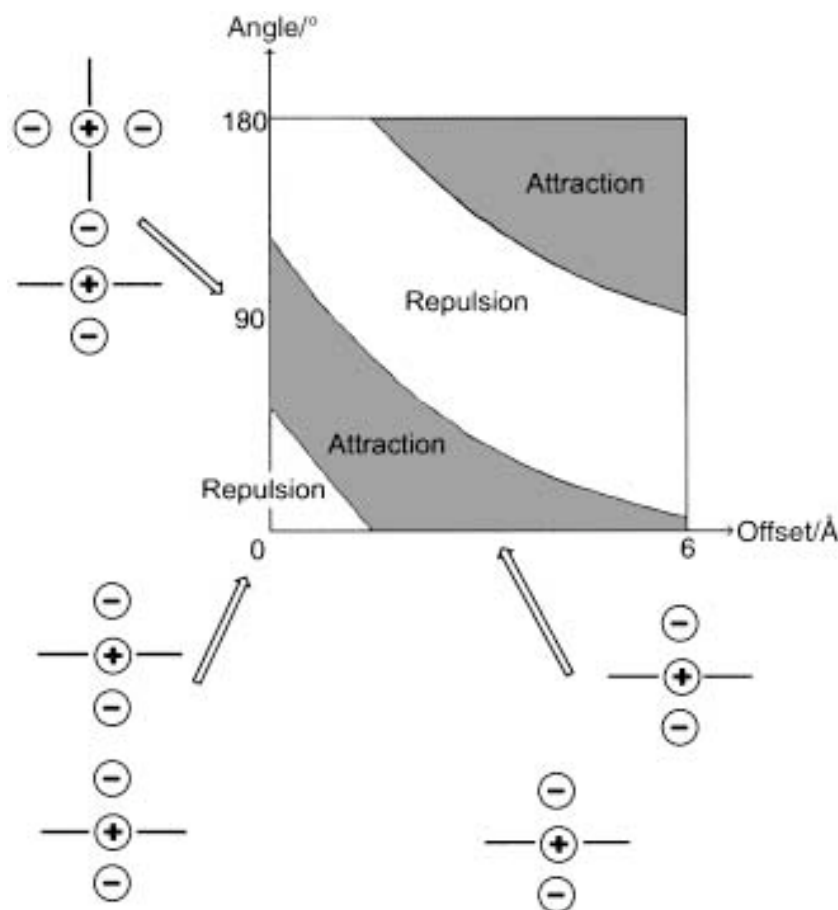


**Figure 7** Interaction between two aromatic rings as a function of distance and angle. Two geometries are shown<sup>29</sup>

The favoured geometries are edge-to-face (T-shaped) and offset stacked (parallel displaced), and these account for the observed benzene dimer and porphyrin stacking geometries. From these findings, the rules which Hunter and Sanders described for non-polarised  $\pi$ -systems are;

Rule 1  $\pi$ - $\pi$  repulsion dominates in a face-to-face  $\pi$  stacked geometry;

Rule 2  $\pi$ - $\sigma$  attraction dominates in an edge-on geometry;

Rule 3  $\pi$ - $\sigma$  attraction dominates in an offset  $\pi$ -stacked geometry.

The stacking interaction is affected by the substituents or a heteroatom in the ring, as this can polarise the aromatic system. An electron withdrawing substituent pulls electron density away from the ring and hence decreases  $\pi$ - $\pi$

repulsion between the two rings. Therefore electron withdrawing substituents led to increased stability of  $\pi$ - $\pi$  interactions. Electron donating substituents increase the electron density associated with the aromatic ring and hence have the opposite effect (Figure 8). The following rules apply for polarised  $\pi$  systems;

Rule 4 For interactions between highly charged atoms, charge-charge interactions dominate;

Rule 5 Favourable interaction with a neutral or weakly polarised site requires the following  $\pi$ -polarisation:

- a) a  $\pi$  deficient atom in a face-to-face geometry,
- b) a  $\pi$  deficient atom in the vertical T-group in the edge-on geometry,
- c) a  $\pi$  rich atom in the horizontal T-group in the edge-on geometry.

Rule 6 A favourable interaction with a neutral or weakly polarised site requires the following  $\sigma$ -polarisation:

- a) a positively charged atom in a face-to-face geometry,
- b) a positively charged atom in the vertical T-group in the edge-on geometry,
- c) a negatively charged atom in the edge-on geometry.

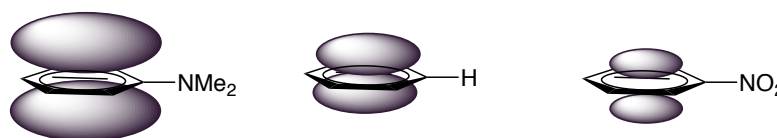
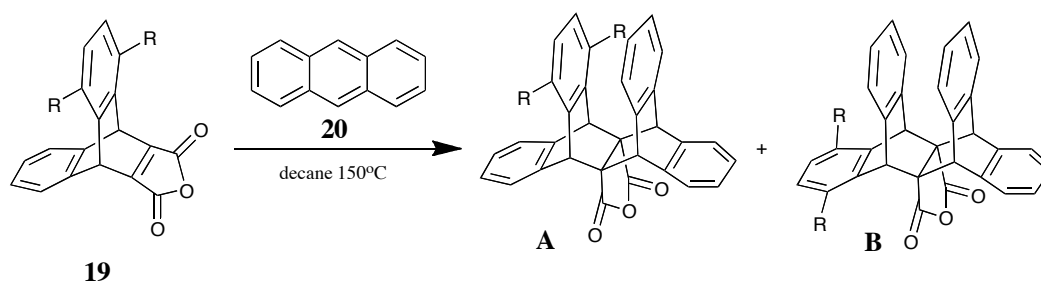


**Figure 8** Representation of the polarisation of benzene by various functional groups

Knowledge of the relative effects of each contribution, allows us to better understand  $\pi$ - $\pi$  interactions. Then the magnitude of the interaction can be calculated by taking into account all the different factors that contribute. From

analysing these different contributions it becomes clear that the main differences between traditional hydrogen bonds and aromatic interactions is the size of the contact area and number of contact points. As a consequence, it is far more complicated to rationalise these interactions with a set of simple rules, as is the case for hydrogen bonding.

A recent paper by Wheeler and Houk questions the validity of the Hunter and Sanders polar/ $\pi$  model and presents a new direct interaction model for interactions between substituted benzene rings.<sup>33, 34</sup> Stereoselective Diels-Alder reactions and theoretical calculations were used to probe substituent effects in  $\pi$ - $\pi$  stacked complexes. Barrier height differences of competing transition states allowed them to calculate stacking free energies for various substituted and unsubstituted benzene dimers, hence providing a measure for relative substituent effects. The Diels-Alder cycloaddition reaction studied is shown in Scheme 1.



**Scheme 1** Diels-Alder reaction of anthracene **20** with various dienophiles **19**

R	Major product (A or B)	Ratio A:B
H	A	-
Me	B	1:3
OMe	A	5:1
Br	A	17:1

**Table 1** Major product, and product ratio (A:B) for the Diels-Alder reaction

It was reported that the product selectivity is a direct result of the free energy differences of the transition states. This was found to be consistent with computational experiments on the system. Proton NMR spectra of the crude

reaction mixtures were used to determine the product ratios. Pronounced selectivity was observed for all substrates and the major products found are shown in Table 1. Interestingly the reaction with the methoxy substituted substrate, favoured a product with a stacking interaction between the incoming anthracene and the substituted ring. However, as the methoxy group is electron donating, using the Hunter and Sanders rules, product A would not be predicted. This led Wheeler and Houk to define a new direct interaction model for understanding substituent effects in  $\pi$ - $\pi$  sandwich complexes, which is shown in Figure 9.

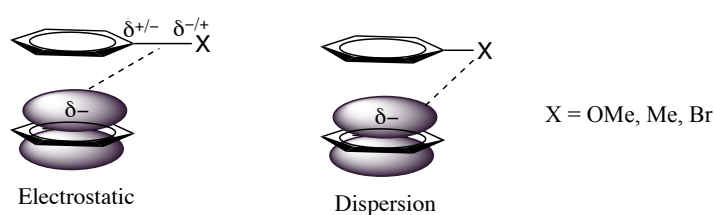


**Figure 9** Direct interaction model for substituent effects in  $\pi$ - $\pi$  sandwich geometry complexes<sup>34</sup>

In this model, the substituent effects in the sandwich geometry of the dimer are attributed to direct interactions between the phenyl ring and the substituent. In contrast to commonly accepted views on  $\pi$ - $\pi$  interactions, these effects rely on inductive effects and not electrostatics. It should be noted that this study only proved this new model to be relevant for the sandwich geometry. Theoretical studies by Wheeler and Houk on the edge-to-face geometry of substituted benzene dimers have shown the direct interaction model to be applicable, however this is yet to be supported by experimental data.<sup>35</sup> Wheeler and Houk have also reported that earlier experimental results by Hunter and Gung *et al.* can be explained by this new model.<sup>36,37</sup>



## 1.3 Interactions between an aromatic ring and a functional group

Aromatic rings can be involved in a weak form of hydrogen bonding, as the aromatic ring can act as a hydrogen bond acceptor and a range of functional groups can act as a hydrogen bond donor. In contrast to conventional hydrogen bonds, X-H/ $\pi$  hydrogen bonds occur between a hard acid and a soft base and they can also form in both polar and non-polar solvents. Although the ability of aromatic rings to form such interactions is not yet as widely studied as arene-arene interactions, it has been reported that they are stronger than  $\pi$ - $\pi$  interactions. However, a detailed understanding of the physical origin of these interactions is yet to be achieved.

### 1.3.1 C-H/ $\pi$ hydrogen bonds

#### 1.3.1.1 Definition and physical properties

Nishio *et al.* first introduced the idea of aromatic rings being involved in a weak form of hydrogen bonding.<sup>38-42</sup> They highlighted how C-H/ $\pi$  hydrogen bonding can account for the folding tendency in a wide range of small organic molecules and how it plays an important role in the conformational behaviour of organic molecules. The enthalpy for a single unit of a C-H/ $\pi$  interaction is small, approximately 0.5 to 2.5 kJ mol<sup>-1</sup>, when an alkyl or aromatic C-H is involved.<sup>43</sup> However the total enthalpy can become sizeable when several C-H groups can simultaneously participate in interactions with  $\pi$  groups. As multiple C-H/ $\pi$  interactions formed between side chains can be significant, they may be considered as one of the driving forces to constrain a peptide conformation and consequently direct specific conformation in many proteins.<sup>44</sup> Using the crystal structure database Nishio *et al.* investigated the C-H/ $\pi$  interactions in peptides.<sup>45-</sup>

<sup>46</sup> Evidence to indicate that 42% of the structures studied exhibited such aromatic

interactions was found. As a consequence the importance of this interaction for the folded conformations of peptides was realised.

In 1993, Sakai reported a computational study of the binding energies and structures of benzene-methane complexes and suggested that the dispersion force was the most important for C-H/ $\pi$  hydrogen bonding (Figure 10).<sup>47</sup> For the most stable methane-benzene complex **21**, the orientation of the methane is above the plane with one hydrogen directed towards the centre of the aromatic ring with an angle approaching 180°, thus although unimportant when considering the binding energy, electrostatics determine the geometry of C-H/ $\pi$  complexes. However, in contrast to conventional hydrogen bonds, the directionality of C-H/ $\pi$  bonds is weak. The binding energy of the most stable complex (**21**) was calculated to be -0.57 kcal per mol.

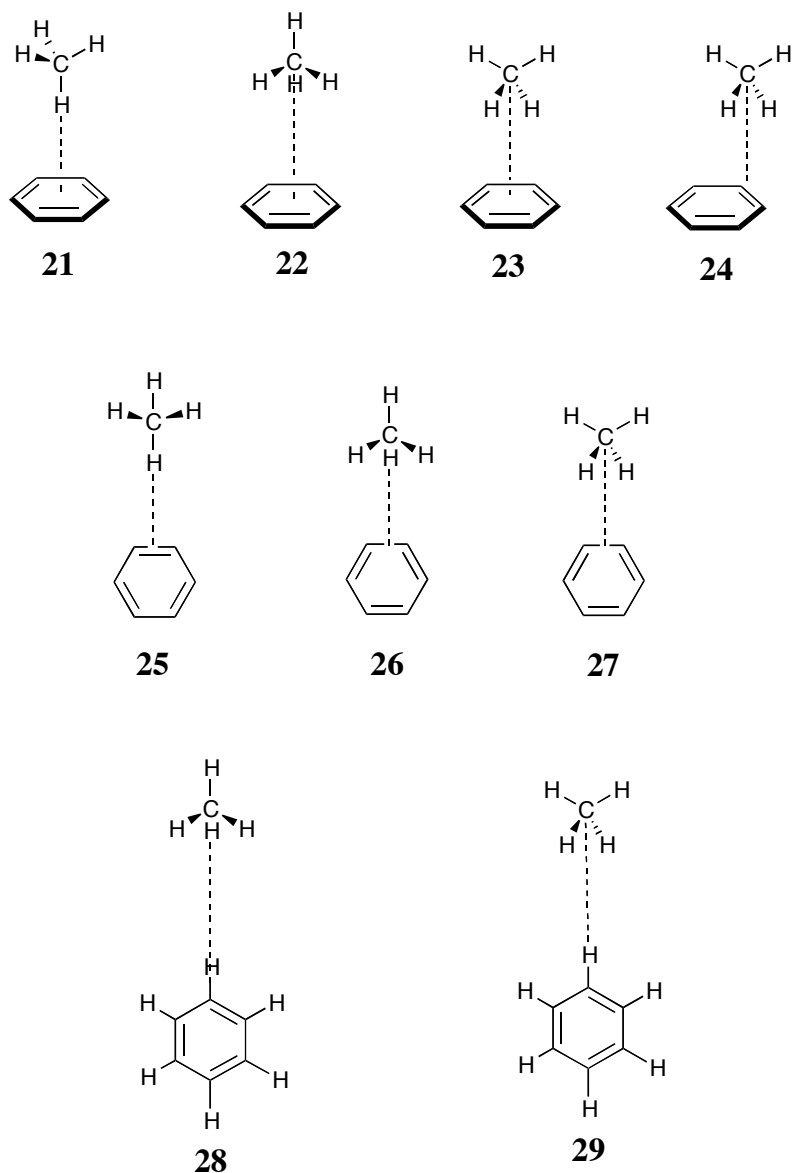


**Figure 10** Geometries of the benzene-methane complexes studied

More recent theoretical studies agree with these findings.<sup>48-52</sup> However, this only holds for a typical  $sp^3$  C-H/ $\pi$  hydrogen bond. For  $sp$  hybridised CH groups the contribution from electrostatic energy becomes significant, and as a consequence such interactions are far more similar in nature to conventional hydrogen bonds than  $sp^3$  C-H hydrogen bonds.<sup>53</sup> In essence, the proportion of electrostatic forces is dependent on the hybridisation of the carbon atom in the C-H bond. Computational studies have also been used to determine the interaction energies

and geometries of the benzene-acetylene and benzene-ethene complexes (Figure 11).<sup>54</sup>

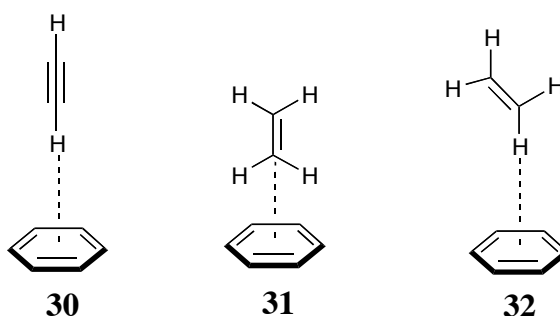


**Figure 11** Preferred geometries of the benzene-acetylene and benzene-ethene complexes

For the acetylene-benzene complex the most stable geometry **30** is a T-shaped stacking between the acetylene and benzene, with a distance of 3.5 Å between the carbon atom of the acetylene and the centre of the ring. In contrast, the ethene-benzene complex has two stable geometries **31** and **32**, and the more stable is complex **32**.

### 1.3.1.2 Intramolecular C-H/ $\pi$ interactions and the conformation of organic compounds

In order to probe the hydrogen bond character of C-H/ $\pi$  interactions, Nishio *et al.* studied the substituent effect on a range of aromatic molecules capable of forming intramolecular C-H/ $\pi$  interactions, by NOE enhancement.<sup>50</sup> The effect of substituents is a useful probe for the hydrogen bond character of C-H/ $\pi$  interactions, as in the formate ester **33** (Figure 12) since, if it behaves like a conventional hydrogen bond, an electron donating substituent on the hydrogen bond acceptor should increase the interaction. From peptide studies it was found that C-H/ $\pi$  interactions are favoured in 5- and 6-membered rings, and this

prompted a further study of a series of organic molecules capable of forming 5-, 6- and 7-membered ring C-H/ $\pi$  interactions (Figure 13).<sup>55, 56</sup>

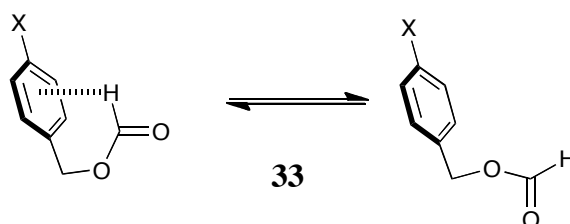
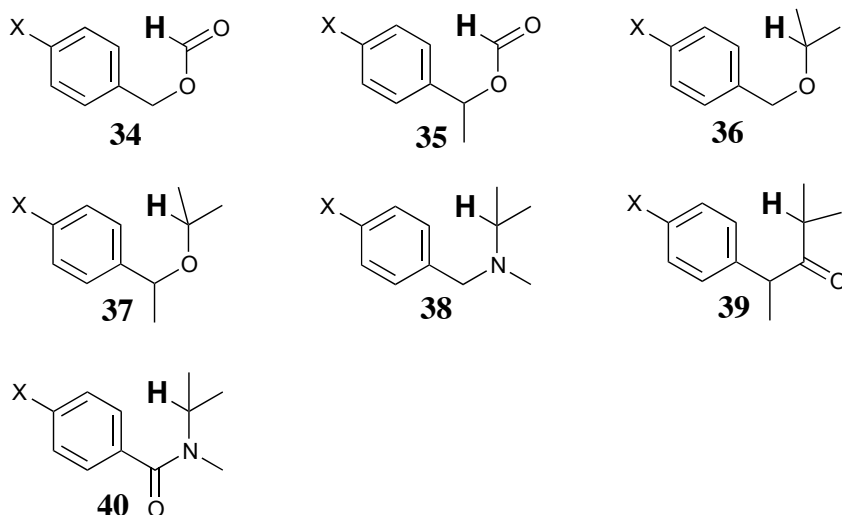


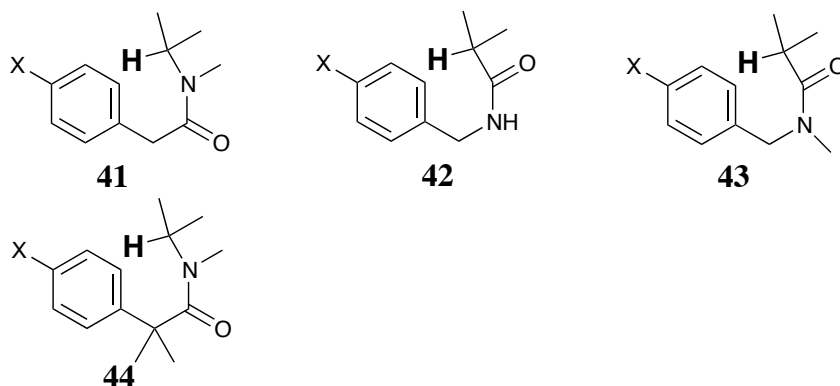
**Figure 12** Conformational equilibria of the folded and stretched conformers of benzyl formate derivatives

NOE enhancements were used to estimate the ratio of the folded and stretched conformations and hence the strength of the C-H/ $\pi$  interactions in the molecules in  $\text{CDCl}_3$  and DMSO. The observation of an upfield shift in the  $^1\text{H}$  NMR of the donor proton was used to confirm the results of the NOE experiments. Molecular mechanics calculations were also applied to estimate the distance between the aromatic acceptor and C-H donor.

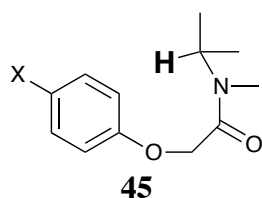
## 5-Membered ring interaction:



## 6-Membered ring interaction:



## 7-Membered ring interaction:



X = OMe, Me, H, Cl  
Br, CF<sub>3</sub>, NO<sub>2</sub>

**Figure 13** Benzylic derivatives studied, in which a C-H/ $\pi$  interaction between the proton (bold) and the aromatic ring, can occur

Electron donating substituents on the aromatic ring should raise the energy of the highest occupied  $\pi$ -orbital, and electron withdrawing substituents on the carbon atom of the C-H donor should lower the C-H antibonding orbital and hence the energy gap of the interacting orbitals required for a C-H/ $\pi$  hydrogen bond, thus

making the interaction favourable. It was proved that this combination of substituents leads to the largest ratio of the folded conformers. With all the series studied, NOE enhancement and hence preference for the folded conformer increased as X became more electron donating. A high-field shift in the NMR of the donor C-H was observed as it is expected to lie just above the ring and as a consequence is subjected to diamagnetic anisotropy. This study also highlighted the effects of the electronegativity of the donor C-H proton. An increase in the acidity of the donor proton leads to an increase in the strength of the C-H/ $\pi$  interaction. Amide **40** showed the most significant NOE enhancement indicating that it has the most stabilised folded conformer. This is attributed to the flexibility of the molecule, which allows the isopropyl group to approach the aromatic ring in the perpendicular plane, allowing for the maximum overlap of the interacting orbitals. In line with previous studies, a 5-membered ring interaction gave the highest ratio of folded conformers and hence is the most favourable interaction. It was reported that when comparing **40**, **41**, and **45** which all have a common  $\text{NCH}(\text{CH}_3)_2$  group but form 5-, 6- and 7-membered ring interactions respectively, the NOE enhancement decreases with increase in ring size. Hence the optimum ring size is 5 for C-H/ $\pi$  hydrogen bonds which can be attributed to the unfavourable entropic effect associated with lengthening the alkyl chain.

### 1.3.1.3 Interactions involving alkyne groups

Several different C-H groups have been shown to participate in C-H/ $\pi$  interactions, including methyl, isopropyl, long chain alkyl groups and the CH groups in aromatic rings. Boese *et al.* determined the X-Ray crystal structures of ethynylbenzene (Figure 16), 1,4-diethynylbenzene (Figure 14) and 1,3,5-triethynylbenzene (Figure 15).<sup>57</sup> These molecules offer a unique opportunity to study the competition of C-H/ $\pi$  and  $\pi$ - $\pi$  interactions, as a terminal ethyne group can be both a hydrogen bond acceptor and donor.

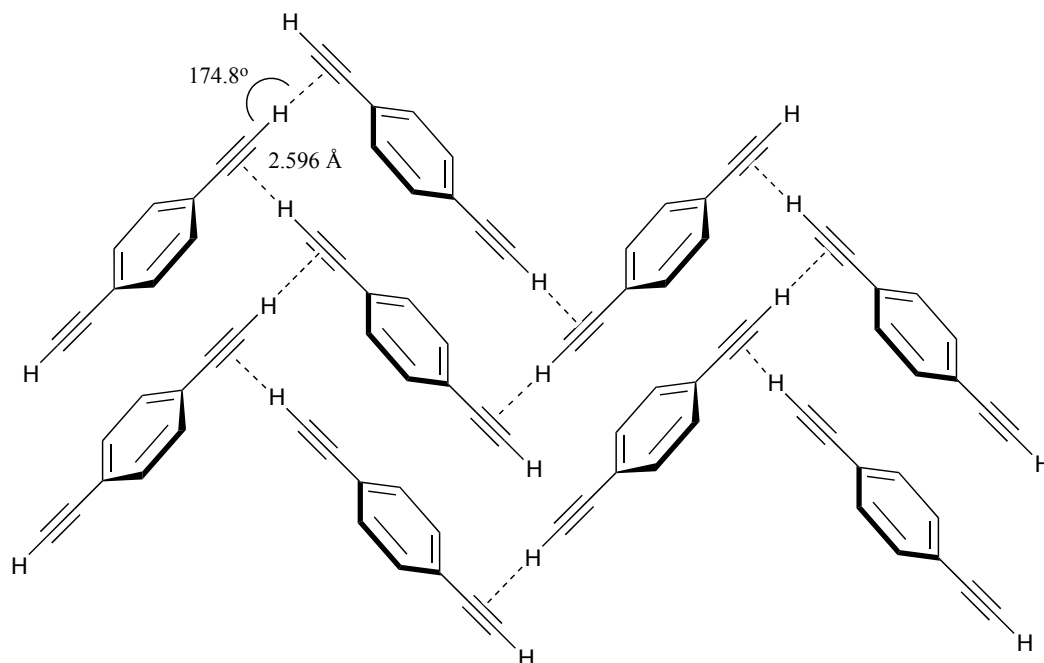


**Figure 14** Packing structure of 1,4-diethynylbenzene

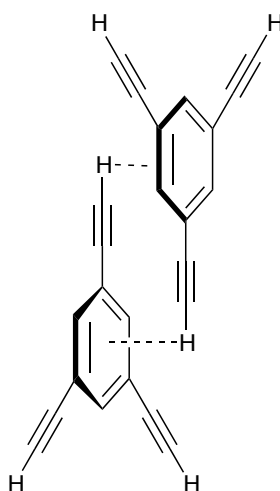


**Figure 15** Packing structure of 1,3,5-triethynylbenzene

All three ethynylbenzenes display distinctly different crystal packing structures. For 1,4-diethynylbenzene a T-shaped geometry is observed and it is stabilised by a C-H/ $\pi$  interaction between the terminal hydrogen of the alkyne group and the  $\pi$ -cloud of a triple bond (Figure 14). This is the sole interaction observed for 1,4-diethynylbenzene. However for 1,3,5-triethynylbenzene the closest contact point



is between the centre of the aromatic ring and the terminal hydrogen of the alkyne (Figure 15). The crystal stacking structure of ethynylbenzene is quite different and shows benzene type edge-to-face interactions, two short contact distances between the alkyne proton and the benzene ring and a further intermolecular interaction with the alkyne  $\pi$ -cloud were observed (Figure 16).

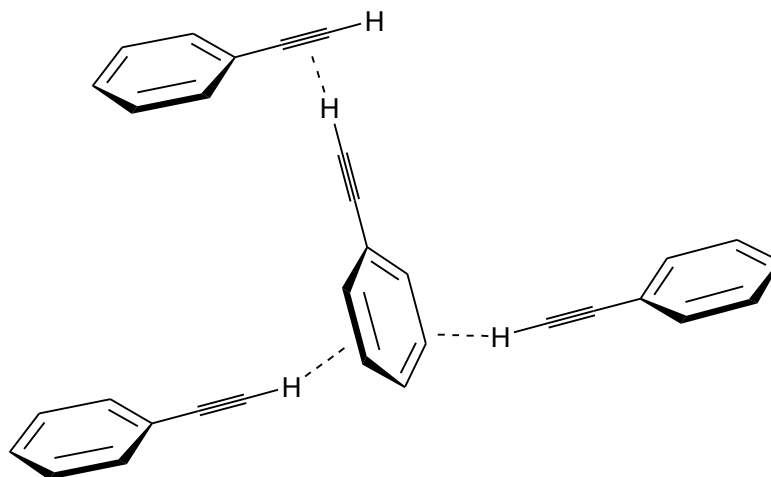


**Figure 16** Packing structure of ethynylbenzene

The physical properties of ethynylbenzene are dramatically different to those of 1,4-diethynylbenzene and 1,3,5-triethynylbenzene, and this may be a reflection of the different packing principles observed. Thus the melting point of ethynylbenzene is  $-45\text{ }^{\circ}\text{C}$ , whereas the melting points of 1,4-diethynylbenzene and 1,3,5-triethynylbenzene are  $97\text{ }^{\circ}\text{C}$  and  $104\text{ }^{\circ}\text{C}$  respectively.

### 1.3.2 X-H/ $\pi$ hydrogen bonds

#### 1.3.2.1 Definition and physical properties

In this form of non-covalent interaction, the  $\pi$  cloud of the aromatic system acts as an acceptor and X-H, in which X is either an oxygen, nitrogen or sulphur

atom, acts as a donor.<sup>58</sup> Like the C-H/ $\pi$  interaction, this interaction can be considered as a “non-conventional” form of hydrogen bonding. Along with conventional hydrogen bonding, this non-conventional form has also contributed to stabilising effects in structural biology.<sup>59,60</sup> Early evidence for X-H/ $\pi$  hydrogen bonding comes from infrared spectroscopy studies conducted in the 1950s and 1960s by Josien and Sourisseau,<sup>61-62</sup> Ōki and Iwamura<sup>63</sup> and Yoshida and Osawa.<sup>64</sup> More recently, extensive searches of the Cambridge Crystallographic Structural Database have confirmed the presence of these interactions in a wide range of organic molecules.<sup>65-67</sup>

The physical evidence for the X-H/ $\pi$  interaction comes from theoretical and experimental studies on the complexes of benzene with different X-H partners.<sup>68,69</sup> In 2000, Tsuzuki *et al.* published a fundamental paper on the comparison of N-H/ $\pi$ , O-H/ $\pi$  and C-H/ $\pi$  interactions, using high level *ab initio* calculations.<sup>70</sup> The geometries of the ammonia-benzene, water-benzene and methane-benzene complexes considered in this study are shown in Figure 17. The interaction energies and intermolecular distances for the most important complexes were calculated (Table 2).

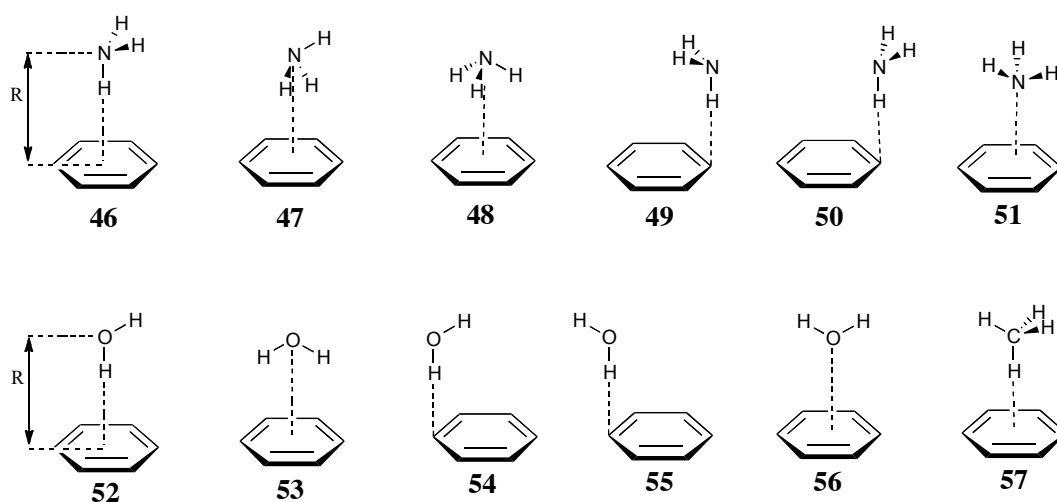


**Figure 17** Geometries of the ammonia-benzene, water-benzene and methane-benzene complexes studied

	<b>46</b>	<b>47</b>	<b>48</b>	<b>49</b>	<b>52</b>	<b>53</b>	<b>54</b>	<b>57</b>
<b>E<sub>tot</sub></b> <b>kcal mol<sup>-1</sup></b>	-2.22	-2.07	-1.72	-1.84	-3.02	-3.17	-2.77	-1.45
<b>E<sub>tot</sub></b> <b>kJ mol<sup>-1</sup></b>	-9.30	-8.65	-7.19	-7.69	-12.62	-13.25	-11.58	-6.06
<b>R (Å)</b>	3.6	3.6	3.6	3.6	3.4	3.4	3.4	3.8

**Table 2** Interaction energies and intermolecular separation R, of selected complexes

It was reported that the attraction between benzene and water or ammonia is weaker than for a conventional hydrogen bond. The interaction energy of the benzene-ammonia complex was found to be approximately 40% of the energy of a conventional hydrogen bond. As expected for hydrogen bonds, the order of magnitude of the  $E_{\text{tot}}$  values is in accordance with the electronegativity of the proton-donating atom, so the strongest interaction occurs in the benzene-water complex. The shortest distance between the centre of the aromatic ring and the atom of the other molecule was also observed for the benzene-water complex. The results also show that in the case of the ammonia complex, the preferred geometry is with the ammonia above the centre of the ring and the N-H bond in the perpendicular plane. This is indicated by the significantly larger interaction energy for complex **46**, as compared to **49** and **50**. For complex **46** a substantial attraction was found at intermolecular distances over 4.0 Å and the energy of the complex was still orientation dependent at these separations. This prompted them to suggest that long range and not short range interactions are the main source of attraction. These results show that the dominating forces are dispersion and electrostatics and not short range forces such as charge transfer.

## 1.4 Cation/ $\pi$ interactions

### 1.4.1 Cation/ $\pi$ interactions in biological systems

Cation/ $\pi$  interactions were once considered to be extremely weak and their contribution to binding processes in biological systems negligible. However the

determination of the active site of acetylcholine esterase completely changed this opinion and attracted a great deal of research interest in this area from both organic and theoretical chemists.<sup>71,72</sup> By the determination of the X-Ray crystal structure, it was demonstrated that the charged  $R-N^+(CH_3)_3$  group of acetylcholine is not in the proximity of a negatively charged anionic group within the enzyme but is instead surrounded by aromatic residues, hence displaying a cation/ $\pi$  interaction. This discovery also led to the development of the anti-Alzheimer drug Aricept **58**, which binds to the active site of acetylcholine esterase (Figure 18).<sup>73,74</sup>

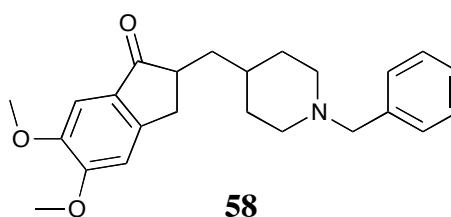


**Figure 18** Molecular structure of Aricept

Cation/ $\pi$  interactions are frequently observed under physiological conditions between protonated side chains and nearby aromatic rings in proteins. This phenomenon was initially observed by Burley and Petsko who reported that NH groups on amino acid side chains display a preference to be near aromatic side chains.<sup>8</sup> Within proteins, cation/ $\pi$  interactions can occur between protonated Lys, Arg or His and Phe, Tyr or Trp. Trp is the most commonly observed  $\pi$  system participating in these interactions, with 26% of all Trp residues involved in energetically significant cation/ $\pi$  interactions.<sup>75</sup>

### 1.4.2 Definition and physical properties

Unlike the other aromatic interactions discussed earlier, the magnitudes of cation/ $\pi$  interactions are substantial and can be similar even to the strongest of

non-covalent interactions.<sup>76</sup> As a consequence, a detailed understanding of the physical origins of this interaction is of vital importance to the field of physical organic chemistry.

Gas phase studies of ion-molecule complexes provided early insight into the fundamental aspects of cation/ $\pi$  interactions. In a pioneering study undertaken by Kebarle *et al.*, water was used as a reference compound and the astonishing relative strengths of these interactions were revealed.<sup>77</sup> The  $K^+$ -benzene complex has a stronger interaction energy than the  $K^+$ -water complex (79 and 75 kJ mol<sup>-1</sup> respectively). Further studies on a range of cations were accomplished by Meot-Ner *et al.*, who established that more complicated cations could also bind strongly to an aromatic system.<sup>78,79</sup> Importantly they showed that the  $NH_4^+$ -benzene complex has a similar binding energy to the  $K^+$ -benzene complex (Table 3).

Cation	Molecule	Experimental binding energy		Computational binding energy	
		kJ mol <sup>-1</sup>	Kcal mol <sup>-1</sup>	kJ mol <sup>-1</sup>	Kcal mol <sup>-1</sup>
$K^+$	Water	74.8	17.9	-	-
$K^+$	Benzene	80.3	19.2	62.7	15.0
$Li^+$	Benzene	160.1	38.3	183.1	43.8
$Na^+$	Benzene	117.0	28.0	113.3	27.1
$NH_4^+$	Benzene	80.7	19.3	74.8	17.9
$NMe_4^+$	Benzene	39.3	9.4	42.6	10.2

**Table 3** Experimental and computational binding energies of various cation-benzene complexes

Several high level computational studies whose results are in agreement with those from the gas phase have also been carried out on various ion-benzene complexes.<sup>80-84</sup>

When comparing the interactions of alkali metals with a benzene ring the following trend is observed,  $Li^+ > Na^+ > K^+ > Rb^+$ . This observed trend follows the classical electrostatic sequence, suggesting that electrostatic forces have a dominant role in cation/ $\pi$  interactions.

Dougherty *et al.* have carried out an extensive body of work on the cation/ $\pi$  interaction using cyclophane receptors, and from these studies, a physical model for the interaction has been suggested.<sup>85-90</sup> In accordance with  $\pi$ - $\pi$  interactions, the electrostatic force arising from the interaction of the quadrupole moment on the aromatic ring and the cation, is often the dominating force. Most of the trends observed for these interactions can be rationalised by an electrostatic model. However the contribution from electrostatics varies with the nature of the aromatic ring. Thus, for example in systems mentioned earlier such as the  $\text{Na}^+$  - benzene complex, the electrostatic contribution is significant, whilst for the  $\text{Na}^+$  - 1,3,5-trifluorobenzene complex, there is no electrostatic contribution. The other contributions to the total binding energy are from dipole interactions, charge transfer and dispersion forces. The combination of these contributions is related to the polarisability of the aromatic ring and the ion component. Forces other than electrostatic will become more important when studying systems with large organic ions and with more complex aromatic systems. An example of a cyclophane receptor and some of the substrates, studied by Dougherty *et al.*, is shown in Figure 19.<sup>91</sup> They found that the cyclophane **59** was a better receptor for quaternary ammonium and iminium ions than for the corresponding neutral molecules. As a control experiment they replaced two of the benzene rings with cyclohexyl units, this seriously impaired the cation binding ability of the host. This observation established that it was the cation/ $\pi$  interaction which was responsible for the binding of the cation.

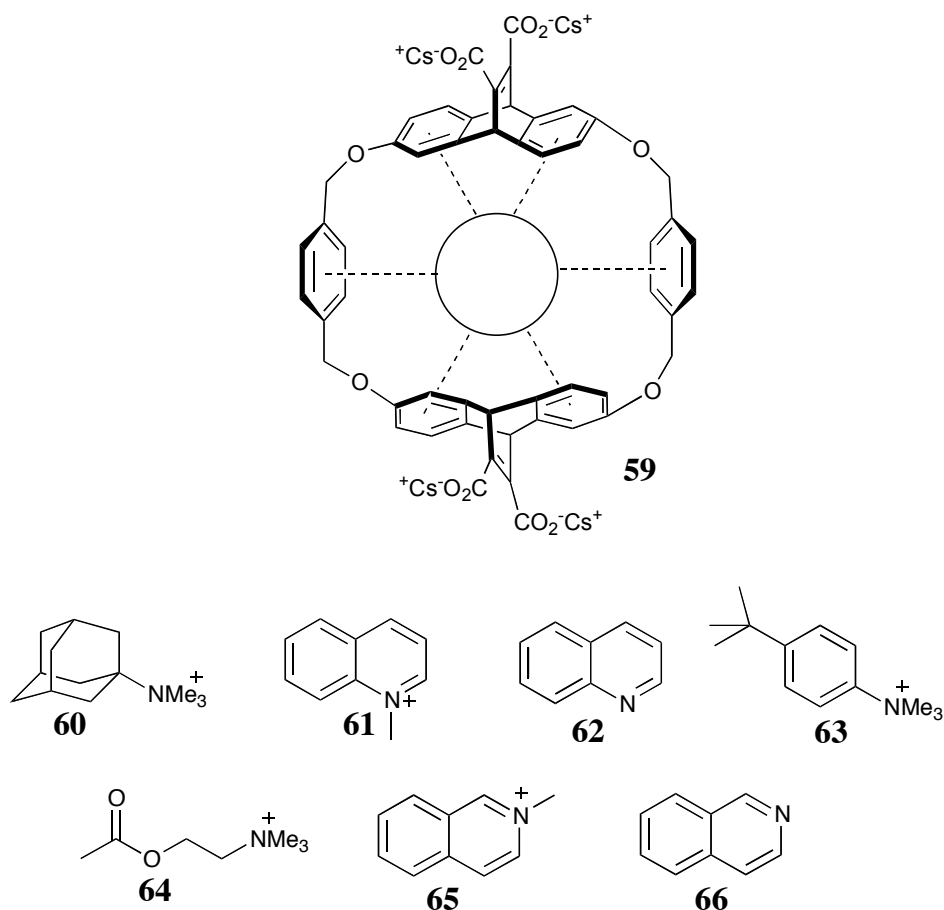


**Figure 19** A cyclophane receptor and examples of substrates used for complexation studies

## 1.5 Molecular balance systems

Molecular balances offer a unique intramolecular approach to measuring weak non-covalent interactions. They overcome many of the problems encountered when using complicated biological systems or supramolecular chemistry to probe  $\pi$ -interactions. Small synthetic modifications in molecular balances, allow for a wide range of fundamental aspects of non-covalent interactions to be studied, such as the variation of interaction geometries, substituent effects and functional groups. Molecular balances can be designed to measure very weak interactions, which are inaccessible by other methods due to entropic requirements. To date, several molecular frameworks for balances have been developed and

successfully used to study  $\pi$ -interactions on both a qualitative and quantitative level.<sup>92</sup>

### **1.5.1 Quantifying $\pi$ -interactions using molecular torsion balances**

A well-designed molecular balance system can allow for the thermodynamic properties of non-covalent interactions to be extracted from the relative stabilities of conformational states. The differences in free energies of the ground-state conformers ( $\Delta G$ ) and the barrier to rotation are often used to evaluate thermodynamics of molecular balance systems. Dynamic NMR studies have been shown to be a valuable tool for determining conformational populations.

### **1.5.2 Wilcox molecular torsion balance**

The group of Wilcox pioneered this field when, in 1994, they reported the use of a novel system described as a “molecular torsion balance” to study edge-to-face aromatic interactions.<sup>93</sup> They postulated that, an experimental probe for aryl-aryl interaction energies could be designed by using a molecule with two distinct conformational states, only one of which would allow for aryl-aryl interactions to occur. With this idea in mind, a series of esters **67**, each capable of either the folded conformation or the open conformation and interconverting by slow rotation were prepared (Figure 20).<sup>94</sup>





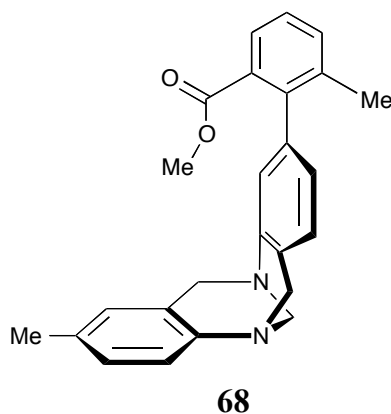


**Figure 21** Methyl ester Wilcox molecular torsion balance

Fortunately, the methyl ester showed no preference for either the folded or the open conformation. As a further probe of the aryl-aryl interaction an analogous range of compounds **69** with varying substituents in the place of the methyl group on the Tröger's base unit were prepared (Figure 22).

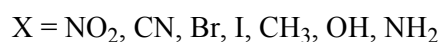
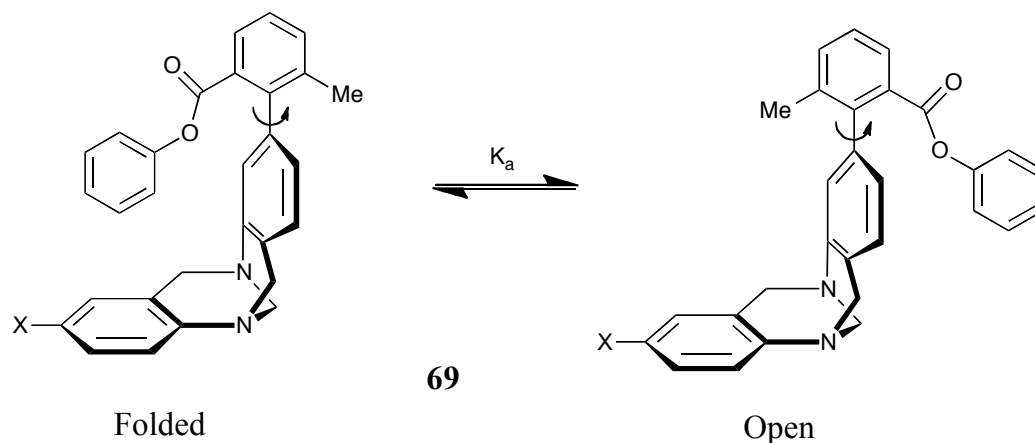


**Figure 22** Molecular torsion balance described by Wilcox for studying substituent effects

As mentioned earlier, electron withdrawing and electron donating substituents on an aromatic ring perturb the quadrupole moment and hence affect the electrostatic forces which govern these interactions. However, it was reported that the nature of the substituent X did not affect the proportion of folded

conformer. This prompted Wilcox to suggest that dispersion forces are dominant in these interactions.<sup>94</sup>

Encouraged by this finding, Diederich and co-workers synthesised a further range of compounds **70** bearing either a phenyl or a 4-(trifluoromethyl)phenyl ester on the edge ring and a range of electron withdrawing and electron donating substituents on the face ring and studied the conformational equilibria (Figure 23, Table 4).<sup>95-97</sup> They chose to study the equilibrium in C<sub>6</sub>D<sub>6</sub> and CDCl<sub>3</sub> after conflicting studies published by Cockroft and Hunter and Wilcox.<sup>98,94</sup> When studying the system in CDCl<sub>3</sub> the  $\pi$ - $\pi$  interaction cannot compete with the solute-solvent interaction and desolvation washes out any substituent effects. However in apolar C<sub>6</sub>D<sub>6</sub>, the solvent cannot compete with the aromatic moiety for binding with the face ring.

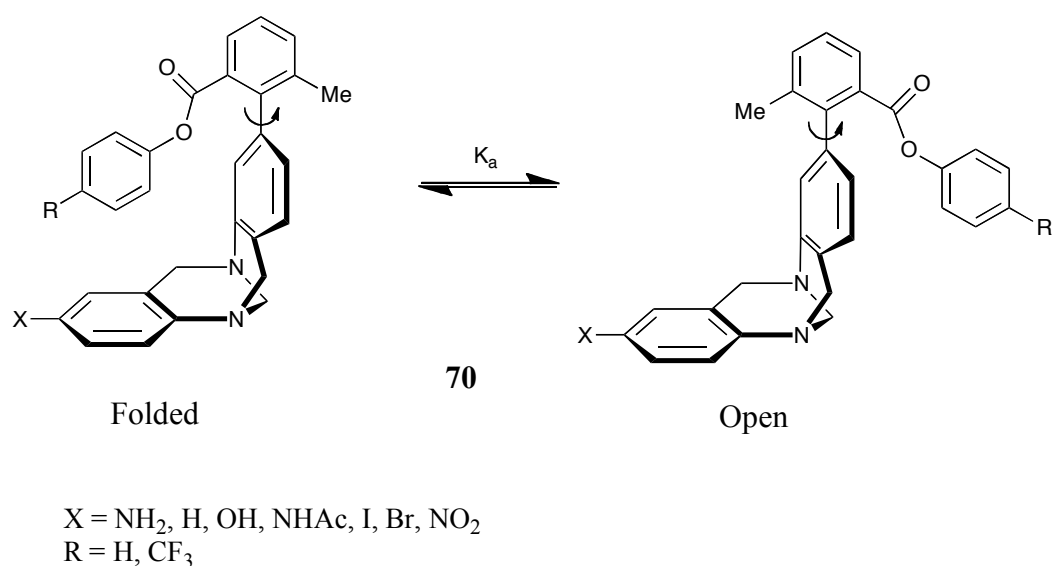


**Figure 23** Wilcox molecular torsion balance derivatives prepared by Diederich and co-workers

R	X	$\Delta G \text{ kJ mol}^{-1}$	
		$\text{C}_6\text{D}_6$	$\text{CDCl}_3$
<b>CF<sub>3</sub></b>	<b>NH<sub>2</sub></b>	-3.91	-2.65
<b>CF<sub>3</sub></b>	<b>H</b>	-3.47	-2.41
<b>CF<sub>3</sub></b>	<b>OH</b>	-3.46	-2.31
<b>CF<sub>3</sub></b>	<b>NHAc</b>	-3.74	-2.74
<b>CF<sub>3</sub></b>	<b>I</b>	-1.52	-0.61
<b>CF<sub>3</sub></b>	<b>Br</b>	-1.89	-1.01
<b>CF<sub>3</sub></b>	<b>NO<sub>2</sub></b>	-0.19	-0.47
<b>H</b>	<b>NH<sub>2</sub></b>	-1.95	-0.89
<b>H</b>	<b>H</b>	-1.56	-1.00
<b>H</b>	<b>OH</b>	-1.61	-1.04
<b>H</b>	<b>NHAc</b>	-1.36	-0.35
<b>H</b>	<b>I</b>	-2.11	-1.37
<b>H</b>	<b>Br</b>	-2.01	-1.41
<b>H</b>	<b>NO<sub>2</sub></b>	-1.28	-0.96

**Table 4** Folding free energies in  $\text{CDCl}_3$  and  $\text{C}_6\text{D}_6$ , of the Wilcox molecular torsion balance derivatives studied by Diederich and co-workers

Interestingly, results from the 4-(trifluoromethyl)phenyl ester **70** contradict Wilcox's earlier observations as they imply that electrostatic effects play an important role in edge-to-face interactions, inasmuch as the folding free energies in both solvents correlated linearly with the Hammett substituent constants. As expected when moving from apolar  $\text{C}_6\text{D}_6$  to  $\text{CDCl}_3$ , the free energies for each substrate decrease. This revealed the significant influence of solvent on the Wilcox molecular balance system, as the edge-to-face interaction competes with solvation of the face ring.

From these recent results on the Wilcox system Hunter and Cockroft reported that the observed trends in the interaction energies of these systems could often be understood by considering a solvent competition model in a generic folding equilibrium (Figure 24, Equation 1).<sup>99</sup>

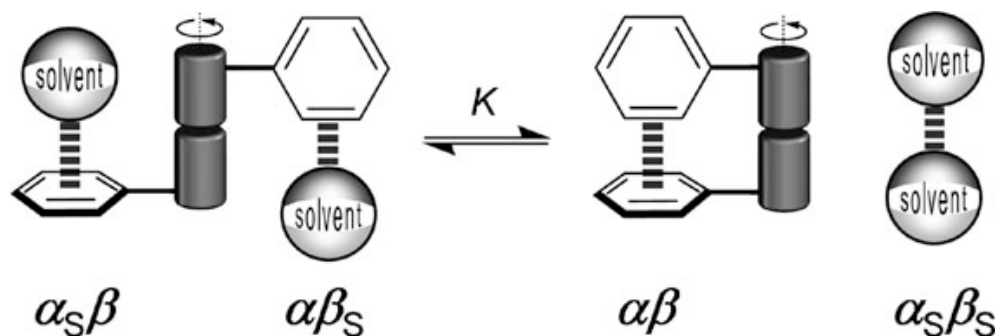


**Figure 24** Generic folding equilibrium for a molecular balance system<sup>99</sup>

$$\Delta\Delta G = -(\alpha - \alpha_s)(\beta - \beta_s)$$

**Equation 1**

Where  $\alpha$  and  $\beta$  are hydrogen bond parameters for the edge and face ring and  $\alpha_s$  and  $\beta_s$  are the corresponding parameters for the solvent. This model takes into account the following contributions for determining the position of equilibrium:

- i)  $\alpha_s\beta$  - the interaction between the aromatic face and the solvent;
- ii)  $\alpha\beta_s$  - the interaction between the edge of the aromatic ring and the solvent;
- iii)  $\alpha\beta$  - the edge-to-face aromatic interaction;
- iv)  $\alpha_s\beta_s$  - the interaction between displaced solvent molecules.

This model is based solely on electrostatic forces, and as the new results from the Diederich group are in agreement with the model it can be concluded that the behaviour of these interactions is dominated by electrostatic forces and not dispersion as was previously thought.

Wilcox and co-workers modified the molecular balance system in order to study C-H/ $\pi$  interactions, by replacing phenolic ester in the flexible unit of the balance with an isopropyl unit **71** (Figure 25).<sup>94</sup>

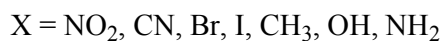
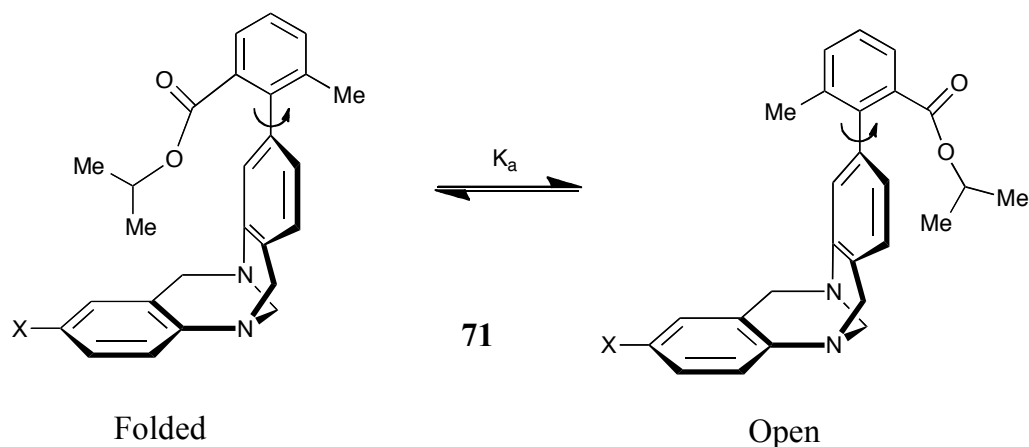


**Figure 25** Wilcox molecular torsion balance for studying C-H/ $\pi$  interactions

Their results show that the isopropyl folding energy is larger than the phenyl folding energy, hence demonstrating the stabilising power of co-occurring C-H/ $\pi$  interactions since the isopropyl group is capable of generating more C-H/ $\pi$  interactions than a phenyl ring. Moreover, they report that for these interactions the predominant force is dispersion.

The Wilcox balance **72** has also been utilized by Diederich *et al.* to study interactions between amides and organic fluorides (Figure 26).<sup>100,101</sup> The work was prompted by the observation of an interaction between an aromatic bound fluoride and a backbone carbonyl group of the serine protease, thrombin. Double-mutant cycles (*vide infra*) were used to quantify the interactions.

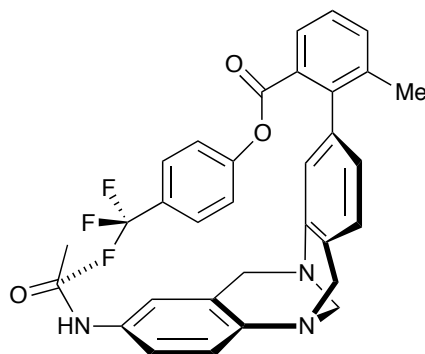
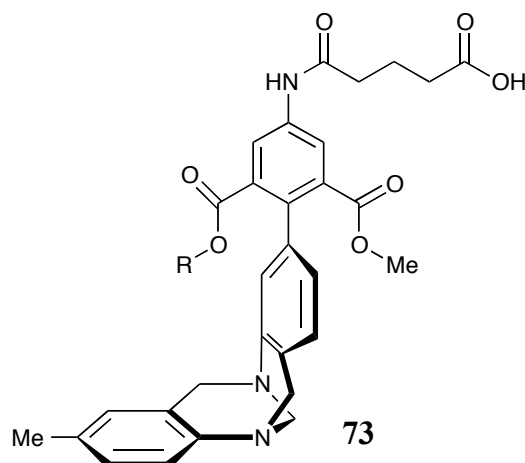


**Figure 26** Wilcox molecular torsion balance used by Diederich and co-workers to study interactions between amides and organic bound fluorides

In 2007, Wilcox and Bhayana reported the use of an improved version of the molecular balance **73** (Figure 27).<sup>102</sup> In order to overcome the problem that the original molecular balance was not water soluble, the structure was modified to include a water solubilising group, thus allowing measurement of the hydrophobic effects on CH- $\pi$  interactions. In this new molecular balance the rotation process exchanges the position of two alkyl groups, so that in the folding event the larger group displaces the solvent from the face of the aromatic ring (Figure 28).



R = CH(CH<sub>3</sub>)<sub>2</sub>, C(CH<sub>3</sub>)<sub>3</sub>, cyclohexyl, 1-adamantyl, CH<sub>3</sub>

**Figure 27** Water soluble molecular torsion balance<sup>102</sup>

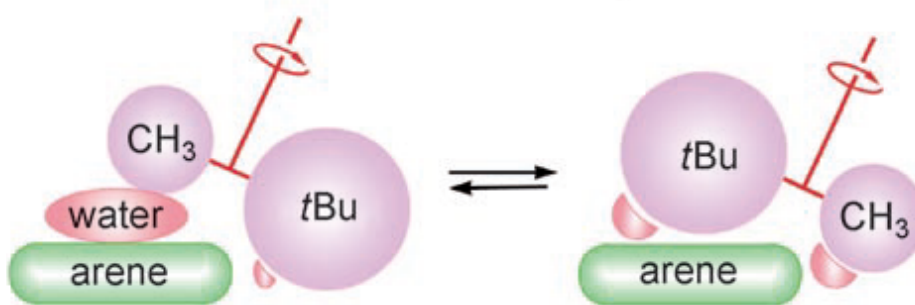


**Figure 28** Folding event of the water soluble molecular torsion balance, in which the solvent is displaced from the face of the aromatic ring by the *t*-butyl group

The folding energies of all the substrates were higher in water, and the difference also increases with increasing size of the alkyl group, this trend is also observed in organic solvents. However, this is only a preliminary study and further interesting results from this new system are expected.

### 1.5.3 Other examples of molecular balance systems

Although they provide an elegant solution for studying non-covalent interactions, molecular balance systems are overshadowed in the literature by other methods such as computational, X-Ray database searches and host-guest chemistry. This is possibly due to the difficulty in designing a molecular balance which allows for these interactions to be quantified. However, since the pioneering work of Wilcox in 1994, there have been several other noteworthy examples of molecular balance systems for studying  $\pi$ -interactions.<sup>93</sup> These will be discussed in turn.



### 1.5.3.1 $\pi$ - $\pi$ interactions

Cozzi *et al.* designed a system based on a series of 1,8-diarylnaphthalenes **74-76**, which was used to study the strength of parallel stacked interactions (Figure 29).<sup>103-106</sup> It was reported that the barrier to rotation of the aryl units could be measured using dynamic  $^1\text{H}$  NMR studies, with the help of the methyl group on the aromatic ring which acts as a label. The barrier to rotation is dependent on the strength of the parallel stacked structure. This property of 1,8-diarylnaphthalenes arises due to the steric effects which force the benzene rings to adopt a stacked geometry.

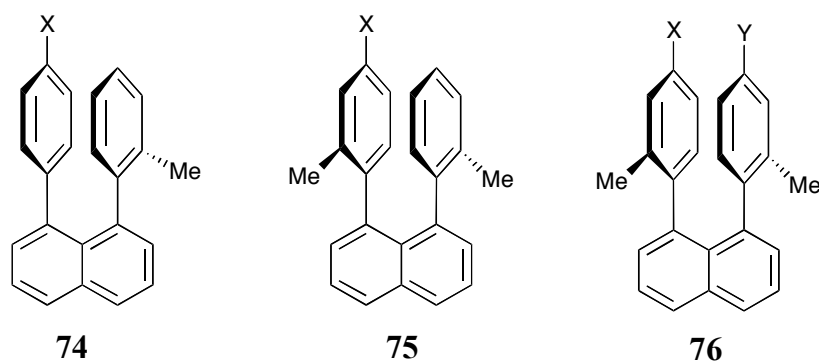


**Figure 29** Series of 1,8-diarylnaphthalene molecular balances

$^1\text{H}$  and  $^{19}\text{F}$  NMR spectroscopy were used to determine the barrier to rotation for a range of 1,8-diarylnaphthalenes with various X and Y groups on the substituted aromatic rings. The barrier to rotation increased as the X substituent became more electron withdrawing, indicating that the interaction becomes stronger as electron density is removed from the aromatic ring. This is in accordance with the Hunter and Sanders model for  $\pi$ - $\pi$  interactions. Cozzi *et al.* have shown that 1,8-diarylnaphthalenes **74-76** provide an effective probe for studying the substituent effects in  $\pi$ - $\pi$  interactions. However the aryl groups are forced into a sterically hindered stacked arrangement. With this in mind, Cozzi and co-workers later developed new systems to study  $\pi$ - $\pi$  interactions without this problem.<sup>107</sup> A 1,8-diarylbiophenylene system **77,78** was chosen (Figure 30). Crucially, in these molecules the arenes are spaced at a van der Waals distance

which is similar to that observed most commonly for stacked arenes. Moreover, the same trends were observed for this new system. However the overall substituent effect was found to be weaker than that observed for the 1,8-diarylnaphthalenes system **74-76**. This was attributed to the difference in orientation and proximity of the rings in the two systems.

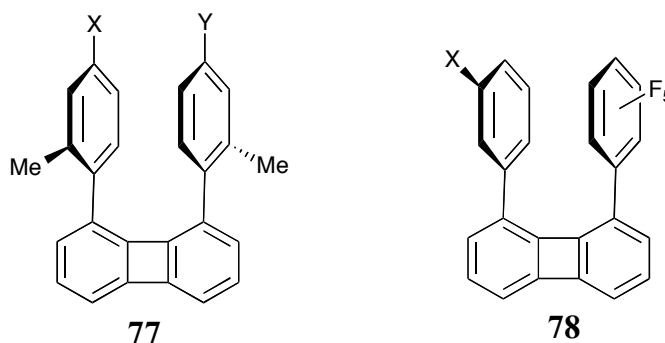


**Figure 30** Series of 1,8-diarylbiphenylene molecular balance systems

The group also developed a system based on conformationally restricted polycyclic systems **79** (Figure 31).<sup>108</sup> Unlike the 1,8-diarylbiphenylenes **77,78** and 1,8-diarylnaphthalenes **74-76**, this system allows for  $\pi$ - $\pi$  interactions to be studied in face-to-face and edge-to-face arrangements. Once again the effect that varying the X substituent has on the barrier to rotation was studied by various NMR techniques and the results were found to be in accordance with previous models, hence providing additional support for the  $\pi$ -polar model for arene interactions.

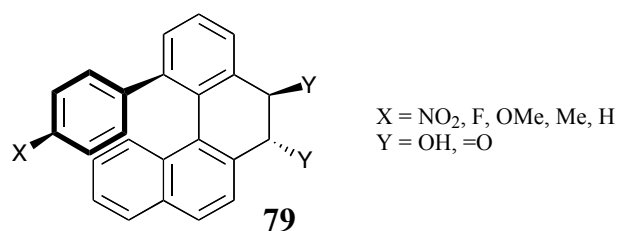


**Figure 31** Conformationally restricted molecular balance system

Several other groups have used the 1,8-diarylnaphthalene framework to study a range of arene interactions. A notable example was reported by Zoltewicz and co-workers, who prepared several different 1,8-diarylnaphthalene derivatives **80-87**, including those with heteroatomic aromatic rings and naphthyl groups instead of substituted phenyl rings (Figure 32).<sup>109-113</sup>

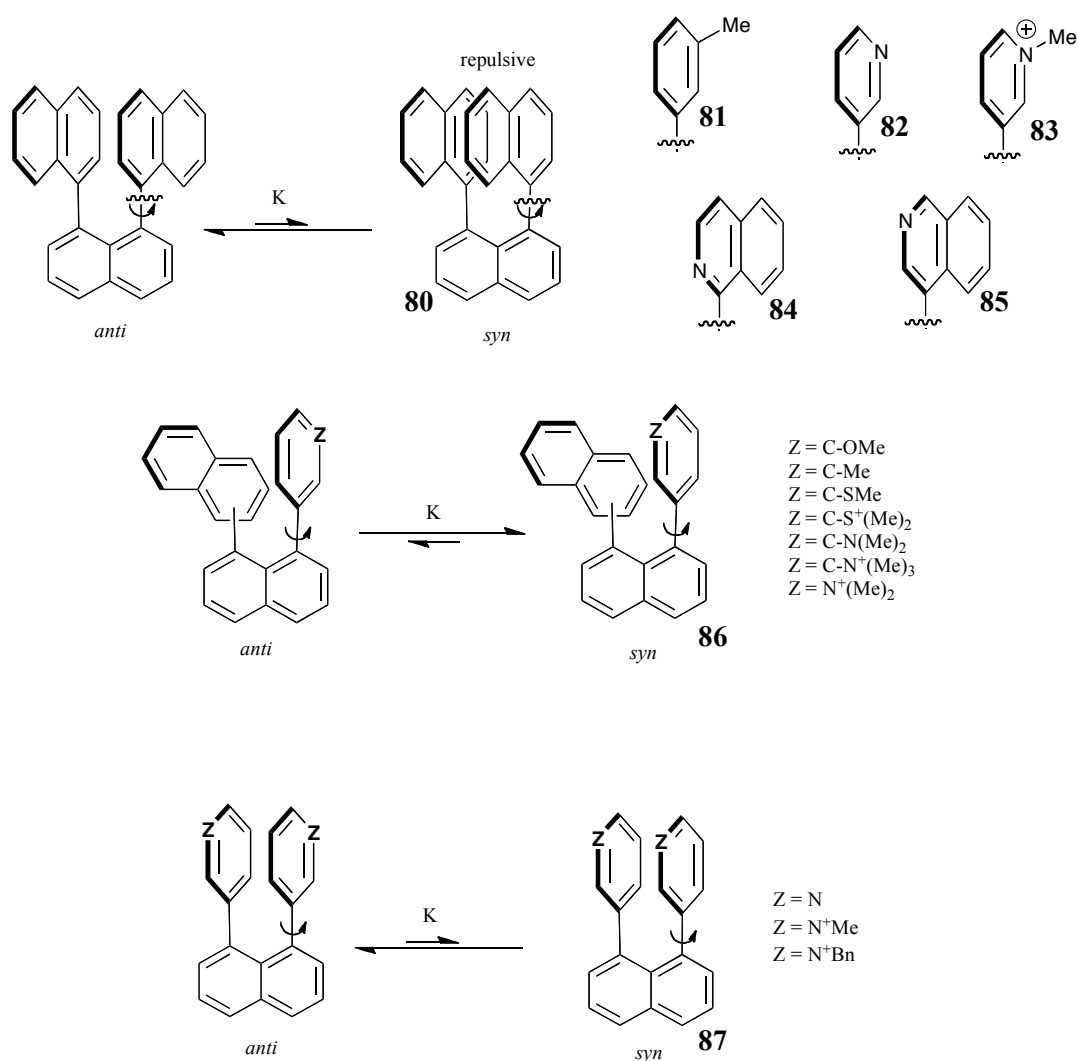


**Figure 32** Series of molecular balance systems based on a 1,8-diarylnaphthalene framework, utilised by Zoltewicz and co-workers

A different approach to studying the interactions was applied. All the derivatives prepared displayed *syn* or *anti* isomers, so information about the arene interactions was extracted from the population ratios calculated by NMR spectroscopy. The pyridyl derivatives **86** and **87** allowed for a study of cation- $\pi$  interactions. A preference for the *syn* isomer and a large upfield shift of the methyl group attached to the nitrogen atom in  $^1\text{H}$  NMR spectroscopy was reported hence indicating the presence of an interaction between the nitrogen centered cation and the aromatic ring.

Using a similar class of rotameric compounds, Rashkin and Waters were able to study arene interactions not only in organic solvents but also in aqueous solution.<sup>114,115</sup> The off-set stacking nature of various *meta* and *para* substituted N-benzyl-2-(2-fluorophenyl)-pyridinium bromides **88** was investigated (Figure 33).

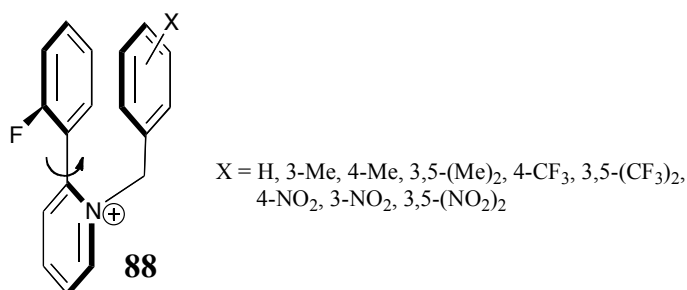


**Figure 33** Rotameric derivatives studied by Rashkin and Waters

Dynamic NMR experiments were used to determine the barrier to rotation around the biaryl bond. As with the previous examples the arene interaction is disrupted by rotation about this bond and hence the barrier to rotation allows for the relative strengths of arene interactions with different substituted aromatic rings to be determined. This system displays only a small variation in the barrier to rotation when varying the substituent. However, as expected, electron withdrawing groups lead to an increased barrier to rotation. Interestingly, they reported that *meta* substituents displayed a larger barrier to rotation than *para* substituents. As both derivatives have a similar amount of electron density on the face ring it cannot be due to change in electron density of the ring. Rashkin and

Waters suggested that an attractive interaction between an edge hydrogen and the electron withdrawing substituent can explain this difference in barrier rotation energy. These findings have been supported by  $^1\text{H}$  NMR chemical shift data and computer modeling.

Developing from earlier qualitative work, in 1997 Gellman *et al.* reported the use of a series of folding molecules **89-92** for quantifying arene-arene interactions.<sup>116,117</sup> The system was designed in such a way that the bond rotation was slow enough to be observed on the NMR time scale and included a carboxylic acid group which can be modified to allow for aqueous solubility (Figure 34). Dynamic NMR experiments were used to determine the *E*:*Z* rotamer ratio in  $\text{CDCl}_3$  and  $\text{D}_2\text{O}$ . In the *E* conformation the aromatic rings are in close contact and are forced into a stacked arrangement and in the *Z* conformation the aromatic rings are far apart.

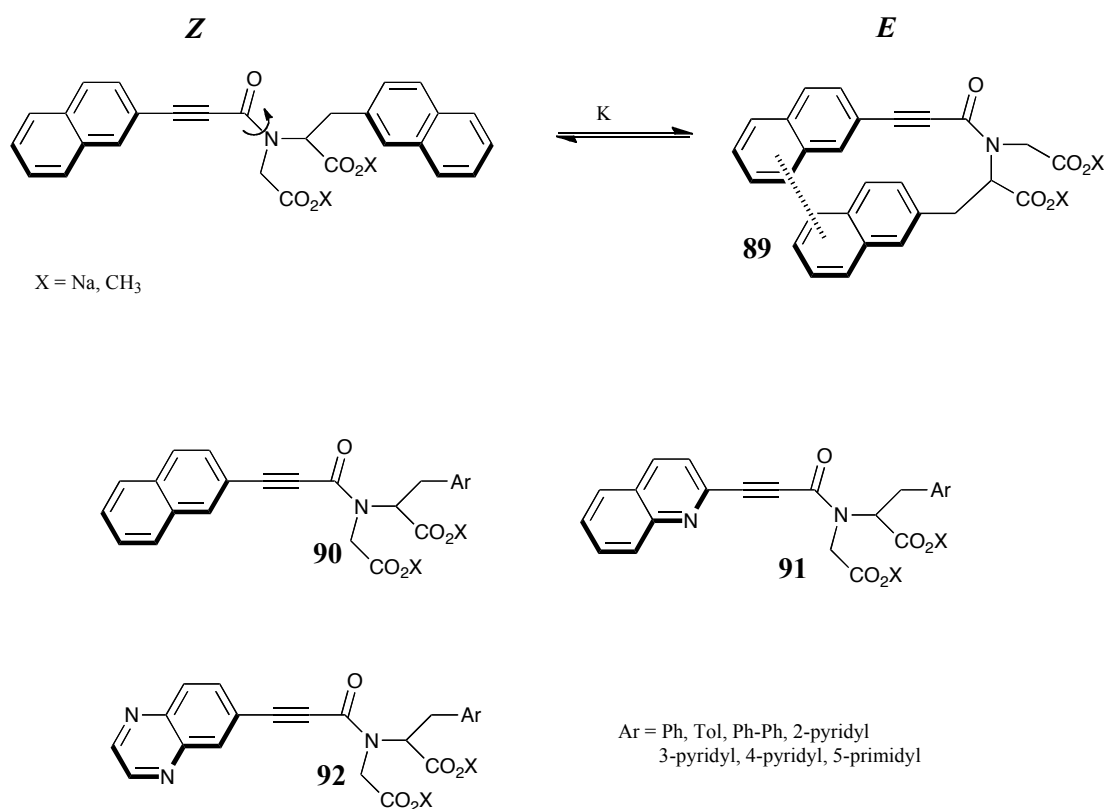


**Figure 34** Series of folding molecules used for studying arene-arene interactions

From initial studies it was proved that an interaction occurs between various substituted phenyl rings and a naphthyl group in both chloroform and water.<sup>118</sup> The terminal aromatic group is free to rotate and as a consequence a twisted propeller conformation of the biaryl compound is observed as the lowest energy conformer. This methodology was later extended to study how this interaction is affected by the introduction of a nitrogen atom into either aromatic ring.<sup>119</sup> These later studies show that the position of the nitrogen atom in the ring affects the conformational ratio and hence the arene-arene interaction.

Building on the early work of Ōki and co-workers, Gung *et al.* used triptycene derivatives **93** to study both face-to-face and offset stacked geometries.<sup>36,120-122</sup> They set out to investigate the contribution of charge transfer effects in aromatic stacking interactions providing more evidence for a polar- $\pi$  model. However no charge transfer bands were observed for any of the mono substituted arenes **93** studied. In the triptycene system two conformational isomers are observed with slow rotation between the two. The *syn* conformer allows for a stacking interaction to occur and the *anti* conformer does not (Figure 35). From the *syn/anti* ratio determined by low temperature NMR studies in various deuterated solvents the free energies of the interaction can be derived.

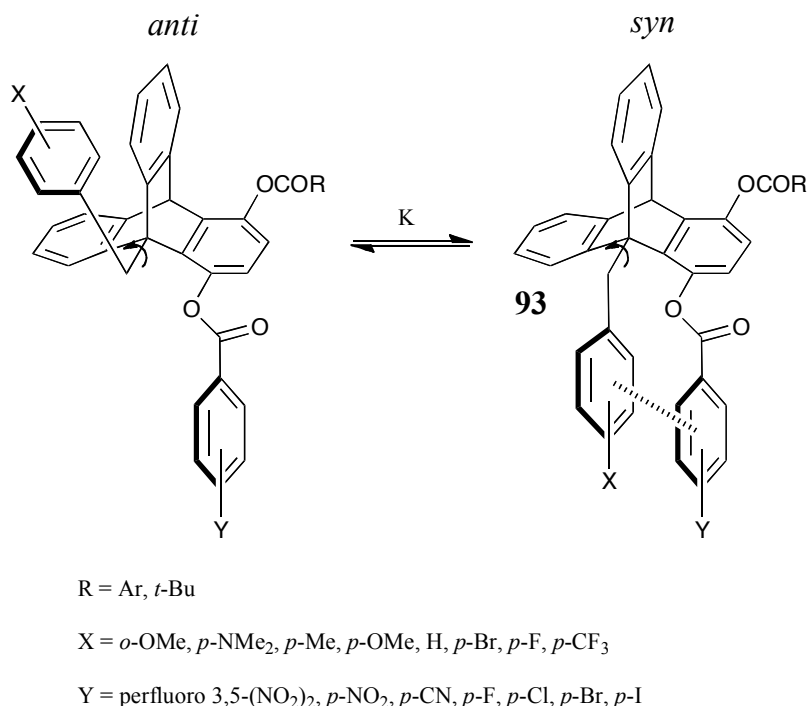


**Figure 35** Conformers of the triptycene based molecular balances, used for studying arene-arene interactions

From computer modeling it was determined that with no interaction present a 2:1 *syn/anti* ratio is expected. Therefore a *syn/anti* ratio of more than 2:1 represents an attractive interaction and a *syn/anti* ratio of less than 2:1 represents a repulsive interaction. When X or Y are electron withdrawing groups the interactions are attractive and when the arenes bear electron donating groups the interaction energy is either slightly repulsive or negligible. Their work was extended to study the interaction between an aromatic ring and a pyridine or pyrimidine ring (Figure 36).<sup>123</sup>

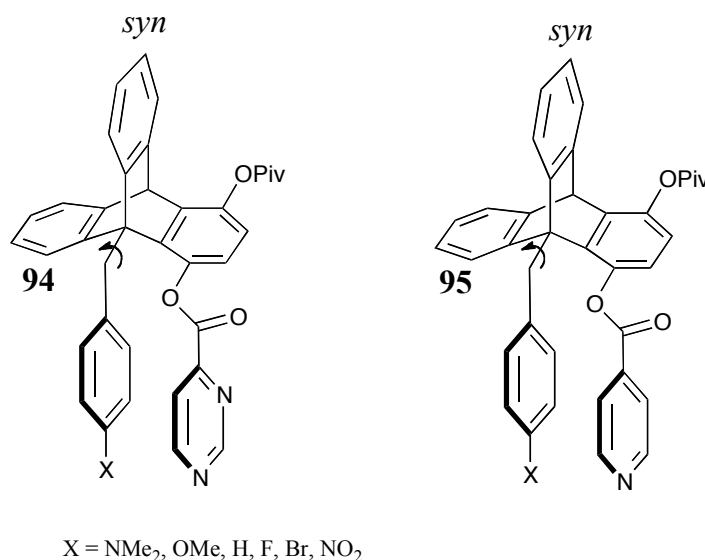


**Figure 36** Triptycene derivatives used for studying interactions between an aromatic ring and a pyridine or pyrimidine ring

Compared to derivatives **93** with an unsubstituted aromatic ring, the heterocyclic derivatives **94**, **95** displayed higher *syn/anti* ratios and hence more attractive interactions between the arene rings. However, in general the substituent effect is far less pronounced for these derivatives **94**, **95**. An X-Ray crystal structure for the substrate with a pyrimidine ring and a bromide as the X substituent was obtained and the *anti* conformation is adopted in the solid state. However, in solution, the *syn* conformation is observed almost exclusively. This highlights the importance of studying  $\pi$ -interactions in both solution and solid state.

Recently Cozzi *et al.* used model systems **96** and **97** based on the [3,3]metaparacyclophane skeleton to study edge-to-face interactions between unsubstituted benzene and fluorinated benzene rings and a pyridine, thiophene or furan ring.<sup>124,125</sup> The energy barrier to topomeric flipping of the *meta*-substituted ring was measured by variable temperature NMR studies (Figure 37) and DFT calculations were used as a predictive tool.



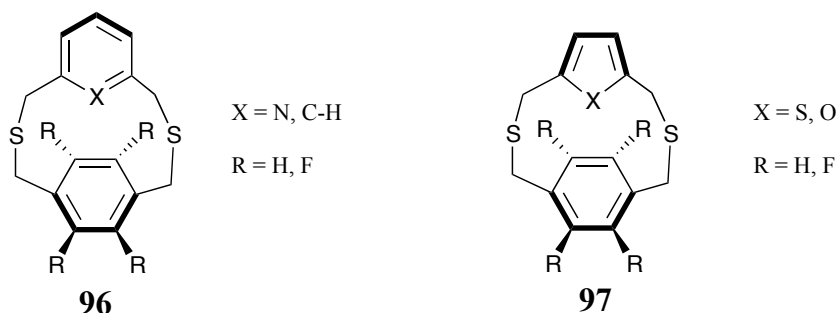


**Figure 37** Topomeric compounds designed by Cozzi *et al.* to measure edge-to-face interactions

Fortunately, the same trends were shown in the experimental NMR data as were predicted by calculations. When comparing the pyridine and benzene derivatives it was found that in all cases the highest barriers to topomerisation were observed for the pyridine derivatives, implying that the interaction is stronger with a pyridine ring. As expected, higher barriers were observed for the fluorinated substrates, in all the series studied. However, the results are difficult to interpret as DFT calculations reveal that, despite similarities in structure, the derivatives prepared, depending on the heterocycle employed, undergo different types of isomerization and have complicated energy landscapes. This prevented a quantitative comparison of the various cyclophane systems **96-97**. A remarkable difference between the furan and thiophene systems was shown, for the furan system an O/ $\pi$  interaction occurs in the ground state, but for the thiophene system the only conformation that allows for an S/ $\pi$  interaction is a high-energy state. This difference was attributed to steric hindrance arising from the large sulphur atom.

### 1.5.3.2 X-H/ $\pi$ interactions

There are fewer examples of molecular torsion balance systems used to quantify X-H/ $\pi$  interactions. The use of triptycene derivatives for studying arene interactions was first reported by Ōki and co-workers in 1976.<sup>63,120</sup> The

compounds **98-99** shown in Figure 38 were synthesised to study C-H/ $\pi$  and halogen or oxygen/ $\pi$  bonds and the X, Y and Z groups were varied.

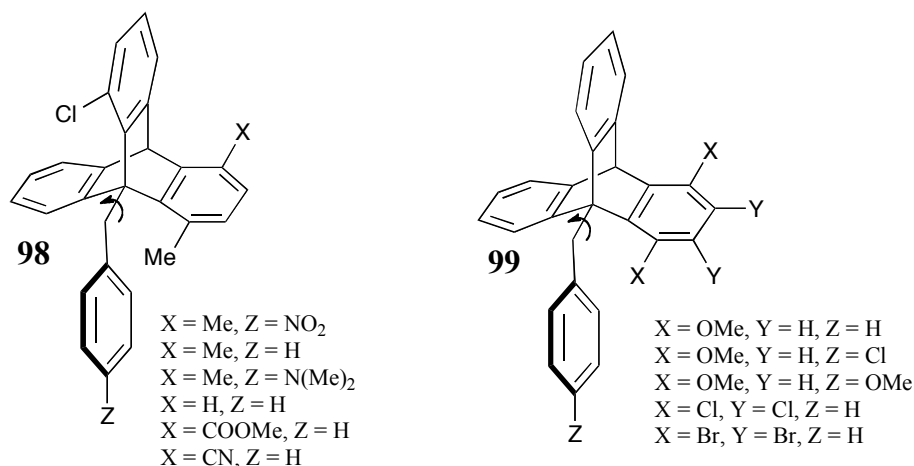


**Figure 38** Triptycene derivatives synthesised by Ōki and co-workers, for studying various non-covalent interactions with aromatic rings

As discussed previously, interactions were studied in CDCl<sub>3</sub> by using NMR to determine the population ratios of the rotamers of the triptycene derivatives. For substrates where X was a methoxy group the population ratio was over the statistical value indicating that an attractive interaction occurred. However, when X was a halogen, a repulsive interaction occurred as the population ratio was below the statistical value. When studying C-H/ $\pi$  interactions it was found that varying the nature of the Z substituent affected the population ratios. The highest ratio was observed for the diethylamino substrate, as this gave rise to the most electron rich aromatic ring.

Following on from their earlier work studying  $\pi$ - $\pi$  interactions, Gung *et al.* modified the triptycene system by replacing an aromatic ring with esters and ethers **100** (Figure 39, Figure 40).<sup>126</sup> Their aim was to quantify the lone pair- $\pi$  interaction which they had previously observed. For this they developed two series of compounds, one to study oxygen/arene interactions **101** and another **102** for studying methoxymethyl/arene interactions. From low temperature NMR studies in CDCl<sub>3</sub> it was found that the majority of the derivatives prepared

showed a preference for the folded *syn* conformer, indicating that an interaction occurs. Both series of substrates also showed a well-defined substituent effect with the strength of the interaction increasing with electron withdrawing groups.

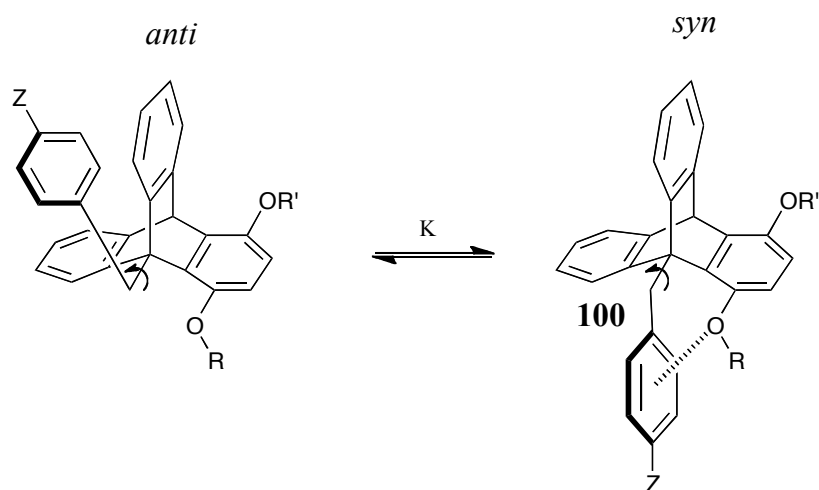


**Figure 39** Conformers of the triptycene balance system, only the *syn* conformer allows for an interaction between the aromatic ring and oxygen atom to occur

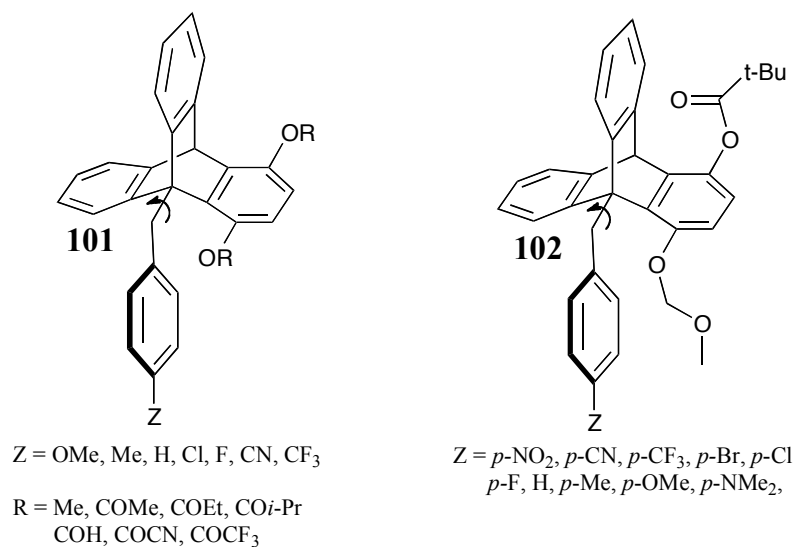


**Figure 40** Series of triptycene derivatives prepared by Gung *et al.* for studying lone pair/ $\pi$  interactions

However, these substrates allow high degrees of conformational freedom and multiple points of contact, which makes interpretation of the results complicated. It is not clear whether the interaction is between an oxygen atom or a CH group and the aromatic ring.

Recently, Cornago reported the use of a molecular balance system **103** based on NH-pyrazoles bearing a benzylphenyl group, to measure the strength of N-H/ $\pi$  hydrogen bonds (Figure 41).<sup>127</sup>

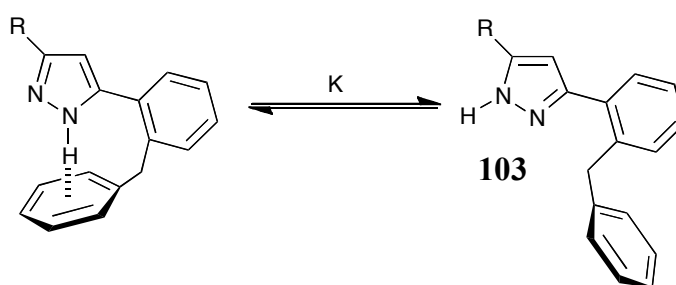


**Figure 41** Molecular balance system for studying N-H/ $\pi$  interaction

This pyrazole system **103** exists in two tautomeric forms and the position of the tautomeric equilibrium was determined by NMR studies in a range of solvents. DFT calculations were also performed to determine the differences in energy for a wide range of substituted pyrazoles. The interaction was found to be strengthened by electron withdrawing groups. When  $R = CF_3$  the tautomer which allows for an interaction, was observed in abundance for each solvent studied. From these preliminary results it was confirmed that the system can be used as a molecular balance to determine the electronic effects of substituents on the strength of such an intramolecular N-H/ $\pi$  hydrogen bond.

### 1.5.3.3 Cation/ $\pi$ interactions

Despite the biological importance of these interactions very few examples of molecular torsion balances being used to study them exist in the literature. Continuing their work on arene-arene interactions, Rashkin and Waters modified the rotameric substrates **104** to study the interaction between phenyl rings and a pyridinium ring in water (Figure 42).<sup>115</sup>

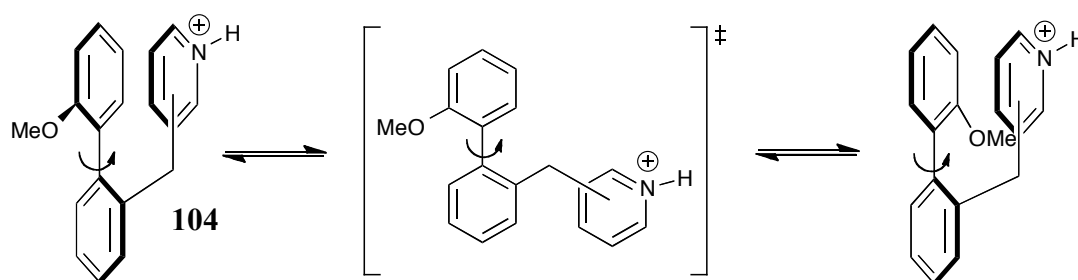


**Figure 42** Molecular balance system for studying interaction between aromatic ring and pyridinium ring in aqueous solution

The design of the system **104** allows for the phenyl and pyridinium ring to align in an offset-stacked arrangement. The position of the nitrogen atom in the pyridinium ring was varied as this affects the overlap of the  $\pi$ -cloud with the anisole system. For each compound, the favoured conformation is the stacked geometry, and evidence for this was provided by comparing the aromatic shifts with those of unstacked control compounds. The largest relative strength of interaction was found for the compound with the nitrogen atom in the *ipso* **105** position followed by the *ortho*, *meta* and *para* substrates (Figure 43).

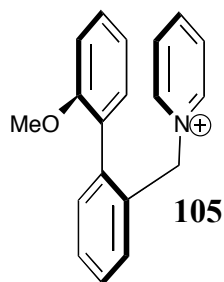


**Figure 43** Derivative **105** which displays the largest relative strength of interaction in the series of molecular balances studied

Upon methylation of the nitrogen atom only very small changes in the strength of the stacking interaction occurred, possibly indicating that the positive charge is delocalized across the entire aromatic surface and the interaction occurs between the surfaces of the two aromatics.

## 1.6 Other methods for studying $\pi$ -interactions

Although molecular torsion balances offer a unique and elegant approach to studying non-covalent interactions, their use is by no means abundant in the current chemical literature. This is most likely due to the difficulties encountered both in the design and synthesis of an efficient molecular torsion balance system. Molecular recognition, double mutant cycles, biological systems and organic reactions are far more commonly employed methods for studying non-covalent  $\pi$ -interactions. Consequently, there is a vast number of such studies in the literature but only a few key examples will be examined in this section.

### 1.6.1 Molecular recognition

Supramolecular recognition in solution is a well established method for studying binding affinities. An insight into the importance of  $\pi$ -interactions can be gained

from systematic studies of the complexation of substrates with a designed receptor in aqueous or organic solvents. These studies have been extensively reviewed.<sup>4,6</sup> Cyclophanes are an important class of synthetic receptor and their complexation chemistry has been thoroughly investigated by Diederich *et al.*<sup>76</sup> In 1986 they reported the use of the designed host-guest complex **106** for quantitative studies of  $\pi$ - $\pi$  interactions (Figure 44).<sup>77</sup>

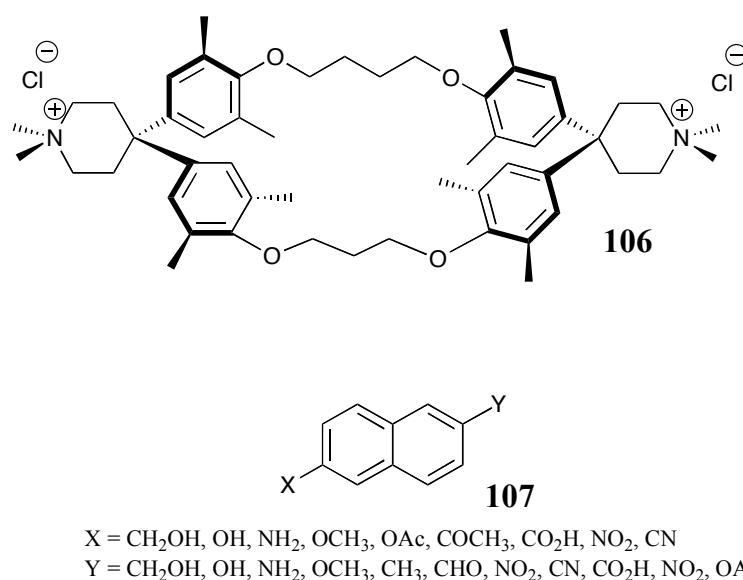


**Figure 44** Synthetic receptor and a range of naphthalene derivative guest molecules

The strength of complexation between the macrocycle host **106** and a range of disubstituted naphthalene derivatives **107** was compared. It was determined from NMR studies in deuterated methanol, that all of the guests form 1:1 complexes with the host as a shift in the <sup>1</sup>H NMR spectra of the naphthyl protons was observed. The hosts prefer to adopt a pseudo-axial geometry in the cavity, thus allowing for  $\pi$ - $\pi$  interactions between the guest and host molecules to occur. The naphthyl protons are arranged in an edge-to-face arrangement with the four aromatic rings in the receptor molecule. From these initial studies it was found that electron deficient guest molecules formed the most stable complexes, emphasising the importance of polar contributions to these interactions. Studies of similar guest-host complexes in aqueous solution and several other organic

solvents were also conducted, including extensive studies with a pyrene guest which exhibited very strong solvent dependency.

Molecular tweezers are a very useful and highly adaptable form of molecular receptor. They can be designed to complex a wide range of guest molecules and have been successfully used to study a considerable number of non-covalent interactions. Klärner and co-workers have extensively investigated the use of molecular tweezers as synthetic receptors.<sup>129-131</sup> By way of example, molecular tweezers containing either benzene **108** or naphthalene **109** spacer units were prepared and selective binding of electron deficient, neutral and cationic aromatic substrates could then be compared in solution (Figure 45).<sup>129-131</sup>

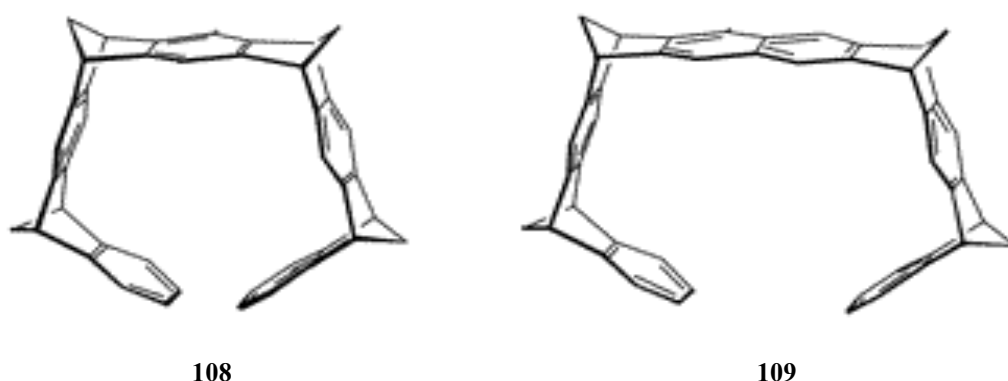


**Figure 45** Structures of the molecular tweezers used as receptors for aromatic substrates

To complement the experimental work, computational studies were undertaken to determine the electrostatic potential surfaces for both the concave and convex faces of the molecular tweezer systems. The results show that the interior of the tweezers has a considerably larger negative potential than the exterior and this explains the high preference for binding electron deficient aromatics in the cavity.



### 1.6.2 Double mutant cycles

Thermodynamic double mutant and triple mutant cycles offer a powerful and elegant method for quantifying non-covalent interactions. Their use in proteins for quantifying non-covalent interactions has now become standard practice and their use in synthetic chemical systems is becoming ever more popular.<sup>132</sup> By cancelling secondary effects in a cycle, thermodynamic information about a major non-covalent interaction can be extracted. Hunter and co-workers have used this methodology to measure the free energy of a wide range of arene interactions, including  $\pi$  stacking, edge-to-face, arene-cation, arene-halogen and arene-carbohydrate interactions.<sup>37,133</sup> One of their earliest double-mutant cycles developed for studying edge-to-face aromatic interactions is shown in Figure 46.

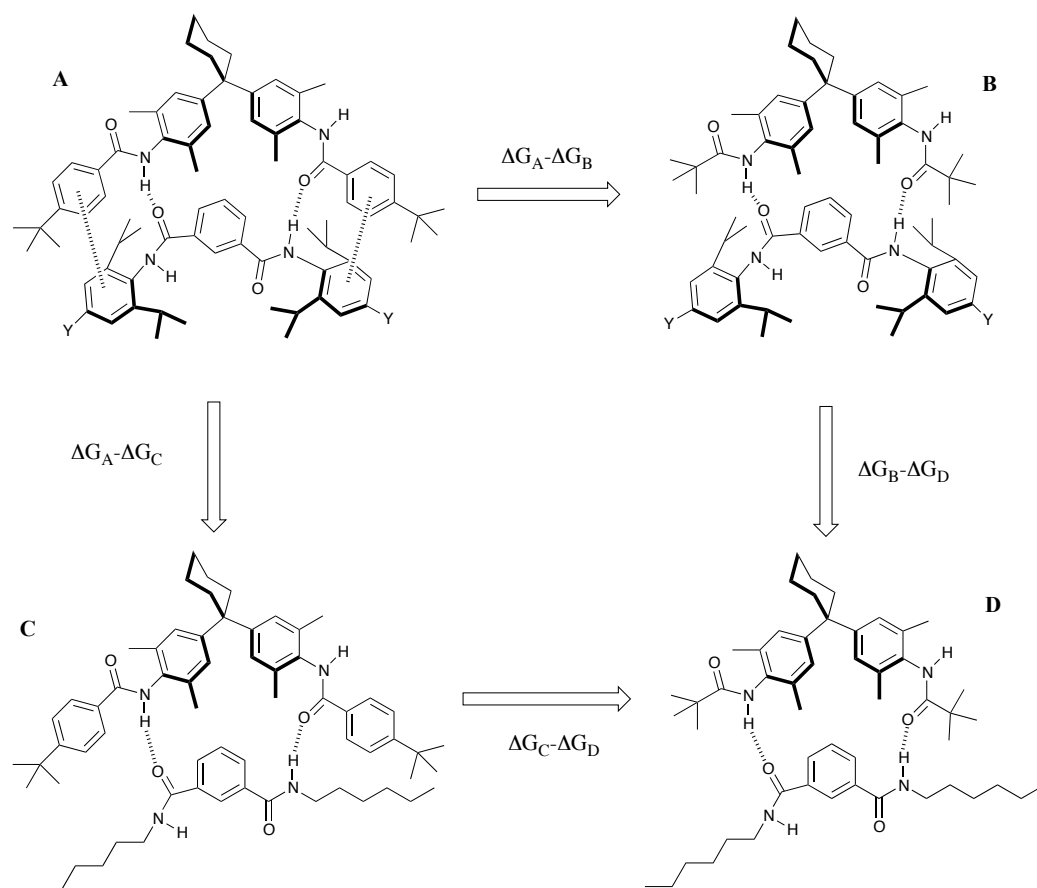


**Figure 46** A double-mutant cycle used for studying edge-to-face aromatic interactions<sup>133d</sup>

The system is based on molecular zipper complexes that in CDCl<sub>3</sub> form a combination of edge-to-face aromatic interactions and hydrogen bonds. By small synthetic changes in either unit of the complex the interactions can be manipulated. For each complex A to D the binding constants and complexation free energies are determined by <sup>1</sup>H NMR titrations, and then, by using the formula shown below, the free energy for the edge-to-face aromatic interactions can be determined (Equation 2).

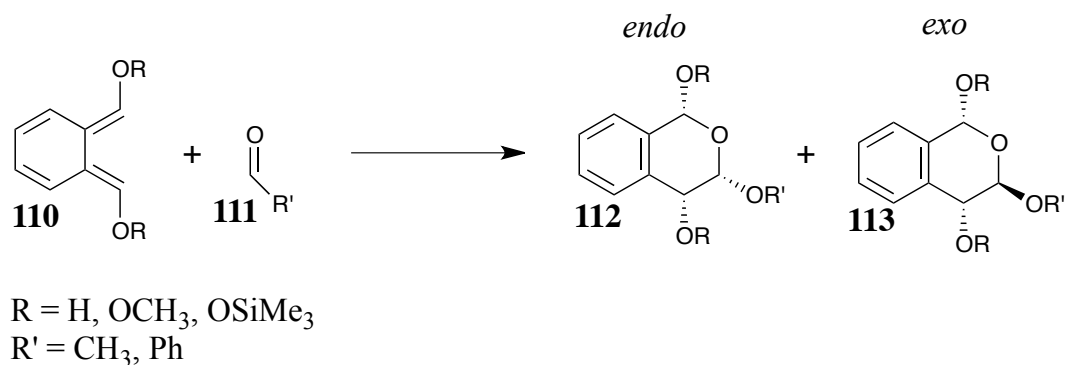
$$\begin{aligned}\Delta\Delta G_{(\pi-\pi)} &= (\Delta G_A - \Delta G_B) - (\Delta G_C - \Delta G_D) \\ &= (\Delta G_A - \Delta G_C) - (\Delta G_B - \Delta G_D)\end{aligned}$$

Equation 2

The geometries of the complexes have also been determined by using dynamic NMR experiments. By changing the Y group the substituent effect was also investigated, and this was shown to have a dramatic effect on the magnitude of the interaction energy hence highlighting the electrostatic nature of these interactions.

### 1.6.3 Organic reactions

The role of  $\pi$ -interactions, in particular the C-H/ $\pi$  interaction, in the stereoselectivity of organic reactions offers a novel insight into these interactions. However this topic has been extensively reviewed and as a consequence an in depth discussion of this topic is not necessary.<sup>134</sup> C-H/ $\pi$  interactions have been shown to influence the stereoselectivity of Diels-Alder reactions,<sup>135</sup> catalytic enantioselective reactions,<sup>136</sup> photochemical reactions<sup>137</sup> and reactions involving transition metal complexes.<sup>138</sup> Recently it has been shown that the cation/ $\pi$  interaction can also be applied to organic synthesis by using it to control regio- and stereoselectivities.<sup>139</sup>



**Scheme 2** Diels-Alder reaction of *o*-xylylene with acetaldehydes used to study non-covalent arene interactions

Houk and co-workers studied the Diels-Alder reaction of *o*-xylylene **110** with acetaldehydes **111** (Scheme 2).<sup>140</sup> They showed that the high *endo* selectivity can be attributed to the formation of a C-H/ $\pi$  interaction in the transition state **114** of the reaction (Figure 47).

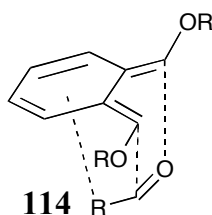


**Figure 47** Transition state of the Diels-Alder reaction studied by Houk *et al.*

## 1.7 Non-covalent interactions involving alkene $\pi$ systems

### 1.7.1 Definition and physical properties

As previously mentioned, the chemical literature on interactions involving olefinic  $\pi$  sources is very limited and they are overshadowed by arene interactions. As a result, little is known about their physical origin, however, double bonds are a common structural motif and reports of their involvement in non-covalent interactions are becoming increasingly frequent.

In 2001 Kim et al. published the results of a high level theoretical investigation into the nature of olefinic and aromatic H- $\pi$  interactions.<sup>141</sup> Using *ab initio* calculations they studied the interactions of ethene and benzene complexes with  $\text{BH}_3$ ,  $\text{CH}_4$ ,  $\text{NH}_3$ ,  $\text{H}_2\text{O}$  and  $\text{HF}$ . For both benzene and ethene, the geometries observed for the complexes with  $\text{BH}_3$  do not allow for a B-H/ $\pi$  interaction to occur. The optimised geometries of the complexes studied are shown in Figure 48.

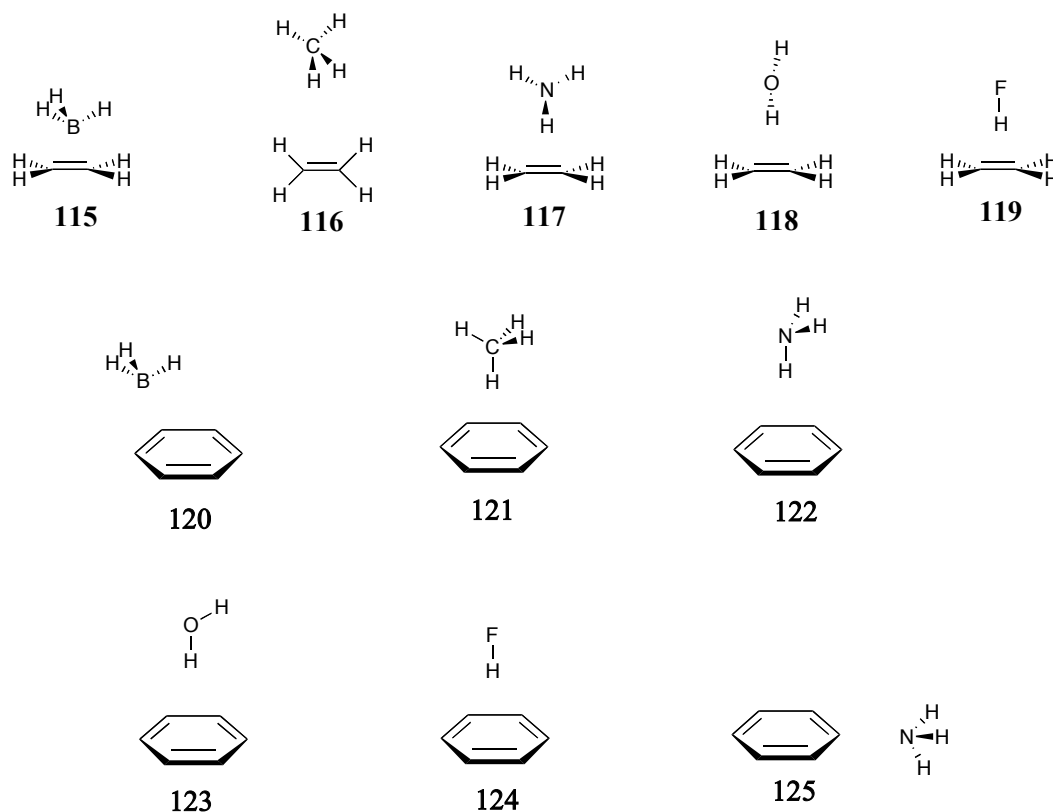


**Figure 48** Optimised geometries of the benzene and ethene complexes studied

On progressing from CH<sub>4</sub> to HF, the strength of the interactions increases and this cannot be explained purely by electrostatic principles, indicating that contributions from other attractive forces, such as dispersion and induction are important for the binding energy of these interactions. For the benzene-NH<sub>3</sub> complex, two optimised geometries are observed. One, in which NH<sub>3</sub> acts as a proton donor **122**, and another in which it acts as a proton acceptor **125**. When compared to the corresponding benzene complexes, ethene complexes have lower binding energies indicating that, in general, the olefinic  $\pi$ -H interactions is weaker than the aromatic  $\pi$ -H interaction. It was reported that for ethene complexes the electrostatic contribution to the total attractive energy is less than 50% and does not vary significantly with the substrate. However, the contribution from induction energy varies from around 20% for the complex with NH<sub>3</sub> **117** to nearly 40% for the complex with HF **119**. It has been suggested that this variation can be attributed to the increased distortion of the electron density of the olefinic  $\pi$  cloud for the HF complex. It was also reported that the binding

energy of the H<sub>2</sub>O ethene complex **118** is almost half that of the water dimer. This study provides some valuable insights into the nature of olefinic  $\pi$ -interactions and indicates that one of the major differences in olefinic and aromatic  $\pi$ -interactions is that the geometries observed arise as a consequence of the distinctly different electron density profiles of the two  $\pi$  systems. However, this study also highlights the need for experimental work in this area.

### 1.7.2 Olefinic $\pi$ -interactions in organic molecules

In 1970 Baker and co-workers observed an O-H/ $\pi$  interaction when studying bicyclo[3.2.2]nona-6,8-dienes. Infrared dilution studies of compound **126** showed that, in contrast to the other alcohols studied which exist as a mixture of conformers, tertiary alcohol **126** exists as one conformation thus suggesting the presence of a strong OH/ $\pi$  interaction (Figure 49).<sup>142</sup> However the group conducted no further studies on this finding.

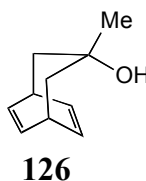
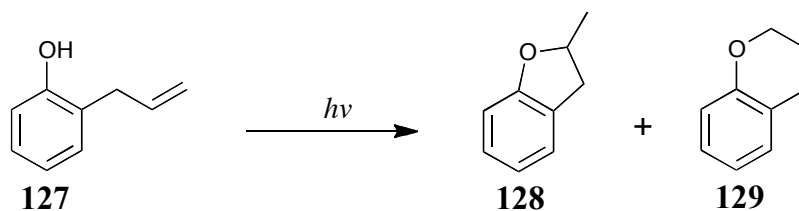


**Figure 49** Bicyclo[3.2.2]nona-6,8-diene studied by Baker and co-workers

The mechanism of photocyclisation of 2-allylphenol **127** was initially proposed by Schmid and Horspool in 1967 and remains essentially valid today (Scheme 3).<sup>143</sup> It is believed that an intramolecular hydrogen bond between the double bond and the hydroxyl group plays a key role in the mechanism.



**Scheme 3** Photocyclisation of 2-allylphenol

As a consequence, the conformational analysis of 2-allylphenol **127** has been undertaken by several groups including those of Baker and Shulgin,<sup>144-145</sup> Ōki and Iwamura,<sup>146</sup> Schaefer,<sup>147</sup> Kim,<sup>148</sup> Berdyshev.<sup>149</sup> The conclusive evidence is that the most stable conformer has a closed structure **130** which is stabilized by O-H/ $\pi$  interactions (Figure 50).



**Figure 50** Open and closed conformers of 2-allylphenol

In order to investigate the nature of these interactions Miranda *et al.* have performed various theoretical and spectroscopic studies on a range of unsaturated phenols **132** (Figure 51).<sup>150</sup>

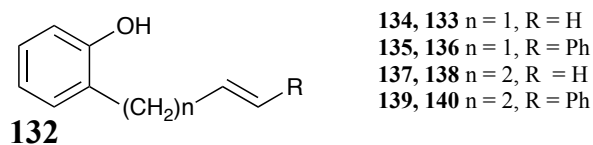


**Figure 51** Series of unsaturated phenols studied by Miranda *et al.*

*Ab initio* calculations were used to determine the optimized conformational structures and the associated energies of these geometries for each compound studied (Figure 52). For substrates with  $n = 1$  the most favourable structures have folded geometries (**134** and **136**) which allow for an O-H/ $\pi$  interaction and when  $n = 2$  a splayed geometry (**137** and **139**) which does not allow for O-H/ $\pi$  interactions is preferred. This is likely to be the result of opposing contributions from the favourable O-H/ $\pi$  interaction and an unfavourable conformational strain arising from the alkene and hydroxyl groups. For the substrates where  $n = 2$  the O-H/ $\pi$  interaction is not strong enough to overcome the conformational strain. Frequency analysis was used to study the nature of the O-H/ $\pi$  interaction and revealed that the interaction is electrostatic in origin. In order to eliminate the possibility of intermolecular interactions the substrates were studied by infrared spectroscopy in the gas phase. The results are in accordance with the computational study. For substrates where  $n = 1$ , two bands are observed in the OH stretching region, corresponding to the free OH and the intramolecularly associated OH. For substrates where  $n = 2$  only one band was observed, which corresponds to the free OH. These findings provide valuable insights into the nature of the O-H/ $\pi$  olefinic hydrogen bond and reveal some similarities to arene interactions.



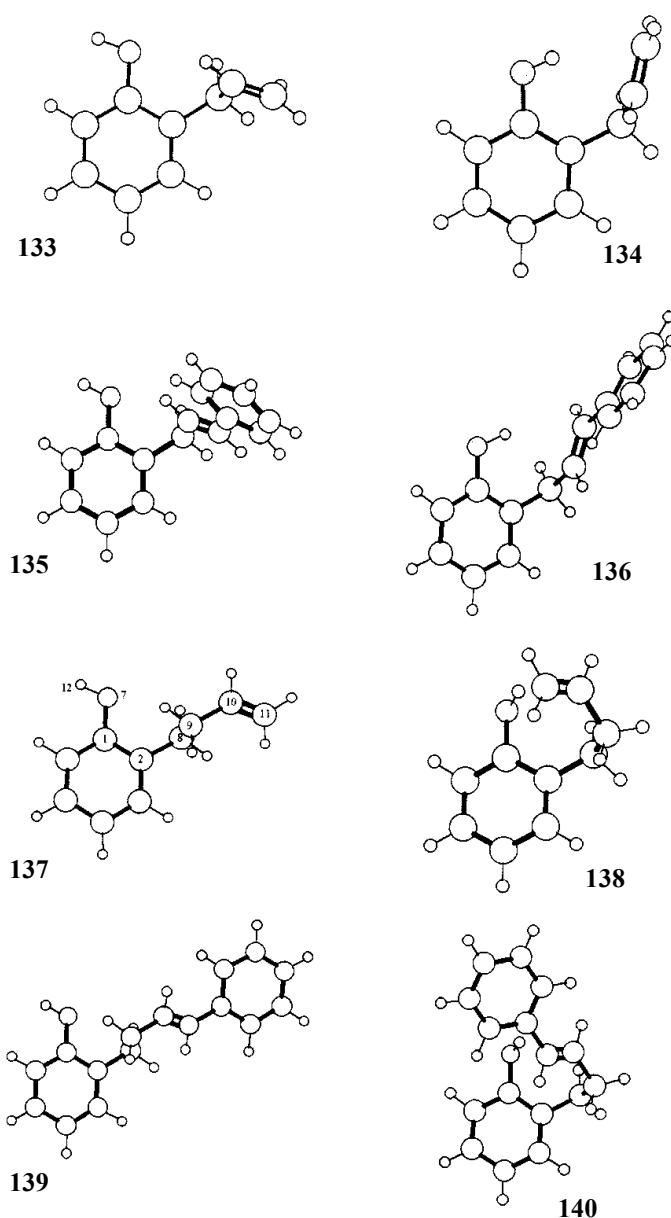


**Figure 52** Various geometries of the unsaturated phenols studied by Miranda *et al.*

Using a similar approach, Miranda and co-workers also confirmed the presence of N-H/ $\pi$  interactions in a series of tetrahydroquinoline compounds **141** (Figure 53).<sup>151</sup> DFT calculated energies were found to be between 2.0 and 2.5 kcal mol<sup>-1</sup> more stable for a folded conformer, in agreement with a favourable N-H/ $\pi$  interaction.

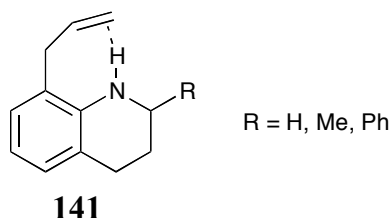


**Figure 53** Tetrahydroquinoline compounds which display N-H/ $\pi$  interactions

In addition to the previous example, Rademacher and co-workers have also extensively studied O-H/ $\pi$  hydrogen bonding in allylphenols.<sup>152</sup> A combination of computational and spectroscopic methods were used to study 4-substituted 2-allylphenols (Figure 54). Due to conformational mobility, all the compounds studied can exist in an open **142** and closed **143** conformer, but the O-H/ $\pi$  hydrogen bond can only occur in the closed conformer. Varying the substituent X enabled the study of the substituent effects on the intramolecular O-H/ $\pi$  interaction.

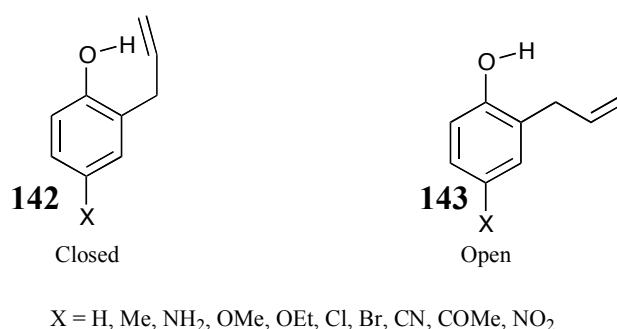


**Figure 54** Conformers of 4-substituted 2-allylphenols studied by Rademacher *et al.*

For 2-allylphenol **127** it was found that the closed conformer was 3.58 kJ mol<sup>-1</sup> more stable than the open form. For all of the substituted 2-allylphenols a preference for the closed conformer was also found but with varying energy differences. As expected on the basis of enhanced acidity, the interaction was strengthened by electron withdrawing substituents and weakened by electron

donating substituents. The compounds were also studied by photoelectron spectroscopy and the results correlated well with the theoretical study.

Chow *et al.* conducted detailed mechanistic studies on the photocyclisation of 2-allyl-1-naphthol **144** and 1-allyl-2-naphthol **145** (Figure 55).<sup>153</sup> It was shown that in accordance with the earlier studies on 2-allylphenol, both compounds exhibited a hydrogen bonding type intramolecular interaction in the ground state.

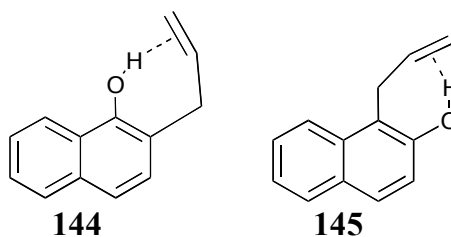


**Figure 55** Intramolecular hydrogen bonding like interaction exhibited by 2-allyl-1-naphthol and 1-allyl-2-naphthol

To gain insight into olefinic C-H/ $\pi$  interaction Tsuzuki *et al.* used high level *ab initio* calculations to study the interaction energies of both ethene and ethane dimers with methane.<sup>154</sup> Although Takagi and co-workers had previously reported calculations on the ethene methane dimer, the basis sets used were considerably smaller and, as a consequence, an analysis of the interaction energies was not possible.<sup>155</sup> The geometries of the ethene-methane dimers **146-152** studied by Tsuzuki *et al.* are shown in Figure 56.

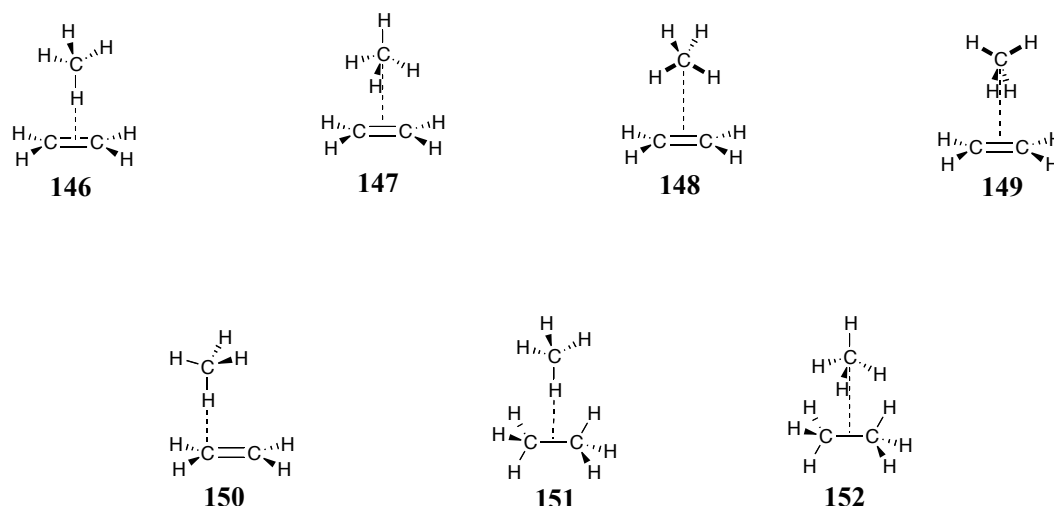


**Figure 56** Geometries of the ethene-methane and ethane-methane dimers studied

Whilst there was no preference for a C-H bond in methane to point to the C-C bond in ethane, the most stable geometry of the ethene-methane complex was found to be dimer **146**. This is indicative of a C-H/ $\pi$  interaction. The calculated interaction energies of the ethene-methane dimers were all of similar magnitude, and the potential energy surface is very flat indicating that the C-H/ $\pi$  interaction in this complex is loose. The results obtained from calculations of the correlation interaction energy indicate that the dispersion energy plays a significant role in the interaction between ethene and methane. It was also reported that the contribution from electrostatic energy is negligible when considering the total interaction energy, but it plays an important role in determining the geometry of the complex.

In a later study Tsuzuki and co-workers calculated the relative energies of the rotamers of various prop-2-enyl ethers in order to investigate the effects of CH- $\pi$  interactions in crownphanes.<sup>156</sup> The optimised geometries of 3-methoxyprop-1-ene **153-157** are shown in Figure 57.

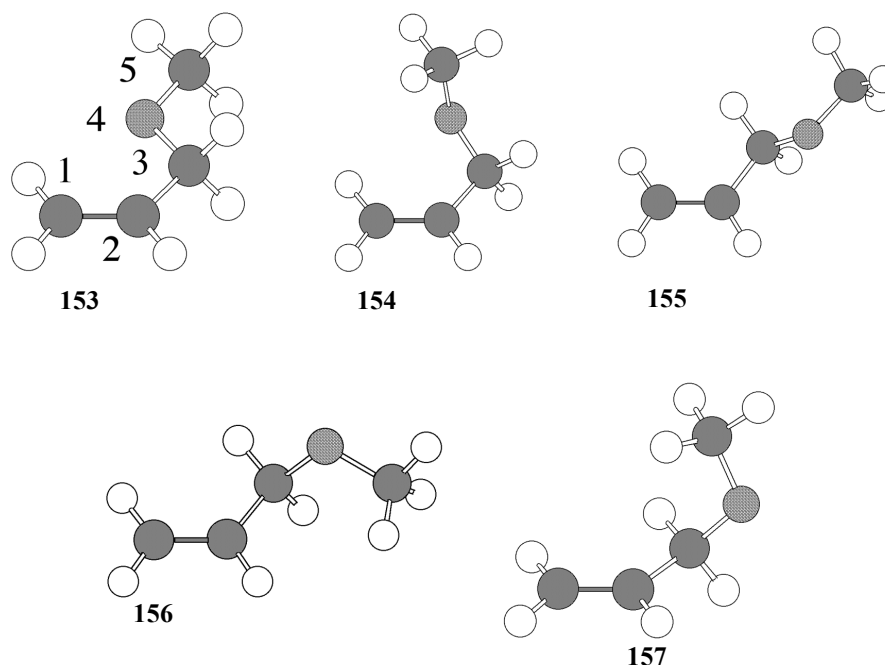


**Figure 57** Optimised geometries of 3-methoxyprop-1-ene as revealed by theoretical studies

The study revealed that the most stable rotamer is **157**, however only a small energy difference between the four rotamers **153**, **154**, **155** and **157** was found. The geometry of rotamer **157** suggests that it is stabilized by an attractive C-H/ $\pi$  interaction as it features a short contact between the double bond and the methyl group.

Roussel *et al.* used several different computational methods to calculate the conformational energy of 1-pentene.<sup>157</sup> Building from the fundamental theoretical work on 1-pentene by Fraser *et al.*, they decided to investigate *syn* **158** and *anti* **160** conformers (Figure 58).<sup>158</sup> The *syn* conformer places a hydrogen atom from the CH<sub>3</sub> group above the double bond and as a result a C-H/ $\pi$  interaction is likely to be present in this conformer.

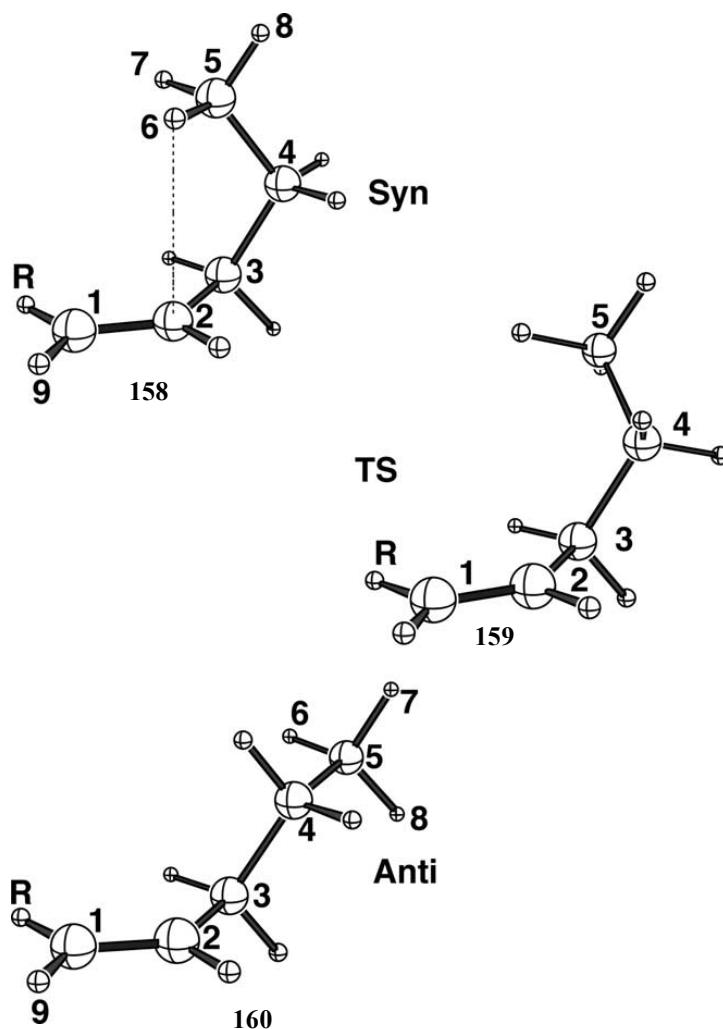


**Figure 58** Conformers of 1-pentene studied by Roussel *et al.*<sup>157</sup>

The *anti* conformer **160** was the most stable conformer, nonetheless the *syn* conformer **158** was only 0.2 kcal mol<sup>-1</sup> less stable. In the case of 1-pentene the weak C-H/ $\pi$  interaction is not strong enough to overcome the unfavourable steric requirements.

It is clear that there are several prominent examples of olefinic  $\pi$ -interactions in the current chemical literature and they are frequently studied in small organic molecules by computational and spectroscopic methods. However to the best of our knowledge these have not been studied in any specifically designed systems such as molecular balances or supramolecular systems. There is also very little mention of their impact on biological systems.

## 1.8 Conclusions and perspectives

From the foregoing chapter, it is evident that a significant research effort in the fields of supramolecular chemistry, crystallography database searches, gas-phase studies and theoretical studies, has helped to enrich our understanding of non-covalent  $\pi$ -interactions. Studies on aromatic interactions, have shown how these interactions are governed by electrostatic forces and that aromatic rings are capable of forming hydrogen bonding like interactions with functional groups. Despite the significant amount of research in this area, a set of general rules for non-covalent interactions of aromatic systems is yet to be established. Due to the importance of these interactions in areas such as drug design, biological chemistry and molecular recognition, a detailed understanding of  $\pi$ -interactions is of great interest. Furthermore, the important role of solvation on these interactions is not yet fully understood.

It is evident that the attention of the majority of research in this area, has been directed to aromatic interactions and in comparison very little research effort has been devoted to olefinic  $\pi$ -interactions. Therefore, far less is known about the physical nature of olefinic  $\pi$ -interactions and a significant amount of research remains to be done.

---

## **CHAPTER 2**

# **RESULTS AND DISCUSSION**



The foregoing introductory review has hopefully highlighted the fact that enormous strides have been made, especially within the last decade, to understand many of the factors involved in the vital role played by non-covalent interactions. It is particularly germane to note that considerable efforts have been made to quantify the strength of such interactions, notably as a function of the solvent in which a given measurement is made. Such information cannot be obtained from single crystal X-Ray diffraction studies. These can only indicate “enforced propinquity” which may arise, either from a genuine non-covalent interaction, or from crystal packing forces. It was with such thoughts in mind that the studies within our group were initiated.

## 2.1 Previous studies within our group

Although, as we have seen, considerable research efforts have been devoted towards studying non-covalent arene interactions, due to the difficulty of measuring such small energies, there have been few studies to quantify these phenomena. Even fewer studies exist on non-covalent olefinic interactions. In previous studies within our own group, a system based on 9,10-propanoanthracenes **161** was therefore designed to quantify weak arene-functional group interactions by a dynamic NMR study of conformational equilibria (**Figure 59**).<sup>159-162</sup>

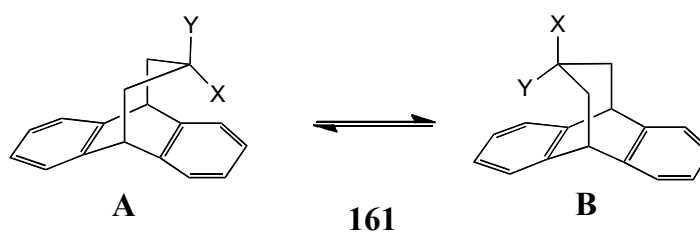


**Figure 59** Conformational equilibrium of the propanoanthracene **161**

The propanoanthracene moiety can be considered as a conformational balance to compare the relative strengths of the interactions of two functional groups, X and Y, and aromatic rings. The framework consists of two independent aromatic systems and a flexible three carbon atom bridge, whose central carbon atom can possess the two different functional groups X and Y. Different substituents on the flexible bridge will affect the conformational equilibrium between **A** and **B**, and the relative abundance of each isomer in solution provides a measure of the relative interaction energies.

NMR experiments were used to quantify the conformational equilibria of this system. The coupling constants between the protons on the 3-membered flexible bridge can be used to calculate the proportion of each conformer in solution. As a result of the fast motion of the flexible bridge, only averaged chemical shifts and coupling constants were observed on the NMR time scale at room temperature.

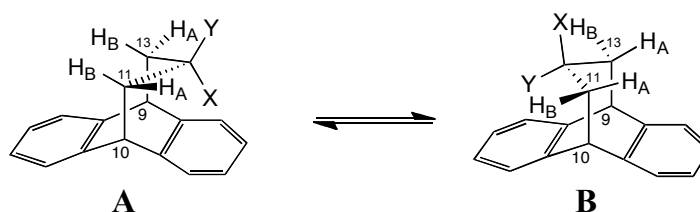


**Figure 60** Detailed structure of the propanoanthracene **161**

Each conformer displays characteristic coupling constants between the protons on the bridge, H<sub>11</sub> and H<sub>13</sub> and those on the bridgehead H<sub>9</sub> and H<sub>10</sub>, and these allow for the population of each conformer **A** and **B** to be determined, if the boundary coupling constants,  $^3J_{10-11A}$  and  $^3J_{10-11B}$  for conformers **A** and **B** are known (Figure 60). These boundary values are the coupling constants found for one conformer in solution, however an exact measurement of these constants was not possible but an estimation can be made. To complement these calculations, NMR experiments at low temperature and in a range of solvents were also conducted.<sup>159,160</sup>

A wide range of functionalised propanoanthracenes were prepared and studied within our group. Figure 61 summarises these functionalised propanoanthracenes and their conformational equilibria in  $\text{CDCl}_3$  solution.

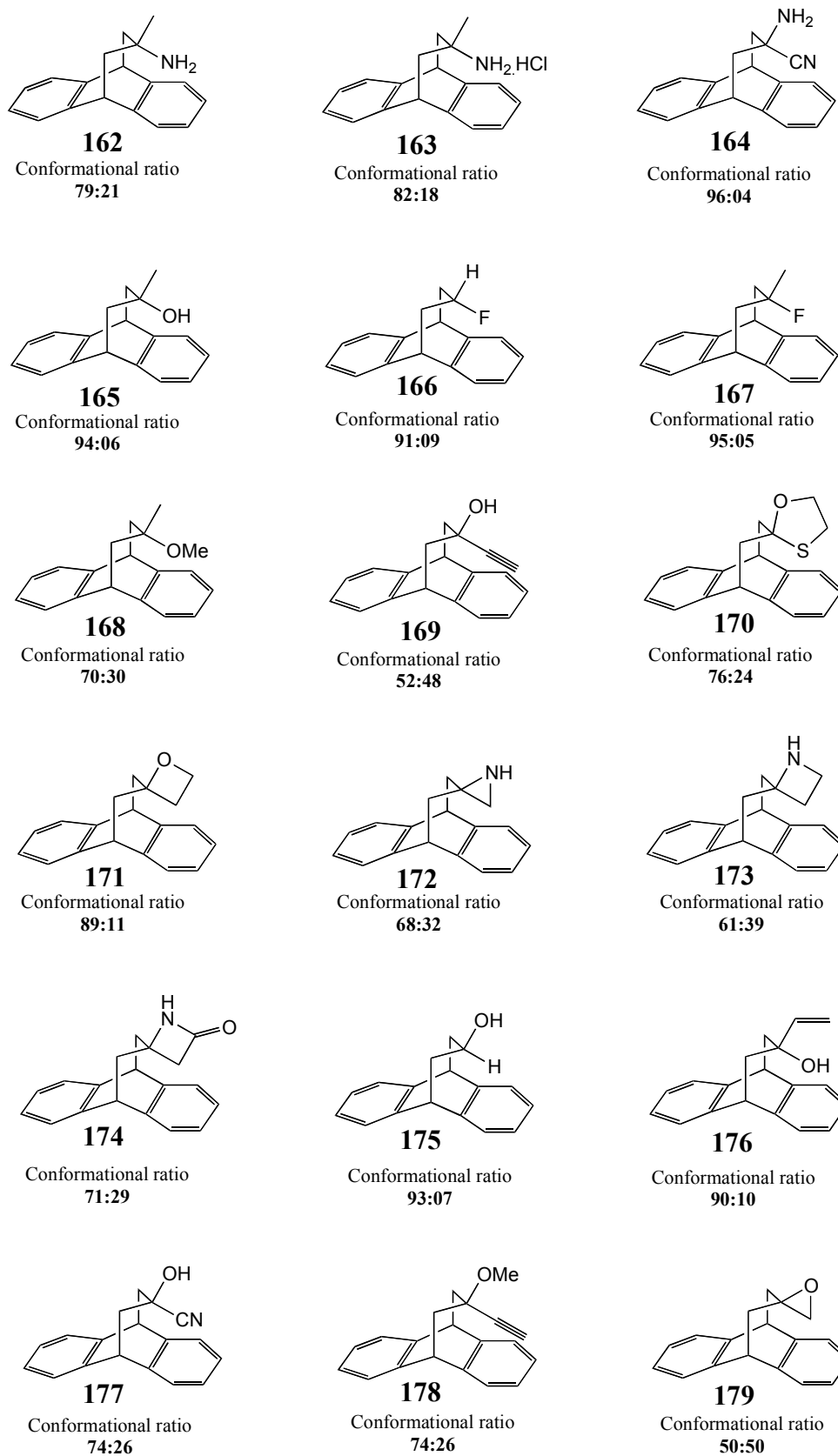


**Figure 61** Major conformation and conformational ratios for the propanoanthracene derivatives in  $\text{CDCl}_3$  at 298 K

## 2.2 Objectives

As established in the foregoing introduction, an area which has often been overlooked is the study of non-covalent olefinic  $\pi$ -interactions and the comparison of these interactions with arene interactions. Accordingly, the primary objective of the present study was to quantify such non-covalent  $\pi$  interactions by dynamic NMR studies of conformational equilibria. Consequently we envisaged that the design and synthesis of a simple molecular balance system featuring alkenes and functional groups would be of great interest. In order to examine these interactions a molecular system with a similar framework to the previously studied propanoanthracene system was selected.<sup>159-162</sup> We decided to use this framework as it had proven to be successful for examining through space arene interactions and we hoped that it would allow for a direct comparison of the alkene and arene balance systems. The molecular balance system was therefore based on the bicyclo[3.2.2]nona-6,8-diene skeleton **180** (Figure 62). We were particularly encouraged to study the potential of this framework as a result of the determination of an intramolecular  $\pi$ -facial hydrogen bond by Baker and co-workers published in the 1970s for the isolated case of the tertiary alcohol (X = Me, Y = OH).<sup>142</sup> For ease of comparison the trivial name for this system in the following account is “the parent diene”.

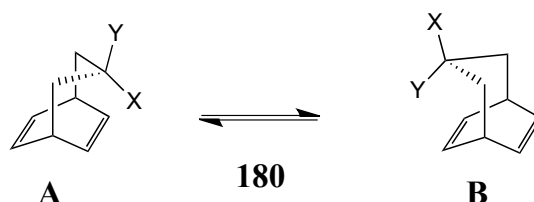


**Figure 62** Conformational equilibrium of the parent diene molecular balance **180**

In addition to this olefinic balance system we decided that it would also be of interest to have a hybrid molecular balance system which allowed for a more direct comparison of olefinic and aromatic interactions, by featuring both an

aromatic ring and an alkene. However in this 6,7-benzobicyclo[3.2.2]nona-6,8-diene system, when X and Y are not equal, two diastereoisomers **181** and **182** are possible (Figure 63). For this system the trivial name propanonaphthalene was adopted.

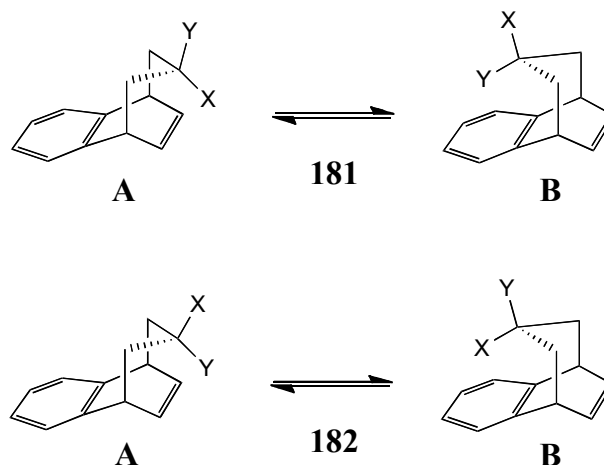


**Figure 63** Conformational equilibrium of the propanonaphthalenes **181** and **182**

As in the propanoanthracene system **161**, the compounds in both new systems exist as a mixture of two easily interconvertible conformers. Consequently, knowledge of the relative abundance of each conformer in solution provides information about the interaction between functional groups and arenes or alkenes as a function of solvent. The conformational equilibria of these systems can be quantified using NMR spectroscopy. The coupling constants between the protons on the bridgehead and the adjacent methylene group can be used to calculate the proportion of each conformer present in solution. Thus, as in the propanoanthracene series, the coupling constants between  $H_5$  and  $H_{4A}$  and  $H_5$  and  $H_{4B}$  are characteristic of each conformer.

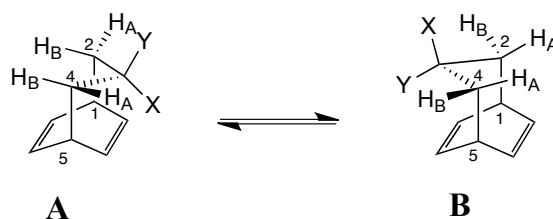


**Figure 64** Detailed structure of the parent diene **180**

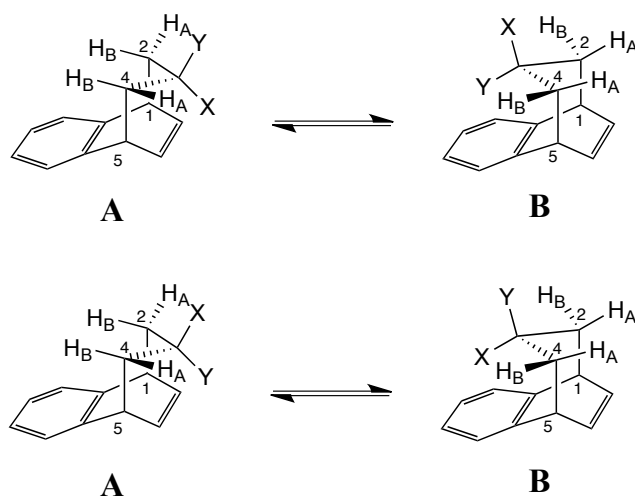
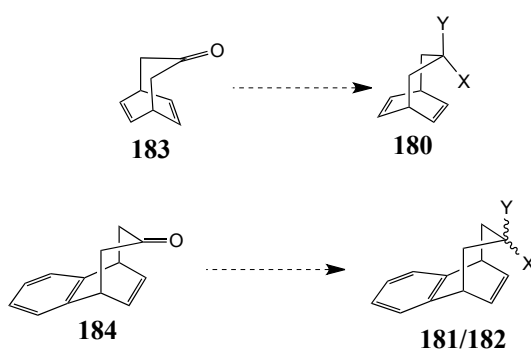


**Figure 65** Detailed structure of the propanonaphthalenes **181** and **182**

With the selection of these frameworks for the study of non-covalent interactions between arenes or alkenes and functional groups in hand, our attention was directed towards their synthesis. As with the propanoanthracene system we decided that in both cases, the carbonyl group would serve as the central precursor for a diverse array of functionalised compounds (Scheme 4).



**Scheme 4**

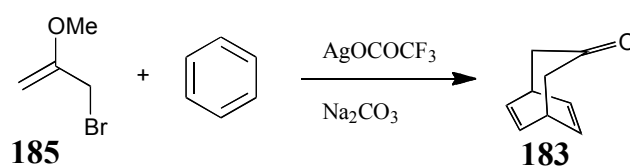
For ease of presentation, the following results and discussion section has been subdivided into synthetic studies followed by the results and discussion of the conformational equilibria of the two families of compounds which were selected.

## 2.3 The synthesis of the “parent diene” system

### 2.3.1 Synthesis of bicyclo[3.2.2]nona-6,8-dien-3-one **183**

The first requirement was of course to access substantial quantities of bicyclo[3.2.2]nona-6,8-dien-3-one, which was to serve as the key intermediate for “parent diene” derivatives.

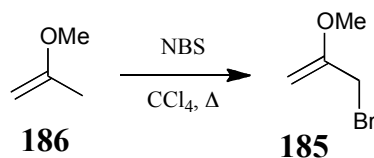
The most spectacular approach to this framework comes from the work of H.M.R Hoffmann *et al.*, who reported the [4+3] cycloaddition reaction between 2-methoxyallyl bromide and benzene in the presence of silver trifluoroacetate, which gave the desired ketone **183** in a single step, albeit in less than 10% yield (Scheme 5).<sup>163,164</sup>



**Scheme 5** Synthetic pathway to ketone **183** developed by Hoffmann *et al.*

However several problems were encountered when this approach was trialed. The first step is to form 2-methoxyallyl bromide **185** by reaction of 2-methoxy-1-propene **186** with N-bromosuccinimide in  $\text{CCl}_4$  (Scheme 6).<sup>163,164</sup>

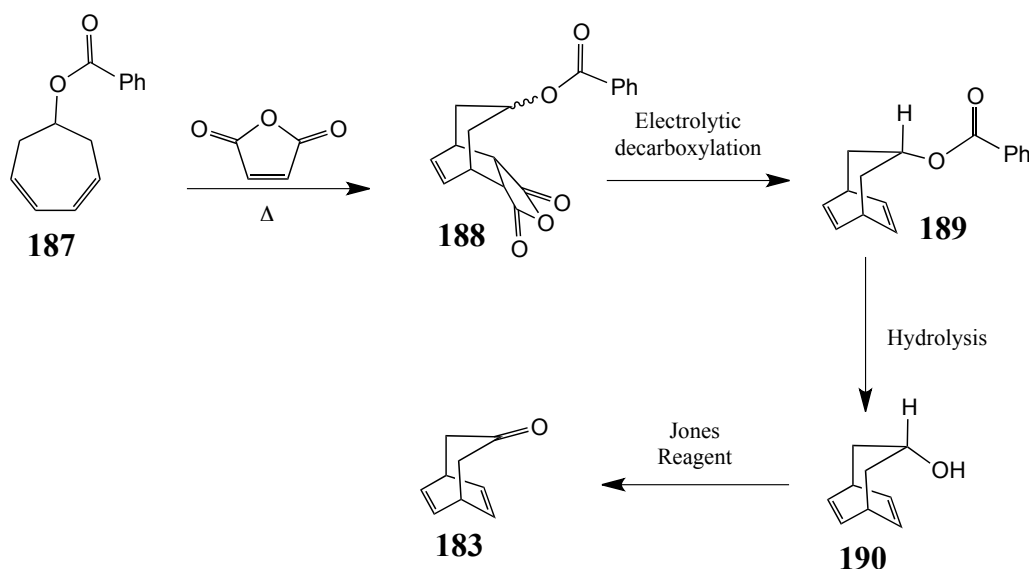




Scheme 6

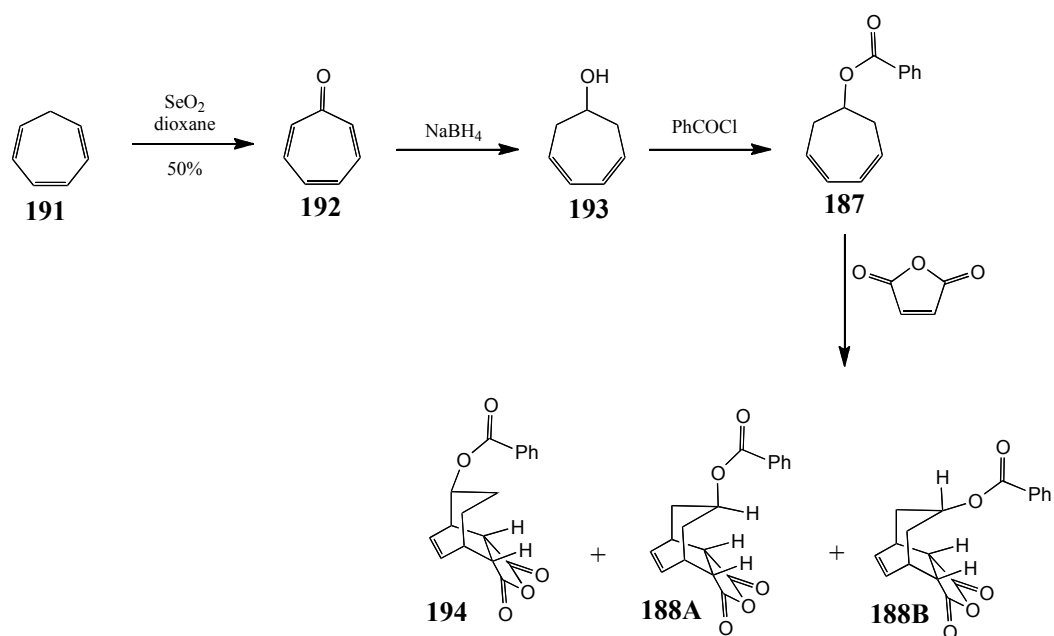
However 2-methoxyallyl bromide **185** is known to be extremely sensitive, decomposing readily in air, and it can therefore only be handled in solution. As a consequence, it was not possible to fully characterise the product or determine the concentration of the solution. The 2-methoxyallyl bromide **185** was subsequently treated with freshly prepared silver trifluoroacetate and benzene, and stirred in the dark. Unfortunately, even after several attempts no bicyclic product was ever isolated from this reaction.

Since the “rapid route” was unsuccessful, it was therefore decided to follow the more classical Diels-Alder strategy which had been used by Baker and co-workers, and wherever possible to shorten or improve the steps, in light of more modern reagents or synthetic equivalents. Unfortunately, Baker and co-workers did not publish full experimental details of this route. The route as outlined in their communication is shown in Scheme 7.<sup>142</sup>



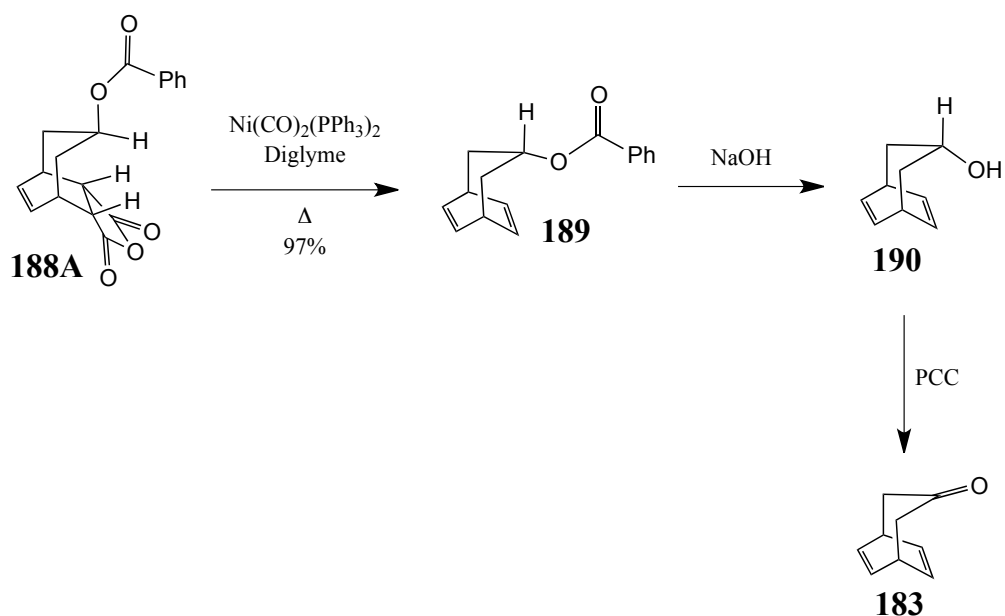
Scheme 7

However, in 1977 Agosta and Takakis reported the results of a study on the synthesis of bicyclononenones, which utilised the route used by Baker *et al.*<sup>142,165</sup> In their case, the diene for the Diels-Alder reaction was prepared in three steps, starting with the selenium dioxide oxidation of cycloheptatriene to tropone, followed by subsequent reduction with sodium borohydride and finally reaction with benzoyl chloride to furnish the diene **187** (Scheme 8).<sup>166,167</sup> They also reported that the Diels-Alder reaction with maleic anhydride yielded not only the expected adducts **188A** and **188B**, but also the isomeric adduct **194**. This observation was also made by Baker *et al.*, but unfortunately, no further information on the formation of the three adducts was provided.<sup>142</sup>



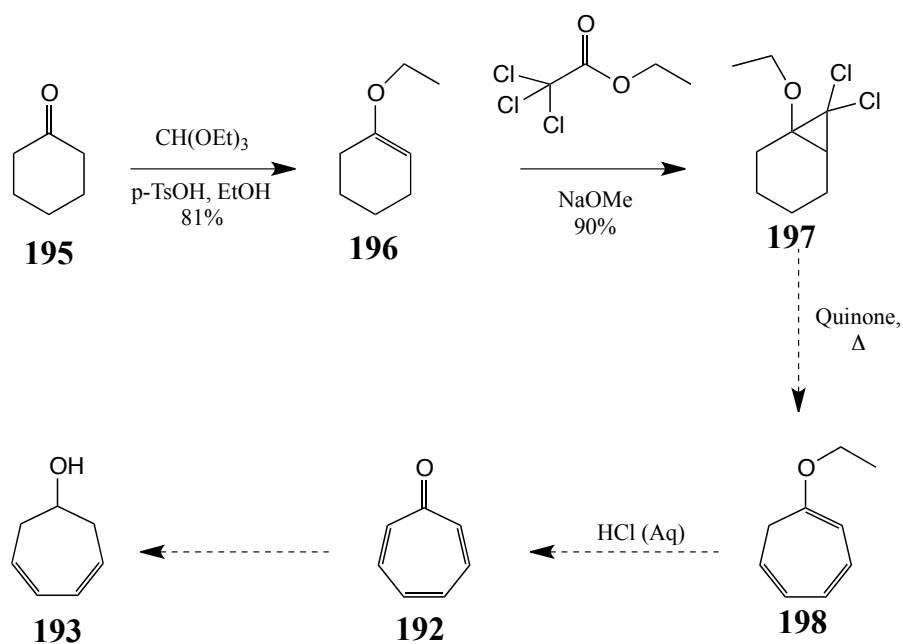
Scheme 8

With the desired adduct separated from the mixture, it was decarboxylated by the use of a nickel catalyst and not the electrolytic method used by Baker and co-workers (Scheme 9). Hydrolysis of the benzoyl group and oxidation with PCC then completed this route to the desired ketone.<sup>165</sup>



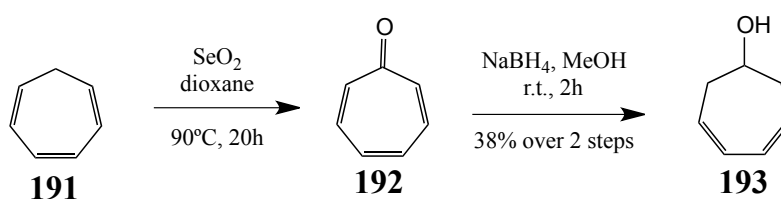
Scheme 9

In our own case, the first route to be investigated involved dichlorocarbene addition to the 1-ethoxy cyclohexene which was, in turn, prepared from the readily available cyclohexanone (Scheme 10).<sup>168</sup>



Scheme 10 Initial route to cycloheptadienol 193

However, after a brief examination this route was found to be too lengthy and unreliable and in the event, selenium dioxide oxidation of cycloheptatriene **191** to tropone **192** *vide supra* proved to be a more practical route. However, when these steps were executed as described in the literature it was found that the oxidation of cycloheptatriene **191** to tropone **192** was low yielding. After several attempts at modifying the reaction conditions, we found that the overall yield could be improved to 38% by reducing the tropone **192** *in situ* before isolation (Scheme 11).



Scheme 11

With the desired cycloheptadienol **193** in hand we were able to prepare a range of protected cycloheptadienols. The protecting groups used were benzoyl,<sup>169</sup> trimethylsilyl<sup>170</sup> and *tert*-butyldimethylsilyl.<sup>171</sup>

A series of different protected cycloheptadienols and acetylene equivalents **199-204** as dienophiles were then screened for the Diels-Alder reaction, in a range of solvents (Figure 66).<sup>172-174</sup> The use of microwave irradiation and sealed tubes was also investigated.

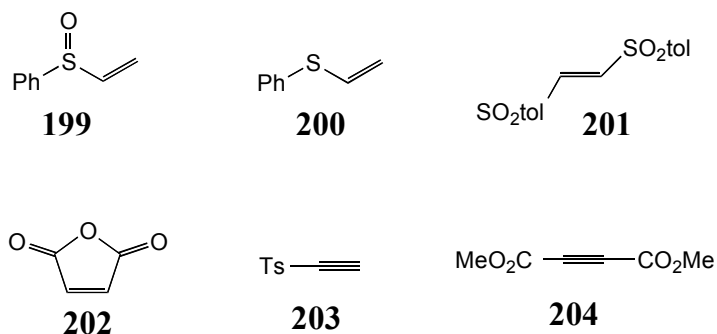
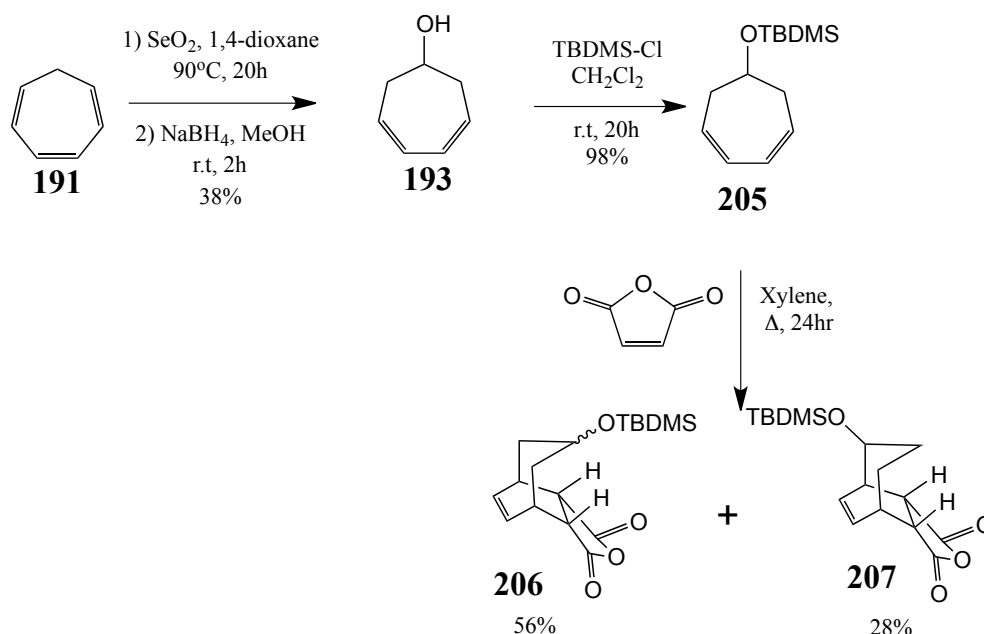


**Figure 66** Range of dienophiles screened

However, few were resistant to the elevated temperatures required for the cycloaddition to occur. We also found that under these conditions, typically refluxing in high boiling solvents, the double bonds in the dienes isomerized, presumably as a consequence of a facile suprafacial 1,5 hydrogen shift. After many failed attempts, the Diels-Alder reaction between *tert*-butyldimethylsilylcycloheptadienol **205** and maleic anhydride as shown in Scheme 12 was chosen. After optimization it was found that the highest yield was obtained when refluxing the starting materials in xylene for 24 hours. Thus, in our final route, the protected cycloheptadienol **205** was prepared in three steps from commercially available cycloheptatriene **191**. The first two steps were executed as described previously and the final step to produce the Diels-Alder precursor was a straightforward silyl protection with *tert*-butyldimethylsilyl chloride which was achieved in excellent yield.<sup>171</sup>

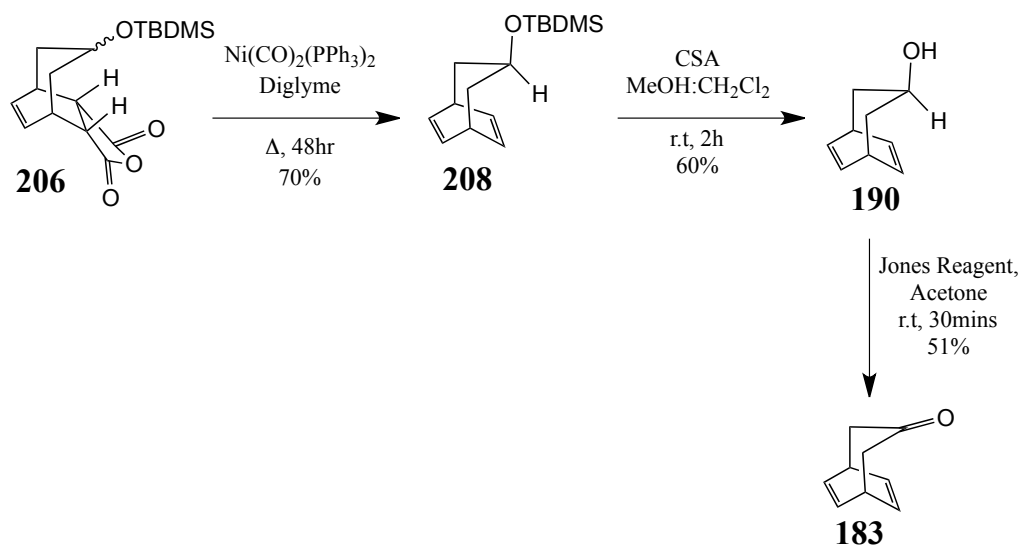


Scheme 12

As well as the desired adduct **206** the Diels-Alder reaction also gave a bicyclic side product **207** in 28% yield. This product is due to prior isomerisation of the double bonds in the parent diene under the high temperatures required for the cyclisation reaction to occur.

With the desired cycloaddition product **206** separated from the byproduct **207**, the ketone **183** could then be obtained in a further 3 steps (Scheme 13). In contrast to the electrolytic protocol adopted in the original synthetic route by Baker and co-workers,<sup>142</sup> the first step of this sequence was a decarboxylation reaction with bis(triphenylphosphine) nickel dicarbonyl, as described by Trost.<sup>175,176</sup> We chose to use this nickel catalyst as several groups have successfully employed it and it avoids the use of alternative toxic lead reagents. The decarboxylation step was found to be very sensitive to the quality of nickel catalyst used, and due to the varying quality of the commercial catalyst we often prepared our own nickel catalyst. Subsequent removal of the tertbutyldimethylsilyl protecting group with camphor sulfonic acid and finally oxidation with Jones reagent yielded the desired ketone **183**.<sup>177</sup> Although the use

of other chromium based oxidising agents was examined, it was found that Jones reagent gave the cleanest product and highest yields.



Scheme 13

However after many attempts at optimisation the yields still remain relatively low and a few of the steps proved to be unreliable and inconsistent. As a consequence it was not possible to synthesise large amounts of ketone **183** and this fact, together with the volatility of this substrate, affected the amount of functionalised substrates which were able to be prepared.

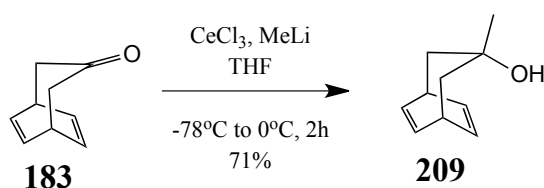
### 2.3.2 Synthesis of alcohol derivatives

With a route to the desired synthetic intermediate **183** now established, we set about the preparation of the functionalised derivatives required for our investigation. Due to the importance of the O-H/ $\pi$  interaction we turned our attention to the synthesis of a range of alcohol derivatives and in order to allow for direct comparison with the propanoanthracene system, an analogous range of functionalised derivatives was planned. Additionally, we decided that it would be



of interest to prepare a compound featuring an ethyl group and a hydroxyl group at the central carbon atom of the propano bridge. The analogous substrate was not prepared in the propanoanthracene series.

The secondary alcohol **190** is of course prepared *en route* to the ketone **183** synthesis and provided us with our first substrate to study non-covalent interactions. We were interested in introducing various groups to the ketone **183** to yield a range of tertiary alcohols. However the reaction of the ketone **183** with either methyl magnesium bromide or methyl lithium, yielded mostly recovered starting material and only trace amounts of the desired products. This may be due to the formation of the metal enolate under the conditions employed. In light of this, we decided to use the corresponding methyl cerium reagent, as it has been reported that cerium based reagents are very efficient in addition reactions with readily enolisable carbonyl compounds.<sup>178</sup> The methyl cerium reagent was therefore prepared from methyllithium and cerium (III) chloride using a literature procedure and gratifyingly, on reaction with the ketone **183**, gave the tertiary alcohol **209** as the sole product and in 71% yield (Scheme 14).<sup>179</sup>

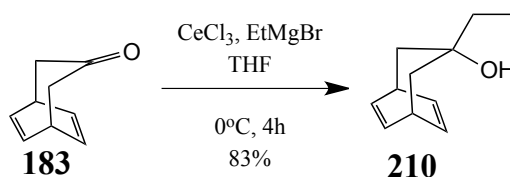


Scheme 14

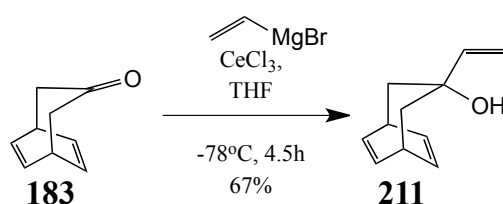
As discussed in the introduction, the hybridisation of the carbon atom in the C-H bond affects the magnitude of the C-H/ $\pi$  interaction, and accordingly we decided that the ethyl substrate **210** could act as a further control. The vinylic alcohol **211** was the next target, as well as gaining further information about the O-H/ $\pi$  interaction, it also provides a probe for the potential alkene-alkene interaction.

Encouraged by the successful introduction of the methyl group we decided to utilise cerium reagents to prepare the analogous ethyl and vinylic congeners (Scheme 15 and Scheme 16). In both cases, the corresponding organo cerium

compound was prepared by the reaction of cerium (III) chloride and the relevant Grignard reagent.<sup>180</sup>



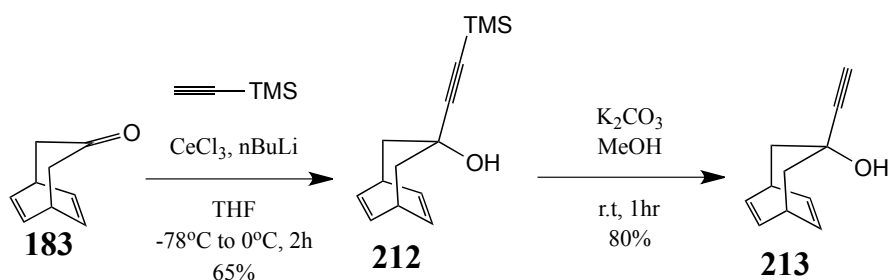
Scheme 15



Scheme 16

In both cases, using two equivalents of organocerium reagent, the reactions proceeded smoothly to completion. The vinylic alcohol was obtained in 67% yield and the ethyl alcohol was obtained in 83% yield.

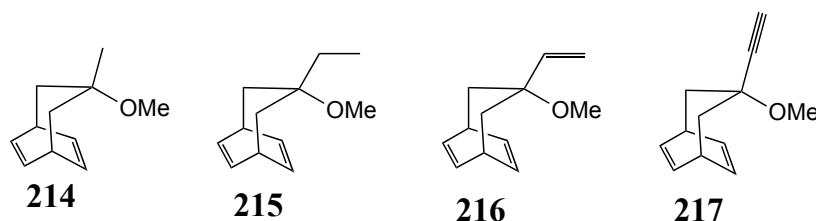
In order to complete the series of alcohol derivatives the propargylic alcohol **213** was then prepared. Once again, the ethynyl moiety was added to the ketone **183** by using an organocerium reagent, generated *in situ* from cerium (III) chloride, *n*-butyllithium and trimethylsilylacetylene (Scheme 17).<sup>181</sup> In this instance, the use of 5 equivalents of the organocerium reagent was necessary for complete conversion of the ketone **183** into the tertiary alcohol **212**. Removal of the trimethylsilyl group was achieved with potassium carbonate in methanol to give the desired propargylic alcohol **213**.



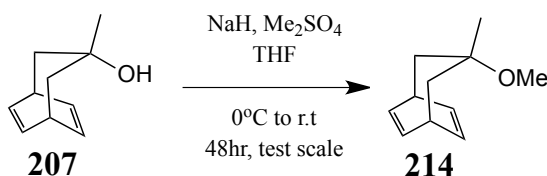
Scheme 17

### 2.3.3 Attempted synthesis of ether derivatives

It was postulated that the comparison of the tertiary alcohols with their corresponding ethers would provide valuable information about the interaction between the hydroxyl group and alkenes (Figure 67).

Figure 67 Corresponding ethers of the tertiary alcohols **209**, **210**, **211** and **212**

Replacement of the proton of the hydroxyl group with a methyl group would eliminate the possibility of an O-H/ $\pi$  interaction from occurring and hence act as an additional control for the alcohol substrates. However, the synthesis of the required ethers was far from trivial.



Scheme 18

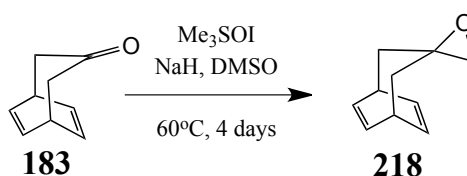
In the first instance, we tried to obtain ether **214** by deprotonation of the tertiary alcohol **209** with sodium hydride and reaction of the subsequent anion with dimethylsulphate (Scheme 18). We were unable to isolate any of the desired product, even although trace amounts of it were detected in the NMR spectrum of the crude product. Unfortunately these reactions have a tendency to work better on a large scale and this was not possible with the amount of material available to us.

#### 2.3.4 Synthesis of substrates with a spirocyclic unit on the flexible bridge

With a range of alcohol derivatives in hand, our attention then turned to the preparation of spiro heterocyclic derivatives. Within the propanoanthracene series, such compounds had proven to be of interest in probing the affinity, or otherwise, of a heteroatom towards the aromatic ring. Unfortunately, within the parent diene system, conversion of the carbonyl group to an exomethylene moiety for further elaboration was not a viable synthetic option and this limited the number of opportunities for comparison with the propanoanthracene system. The greater chemical reactivity of the alkene groups in the parent diene also posed problems.

### 2.3.4.1 Attempted synthesis of epoxide derivative 218

The first spirocyclic derivative examined was the epoxide **218**. In order to prepare the epoxide derivative **218** we decided to employ a sulphur ylide generated *in situ* from trimethylsulfoxonium iodide (Scheme 19).<sup>182</sup>

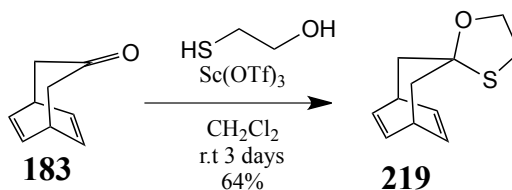


Scheme 19

After 4 days the reaction appeared by TLC to have gone to completion. However, all attempts to purify the crude product led to decomposition by ring opening of the epoxide **218**. Consequently, it was not possible to fully characterize the product. Nevertheless some interesting information could be extracted from the  $^1\text{H}$  NMR spectrum of the crude product (*vide infra*).

### 2.3.4.2 Synthesis of oxathiolane derivative 219

The oxathiolane derivative **219** was selected for direct comparison of the S- $\pi$  and O- $\pi$  interactions. Accordingly, the ketone **183** was reacted with 2-mercaptoethanol in the presence of catalytic scandium (III) triflate and stirred for 3 days to generate the oxathiolane **219** in 64% yield, as a somewhat labile compound whose rigorous purification proved to be somewhat problematic (Scheme 20).<sup>183</sup>

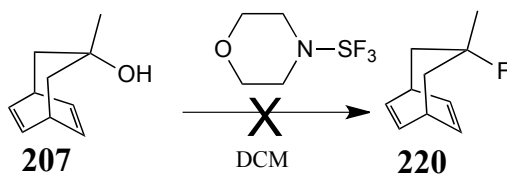


Scheme 20

### 2.3.5 Replacement of the hydroxyl group by a fluorine atom

The incorporation of fluorine atoms or fluorinated groups into biologically active compounds is of considerable interest to medicinal chemists as it can increase the lipophilicity of organic compounds. The physical, chemical and biological properties can be drastically modified by substitution of a hydrogen atom by fluorine. It is therefore of importance to probe non-covalent interactions involving fluorine atoms. Consequently, efforts were made to prepare a range of fluorine derivatives by substituting the hydroxyl group in the previously prepared alcohol derivatives, for a fluorine atom.

We examined the use of DAST and morpholinosulphur trifluoride, both of which are commonly used fluorinating agents. Unfortunately all attempts to prepare the fluoride derivative **220** gave a complex mixture of products and, after many attempts, none of the desired product **220** was obtained (Scheme 21). These reactions once again emphasised that the parent diene was a much more reactive chemical entity than the dibenzo analogue. Consequently the synthesis of fluorinated derivatives was abandoned.

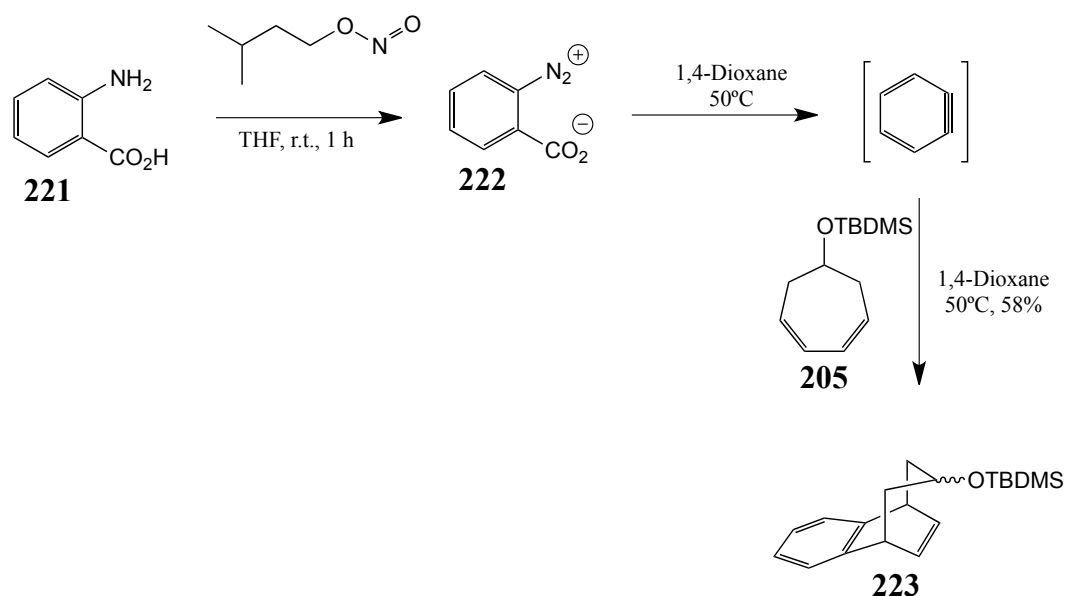


Scheme 21

## 2.4 Synthesis of the “propanonaphthalene system”

### 2.4.1 Synthesis of 6,7-benzobicyclo[3.2.2]nona-6,8-dien-3-one **184**

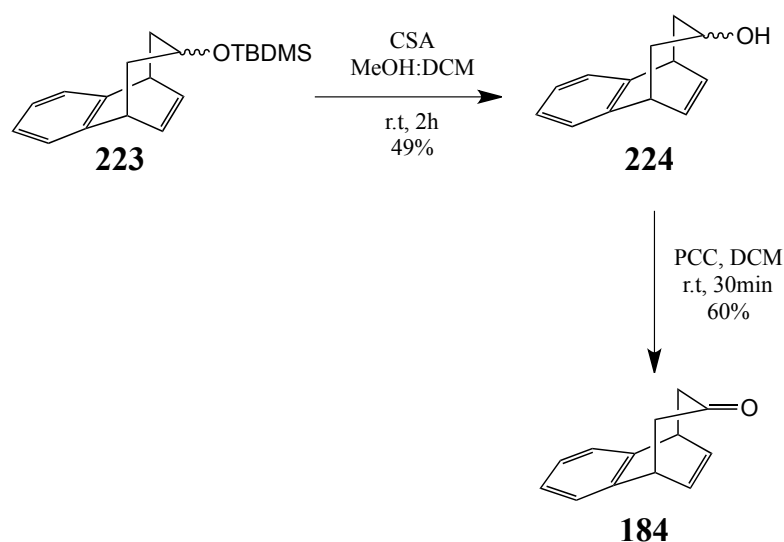
For the synthesis of the key ketone intermediate **184** for the propanonaphthalene series, a similar protocol was adopted, but using benzyne as the dienophile for the Diels-Alder reaction (Scheme 22).<sup>184</sup>



Scheme 22

Benzyne was generated *in situ* from 2-diazo benzoate **222**, which was formed by the reaction of anthranilic acid **221** and isoamyl nitrite.<sup>185</sup> The use of 2-(trimethylsilyl)phenyl trifluoromethanesulfonate to generate the benzyne intermediate was also examined, however the conditions required were found to be incompatible with the diene substrate **205**.<sup>186</sup> The Diels-Alder reaction proceeded smoothly to yield the bridged bicyclic compound **223** in 58% yield as a mixture of diastereoisomers which at this point were not separated. By NMR the product was determined to be a 86:14 mixture of the two diastereoisomers.

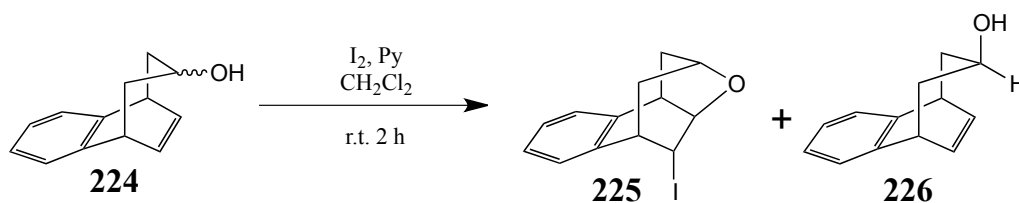
The low yield of this reaction is believed to be affected by the short lifetime of the benzyne intermediate, with up to 20% of the starting protected alcohol **205** recovered. The bicyclic compound **223** was deprotected upon treatment with camphor sulphonic acid in low yield 49% (Scheme 23). The deprotected alcohol **224** was obtained as a 10:1 mixture of diastereoisomers **226** and **225**. Subsequent oxidation with pyridinium chlorochromate then furnished the desired ketone **184**.<sup>187</sup>



Scheme 23

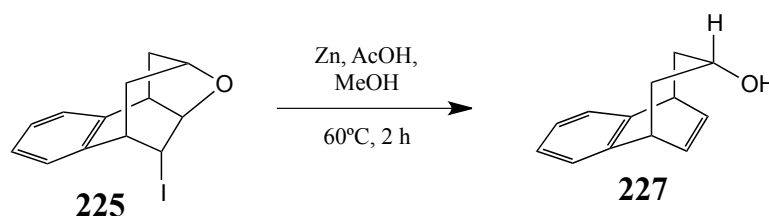
To fully characterise the diastereoisomers of the alcohol **224** they needed to be separated. However, after several attempts, separation by flash column chromatography proved to be impossible. Hence, it was decided to separate the two diastereoisomers **226** and **227** chemically using an iodoetherification reaction (Scheme 24). When the mixture is reacted with iodine, only one of the diastereoisomers can react to form the iodoether **225**. This reaction proceeded smoothly to yield the desired products which were then readily separated by flash column chromatography.





Scheme 24

The cyclic compound **225** was then ring opened with zinc and acetic acid to reform the other diastereoisomeric alcohol **227** (Scheme 25). With both diastereoisomers of the alcohols **224** separated we were able to use them for our studies. This chemical reaction also allowed unambiguous structural assignment of each diastereoisomer by classical chemical correlation.

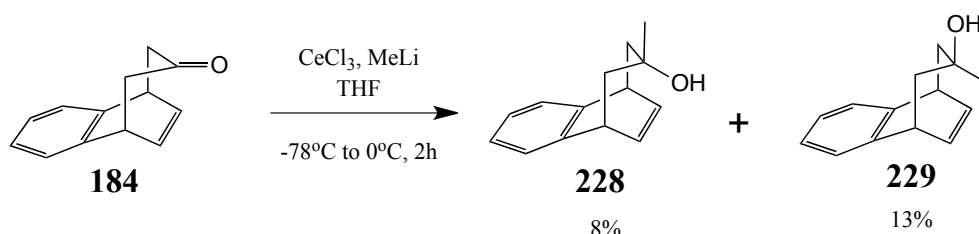


Scheme 25

### 2.4.2 Synthesis of alcohol derivatives

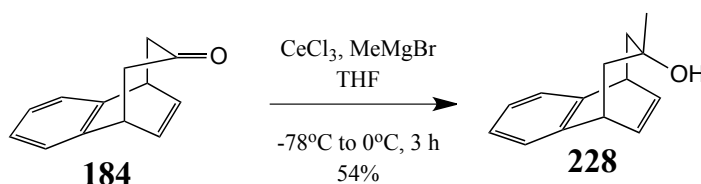
With the key ketone intermediate **184** in hand we set about to prepare an analogous range of alcohol derivatives to allow us to compare the three systems. From experience with the secondary alcohols **224**, we anticipated that separating the diastereoisomers would be far from trivial. Firstly we prepared the methyl alcohol derivatives **228** and **229** (Scheme 26). However using the same organocerium methodology as employed for the parent diene system, this reaction was found to be low yielding.<sup>179</sup> Fortunately we were able to separate the two diastereoisomers **228** and **229** by flash column chromatography. We

initially believed that the low yield was due to incomplete reaction and product loss during purification. However longer reaction times and the use of more equivalents of organocerium reagent had little impact on the yield of the reaction.



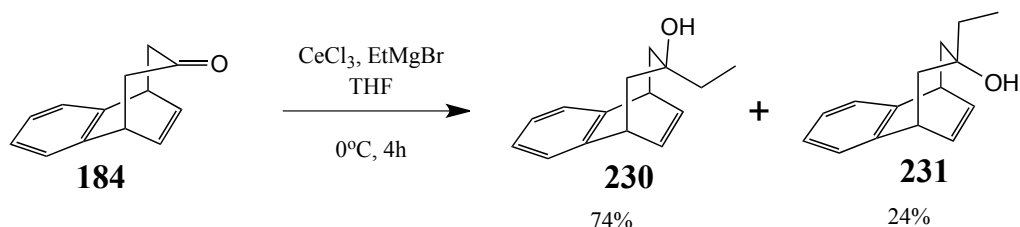
Scheme 26

Following from the success of our earlier work, we decided to prepare the organocerium reagent from methylmagnesium bromide.<sup>180</sup> To our surprise, the selection of the Grignard reagent led, not only to a substantial improvement in the yield of the desired tertiary alcohol (54%), but also to the single diastereoisomer **228** (Scheme 27). A possible rationalization for this observation may involve some form of complexation of the double bond with magnesium salts.

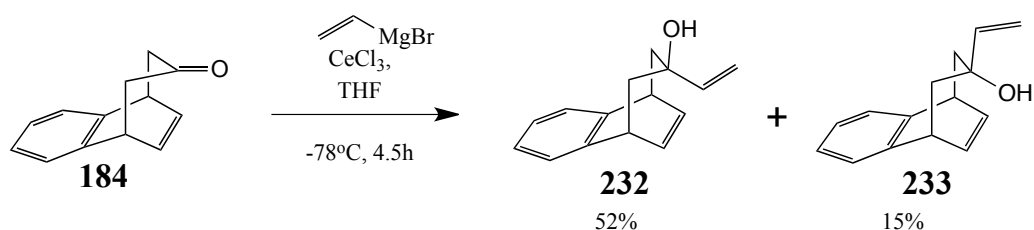


Scheme 27

We next turned our attention to the synthesis of the vinylic **232** and **233** and ethyl **230** and **231** alcohols (Scheme 28 and Scheme 29). Once again, as for the parent diene system it was also possible to obtain the derivatives in excellent yield and also to separate the diastereoisomers by flash column chromatography.

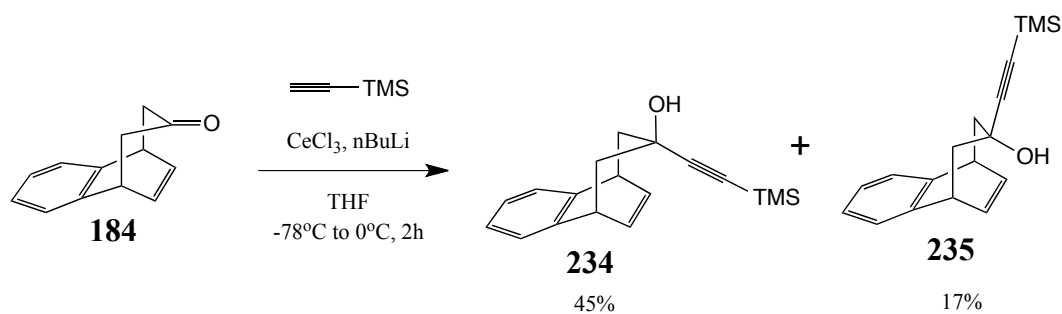


Scheme 28



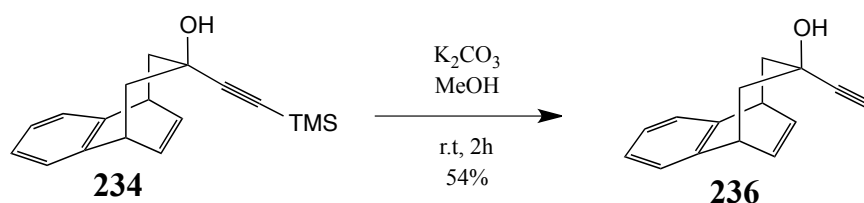
Scheme 29

The propargylic alcohols **236** and **237** were prepared in similar fashion using the organocerium reagent generated *in situ* as described previously (Scheme 30).<sup>181</sup> However, even when 5 equivalents of the organocerium agent were employed, the reaction failed to go to completion, as some unreacted starting material was isolated. The two diastereoisomers were successfully separated by column chromatography to give the propargylic alcohols **234** and **235**.

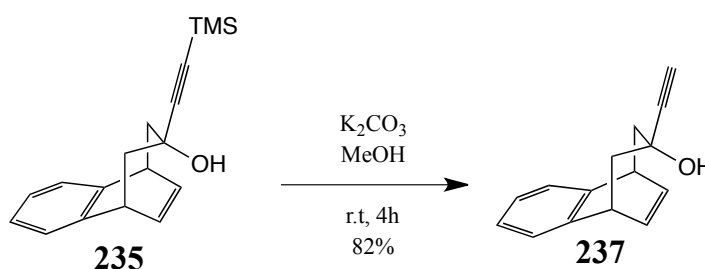


Scheme 30

With the diastereoisomers separated, they were each treated with potassium carbonate in methanol to remove the trimethylsilyl group to yield alcohols **236** and **237** (Scheme 31 and Scheme 32).



Scheme 31

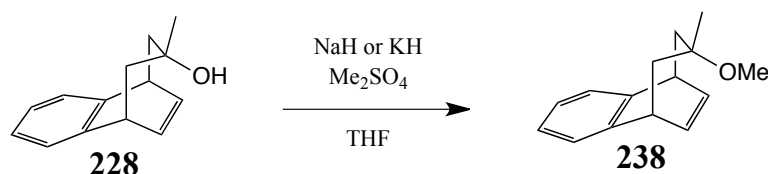


Scheme 32

### 2.4.3 Attempted synthesis of ether derivatives

In order to gain valuable information about O-H/ $\pi$  interactions the synthesis of the methyl ether **238** from the tertiary alcohol **228** was attempted. Initially, the same method as used for the parent diene system was employed. However, treatment of alcohol **228** with sodium hydride followed by dimethylsulphate led to the recovery of the starting alcohol **228** (Scheme 33). As we were fortunate enough to have more starting material in hand we examined the use of potassium hydride. The tertiary alcohol substrate **228** was deprotonated with oil free potassium hydride before the resulting anion was reacted with dimethylsulphate. Unfortunately this reaction led to a complex mixture of products and none of the

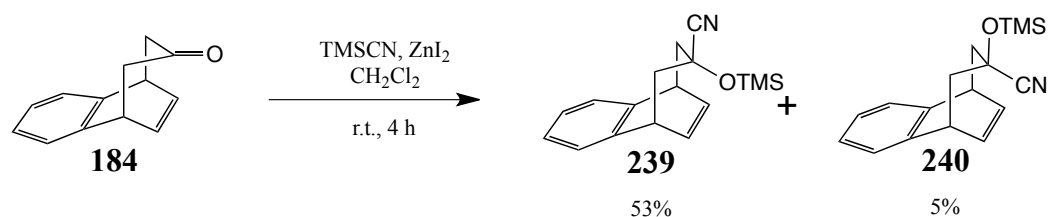
desired product **238** could be isolated. At this moment in time, there seems to be no obvious mechanistic pathway to explain the instability of the potassium alkoxide.



Scheme 33

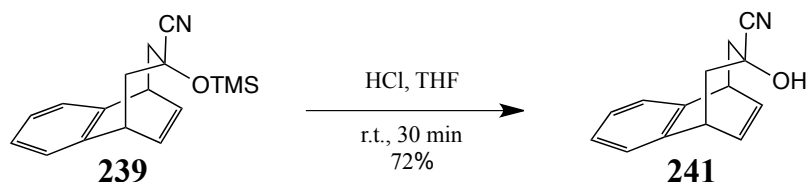
#### 2.4.4 Synthesis of cyanohydrin derivatives **241** and **242**

As the synthesis of the propanonaphthalene ketone **184** was more robust and higher yielding than that of the parent diene ketone congener, we were able to prepare a larger amount and hence had the opportunity to prepare a wider range of functionalised derivatives. To complement the tertiary alcohol series it was decided to prepare the cyanohydrins **241** and **242** (Scheme 34). This derivative also offered the opportunity to compare the cyano group with the terminal alkyne. Trimethylsilyl cyanide was employed as a source of cyanide anion, reaction with the ketone **184** led to the formation of the intermediate silyl protected derivatives **239** and **240** in overall 58% yield.<sup>188</sup>

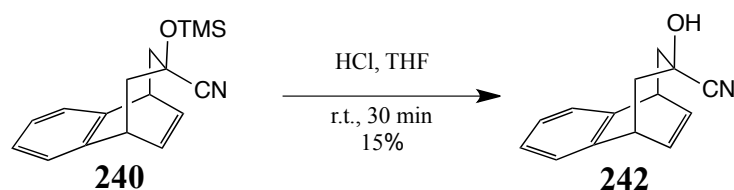


Scheme 34

The diastereoisomers were then separated by flash column chromatography and treated with aqueous HCl to give the desired cyanohydrins **241** and **242** (Scheme 35 and Scheme 36).



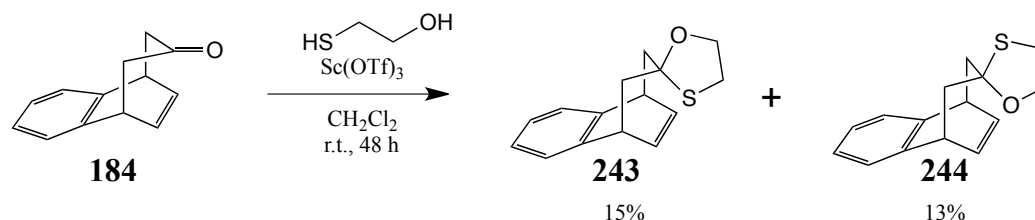
Scheme 35



Scheme 36

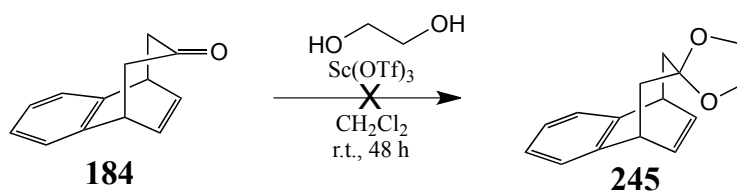
#### 2.4.5 Synthesis of substrates with a spirocyclic unit on the flexible bridge

Since our initial studies with the parent diene series had revealed the oxathiolane **219** to be a very interesting substrate, the propanonaphthalene analogues became the first focus of attention. To prepare the oxathiolanes **243** and **244**, the ketone **184** was reacted with 2-mercaptoethanol and a catalytic amount of scandium (III) triflate (Scheme 37). <sup>183</sup>The reaction proceeded smoothly and after 48 h, TLC of the reaction mixture showed that all the ketone **184** starting material had been consumed. However the two diastereoisomers **243** and **244** were very difficult to separate by flash column chromatography, and a significant amount of product was lost, in the interest of isolating pure samples of both isomers.

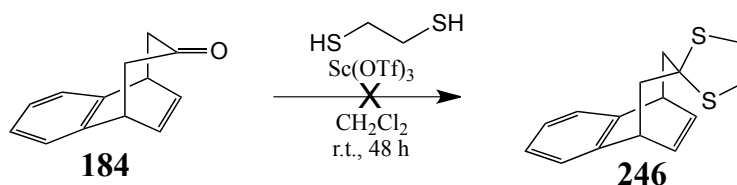


Scheme 37

As more ketone substrate **184** was available, it was decided to attempt preparation of the dioxolane **245** and the dithiolane **246** derivatives (Scheme 38 and Scheme 39). However we had little success when the same methodology was applied. In the case of the dioxolane **245** the product was unstable and a complex mixture was obtained. For the dithiolane **246**, even after 48 hours, only unreacted starting material was recovered. We envisaged that these substrates would offer us an opportunity to directly compare the olefinic and aromatic  $\pi$ -interactions with sulphur and oxygen atoms.



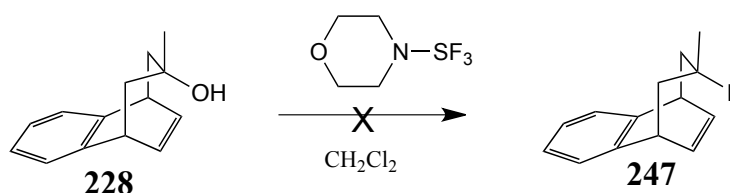
Scheme 38



Scheme 39

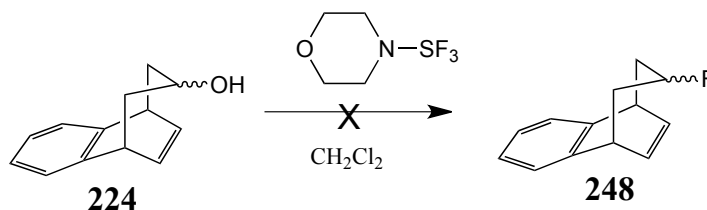
## 2.4.6 Replacement of the hydroxyl group by a fluorine atom

Although efforts to prepare fluorinated derivatives of the parent diene had been unsuccessful, we nevertheless decided to attempt the synthesis of these derivatives in the propanonaphthalene series. Once again, morpholinosulphur trifluoride was selected, since it had been shown to be successful for the fluorination of a tertiary alcohol in the propanoanthracene series. As with the parent diene system, we initially attempted the fluorination of the methyl tertiary alcohol **228** (Scheme 40).



Scheme 40

Unfortunately, we were unable to isolate any of the desired product **247**. We decided that this might be due to the quality of morpholinosulphur trifluoride used and as a consequence, we repeated the experiment with a brand new bottle of the reagent and the same result was obtained. Undeterred by this result fluorination of the secondary alcohol **224** was also attempted (Scheme 41).



Scheme 41



Once again the desired product **248** was not formed and only a complex mixture of products, which defied further purification by column chromatography was obtained.

## 2.5 Synthetic summary

The following series of bicyclo[3,2,2]nona-6,8-dienes and propanonaphthalenes with various functional groups on the central carbon of the flexible bridge as summarised in Figure 68 have therefore been prepared.

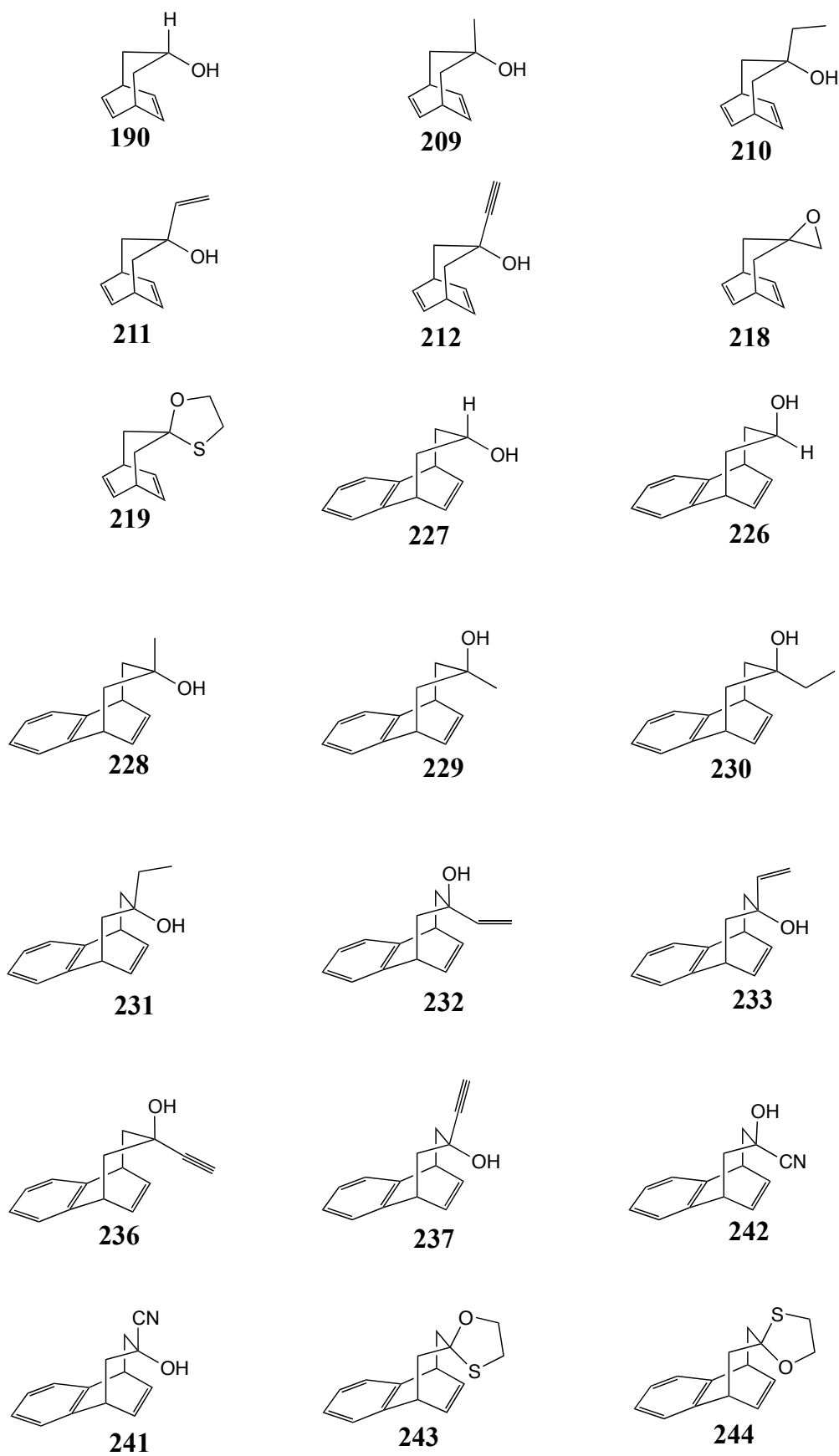


Figure 68

From a purely synthetic perspective, it is frustrating to record that the relatively lengthy and low yielding sequence to the parent diene system, when coupled with the instability of the compounds and the often undesirable chemical reactivity of the alkene  $\pi$ -clouds, precluded the preparation of several desired substrates. By way of contrast, synthetic studies in the propanonaphthalene series were comparatively straightforward, save for the sacrificial chromatography which was often necessary to achieve separation of the two diastereoisomers.

## **2.6 NMR spectroscopy techniques used to study conformational equilibria**

The structures of the propanonaphthalene and parent diene derivatives have been specifically designed to allow the conformational equilibrium between the conformers **A** and **B** to be measured by NMR spectroscopy. However the interconversion energy barriers are very small, and, as a consequence previous studies within the group have shown that the usual approach of reaching a slow exchange limit on the NMR timescale by operating at low temperature failed. As a result of the fast motion of the flexible bridge, only averaged chemical shifts and coupling constants are observed on the NMR time scale at room temperature.

### **2.6.1 Dihedral angle**

The torsional angle of the parent diene system **181** is shown in the following Newman projection (Figure 69).

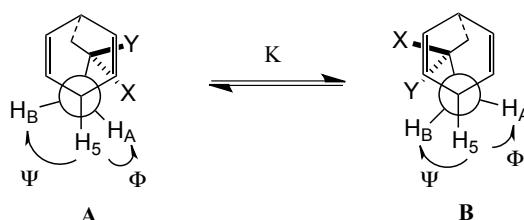


**Figure 69** Newman projection of conformers A and B for the parent diene **181**

If the conformer **A** predominates, the dihedral angle  $\Psi$  will be greater than  $60^\circ$  thus giving  $^3J_{5-4A} > ^3J_{5-4B}$  from the Karplus equation. If the other conformer **B** predominates, the dihedral angle  $\phi$  will be greater than  $60^\circ$  thus giving  $^3J_{5-4A} < ^3J_{5-4B}$ .

The dihedral angles of the parent diene framework **181** have been predicted by Dr. A. Aliev, using theoretical calculations. The predicted values for the dihedral angles  $\phi$  and  $\Psi$  are approximately  $40^\circ$  and  $73^\circ$  respectively. The dihedral angles are directly related to the values of the coupling constants  $^3J_{5-4A}$  and  $^3J_{5-4B}$  for one conformer.

The torsional angles of the two diastereoisomers **181** and **182** of the propanonaphthalene system are shown in the following Newman projection (Figure 70).

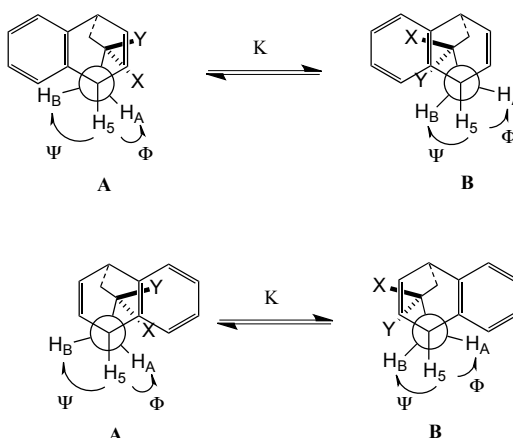


**Figure 70** Newman projections for both diastereoisomers **181** and **182** of the propanonaphthalene derivatives

From calculations, the values of the dihedral angles for the propanonaphthalene system **181** and **182** were found to be of the same magnitude (i.e.  $\phi = 40^\circ$  and  $\Psi = 73^\circ$ ) as those of the parent diene system.

### 2.6.2 Determination of the predominant conformer by NOE measurements

The nuclear Overhauser effect provides a convenient method by which the through space proximity of two nuclei can be determined since the NOE enhancement is dependent on the internuclear distance,  $r$ , of the two nuclei and not connectivity.<sup>189</sup> Consequently, it has frequently been used for determining the geometry of conformers in a rapidly exchanging mixture. This type of NMR experiment was also used for both the parent diene and propanonaphthalene systems to help determine the major conformer in solution.

### 2.6.3 Determination of the conformational ratios using the coupling constants between the protons on the central bridge

The coupling constants between the protons on the bridge,  $H_4$  and  $H_2$  and those on the bridgehead  $H_1$  and  $H_5$  allow for the population of each conformer **A** and **B** to be determined, if the boundary coupling constants,  ${}^3J_{5-4A}$  and  ${}^3J_{5-4B}$  for conformers **A** and **B** are known (Figure 71). These boundary values are the coupling constants found for one conformer in solution, however an exact measurement of these constants was not possible but an estimation can be made.

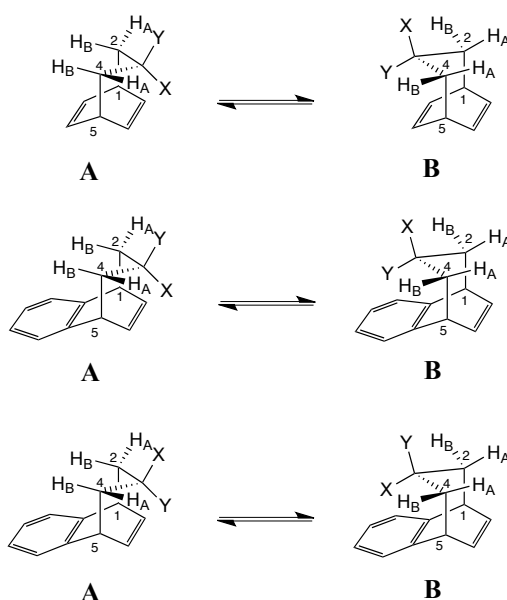


Figure 71

For both molecular balance systems, as a result of the symmetry of the framework, the largest coupling constant for **A** equals the smallest in **B** and the converse also applies. The boundary values were found to be  ${}^3J_{5,4A} = J_L = 6.5$  Hz when X is directed towards the alkene and  ${}^3J_{5,4A} = J_S = 1.1$  Hz when X is directed away from the alkene for the parent diene system and  ${}^3J_{5,4A} = J_L = 6.7$  Hz and

${}^3J_{5,4A} = J_S = 1.2$  Hz for the propanonaphthalene system. The boundary values were obtained from the lowest and highest observed coupling constants, which for the parent diene system was from substrate **209** at 210 K and for the propanonaphthalene system was from substrate **229** at 210 K. For the disubstituted derivatives, the coupling constants  ${}^3J_{5,4A}$  and  ${}^3J_{5,4B}$  are dependent on the dihedral angles and the electronegativity of the substituents.

$P_A$  is the population of the conformer **A** and similarly for conformer **B**,  $P_B$  is  $1 - P_A$ . The conformation ratios will be given as percentages and therefore  $P_B = 100 - P_A$ . The values for the coupling constant between  $H_5$  and  $H_{4A}$  can be calculated using Equation 3 and Equation 4:<sup>159,160</sup>

$${}^3J_{5,4B} = \frac{P_A}{100} \cdot J_S + \left[1 - \frac{P_A}{100}\right] \cdot J_L$$

Equation 3

$${}^3J_{5,4A} = \frac{P_A}{100} \cdot J_L + \left[1 - \frac{P_A}{100}\right] \cdot J_S$$

Equation 4

Where:

$P_A$  the proportion of time spent in the conformer A

$J_L$  the coupling constant between the protons  $H_5$  and  $H_{4A}$  in the conformer A

$J_S$  the coupling constant between the protons  $H_5$  and  $H_{4A}$  in the conformer B

${}^3J_{5-4A}$  the observed average coupling constant between protons  $H_5$  and  $H_{4A}$

${}^3J_{5-4B}$  the observed average coupling constant between protons  $H_5$  and  $H_{4B}$

Consequently,

$$P_A = \frac{(J_L - {}^3J_{5,4B})}{(J_L - J_S)} \times 100 = \frac{({}^3J_{5,4A} - J_S)}{(J_L - J_S)} \times 100$$

**Equation 5**

The equilibrium constant  $K_a$  can then be directly calculated from the proportion of time spent in the conformer A by the following equation:

$$K_a = \frac{P_A}{100 - P_A}$$

**Equation 6**

The free energy difference  $\Delta G^\circ$  can then be determined from the conformational ratio by using the following equation:

$$\Delta G^\circ = RT \ln K_a$$

**Equation 7**

Where:

$\Delta G^\circ$  Free energy difference between conformers ( $\text{J mol}^{-1}$ )

R Universal gas constant ( $R = 8.314 \text{ JK}^{-1} \text{ mol}^{-1}$ )

T Temperature (K)

$K_a$  Equilibrium constant determined from the conformational ratio

Equation 5 shows that the sum of the boundary values  $J_L$  and  $J_S$  are approximately equivalent to the sum of the coupling constants  ${}^3J_{5-4A}$  and  ${}^3J_{5-4B}$ .



This allows for an internal check in the system and for an approximation of coupling constants that cannot be measured. When the conformational populations are calculated using two different  ${}^3J_{5-4A}$  and  ${}^3J_{5-4B}$  couplings for each substrate the agreement is within 2%. In this system, the error in the population measurements arises from the accuracy of the boundary values  $J_L$  and  $J_S$ , assuming that these values are accurate to within  $\pm 0.3$  Hz, then the error in the population measurements is  $\pm 5\%$ .

#### 2.6.4 Temperature dependence

The conformational equilibrium can be perturbed by varying the temperature at which it is studied, as it can slow down the motion of the bridge and increase the time spent in the more stable conformer on the NMR time scale. Consequently,  ${}^1\text{H}$  NMR studies were undertaken over a range of temperatures for all of the substrates in  $\text{CDCl}_3$ . It was found that for both molecular balance systems, the chemical shifts and conformational ratios were significantly affected by the gradient of temperature. This often allowed us to confirm the more stable conformer. Variable temperature studies were also used to determine the boundary values as for both systems we were unable to prepare the spirocyclic cyclopropane derivative. In previous studies with the propanoanthracene system, the cyclopropane derivative was used to help calculate the boundary values.

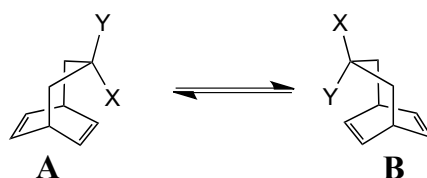
The observed chemical shifts of the protons of the conformational balance are an average between the theoretical chemical shifts of the two conformers **A** and **B** and as a consequence changes in the conformational ratio also affect the chemical shifts of the protons in the bridge. With the propanonaphthalene series an upfield shift of the substituent directed towards the aromatic ring should be observed as the close through space location of the aromatic ring increases the electron density on the substituent directly above it. As a consequence, the temperature dependence of the chemical shifts and the conformational ratios provide a further tool in the determination of the conformational equilibria.

## 2.7 Results from the parent diene system

The primary objective of this work is to gain insight into various intramolecular non-covalent olefinic and aromatic  $\pi$ -interactions occurring in a series of specifically designed molecular balance systems. It is apparent that numerous interactions play a part in the stabilisation of one conformer over the other. Unfortunately, as discussed in the introductory chapter, the direct experimental investigations of  $\pi$ -interactions are not possible. Many research groups have circumvented this problem by systematic variation of one parameter. Although our molecular balance systems are designed to limit interference from other interactions on the conformational equilibrium, they cannot always be neglected and of course solvent effects are of vital significance. For our studies we have tried to select substituents on the bridge that would have comparable steric hindrance, as the difference in van der Waals radii between substituents may have significant effects on the position of the conformational equilibrium. Measurements of the conformational ratios have been obtained under comparable conditions of temperature and solvent. In this section attempts will be made to provide accurate quantitative data to compare the series of substrates.

### 2.7.1 Relative strengths of functional group interactions in $\text{CDCl}_3$

The structures of the predominant conformers and their conformational ratios and the free energy difference between the conformers have been determined for a series of parent diene derivatives, using the methods described. The results of these studies in  $\text{CDCl}_3$  are presented in Table 5.



	X	Y	$^3J_{5,4A}$ (Hz)	$^3J_{5,4B}$ (Hz)	$P_A$	$\Delta G^\circ$ (kJ mol <sup>-1</sup> )
<b>190</b>	H	OH	6.6	1.3	98:02	9.6
<b>209</b>	OH	Me	6.7	1.1	100:0	-
<b>210</b>	OH	Et	6.5	1.3	98:02	9.6
<b>211</b>	OH	CH=CH <sub>2</sub>	6.5	1.2	96:04	7.9
<b>213</b>	OH	C≡CH	4.7	2.9	67:33	1.8
<b>218</b>	-O-	-CH <sub>2</sub> -	3.8	3.7	51:49	0.2
<b>219</b>	-S-	-O-	6.3	1.7	92:08	6.1

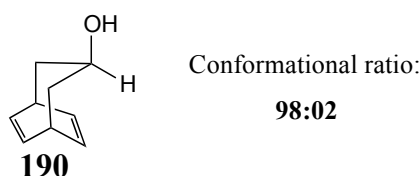
**Table 5** Equilibrium ratios, experimental coupling constants and energy differences between conformers of the parent diene derivatives in CDCl<sub>3</sub> at 298 K

To determine the predominant conformers a combination of methods were used as they cannot be determined by the use of only one method. Due to the complexity of the system and the fact that small changes in the structure may be hard to detect by <sup>1</sup>H NMR, several possible interpretations of the results we obtained may be possible. In this section the results presented in the above table will be analysed and their interpretations discussed. A comparison of the results will be done to gain an understanding into the relative strengths of olefinic  $\pi$ -interactions. To complement our results, variable temperature <sup>1</sup>H NMR experiments were also undertaken for each substrate in CDCl<sub>3</sub>, these results, where interesting patterns were found will be discussed later. Unfortunately no X-Ray crystal structures could be obtained for any of the substrates in the parent diene series. For all substrates NOE experiments were undertaken to help confirm the predominant conformers.

### 2.7.1.1 Alcohol derivatives – Importance of O-H/ $\pi$ interaction

As emphasised in the introduction, the hydrogen bonding like interaction between a hydroxyl group and an aromatic ring is now a well-established non-covalent interaction. The series of alcohol derivatives within the parent diene system now allows us to study the analogous interaction between a hydroxyl group and the simple  $\pi$ -cloud of an alkene.

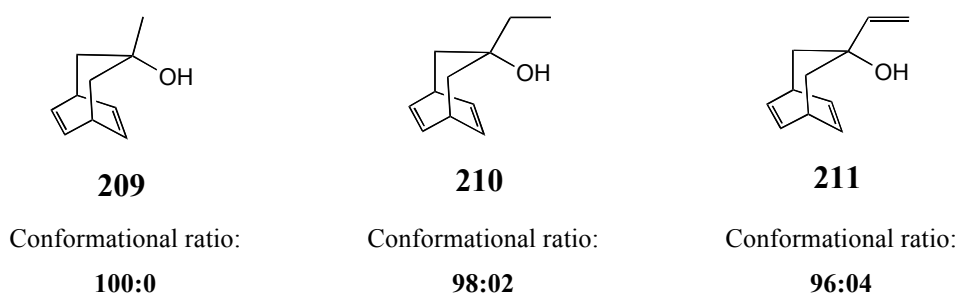
In solution the population of the predominant conformer of the secondary alcohol **190** is 98%, with the hydrogen atom positioned above the double bond (Figure 72).



**Figure 72** Representation of the predominant conformer of **190** in  $\text{CDCl}_3$  solution

However in this substrate there is a significant steric difference between the hydroxyl group and the hydrogen atom. In the propanoanthracene series the analogous conformer was also observed as the major conformer.<sup>159,160</sup> It therefore seems reasonable to postulate that the formation of a hydrogen bond with either the aromatic ring or with a simple alkene is not strong enough to compensate for the difference in van der Waals radii.

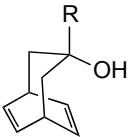
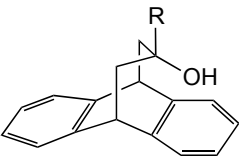
For the tertiary alcohols **209**, **210** and **211** one predominant conformer (> 90%) was observed, thus the energetic difference between two conformers must be higher than  $7 \text{ kJ mol}^{-1}$  (Figure 73). NOE enhancements were used to prove that the hydroxyl group was directed towards the double bond.



**Figure 73** Representation of the predominant conformers of tertiary alcohols **209**, **210** and **211** in  $\text{CDCl}_3$  solution at 298 K

The conformational ratios of the derivatives **209**, **210** and **211** are 100%, 98% and 96% respectively, with the hydroxyl group orientated towards the double bond. For the methyl alcohol **209**, the observed coupling constants are very similar in magnitude to the boundary values, hence predominance for one conformer is observed and the conformational ratio is approximately 100%. This indicates that the O-H/ $\pi$  interaction may be sufficiently strong to compensate for the difference in steric bulk between a vinyl group and a methyl group. Also of note is that these results show that varying the size of the alkyl group does not have a significant effect on the stabilisation of the conformer. Initially these alcohols were synthesised to study the effects of the hybridized orbitals of the carbon atom of the substituent on the conformational ratio. Accordingly they have shown that the ratio decreases on increasing the degree of unsaturation at the carbon atom. If steric hindrance was of crucial importance to the conformational ratio, the opposite results would be expected, as the vinyl group is significantly larger than the methyl group. Although there is only a small difference in the conformational ratios, these results could suggest that the C-H/ $\pi$  interaction is stronger for a vinylic C-H than an alkyl C-H and such interactions will be further discussed at a later stage. Further evidence for this interaction could be provided by studying the conformational ratios of the corresponding ethers. However, in this instance it was not possible to prepare them.

Even at this preliminary stage it was of course, almost impossible to resist the temptation of comparing the results from these three tertiary alcohols with those which had been obtained earlier in the propanoanthracene series.<sup>159,160</sup>

R		
Me	100:0	96:04
Et	98:02	n/a
CH=CH <sub>2</sub>	96:04	90:10

**Table 6** Equilibrium ratios of the parent diene and propanoanthracene tertiary alcohol derivatives in CDCl<sub>3</sub> at 298 K

The small but distinct preference for the presence of an intramolecular  $\pi$ -facial hydrogen bond of an alkene over an arene, was of considerable interest.



**Figure 74** Representation of *gauche* and *trans* rotamers that the hydroxyl group in alcohol derivatives can adopt

Even though these molecular balance systems restrict the degree of conformational freedom, there is nonetheless sufficient freedom retained. The hydroxyl group in all of the alcohol substrates can adopt a *gauche* or *trans* orientation relative to the other substituent on the flexible bridge (Figure 74). Only the *trans* rotamer allows for the correct geometry required for a  $\pi$ -interaction to occur.<sup>162</sup> For the vinylic alcohol **211**, detailed NMR measurements were undertaken in order to determine the orientation of the

hydroxyl group and hence verify the existence of an O-H/ $\pi$  interaction in solution. From selectively decoupled  $^{13}\text{C}$  and 2D  $J$ -resolved measurements, the  $^3J_{\text{CH}}$  coupling for the  $^{13}\text{C}$ , OH pair was determined to be 7.34 Hz. A Karplus type relationship indicates that a coupling of this magnitude suggests that the *trans*-rotamer about the C-O bond is the major rotamer, hence, confirming the presence of an O-H/ $\pi$  interaction in solution for this substrate.

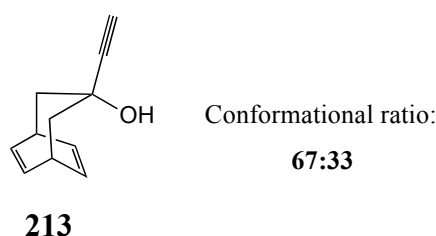


**Figure 75** Representation of the major conformer of the tertiary alcohol **213** in  $\text{CDCl}_3$  solution at 298 K

In contrast, the conformational ratio of the propargylic alcohol **213** does not show one predominant conformer. The major conformer has the hydroxyl group orientated towards the double bond with a conformational population of 67% (Figure 75). However, the lack of a predominant conformer meant that selective NOE experiments proved to be inconclusive. Thus, in order to determine the geometry of the major conformer, further NMR experiments were undertaken. From selectively decoupled  $^{13}\text{C}$  and 2D  $J$ -resolved measurements from a  $J$ -HMBC experiment, the  $^3J_{\text{CH}}$  couplings for the quaternary acetylene carbon and  $\text{H}_\text{A}$  and  $\text{H}_\text{B}$  have been determined. The values of the  $^3J_{\text{CH}}$  and  $^3J_{\text{CHA}}$  are 3.4 Hz and  $^3J_{\text{CHB}}$  is 3.9 Hz (Figure 76). A Karplus type relationship indicates that this corresponds to the geometry with the hydroxyl group orientated towards the double bond. For the opposite geometry, one large and one small  $^3J_{\text{CH}}$  coupling constants are expected, based on the Karplus relationship.

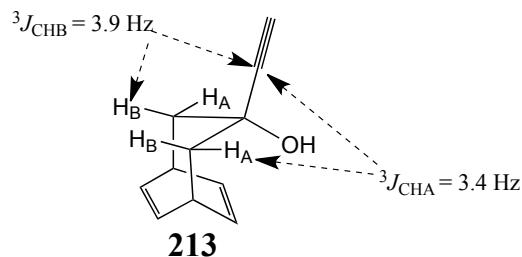


**Figure 76** Representation of the torsional angles of alcohol **213** measured from  $J$  HMBC NMR experiments in  $\text{CDCl}_3$

To complement these NMR experiments, DFT calculations were carried out by Dr Aliev. To determine the boundary values for the  $^3J_{\text{CH}}$  couplings, calculations were done at the B3LYP level of theory using Gaussian 09. In the conformation where the hydroxyl group is orientated towards the double bond, the boundary values are  $^3J_{\text{CHA}} = 5.42$  Hz and  $^3J_{\text{CHB}} = 6.48$ . For the opposite conformer, the boundary values are  $^3J_{\text{CHA}} = 1.09$  Hz and  $^3J_{\text{CHB}} = 3.52$ . Using these boundary values and the measured values for the  $^3J_{\text{CH}}$  coupling constants, the conformational population for the conformer with the hydroxyl group orientated towards the double bond can be estimated as 57%. The difference between the calculated and experimental values for the conformational population is 10%.

This provides an intriguing result, demonstrating once again that, as in the propanoanthracene series, the strength of the O-H/ $\pi$  interaction can be counterbalanced by the terminal alkyne.

#### 2.7.1.2 Oxathiolane 219 and epoxide 218 derivatives

Spirocyclic substrates, provide the opportunity to study the influence of a heteroatom in proximity to a  $\pi$ -cloud. Unfortunately, in the parent diene series we were unable to prepare a pure sample of the epoxide derivative **218** as it readily decomposed. However it was possible to draw some preliminary conclusions about its conformational population from the coupling constants measured from the  $^1\text{H}$  NMR spectrum of the crude reaction product.



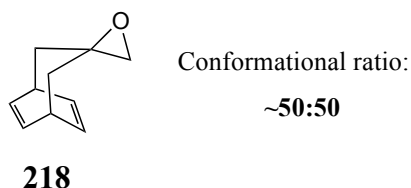


**Figure 77** Representation of the epoxide derivative **218**

No preference for either conformer was observed, suggesting that the strained geometry of the three-membered ring prevents either the oxygen atom or the methylene protons from interacting with the  $\pi$  cloud of the double bond (Figure 77). A similar situation was previously encountered in the propanoanthracene series, and hence, this was not a surprising observation. However this is only a preliminary result, and to confirm the conformational ratio of this substrate further work is required.

By way of contrast, for the oxathiolane substrate **219**, one predominant conformer was observed in  $\text{CDCl}_3$  solution (Figure 78). Due to the large steric difference between an oxygen and a sulphur atom, most organic chemists are tempted to predict that the oxygen atom would be positioned above the double bond.

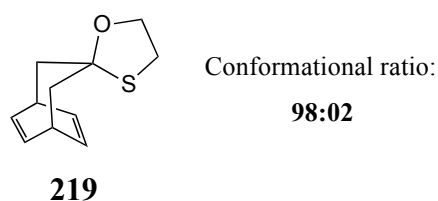


**Figure 78** Representation of the predominant conformer of the oxathiolane **219** in  $\text{CDCl}_3$  solution at 298 K

However, the  $^1\text{H}$  NMR spectra and NOE data, confirm that, in actual fact, the sulphur atom is positioned above the double bond. With a conformational population of 92%. Thus, the S- $\pi$  interaction appears to be significantly stronger

than the O- $\pi$  interaction. This tendency, which had previously been observed to a lesser extent in the propanoanthracene system<sup>159,160</sup> (conformational ratio 77:23) can possibly be attributed to the enhanced polarisability of the sulphur atom and the availability of its empty 3*d*-orbitals.

### 2.7.2 Effects of temperature on the parent diene system in CDCl<sub>3</sub>

As the conformational ratio can be perturbed by varying the temperature at which it is studied, the parent diene derivatives were studied at a range of temperatures. However, as the predominant conformer is overwhelmingly observed at room temperature for many of the derivatives, no significant observations were made.

Thus, for the tertiary alcohols, the conformational ratio was not significantly perturbed by varying the temperature at which it was studied. Consequently little information about the nature of the O-H/ $\pi$  interaction can be extracted from these experiments. The effects of temperature gradient on the conformational ratio and chemical shifts of the methyl alcohol **209** are shown in Table 7.

T (K)	$\Delta\delta$ (ppm)				$^3J_{5,4A}$ (Hz)	$^3J_{5,4B}$ (Hz)	$P_A$
	H <sub>4A</sub>	H <sub>4B</sub>	OH	CH <sub>3</sub>			
334	0.01	0.01	-0.18	0.01	6.4	1.4	100:0
320	0.01	0.01	-0.11	0.01	6.4	1.3	100:0
297	0	0	0	0	6.5	1.3	100:0
276	-0.01	0	0.08	0	6.5	1.3	100:0
254	-0.01	-0.01	0.17	0	6.5	1.2	100:0
232	-0.03	-0.01	0.24	0	6.5	1.2	98:02
210	-0.02	-0.02	0.29	0	6.5	1.1	99:01

**Table 7** Difference of chemical shifts and conformational ratios over a range of temperatures for the tertiary alcohol **209**

Studying the tertiary alcohols **209**, **210** and **211** at low temperature proved that the one conformer is predominant at room temperature as there was little change in the coupling constants at low temperature. It is also of note that the oxathiolane shows similar behaviour to the tertiary alcohols at low temperatures.

### 2.7.2.1 Studies of the propargylic alcohol at low temperatures

The propargylic alcohol **213** (Figure 79) however displayed much more interesting behaviour at low temperatures. Thus at room temperature the ratio of the two conformers was 67:33 and, on cooling it increased to 86:14 at 210 K. Accordingly, the conformational ratio is clearly dependent on the temperature at which it is studied.

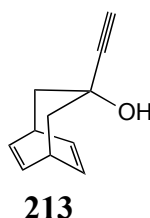


Figure 79

The structure of the predominant conformer was confirmed by selective NOE experiments which were conducted at 232 K and 210 K, as the major conformer is more dominant at this temperature. On cooling, a small downfield shift is observed for both the hydroxyl and acetylene protons in the  $^1\text{H}$  NMR spectrum (Table 8). A more interesting observation at low temperature is that the chemical shifts of  $\text{H}_{4\text{A}}$  and  $\text{H}_{4\text{B}}$  switched place, and at 276 K and 254 K the two peaks overlap.

T (K)	$\Delta\delta$ (ppm)				$^3J_{5,4A}$ (Hz)	$^3J_{5,4B}$ (Hz)	$P_A$
	H <sub>4A</sub>	H <sub>4B</sub>	OH	CH			
334	-0.03	0.03	-0.24	-0.02	4.5	3.2	61:39
320	-0.02	0.02	-0.15	-0.02	4.6	3.2	63:37
297	0	0	0	0	4.7	3.0	66:34
276	n/a	n/a	0.16	0.02	4.5	3.2	63:37
254	n/a	n/a	0.31	0.03	4.6	3.1	64:36
232	0.10	-0.06	0.47	0.05	5.3	2.3	78:22
210	0.12	-0.08	0.60	0.07	5.7	1.8	86:14

**Table 8** Difference of chemical shifts and conformational ratios over a range of temperatures for the tertiary alcohol **213**

Unusual behaviour of the tertiary acetylenic alcohol had previously been observed in the propanoanthracene series which had exhibited an approximately equal population of both conformers in CDCl<sub>3</sub> at 298 K.<sup>160</sup> On cooling a CFCl<sub>3</sub>/CD<sub>2</sub>Cl<sub>2</sub> solution, a very significant upfield shift for the acetylenic proton occurred from  $\delta = 2.07$  ppm at 235 K to  $\delta = 0.51$  ppm at 163 K. Based on the anisotropy of the ring current effect this shift was indicative of dimer formation with an acetylenic C-H/ $\pi$  interaction and this was further supported by a single crystal X-Ray crystal structure determination, which is reproduced in Figure 80.

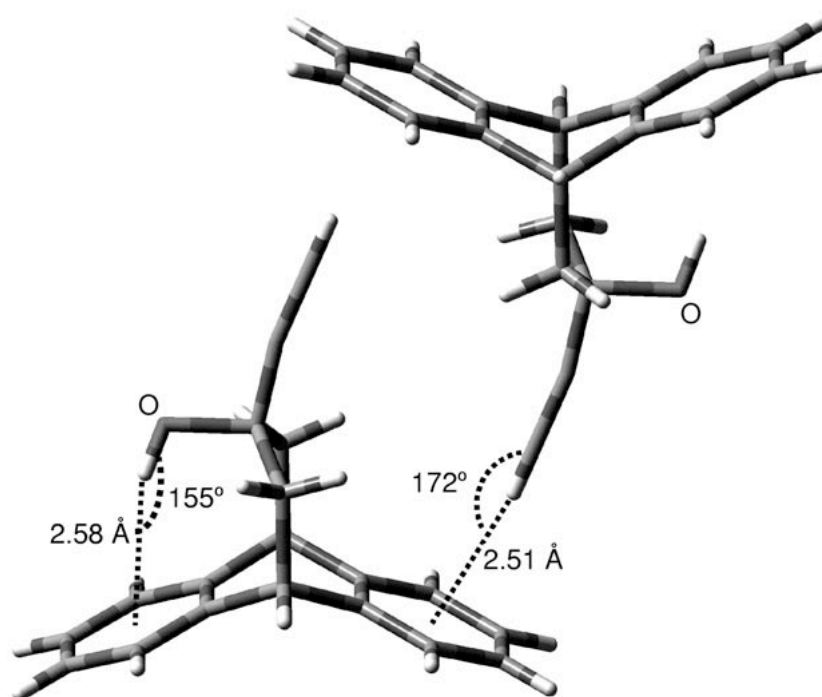


**Figure 80** Crystal structure of alcohol **169** which presents the intermolecular C-H/ $\pi$  interaction<sup>161</sup>

In the present instance, for the tertiary acetylenic alcohol in the parent diene system, conversely, a small downfield shift in the acetylenic proton occurs on cooling. However, dimer formation may still occur in this substrate, and the overlapping of the chemical shifts of  $H_{4A}$  and  $H_{4B}$  is indicative of this. Unfortunately further evidence of this phenomenon could not be obtained, as it was not possible to obtain an X-Ray crystal structure for this substrate.

### 2.7.3 Solvent dependence studies

It is well recognised that the nature of the solvent can have a profound effect on any non-covalent arene interaction and hence this is always a very important topic in molecular recognition. As emphasized earlier, a considerable advantage of any dynamic molecular balance system over single crystal X-Ray diffraction is that it allows such solvation effects to be explored. As the magnitudes of stabilisation energy of weak non-covalent interactions and that of solvation are

often similar, it is important to study such interactions in a range of polar and non-polar solvents. As in our earlier studies in the propanoanthracene series, we therefore decided to investigate the solvent dependence of the parent diene derivatives in various different deuterated solvents at room temperature. From the range of solvents chosen, we thought that deuterated benzene may display interesting results as it gives the opportunity for a competing  $\pi$ -interaction to occur. We also chose to study the derivatives in a range of solvents that display high polarity and hydrogen-bond forming capacity with the expectation that these would perturb the interactions and significantly alter the conformational ratios. The conformational ratios calculated for the parent diene derivatives in a range of solvents are reported in Appendix 1. The results clearly show the dramatic impact that varying the nature of the solvent can have on the conformational ratios.

For ease of comparative assimilation the results of the solvent studies are also presented as a range of graphs. For the horizontal axis we chose to order the solvents by their hydrogen bond forming capacity and not by their dielectric constant as the results correlate better with this parameter, as shown by previous studies within our group (Table 9).<sup>160</sup>

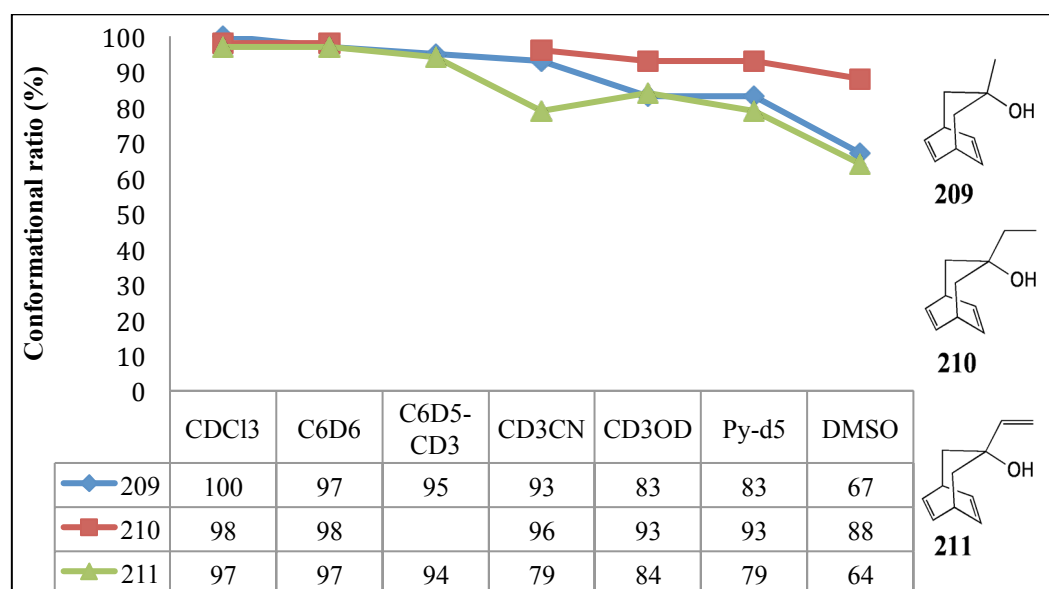
	<b>CDCl<sub>3</sub></b>	<b>C<sub>6</sub>D<sub>6</sub></b>	<b>C<sub>6</sub>D<sub>5</sub>- CD<sub>3</sub></b>	<b>CD<sub>3</sub>CN</b>	<b>CD<sub>3</sub>OD</b>	<b>Py-<i>d</i><sub>5</sub></b>	<b>DMSO</b>
<b><math>\epsilon</math></b>	4.7	2.3	2.4	35.7	32.6	12.3	46.8
<b><math>\beta</math></b>	0.8	2.2	2.2	4.7	5.8	7.0	8.9

**Table 9** Dielectric constant  $\epsilon$  and hydrogen bond acceptor parameter  $\beta$  for the range of solvents used

### 2.7.3.1 Effects of the solvent nature on the conformational equilibria of alcohol derivatives

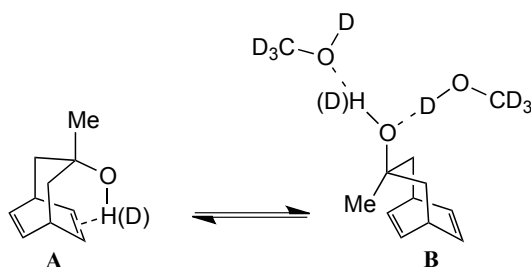
The behaviour of the tertiary alcohols **209**, **210** and **211** clearly illustrate the importance of the nature of the solvent on the conformational equilibrium. For the methyl alcohol **209**, the population of the predominant conformer decreases

drastically on increasing the hydrogen bond acceptor character of the solvent, as illustrated by Figure 81. In apolar solvents such as  $C_6D_6$  and  $CDCl_3$ , the conformer with the hydroxyl group directed towards the alkene is preferred almost exclusively but in solvents capable of forming hydrogen bonds with the hydroxyl group, the conformational ratio significantly drops as the minor conformer is stabilized by hydrogen bonding to solvent. However, the ethyl alcohol **210**, displays a less drastic variation of the conformational ratio and this is possibly due to steric hindrance of the more bulky ethyl group. Overall, similar behaviour was noted for the  $sp^2$  hybridised vinyl alcohol **211**.



**Figure 81** conformational ratios of tertiary alcohols **209**, **210** and **211** in a range of solvents, ranked in order of their hydrogen bond forming capacity at 298 K

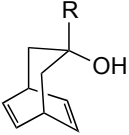
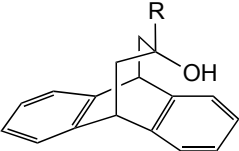
These results confirm, as expected that, solvents with high hydrogen bond forming capability such as  $CD_3OD$ , pyridine- $d_5$  or  $DMSO-d_6$ , can counterbalance the intramolecular  $\pi$ -interaction and hence have an effect on the conformational ratio (Figure 82).



**Figure 82** Conformational equilibrium of tertiary alcohol **209** between conformers A and B, which are stabilised by intramolecular O-H/ $\pi$  interactions and by solute-solvent interactions respectively

Interestingly the conformational ratio for the alcohol **209** in  $\text{CD}_3\text{OD}$  is 83%, indicating that the hydrogen bond donor properties of methanol do not participate significantly in the solvation of the hydroxyl group. For all three of the alcohols, the conformational ratio in  $\text{CD}_3\text{OD}$  remains above 50%, indicating that the solute-solvent interaction does not dominate over the intramolecular O-H/ $\pi$  interaction.

At this moment in time, it was particularly exciting to compare the solvent behaviour with those tertiary alcohols which had previously been studied in the propanoanthracene series (Table 10).<sup>159,160</sup>

Solvent	R		
<b><math>\text{CD}_3\text{OD}</math></b>	Me	82:18	60:40
	$\text{CH}=\text{CH}_2$	84:16	62:38
<b>Py-<math>d_5</math></b>	Me	82:18	51:48
	$\text{CH}=\text{CH}_2$	79:21	n/a
<b>DMSO</b>	Me	66:34	50:50
	$\text{CH}=\text{CH}_2$	64:36	55:45

**Table 10** Conformational ratios for methyl and vinylic alcohols in the parent diene and propanoanthracene series in a range of solvents at 298 K



Examination of these results from the standpoint of comparing the relative strengths of a  $\pi$  facial intramolecular hydrogen bond either to an aromatic ring or to an alkene would suggest that a stronger hydrogen bond is formed in the latter case. It should be emphasised however that such comparisons are dangerous since solvation effects are not limited to functional groups but to the entire molecular architecture which, in the present case is substantially different.

It was significant to note that, as in the propanoanthracene case, the propargylic alcohol **213** displayed significantly different solvent effects when compared to the other tertiary alcohols.<sup>160</sup> In this case, the predominant conformer was very dependent on the nature of the solvent (Figure 83). Unfortunately however, the sample decomposed in deuterated pyridine, and so it was not possible to obtain any information about the interaction in this solvent.

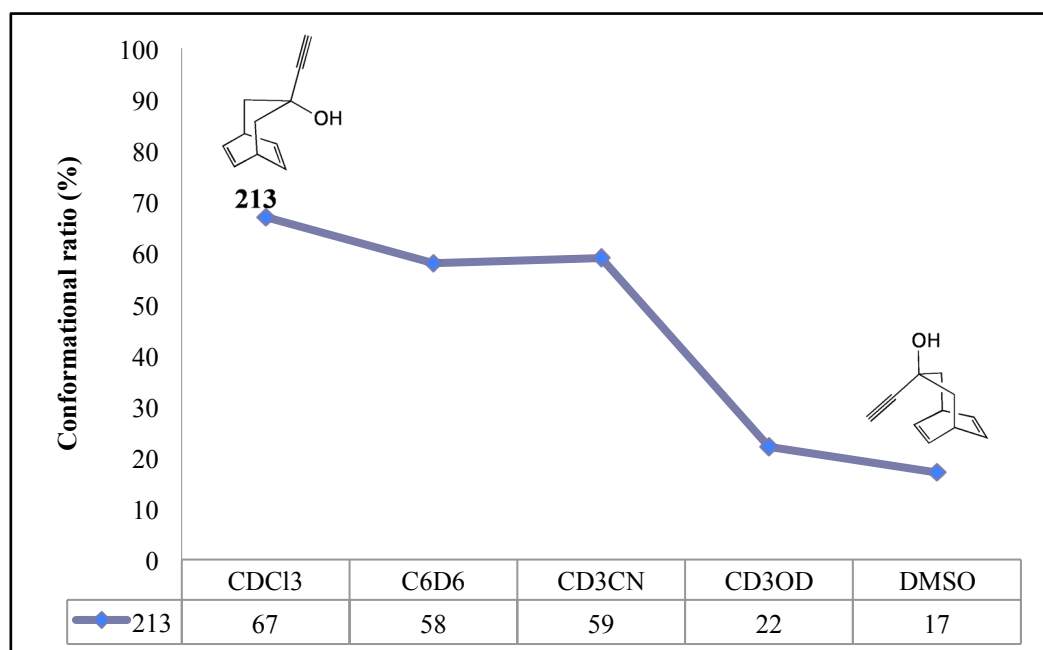


**Figure 83** Conformational ratio of tertiary alcohol **213** in a range of solvents, ranked in order of their hydrogen bond forming capacity at 298 K

In general, the conformational ratio decreases when progressing from apolar to solvents with more hydrogen bonding capability. In apolar solvents, the major conformer has the hydroxyl group orientated towards the double bond. However, in polar solvents, the opposite conformer is predominant with the

alkyne group orientated towards the double bond, with conformational ratios of up to 83% (Figure 84). This provides a powerful demonstration of the influence that solute-solvent interactions can have on the total stabilisation of the conformer. For this substrate, the O-H/ $\pi$  interaction can be effectively counterbalanced by the interaction between the hydroxyl group and the solvent.

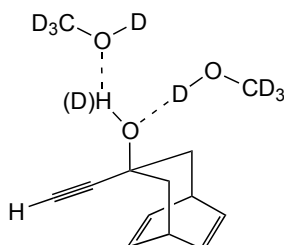


**Figure 84** Representation of the major conformer of alcohol **213** in CD<sub>3</sub>OD solution at 298 K

In polar solvents the chemical shifts of the H<sub>4A</sub> and H<sub>4B</sub> protons switch places, and this alerted us to the change in predominant conformer. The differences in chemical shifts relative to CDCl<sub>3</sub> for the propargylic alcohol **213** are shown in Table 11.

Solvent	$\Delta\delta$ (ppm)				$^3J_{5,4A}$ (Hz)	$^3J_{5,4B}$ (Hz)	$P_A$
	H <sub>4A</sub>	H <sub>4B</sub>	OH	C $\equiv$ CH			
C <sub>6</sub> D <sub>6</sub>	-0.16	-0.1	-0.56	-0.35	4.4	3.5	58:42
CDCl <sub>3</sub>	0	0	0	0	4.7	2.9	67:33
CD <sub>3</sub> CN	0.03	-0.39	0.28	0.2	4.4	3.4	59:41
CD <sub>3</sub> OD	-0.4	0.04	n/a	0.3	5.5	2.5	22:78
DMSO	-0.56	-0.11	2.09	0.72	5.7	2.2	17:83
D <sub>2</sub> O	-0.36	0.09	n/a	0.45	5.3	2.6	26:74

**Table 11** Difference of chemical shifts, conformational ratios and observed coupling constants for the tertiary alcohol **213** in a range of solvents at 298 K

Interestingly, this substrate displays different behaviour in CDCl<sub>3</sub> and C<sub>6</sub>D<sub>6</sub> whereas most of the other alcohol derivatives have similar conformational ratios in both solvents. The chemical shift of the acetylenic proton is shifted upfield

by 0.35 ppm. This may be due to the aromatic ring of the solvent forming non-covalent interactions with the functional groups on the bridge. Unfortunately, when studying the interaction in CD<sub>3</sub>OD the alkyne proton is readily deuterated, and this hindered any attempts to prove the structure by NOE experiments. Therefore alternative NMR techniques were employed to confirm the structure of the major conformer in CD<sub>3</sub>OD. From selectively decoupled <sup>13</sup>C and 2D *J*-resolved measurements, the <sup>3</sup>*J*<sub>CH</sub> couplings for the quaternary acetylene carbon and H<sub>A</sub> and H<sub>B</sub> have been determined. The values of the <sup>3</sup>*J*<sub>CH</sub> are <sup>3</sup>*J*<sub>CHA</sub> is 5.4Hz and <sup>3</sup>*J*<sub>CHB</sub> is 6.2Hz. A Karplus type relationship indicates that a coupling of this magnitude correspond to torsional angles of 39° (5.4Hz) and 154° (6.2Hz), which correspond to the geometry with the alkyne orientated towards the double bond (Figure 85). For the opposite conformer torsional angles of 40° and -70° would be expected.

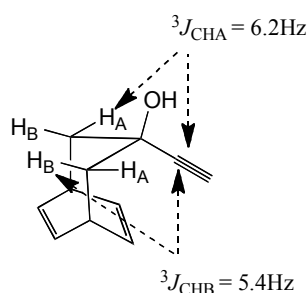


**Figure 85** Representation of the torsional angles of alcohol **213** measured from *J* HMBC NMR experiments in CD<sub>3</sub>OD

## 2.8 Results from the propanonaphthalene system

### 2.8.1 Introduction

In the first instance, it must be admitted that the decision to prepare derivatives of a propanonaphthalene system was taken largely on synthetic grounds and as a result of the frustrations experienced when faced by the volatility and high

chemical reactivity of the parent diene system, which had precluded the preparation of several desirable derivatives.

From the standpoint of comparing and contrasting non-covalent functional group interactions of aromatic and olefinic systems, it was argued that such a series would serve as an interesting system in its own right and also as a further excellent internal check on the measurements already made. Thus, as illustrated in Figure 86, the considerable advantage of being able to prepare both diastereoisomers of this system would allow comparative solvent studies to be made within a single molecular framework.

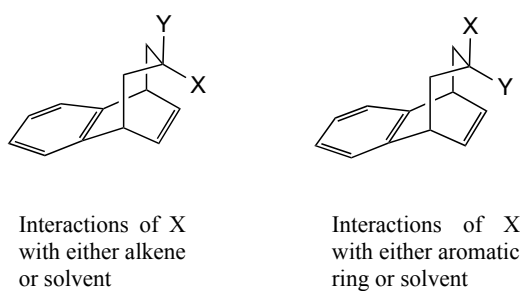


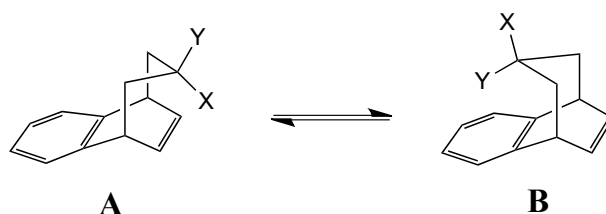
**Figure 86** Interactions present in diastereoisomers **181** and **182** of the propanonaphthalene system

### 2.8.2 Relative strengths of functional group interactions in $\text{CDCl}_3$

As with the parent diene system measurements of the conformational ratios were obtained under comparable conditions of temperature and solvent. In this section attempts will be made to provide accurate quantitative data to compare a series of propanonaphthalene derivatives. The structures of the predominant conformers and their conformational ratios have been determined using the methods described earlier. As it is of interest to compare the behaviour in solution with that in the solid state, wherever possible, single crystal structures

of the derivatives were obtained, particularly since this proved to be problematic in the parent diene system.

The results of the studies in  $\text{CDCl}_3$  are presented in Table 12. In all cases, the structure of the diastereoisomers and the predominant conformers were determined by NOE experiments.



	X	Y	$^3J_{5,4A}$ (Hz)	$^3J_{5,4B}$ (Hz)	$P_A$	$\Delta G^\circ$ $\text{kJ mol}^{-1}$
<b>226</b>	H	OH	7.4	0.9	100:0	7.3
<b>227</b>	OH	H	6.5	1.2	12:88	4.9
<b>229</b>	Me	OH	6.5	1.5	05:95	7.3
<b>228</b>	OH	Me	6.5	1.5	95:05	7.3
<b>230</b>	Et	OH	6.7	1.2	0:100	0
<b>231</b>	OH	Et	6.7	1.3	99:01	11.4
<b>232</b>	$\text{CH}=\text{CH}_2$	OH	6.0	1.9	13:87	3.6
<b>233</b>	OH	$\text{CH}=\text{CH}_2$	6.3	1.7	92:08	6.1
<b>236</b>	$\text{C}\equiv\text{CH}$	OH	5.2	2.8	28:72	2.3
<b>237</b>	OH	$\text{C}\equiv\text{CH}$	4.4	3.7	44:56	0.6
<b>242</b>	CN	OH	6.0	2.2	85:15	4.3
<b>241</b>	OH	CN	4.9	3.1	34:66	1.6
<b>244</b>	-O-	-S-	6.4	1.9	09:91	5.7
<b>243</b>	-S-	-O-	6.1	2.2	85:15	4.3

**Table 12** Equilibrium ratios, experimental coupling constants and energy differences between conformers of the propanonaphthalene derivatives in  $\text{CDCl}_3$  at 298 K

### 2.8.2.1 Alcohol derivatives – Importance of the O-H/ $\pi$ interaction

As we have already stated, the intramolecular  $\pi$  facial hydrogen bond between a hydroxyl group and an aromatic ring is a well established non-covalent interaction, especially relative to the lesser known analogous interaction with an

olefinic  $\pi$ -cloud. Consequently, it was certainly of interest to study both of these interactions within the propanonaphthalene system.

For the secondary alcohols, the two diastereoisomers **226** and **227** were separated chemically, as described previously. In solution, the populations of the predominant conformers of the secondary alcohol are 100 and 88% respectively, with the hydrogen atom positioned above either the double bond or the aromatic ring as shown in Figure 87.

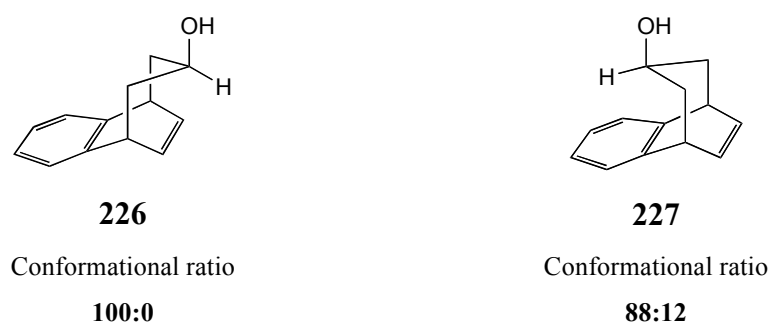


**Figure 87** Representation of the major conformers of alcohols **226** and **227** in  $\text{CDCl}_3$  solution at 298 K

In these substrates there is a significant steric difference between the hydroxyl group and the hydrogen atom and the O-H/ $\pi$  interactions with either the aromatic ring or the double bond does not appear to be strong enough to compensate for the difference in van der Waals radius. For both diastereoisomers **226** and **227**, the preferred conformer can therefore be attributed to the significant steric difference between the substituents on the flexible bridge.

For the tertiary alcohols **228**, **229**, **230** and **231** one predominant conformer (> 90%) was observed (Figure 88). For the methyl alcohols **228** and **229** the conformational ratios are 95% for each diastereoisomer, and for the ethyl alcohols **230** and **231** the conformational ratios are 100 and 99% respectively. This indicates that the energetic difference between the two conformers is above  $7 \text{ kJ mol}^{-1}$ , and for each diastereoisomer, the OH/ $\pi$  interaction is dominant.

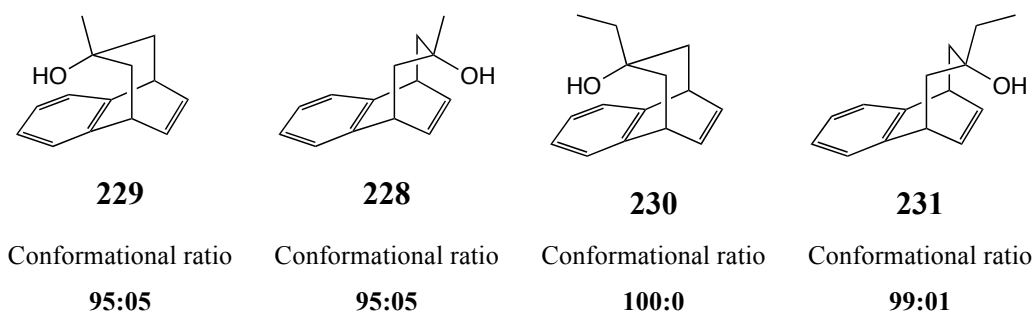


**Figure 88** Representation of the predominant conformers of alcohols **228**, **229**, **230** and **231** in  $\text{CDCl}_3$  solution at 298 K

These results signify that in this case varying the size of the alkyl group does not have a significant effect on the stabilisation of the conformer and also that the olefinic and aromatic interactions are of similar strengths for these substrates in this solvent.

However the vinylic alcohol derivatives **232** and **233** do not adhere strictly to this trend, as the diastereoisomer **232** with the hydroxyl group orientated towards the aromatic ring displays a slightly lower conformational ratio as shown in Figure 89.

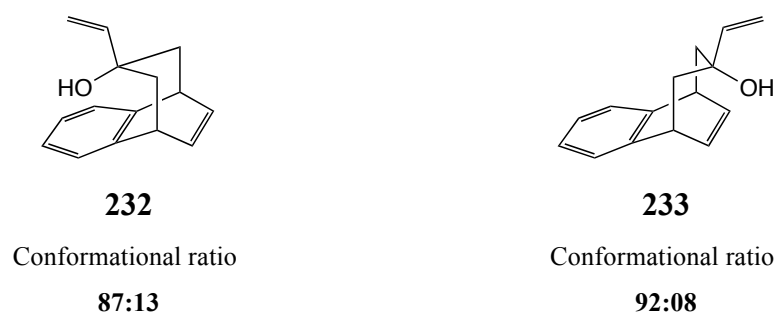


**Figure 89** Representation of the major conformers of alcohols **232** and **233** in  $\text{CDCl}_3$  solution at 298 K

This observation was initially attributed either to the increased steric hindrance between the aromatic ring and the vinyl group when compared to the alkene and

the vinyl group, however difference in the two conformational ratios is within the error range calculated for this system.

Once again, the conformational ratios of the propargylic alcohols **236** and **237** do not show one predominant conformer. Unlike the  $sp^3$  and  $sp^2$  hybridised tertiary alcohol derivatives, the two diastereoisomers **236** and **237** have opposing major conformers. Thus in this case there was found to be a considerable difference between the conformational ratios of the two diastereoisomers **236** and **237**, being 72 and 56% respectively (Figure 90).

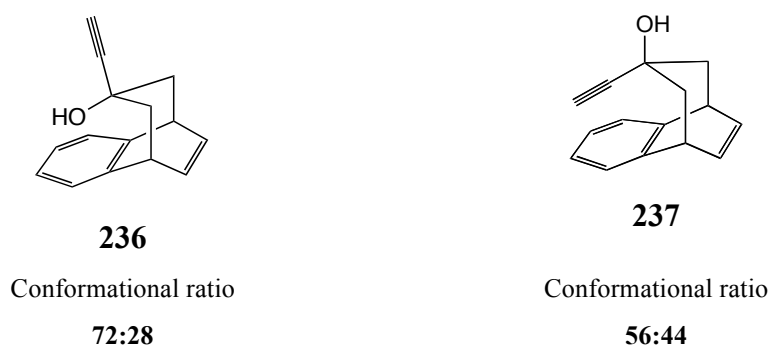


**Figure 90** Representation of the major conformers of alcohols **236** and **237** in  $CDCl_3$  solution at 298 K

This exciting result demonstrates a significant difference between olefinic and aromatic  $\pi$ -interactions. For the diastereoisomer **237**, the two conformers are almost equally populated suggesting that any interaction between the terminal alkyne and either the solvent or the aromatic ring is of a similar strength to the O-H/ $\pi$  interaction. Even more surprisingly perhaps is the conclusion that, in  $CDCl_3$ , the O-H/ $\pi$  interaction is stronger with the aromatic ring than with the alkene.



### 2.8.2.2 Cyanohydrin derivatives – The influence of a cyano group

For both diastereoisomers of the cyanohydrin derivatives **241** and **242**, the conformer with the nitrile group orientated towards the aromatic ring or double bond is favoured. The conformational ratios of the two diastereoisomers **241** and **242** are 85 and 66% respectively (Figure 91). The absolute stereochemistry and major conformer of these derivatives was determined by NOE experiments.

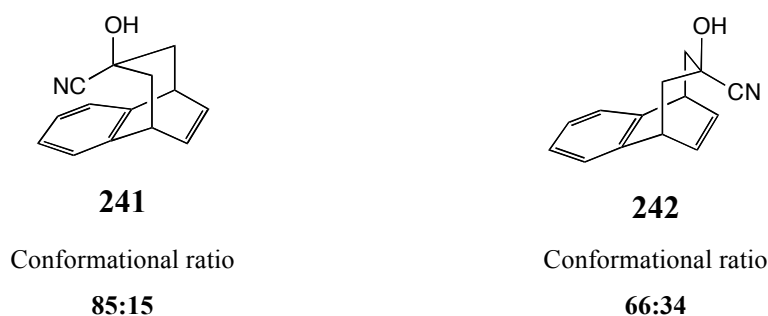


**Figure 91** Representation of the major conformers of alcohols **241** and **242** in CDCl<sub>3</sub> solution at 298 K

For the derivative **242** the conformational ratio suggests that the O-H/ $\pi$  interaction is strong enough to counterbalance the interaction between the nitrile and the double bond. The significant difference in the two conformational ratios implies that the C $\equiv$ N/ $\pi$  interaction is stronger with an aromatic  $\pi$  source, and, given the presumably similar steric requirements of a terminal alkyne, comparison of **241** with **237** may imply a polar component to this interaction. Unfortunately we were unable to prepare the analogous substrate for the parent diene system. This would allow us to gain further insight into the interactions present.

### 2.8.2.3 Oxathiolane derivatives **243** and **244**

As with the parent diene system, NOE experiments proved that for both substrates **243** and **244**, the sulphur atom prefers to be orientated towards the

aromatic ring or double bond. The conformational ratios in  $\text{CDCl}_3$  solution were determined to be 91 and 85% respectively (Figure 92).

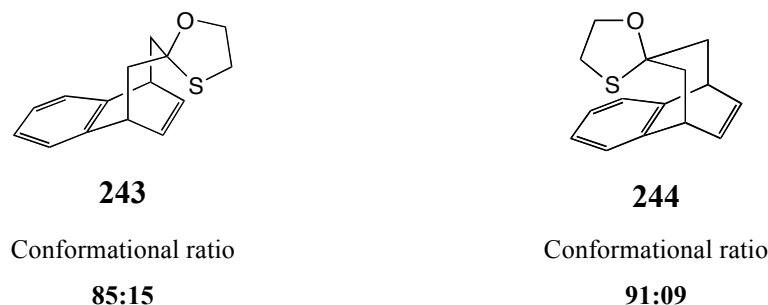


**Figure 92** Representation of the major conformers of alcohols **243** and **244** in  $\text{CDCl}_3$  solution at 298 K

The dominance of the conformer with the sulphur atom down in both diastereoisomers suggests that the S- $\pi$  interaction is significantly stronger than the O- $\pi$  interaction for both an aromatic ring and for an alkene. This remarkable result can perhaps be attributed to the enhanced polarisability of the sulphur atom and the availability of its empty 3*d*-orbitals.

### 2.8.3 Effects of temperature on the propanonaphthalene system in $\text{CDCl}_3$

As mentioned when studying the parent diene system, it is important to study the propanonaphthalene substrates at a range of temperatures as the conformational ratio can be perturbed by varying the temperature at which it is studied. Once again, for many of the substrates a predominant conformer is observed at room temperature and therefore no significant observations were made when studying these substrates over a range of temperatures. However, substrates such as the propargylic alcohols **236** and **237** and the cyanohydrins **241** and **242** show interesting results when studied over a range of temperatures.

### 2.8.3.1 Effects of temperature on the propargylic alcohols **236** and **237**

At low temperatures there is little change in the conformational ratio of the alcohol **236**, at room temperature the conformation ratio is 72% and on cooling it increases to 77% at 210 K.

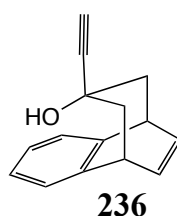


Figure 93

There is also little variation in the chemical shifts of the acetylene, hydroxyl and the protons on the flexible bridge, as shown in Table 13.

T (K)	$\Delta\delta$ (ppm)				$^3J_{5,4A}$ (Hz)	$^3J_{5,4B}$ (Hz)	$P_A$
	H <sub>4A</sub>	H <sub>4B</sub>	OH	C≡CH			
334	0.01	0.03	-0.01	-0.01	4.9	3.0	68:32
320	0.01	0.02	0	-0.01	5.0	3.0	68:32
297	0	0	0	0	5.1	2.8	72:29
276	0.03	0	0.03	0.04	5.2	2.8	72:28
254	0.04	-0.01	0.05	0.07	5.3	2.6	74:26
232	0.05	-0.01	0.06	0.08	5.4	2.6	76:24
210	0.06	-0.02	0.08	0.09	5.5	2.5	77:23

Table 13 Difference of chemical shifts and conformational ratios over a range of temperatures for the tertiary alcohol **236**

However, the diastereoisomeric propargylic alcohol **237** displays slightly more interesting behaviour when studied over a range of temperatures. Since at low temperatures, protons H<sub>4A</sub> and H<sub>4B</sub> overlap, it was only possible to get an estimate of the conformational ratio at 232 K.

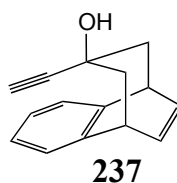


Figure 94

At room temperature the two conformers are almost equally populated, however at 254 K no preference for either conformer is observed and there is a slight downfield shift of the hydroxyl and acetylene protons in the  $^1\text{H}$  NMR spectrum (Table 14).

T (K)	$\Delta\delta$ (ppm)				$^3J_{5,4A}$ (Hz)	$^3J_{5,4B}$ (Hz)	$P_A$
	$H_{4A}$	$H_{4B}$	OH	$C\equiv CH$			
<b>334</b>	0.02	-0.03	-0.2	-0.04	4.6	3.3	62:38
<b>320</b>	0.01	-0.02	-0.13	-0.02	4.5	3.5	60:40
<b>297</b>	0	0	0	0	4.4	3.7	57:43
<b>276</b>	-0.01	0.02	0.14	0.04	4.1	3.9	53:47
<b>254</b>	-0.07	0.10	0.31	0.07	4.1	4.0	51:49
<b>232</b>	n/a	n/a	n/a	n/a	4.0	4.0	49:51

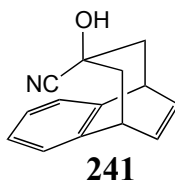
**Table 14** Difference of chemical shifts and conformational ratios over a range of temperatures for the tertiary alcohol **237**

When the substrate is studied at high temperatures, the rate of conformational motion should increase, and a slight increase in preference of one conformer over the other is observed.

### 2.8.3.2 Effects of temperature on the cyanohydrins **241** and **242**

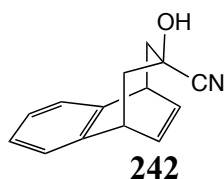
When studying the cyanohydrin, both diastereoisomers **241** and **242** display a clear trend. When the temperature is decreased the conformational ratio approaches 100 and when studying the conformational ratio at elevated

temperatures the ratio decreases. The effects of the temperature gradient on the conformational ratio and chemical shifts of the cyanohydrin substrates are shown in Table 15 and Table 16.



T (K)	$\Delta\delta$ (ppm)			$^3J_{5,4A}$ (Hz)	$^3J_{5,4B}$ (Hz)	$P_A$
	H <sub>4A</sub>	H <sub>4B</sub>	OH			
334	-0.01	0.02	-0.14	5.8	2.4	81:19
320	-0.01	0.02	-0.10	5.8	2.3	82:18
297	0	0	0	5.9	2.1	84:16
276	0	-0.02	0.13	6.1	2.0	87:13
254	0.01	-0.05	0.32	6.3	1.8	91:09
232	0.01	-0.07	0.43	6.4	1.7	93:07
210	0.01	-0.11	0.62	6.5	-	96:04

**Table 15** Difference of chemical shifts and conformational ratios over a range of temperatures for the tertiary alcohol **241**



T (K)	$\Delta\delta$ (ppm)			$^3J_{5,4A}$ (Hz)	$^3J_{5,4B}$ (Hz)	$P_A$
	H <sub>4A</sub>	H <sub>4B</sub>	OH			
334	-0.01	0.03	-0.17	4.7	3.1	64:36
320	-0.01	0.02	-0.14	4.8	3.1	65:35
297	0	0	0	4.9	3.0	67:33
276	0.01	-0.03	0.17	5.2	3.0	70:30
254	0.02	-0.06	0.45	5.5	2.7	75:25
232	0.04	-0.10	0.73	5.5	2.5	77:23
210	0.05	-0.16	1.16	6.1	1.8	89:11

**Table 16** Difference of chemical shifts and conformational ratios over a range of temperatures for the tertiary alcohol **242**

Temperature also has an interesting effect on the chemical shifts of the hydroxyl and bridgehead protons. Clear trends can be observed for both diastereoisomers **241** and **242**. The hydroxyl group is significantly shifted downfield as the temperature is decreased. It is also worth noting that the change in chemical shift of H<sub>4A</sub> is less significant than for H<sub>4B</sub>.

### 2.8.3.3 Some preliminary conclusions from the studies of the propanonaphthalene derivatives in CDCl<sub>3</sub> solution

The results from our studies in CDCl<sub>3</sub> solution have shown that the propanonaphthalene system can act as a balance and allow us to compare the various interactions present. By studying the different diastereoisomers we have gained an insight into the differences between olefinic and aromatic  $\pi$ -interactions. Whilst confirming the overwhelming preference for the tertiary alkyl alcohols to exhibit a strong O-H/ $\pi$  interaction, little information can be gleaned from the studies in CDCl<sub>3</sub> alone as to the relative strengths of the O-H/ $\pi$  (arene) versus the O-H/ $\pi$  (alkene) interaction.

However, the vinyl alcohols **232** and **233** do not at first sight appear to follow this trend. This result may arise from an increase in steric hindrance. Once again, the propargylic alcohols **236** and **237** display interesting results, indicating the importance of sterics and the acidity of the acetylenic proton of this functional group. The cyanonhydrins **241** and **242** are interesting substrates, especially when compared with the propargylic alcohols **236** and **237**. Once again the oxathiolane substrates **243** and **244** offer an exciting insight into the relative strengths of S/ $\pi$  interactions and strengthen the observations made in the parent diene system.

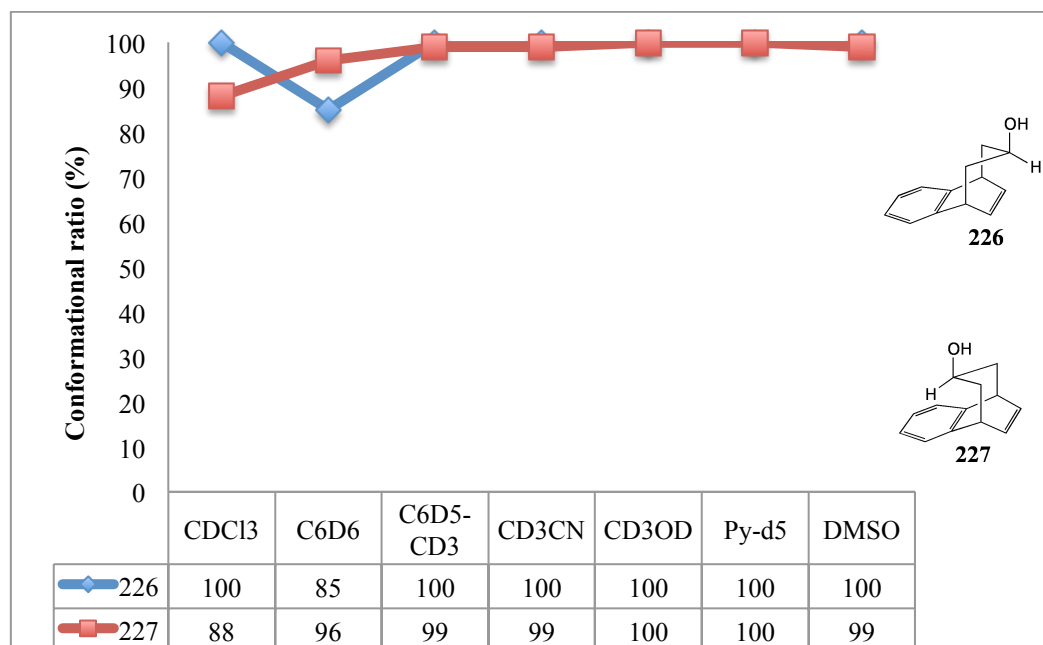
## 2.8.4 Solvent dependence studies

As already established, it is of fundamental importance to study non-covalent  $\pi$  interactions in a range of different solvents. Consequently, we decided to study the conformational ratios of the propanonaphthalene series in a range of different solvents in an analogous fashion to the parent diene system. The conformational ratios calculated for the propanonaphthalene derivatives in a range of solvents are reported in Appendix 2. The results show the dramatic impact that varying the solvent can have on the  $\pi$ -interactions.

As in the parent diene system the results of the solvent studies are also presented as a range of graphs with the horizontal axis chosen to order the solvents by their hydrogen bond forming capacity and not their dielectric constant. The conformational ratio as a percentage is plotted on the vertical axis.

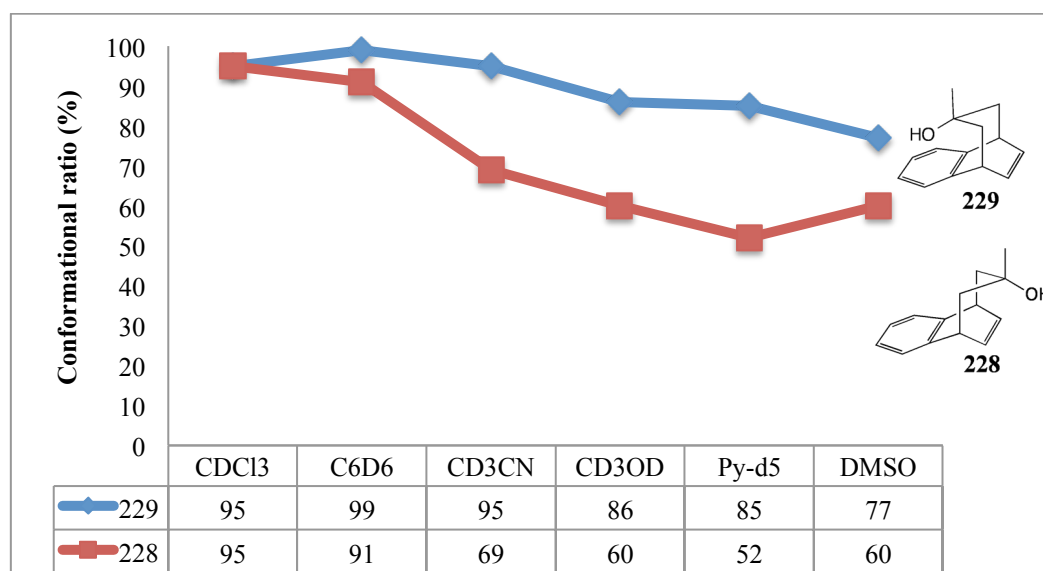
### 2.8.4.1 Effects of the solvent nature on the conformational equilibria of alcohol derivatives

For the secondary alcohol derivatives **226** and **227**, little change was seen in the conformational ratio when the solvent was varied (Figure 95). As discussed previously, few interesting conclusions can be drawn from these substrates due to the significant difference in van der Waals radii of the two substrates.



**Figure 95** Conformational ratio of tertiary alcohols **226** and **227** in a range of solvents, ranked in order of their hydrogen bond forming capacity at 298 K

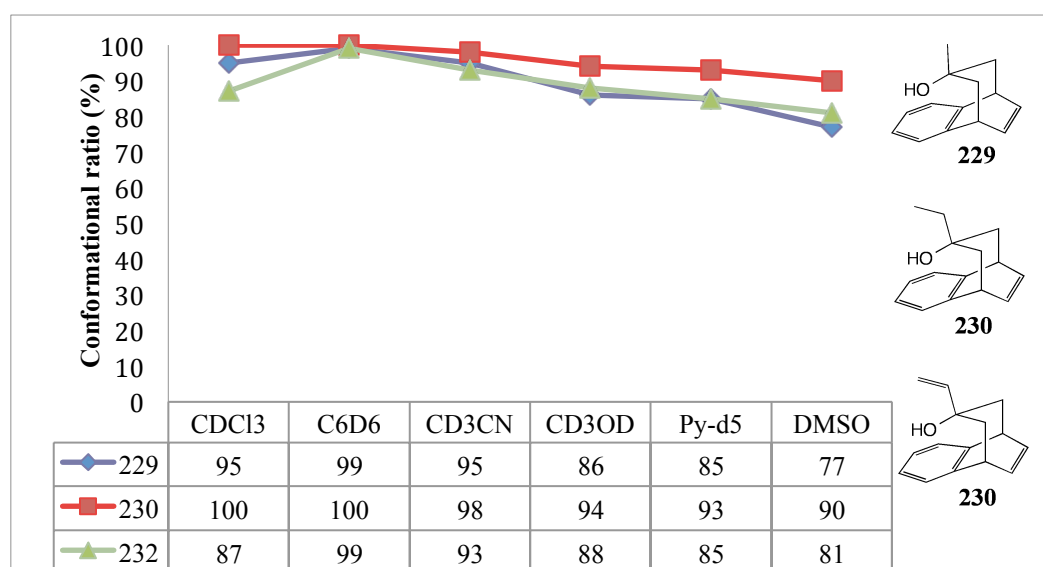
The tertiary alcohols **228** and **229** however display much more interesting behaviour over the range of solvents employed.



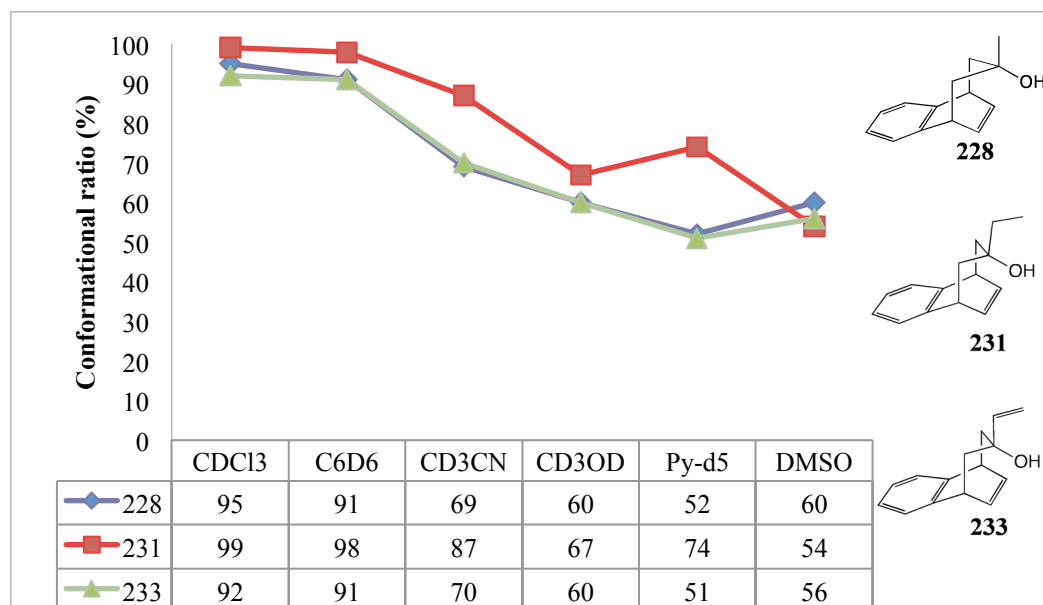
**Figure 96** Conformational ratio of tertiary alcohols **228** and **229** in a range of solvents, ranked in order of their hydrogen bond forming capacity at 298 K



Thus, as illustrated in Figure 96 for the case of the two  $sp^3$  hybridised methyl alcohols **228** and **229**, the two diastereoisomers display significantly different behaviour when varying the solvent. Indeed, this pattern can also be detected for all of the tertiary alcohols studied and it is always the diastereoisomer in which the hydroxyl group is orientated towards the double bond whose conformational ratio is clearly much more influenced by solvent. This statement can be easily seen by comparison of the two graphs, in Figure 97 where a  $\pi$  facial intramolecular hydrogen bond can be made to the aromatic ring, and Figure 98 where the O-H/ $\pi$  interaction is with the alkene.



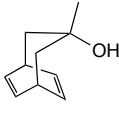
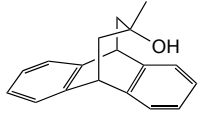
**Figure 97** Conformational ratio of tertiary alcohols **229**, **230** and **232** in a range of solvents, ranked in order of their hydrogen bond forming capacity at 298 K



**Figure 98** Conformational ratio of tertiary alcohols **228**, **231** and **233** in a range of solvents, ranked in order of their hydrogen bond forming capacity at 298 K

The pattern observed in this case would clearly suggest that the O-H/ $\pi$  (alkene) interaction is much more affected by the nature of the solvent and hence weaker than the O-H/ $\pi$  (arene) interaction.

Such a conclusion however contradicts that made when a comparison was drawn between the behaviour of the tertiary methyl alcohols of the propanoanthracene and parent diene systems as reproduced in Table 17 below.<sup>159,160</sup>

Solvent	Conformational ratio	
	 <b>209</b>	 <b>165</b>
<b>CDCl<sub>3</sub></b>	100:0	93:07
<b>C<sub>6</sub>D<sub>6</sub></b>	95:05	89:11
<b>CD<sub>3</sub>CN</b>	93:07	74:26
<b>CD<sub>3</sub>OD</b>	82:18	51:49
<b>Py-d<sub>5</sub></b>	82:18	52:48
<b>DMSO</b>	66:34	50:50

**Table 17** Conformational ratio of the methyl alcohol derivatives in the parent diene and propanoanthracene series in a range of solvents at 298 K

Whilst solvation effects for each molecular system are certainly different, it was clear at this moment that further thought was necessary to provide a full internally consistent rationalisation of our results.

Once again, the propargylic alcohols **236** and **237** display interesting behaviour when varying the nature of the solvent (Figure 99). For the diastereoisomer **236** with the hydroxyl group orientated towards the aromatic ring, the major conformer changes in polar solvents. Indeed, the opposite conformer to that observed in apolar solvents is preferred by up to 74% in polar solvents.

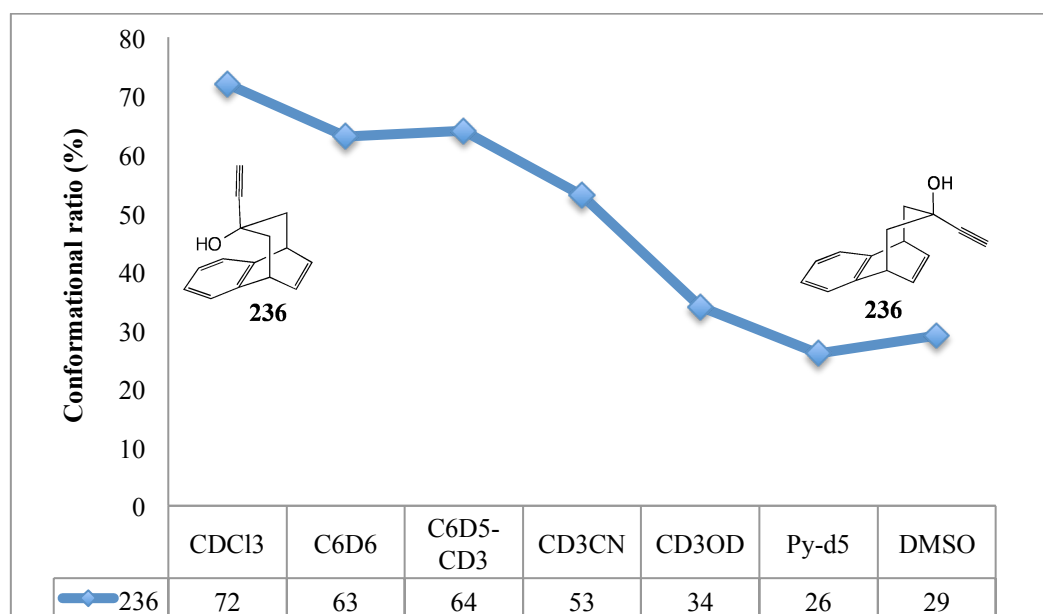


**Figure 99** Conformational ratio of tertiary alcohol **236** in a range of solvents, ranked in order of their hydrogen bond forming capacity at 298 K

Once again this demonstrates the influence that solute-solvent interactions can have on the total stabilisation of the conformer. In polar solvents the O-H/ $\pi$  interaction is effectively counterbalanced by the interaction between the hydroxyl group and the solvent as illustrated in Figure 100.

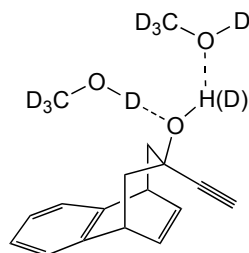


**Figure 100** Representation of the solute-solvent interaction which stabilises the major conformer of alcohol **236** in CD<sub>3</sub>OD

As in previous cases, we were alerted to the change in predominant conformers by studying the changes in chemical shifts for protons H<sub>4A</sub> and H<sub>4B</sub>. As before significant deuteration of the acetylenic proton was observed in polar solvents and further NMR experiments were undertaken. From selectively decoupled <sup>13</sup>C and 2D *J*-resolved measurements, the <sup>3</sup>*J*<sub>CH</sub> couplings for the quaternary acetylene carbon and H<sub>4A</sub> and H<sub>4B</sub> have been determined. The values of the <sup>3</sup>*J*<sub>CH</sub> are <sup>3</sup>*J*<sub>CHA</sub> is 4.6Hz and <sup>3</sup>*J*<sub>CHB</sub> is 5.1Hz. A Karplus type relationship indicates that this corresponds to the geometry with the acetylene orientated towards the double bond.

The difference in chemical shifts relative to CDCl<sub>3</sub> for the propargylic alcohol **236** is shown in Table 18.

Solvent	$\Delta\delta$ (ppm)				<sup>3</sup> <i>J</i> <sub>5,4A</sub> (Hz)	<sup>3</sup> <i>J</i> <sub>5,4B</sub> (Hz)	<i>P</i> <sub>A</sub>
	H <sub>4A</sub>	H <sub>4B</sub>	OH	C≡CH			
C <sub>6</sub> D <sub>6</sub>	-0.13	-0.09	-0.35	-0.23	4.7	3.3	63:37
CDCl <sub>3</sub>	0	0	0	0	5.3	2.8	72:28
C <sub>6</sub> D <sub>5</sub> -CD <sub>3</sub>	-0.16	-0.11	-0.36	-0.32	4.7	3.1	64:36
CD <sub>3</sub> CN	-0.26	-0.16	0.11	1.2	4.1	3.8	53:47
CD <sub>3</sub> OD	0.23	-0.53	0.34	-	4.8	3.1	33:66
Py- <i>d</i> <sub>5</sub>	0.50	-0.19	0.88	-	5.5	2.9	26:74
DMSO	0.08	-0.68	-	1.18	5.1	2.9	29:71

**Table 18** Difference of chemical shifts, conformational ratios and observed coupling constants for the tertiary alcohol **236** in a range of solvents at 298 K

However, for the other diastereoisomer **237** the opposite trend is observed. The predominant conformer is stabilised in polar solvents (Figure 101). In addition, for this substrate selective NOE experiments were conducted in CD<sub>3</sub>OD, to confirm the structure of the major conformer.

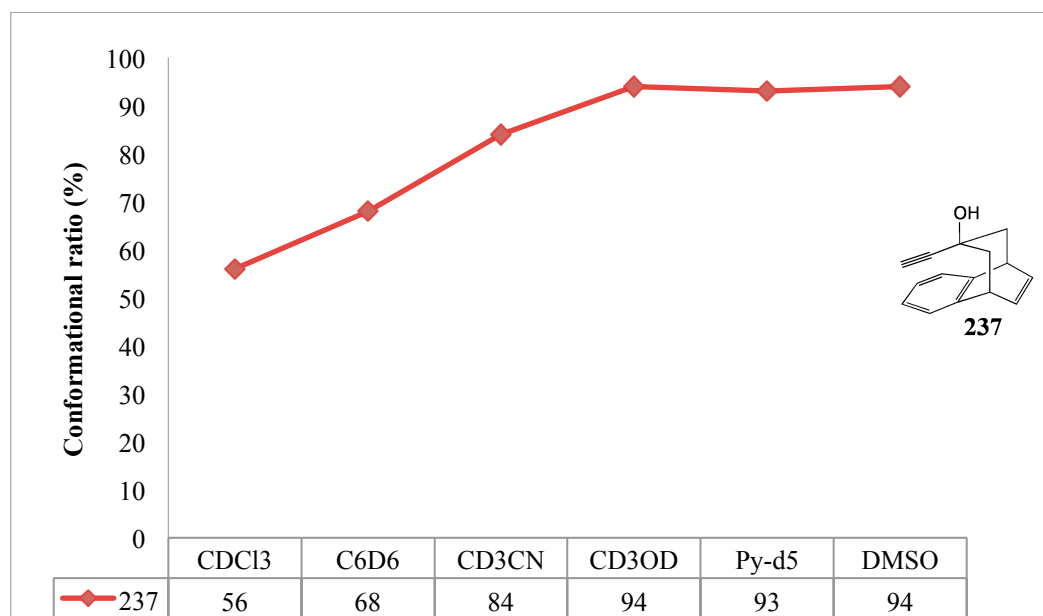


**Figure 101** Conformational ratio of tertiary alcohol **237** ranked in order of their hydrogen bond forming capacity at 298 K

In CDCl<sub>3</sub>, the two conformers are almost equally populated. However, in polar solvents such as CD<sub>3</sub>OD and DMSO, there is clearly one predominant conformer. This demonstrates the ability of solute-solvent interactions to stabilise a conformer. These results also imply that for this substrate the olefinic O-H/ $\pi$  interaction cannot compete with the interaction between the hydroxyl group and such solvents.

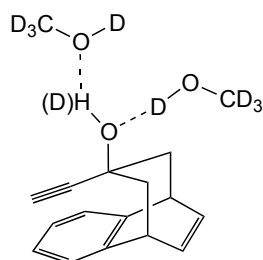


**Figure 102** Representation of the solute-solvent interaction which stabilises the major conformer of alcohol **237** in CD<sub>3</sub>OD

Interestingly, for the propargylic alcohol derivatives **236** and **237**, different conformational ratios are observed in CDCl<sub>3</sub> and C<sub>6</sub>D<sub>6</sub>. This phenomenon was also noted for the propargylic alcohol **213** in the parent diene system and the reason for this observation is not apparent to us. Both substrates also display an upfield shift of the acetylenic proton.

In global terms, the cyanohydrin derivatives display a similar trend to those observed in the case of the propargylic alcohol **237**. The variation of conformational ratio with solvent for the cyanohydrin derivatives is shown in Figure 103.

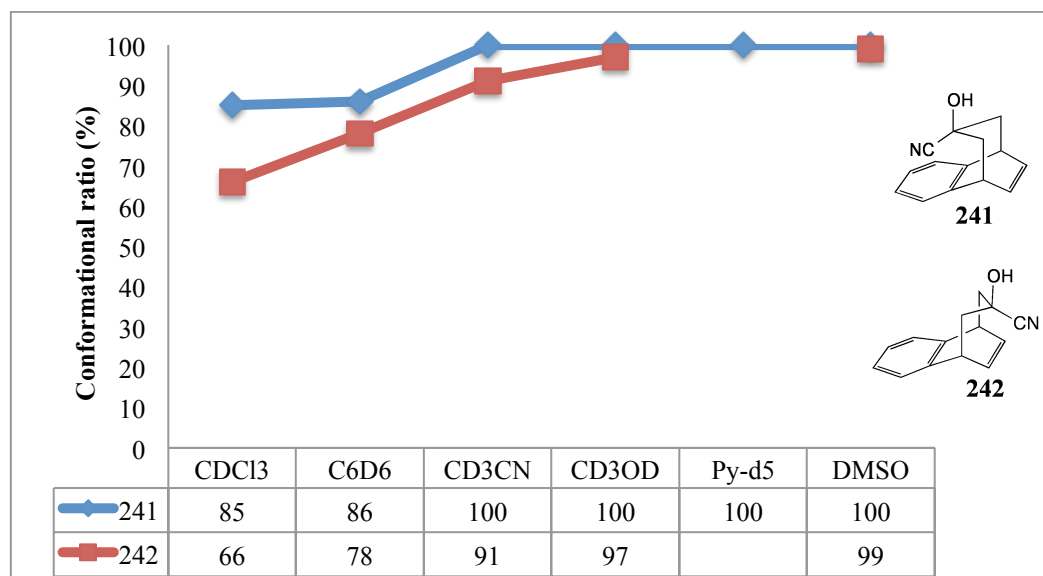


**Figure 103** Conformational ratio of cyanohydrins **241** and **242** ranked in order of their hydrogen bond forming capacity at 298 K

In apolar solvents, the O-H/ $\pi$  interaction is almost counterbalanced by the nitrile. However, in more polar solvents one predominant conformer is observed. In these solvents the interaction between the hydroxyl group and the solvent is dominant.

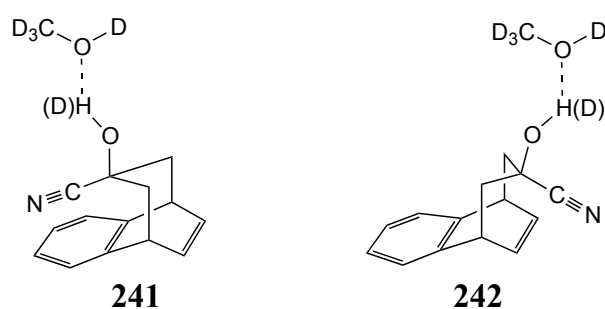


**Figure 104** Representation of the solute-solvent interaction which stabilises the major conformer of cyanohydrins **241** and **242** in CD<sub>3</sub>OD

These results imply that although the nitrile group is known to participate in traditional hydrogen bonding, solvation of the nitrile group is not of great importance. The solvent effects on the conformational population in polar solvents are similar to those of the propargylic alcohol **236**. In both of these substrates an *sp* hybridised carbon atom competes with a hydroxyl group.

However in  $\text{CDCl}_3$ , the opposite conformer is preferred for the propargylic alcohol **236** (Figure 105).

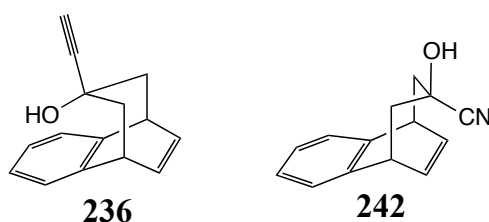
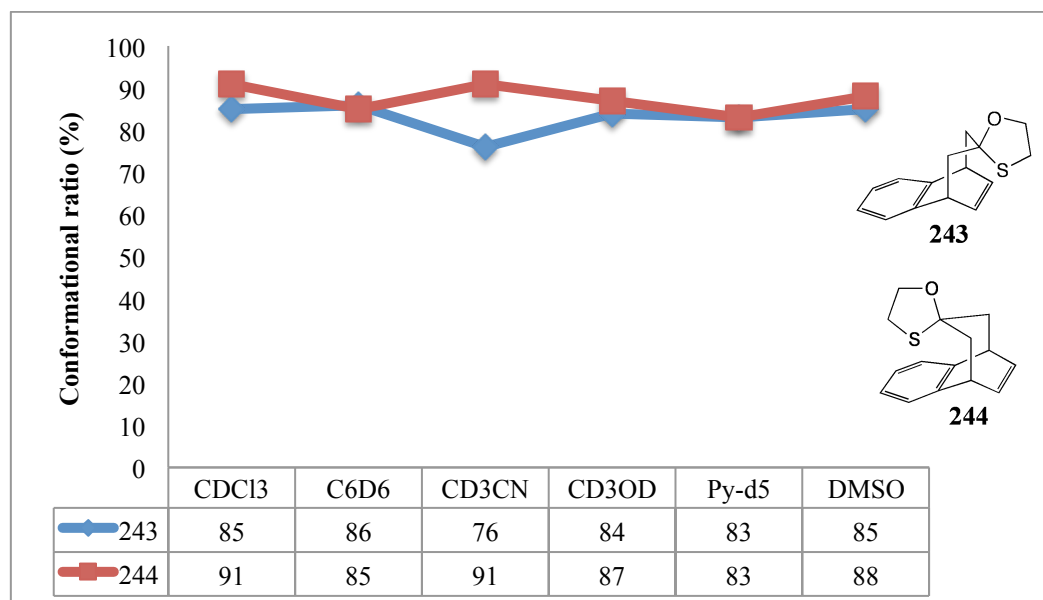


Figure 105

#### 2.8.4.2 Effects of the solvent nature on the conformational equilibria of oxathiolane derivatives **243** and **244**

As we have already seen, the oxathiolane derivatives revealed the relative strength of the  $\text{S}/\pi$  interaction compared to the  $\text{O}/\pi$  interaction. The oxathiolanes also provide us with our only derivatives not to feature a hydroxyl group. It was found that the population of the predominant conformer is not greatly affected by the nature of the solvent (Figure 106).





**Figure 106** Conformational ratio of oxathiolanes **243** and **244** in a range of solvents at 298 K

As there is no drastic change in the conformational ratio of either diastereoisomer **243** and **244** in the range of solvents, the possible solute-solvent interactions with the oxygen or sulphur atom do not compete with the S/ $\pi$  interaction. For all of the four components studied, the oxathiolanes **243** and **244** therefore provided an internally consistent series in which the S/ $\pi$  interaction is always clearly featured.

#### 2.8.4.3 X-Ray Studies

When studying non-covalent interactions, it is always of interest to compare the behaviour in solution with that in the solid state, especially since crystallographic database mining is a very popular method for detecting non-covalent interactions. Wherever possible, X-Ray crystallography data were therefore obtained for the derivatives studied, some of the successful cases are outlined below.

#### 2.8.4.4 Crystal structure of propargylic alcohol **237**

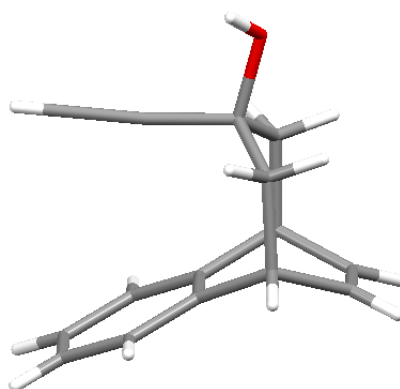


**Figure 107** Crystal structure of the propargylic alcohol **237**

In the solid state, propargylic alcohol **237** exists as only one conformer, with the acetylenic group orientated over the aromatic ring (Figure 107). The distance between the centre of the aromatic ring and the acetylenic proton was found to be 3.87 Å. NOE enhancement experiments conducted in CDCl<sub>3</sub> solution proved the predominance of the same conformer.

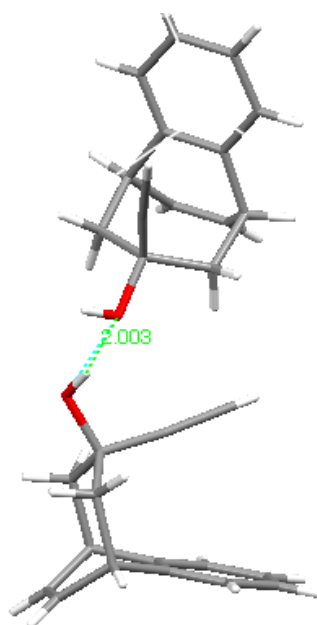


**Figure 108** Intermolecular hydrogen bonding between two hydroxyl groups in the crystal structure of propargylic alcohol **237**

The structure also exhibits intermolecular interactions. The oxygen atom of one molecule participates in hydrogen bonding with the proton of the hydroxyl group on another molecule. Each molecule participates in two intermolecular hydrogen bonding interactions. The distance from the hydroxyl proton to the oxygen atom was found to be 2.00 Å and the O-H-O angle was found to be 147.9°, both of which are a slight deviation from the values measured for hydrogen bonding in water (1.88 Å and 162°). This difference may be explained by the fact that each hydroxyl group is involved in two hydrogen bonds and as a consequence the oxygen atom becomes electron deficient.

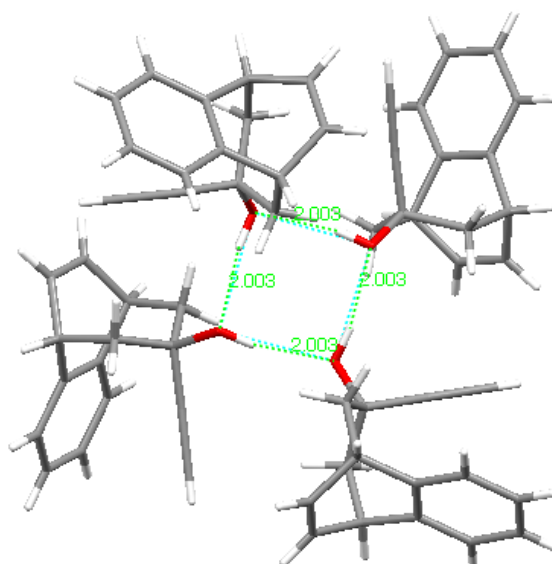


**Figure 109** Representation of the intermolecular hydrogen bonding in the crystal structure of propargylic alcohol **237**

No intermolecular O-H/ $\pi$  interactions with the aromatic ring or double bond were detected for this substrate.

#### 2.8.4.5 Crystal structure of the cyanohydrin **241**

In the solid state, the major component of the unit cell is present as a dimer in which the cyanohydrin **241** adopts two slightly different geometries. In both geometries the nitrile group is orientated above the aromatic ring. However the proton of the hydroxyl group adopts a different orientation in each geometry to allow it to form intermolecular hydrogen bonds.

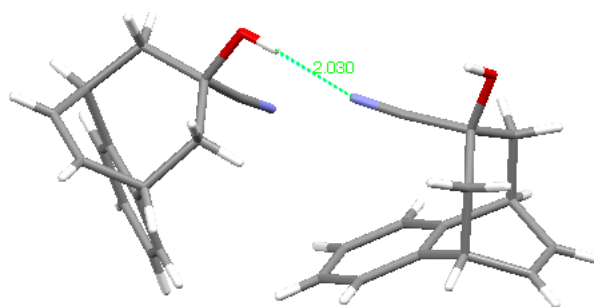


**Figure 110** Crystal structure of the cyanohydrin **241**

In each molecule an intermolecular hydrogen bond is formed between the nitrile group and the proton from the hydroxyl group on another molecule. The N-H distance and the H-N-C angle were found to be 2.03 Å and 174°.

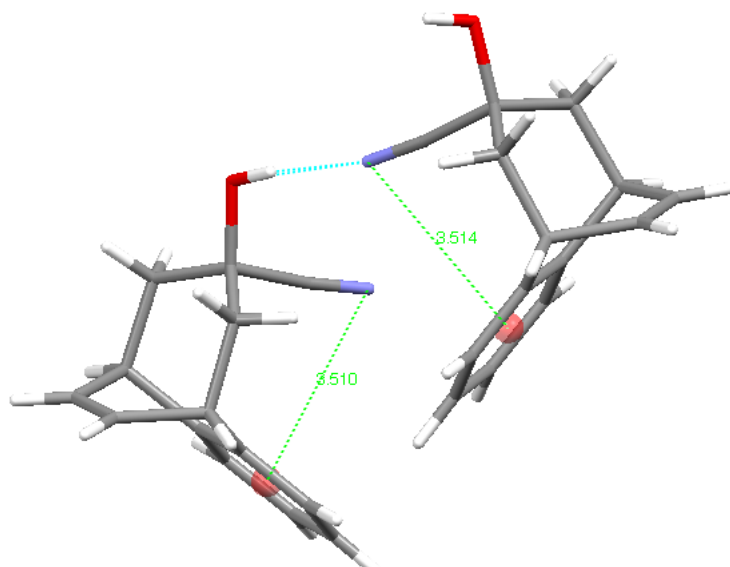


**Figure 111** Intermolecular hydrogen bond between a hydroxyl and a nitrile group in the crystal structure of the cyanohydrin **241**

Although two different components are observed, their geometry corresponds to only one conformer. In solution, NOE experiments predict the same major conformer with the nitrile group orientated above the aromatic ring.

## **2.9 Comparison of the parent diene, propanonaphthalene and propanoanthracene molecular balance systems**

### **2.9.1 Introduction**

The primary objective of this work was to gain further insight into the nature of non-covalent olefinic  $\pi$ -interactions and to compare them with the better studied aromatic  $\pi$ -interactions. Consequently, in this section, irrespective of the merits or otherwise of examining different molecular structures, we aim to bring together the results from the three molecular balance systems studied within our group and compare and contrast them. However, within these balance systems several different interactions compete to contribute to the overall conformational ratio, and so the results are far from trivial to interpret; moreover several interpretations may be possible.

In particular, we were concerned to note that comparison of very small subsets of data could lead to diametrically opposed conclusions. Thus, comparison of the tertiary alcohols in the propanoanthracene system with those of the parent diene had implied that the olefinic  $\pi$ /O-H interaction could be stronger than the arene  $\pi$ /O-H interaction (*vide infra*), whereas comparison of the diastereomeric tertiary alcohols in the propanonaphthalene system had led to exactly the opposite conclusion. It was therefore highly desirable that some internally consistent explanation could be provided for all of the data which had been collected.

We therefore turned to a careful scrutiny of the four molecular frameworks which had been assembled and in the most general way tabulated the potential non-covalent interactions which could be involved in such systems. The overview is shown in Figure 112.

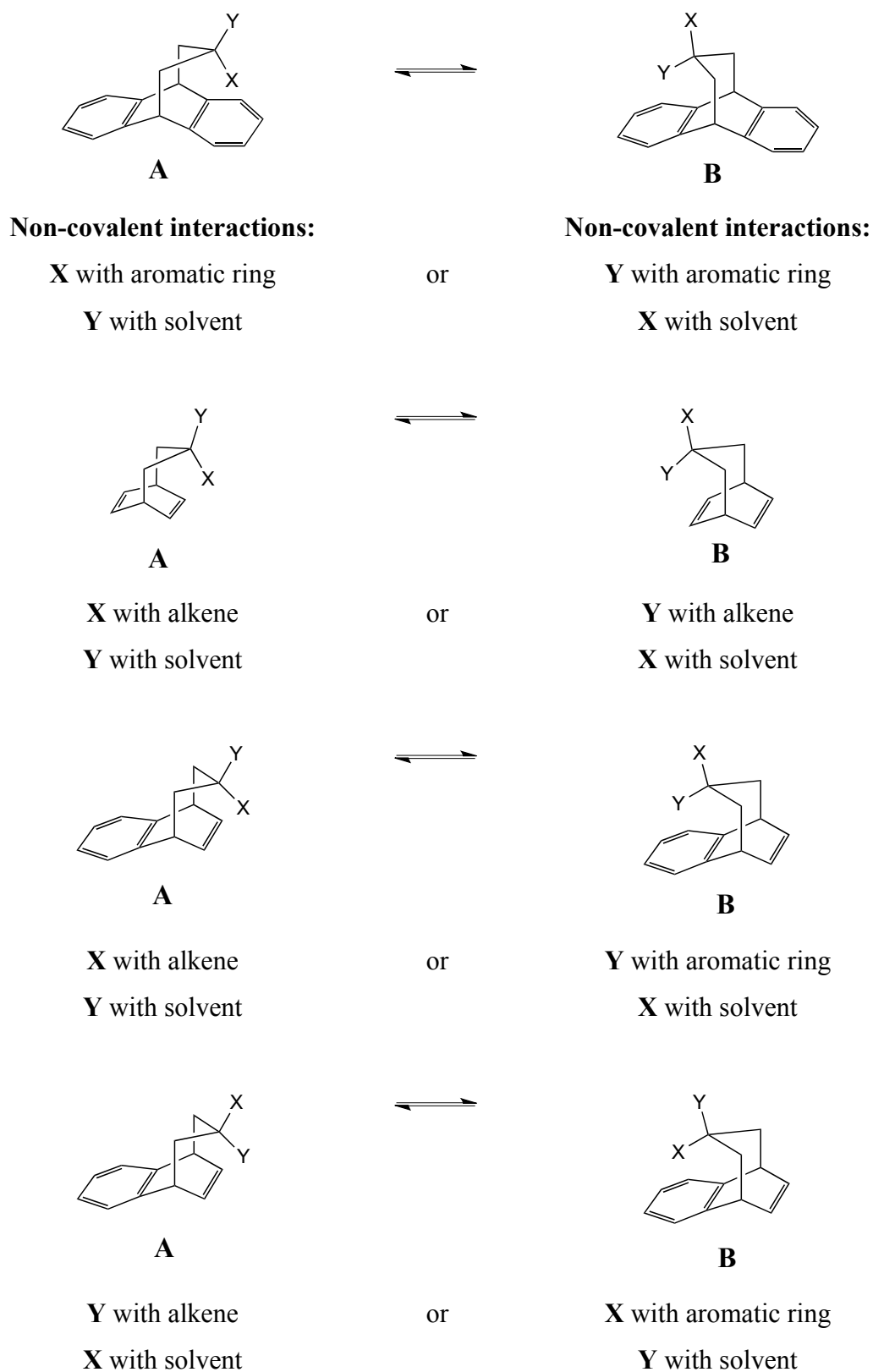


Figure 112

At this moment in time, realisation dawned that there are two functional groups X and Y on the central carbon atom of the flexible bridge, and that, because of

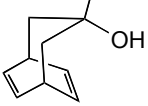
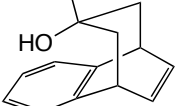
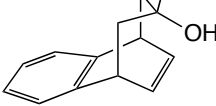
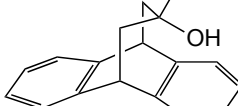


our focus on  $\pi$  facial hydrogen bonding in tertiary alcohols, the alkyl group had effectively been dismissed as a spectator of differing steric bulk. The propargylic alcohols, cyanohydrins and oxathiolanes had always been regarded as more special and different subsets within our programme.

In light of this overview, careful reexamination of the data led to the insight that all four molecular balances could also undergo C-H/ $\pi$  interactions as well as O-H/ $\pi$  interactions. Even although such interactions are weaker, they should not be neglected.

## 2.9.2 Alcohol derivatives

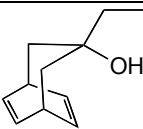
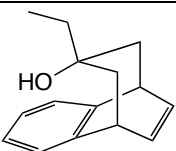
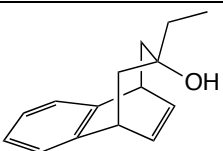
Thus, for the collated set of tertiary methyl alcohols shown once again in Table 19, the myopic comparison leads to a contradiction wherein examination of the results from the parent diene and propanoanthracene systems lead to the conclusion that the O-H/ $\pi$  interactions with an alkene is stronger, whereas comparison of the two diastereoisomers of the propanonaphthalene system would suggest that the  $\pi$ -facial hydrogen bond to the aromatic ring is preferred.

Solvent	Conformational ratio			
	 <b>209</b>	 <b>229</b>	 <b>228</b>	 <b>165</b>
<b>CDCl<sub>3</sub></b>	100:0	95:05	95:05	94:06
<b>C<sub>6</sub>D<sub>6</sub></b>	97:03	99:01	91:09	89:11
<b>C<sub>6</sub>D<sub>5</sub>-CD<sub>3</sub></b>	95:05	99:01	-	88:12
<b>CD<sub>3</sub>CN</b>	93:07	95:05	69:31	74:26
<b>CD<sub>3</sub>OD</b>	82:18	86:14	60:40	51:49
<b>Py-<i>d</i><sub>5</sub></b>	82:18	85:15	52:48	52:48
<b>DMSO</b>	66:34	77:23	70:30	50:50

**Table 19** Conformational ratios of tertiary alcohols **209**, **228**, **229** and **165** in a range of solvents at 298 K

If, however, attention is focused on the methyl group and all four structures are examined, it can be stated that the orientation of a methyl group over a simple alkene is certainly disfavoured relative to its placement over an aromatic ring.<sup>159-162</sup> The alternative way of phrasing this conclusion is that the arene  $\pi$ /C-H interaction is considerably stronger than the weak or non-existent olefin  $\pi$ /C-H interaction in these systems.

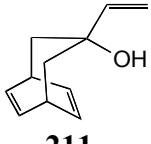
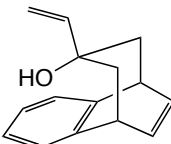
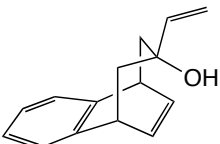
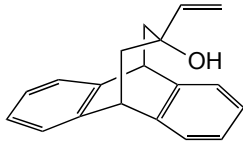
Within the congeneric series of the three tertiary ethyl alcohols which were prepared, a similar pattern can be discerned with the parent diene derivative **210** and the propanonaphthalene diastereoisomer **230** exhibiting  $\pi$  facial hydrogen bonding to the alkene or arene respectively and almost irrespective of the nature of the solvent (Table 20). By way of contrast, in diastereoisomer **231**, the intramolecular  $\pi$  facial hydrogen bond to the alkene can be effectively counterbalanced both by the hydrogen bonding in more polar solvents and also presumably by an arene  $\pi$ /C-H interaction, even involving the larger ethyl group. The remarkable difference between **230** and **231** in DMSO certainly cannot be attributed to the solute-solvent interaction alone.

Solvent	Conformational ratio		
	 <b>210</b>	 <b>230</b>	 <b>231</b>
<b>CDCl<sub>3</sub></b>	98:02	100:0	99:01
<b>C<sub>6</sub>D<sub>6</sub></b>	98:02	100:0	98:02
<b>CD<sub>3</sub>CN</b>	96:04	98:02	87:13
<b>CD<sub>3</sub>OD</b>	93:07	94:06	67:33
<b>Py-<i>d</i><sub>5</sub></b>	93:07	93:07	74:26
<b>DMSO</b>	88:12	90:10	54:46

**Table 20** Conformational ratios of the tertiary alcohols **210**, **230** and **231** in a range of solvents at 298 K

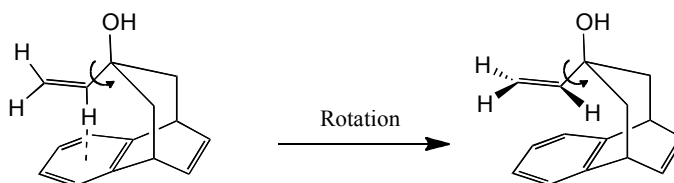
For the vinylic alcohols when studied in CDCl<sub>3</sub> solution, the conformational ratios obtained are of comparable values (Table 21). The highest value was observed for the parent diene derivative **211**, where the predominant conformer

has the hydroxyl orientated towards the alkene. The substantial preference for this conformer can be attributed to the strength of the O-H/ $\pi$  interaction compared to that of the C-H/ $\pi$  interaction.

Solvent	Conformational ratio			
	 <b>211</b>	 <b>232</b>	 <b>233</b>	 <b>176</b>
<b>CDCl<sub>3</sub></b>	97:03	92:08	87:19	90:10
<b>C<sub>6</sub>D<sub>6</sub></b>	97:03	91:09	99:01	89:11
<b>CD<sub>3</sub>CN</b>	79:21	70:30	93:07	-
<b>CD<sub>3</sub>OD</b>	84:16	60:40	88:12	62:38
<b>Py-<i>d</i><sub>5</sub></b>	79:21	51:49	85:15	-
<b>DMSO</b>	64:36	56:44	81:19	55:45

**Table 21** Conformational ratios of tertiary alcohols **211**, **232**, **233** and **176** in a range of solvents at 298 K

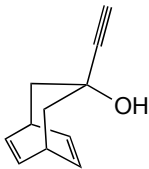
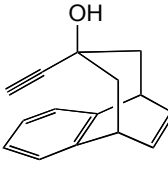
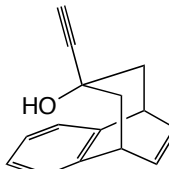
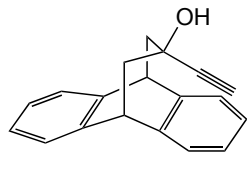
Interestingly, the conformational ratios of the four substrates show different variations when varying the nature of the solvent. The vinyl group is a somewhat problematic one to analyse in terms of its interactions or otherwise with the alkene or the arene because of free rotation. Thus for example, whilst the greater acidity of the vinylic hydrogen atom attached to the sp<sup>2</sup> hybridised carbon might lead to a stronger arene  $\pi$ /C-H interaction, simple rotation then leads to  $\pi$ - $\pi$  or  $\pi$ - $\pi^*$  interactions which seem less favourable (Figure 113).



**Figure 113** Representation of free rotation of the vinyl group as observed in the vinylic alcohols **232** and **233**

However, it should be noted that substantial overlap of the protons on the bridge was observed and this may influence the accuracy of the measured  $J$  values in this series.

Throughout our studies, tertiary propargylic alcohols and cyanohydrins (*vide infra*) possessing an  $sp$  hybridised carbon atom have always proven to be of interest. Unlike the alkyl groups they must be considered much more promiscuous functional groups in their own right, especially in terms of potential non-covalent interactions. Thus, as the earlier study in the propanoanthracene series revealed, the acetylenic proton can be used, both in solution and in the solid state, to form dimers in which a clear intermolecular arene  $\pi/C-H$  interaction is involved.<sup>160</sup> Moreover, in terms of solvation, both the  $\pi$ -systems and the “acidic” proton can be involved. As a linear rod this functional group is less sterically demanding than the alkyl or vinyl groups and cannot participate in  $C-H/\pi$  interactions with either the arene or alkene, because of the internal  $sp$  hybridised carbon atom.

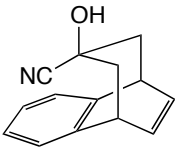
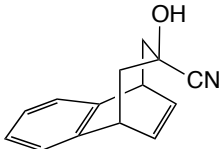
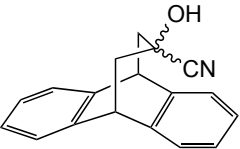
Solvent	Conformational ratio			
	 <b>213</b>	 <b>237</b>	 <b>236</b>	 <b>169</b>
<b>CDCl<sub>3</sub></b>	67:33	56:44	72:28	52:48
<b>C<sub>6</sub>D<sub>6</sub></b>	58:42	68:32	63:47	52:48
<b>C<sub>6</sub>D<sub>5</sub>- CD<sub>3</sub></b>	-	-	64:46	67:33
<b>CD<sub>3</sub>CN</b>	59:41	84:16	53:47	70:30
<b>CD<sub>3</sub>O D</b>	22:78	94:06	34:66	82:18
<b>Py-<i>d</i><sub>5</sub></b>	-	93:07	26:74	82:18
<b>DMSO</b>	17:83	94:06	29:71	78:22

**Table 22** Conformational ratios of tertiary alcohols **213**, **237**, **236** and **169** in a range of solvents at 298 K

Comparative examination of the results for the four acetylenic alcohols (Table 22) serves to confirm that competing solute-solvent interactions in this series can effectively counterbalance both the arene and olefinic O-H/ $\pi$  interactions but, in general, in polar solvents strong solute-solvent interactions can occur with the hydroxyl group and stabilise the conformer in which the acetylene is orientated towards either the aromatic ring or the double bond. Alcohols **213** and **237** show different predominant conformers in apolar and polar solutions, highlighting the great effects that the nature of the solvent can play. Furthermore, comparison of the behaviour of diastereoisomers **236** and **237** in terms of their relative ability to form a  $\pi$ -facial intramolecular hydrogen bond would suggest that the arene is certainly preferred to the alkene.

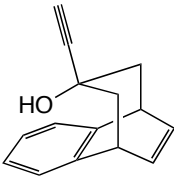
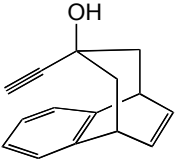
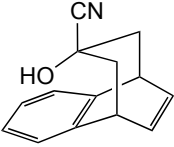
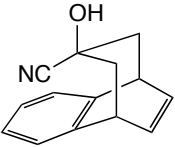
### 2.9.3 Cyanohydrins

Unfortunately, because of synthetic problems, it was not possible to prepare the cyanohydrin derivative for the parent diene series. It was also not possible to determine the structure of the predominant conformer of the propanoanthracene substrate **177**, as neither of the substituents on the bridge contain a proton suitable for NOE enhancements.<sup>160</sup> However, in the propanonaphthalene system the alkene makes NOE enhancements possible and the structures of the major conformers could be determined. Examination of the conformational ratios for both diastereoisomers **241** and **242** (Table 23) leads to the remarkable observation that, irrespective of the nature of the solvent, the dominant conformer is that in which the nitrile group is orientated towards either the aromatic ring **241** or the alkene **242**. From these results it seems appropriate to conclude that the major conformer of the propanoanthracene derivative **177** would also have the nitrile group orientated towards the aromatic ring. Whilst the interaction of the hydroxyl group with the more polar solvents is always observed and readily understood, the influence of the cyano groups in effectively diminishing the contribution from the O-H/ $\pi$  interaction in polar solvents is very intriguing.

Solvent	Conformational ratio		
	 <b>241</b>	 <b>242</b>	 <b>177</b>
<b>CDCl<sub>3</sub></b>	85:15	66:34	74:26
<b>C<sub>6</sub>D<sub>6</sub></b>	86:14	78:22	76:24
<b>CD<sub>3</sub>CN</b>	100:0	91:09	93:07
<b>CD<sub>3</sub>OD</b>	100:0	97:03	96:04
<b>Py-<i>d</i><sub>5</sub></b>	100:0	-	-
<b>DMSO</b>	100:0	99:01	95:05

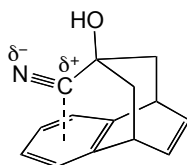
**Table 23** Conformational ratios of cyanohydrins **241**, **242** and **177** in a range of solvents at 298 K

Any naïve assumption that the nitrile group functions in the same manner as the alkyne, i.e. merely as a small linear rod of similar steric bulk and an sp hybridised carbon atom, is clearly wrong and this is emphasized by comparison of the four diastereoisomers in Figure 114.

		
	<b>236</b>	<b>237</b>
CDCl <sub>3</sub>	72:28	56:44
C <sub>6</sub> D <sub>6</sub>	63:47	68:32
		
	<b>242</b>	<b>241</b>
CDCl <sub>3</sub>	34:66	85:15
C <sub>6</sub> D <sub>6</sub>	22:78	86:14

**Figure 114** Comparison of conformational ratios of propargylic alcohol derivatives **236** and **237** with cyanohydrin derivatives **241** and **242** in CDCl<sub>3</sub> and C<sub>6</sub>D<sub>6</sub>

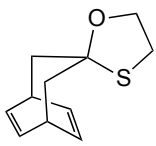
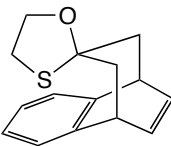
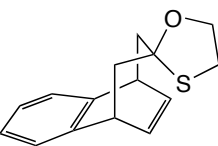
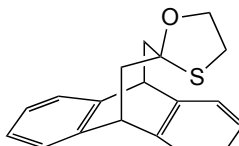
On comparison of these four propanonaphthalene derivatives it would appear that the  $\pi$ -interactions of both the alkene and the arene with the cyano group are stronger than the O-H/ $\pi$  interactions and the values also suggest that the arene  $\pi$ /C $\equiv$ N interaction is stronger than the alkene  $\pi$ /C $\equiv$ N interaction. Given the stronger electrophilic character of the sp hybridised carbon atom of the nitrile relative to that of an alkyne, it is tempting to suggest that the cyano group is ideally positioned to benefit from the negative charge associated with the nuclear quadrupole moment of the aromatic ring as implied in Figure 115.



**Figure 115** Representation of the predominant conformer of cyanohydrin **241** in CDCl<sub>3</sub> and C<sub>6</sub>D<sub>6</sub> at 298 K.

## 2.9.4 Oxathiolane derivatives

Given the importance of sulphur interactions in biological systems, the oxathiolane derivatives offer a fascinating insight into the nature of S/ $\pi$  interactions. On account of the significant difference in van der Waals radii between sulphur and oxygen atoms, the prediction might have been made that the oxygen atom would be orientated towards the  $\pi$ -cloud. However, the earlier study of the propanoanthracene hemithioacetal **170** had given a conformational equilibrium of 76:24 in favour of the S/ $\pi$  interaction in CDCl<sub>3</sub> which translates into a free enthalpy difference of -0.7 kcal mol<sup>-1</sup>. In similar fashion, the major conformer in each case for the remaining three derivatives has the “softer” sulphur atom orientated towards the aromatic ring or the double bond. These results highlight how properties such as polarisability are often of greater importance than steric effects when studying non-covalent interactions and indeed there is a very large difference in polarisability between sulphur ( $3 \times 10^{-24}$  cm<sup>3</sup>) and oxygen ( $0.62 \times 10^{-24}$  cm<sup>3</sup>).<sup>190</sup>

Solvent	Conformational ratio			
	 <b>219</b>	 <b>244</b>	 <b>243</b>	 <b>170</b>
CDCl <sub>3</sub>	98:02	91:09	85:15	77:23
C <sub>6</sub> D <sub>6</sub>	-	85:15	86:14	64:36
CD <sub>3</sub> CN	-	91:09	76:24	71:29
CD <sub>3</sub> OD	-	87:13	84:16	-
Py- <i>d</i> <sub>5</sub>	-	83:17	83:17	-
DMSO	-	88:12	85:15	-

**Table 24** Conformational ratios of the oxathiolane derivatives **243**, **242** and **170** in a range of solvents at 298 K



Unfortunately only limited results from solvent experiments were available to us. However, from these results it can be deduced that the nature of the solvent does not greatly affect the S/ $\pi$  interaction as there is little variation in the conformational ratio whether it is measured in an apolar or polar solvent (Table 24). This indicates that an interaction between the solvent and the sulphur atom does not compete with the S/ $\pi$  interaction.

---

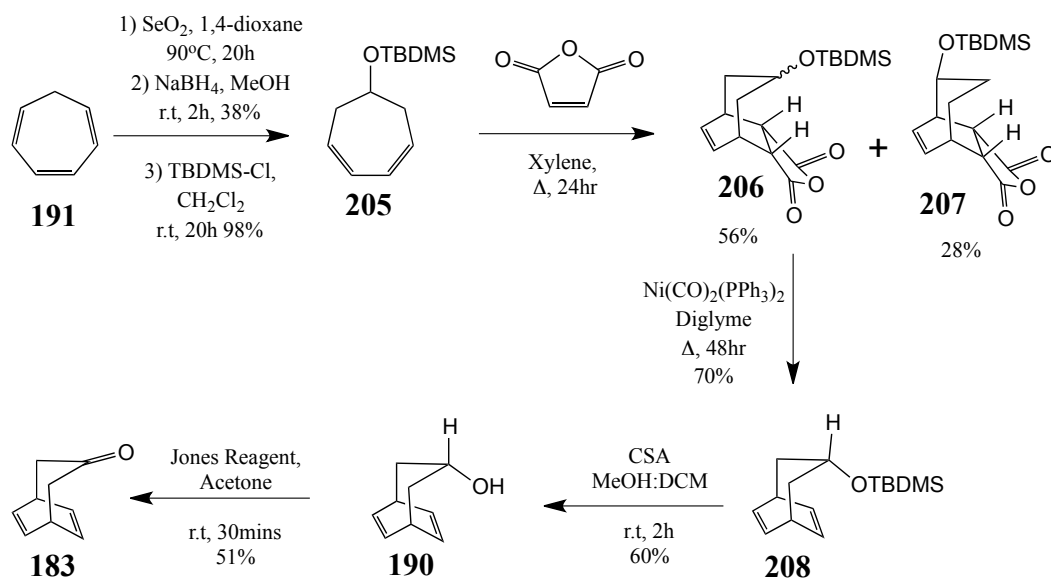
## **CHAPTER 3**

# **CONCLUSIONS AND PERSPECTIVES**

The Primary objective of this work was to study non-covalent olefinic  $\pi$ -interactions and compare and contrast these interactions with the analogous arene interactions. In order to achieve this, a series of molecular systems capable of acting as conformational balances for such interactions were designed, synthesised and subsequently studied in a range of solvents.

### 3.1 Synthetic studies

In the first instance, as with the propanoanthracene system, a carbonyl group on the central carbon of the propano bridge of a bridged bicyclic system was elected as the vital element for a diverse array of derivatives. Thus, the “parent diene” ketone **183**, was prepared in seven steps using a modified version of the route utilised by Baker and co-workers (Scheme 42).

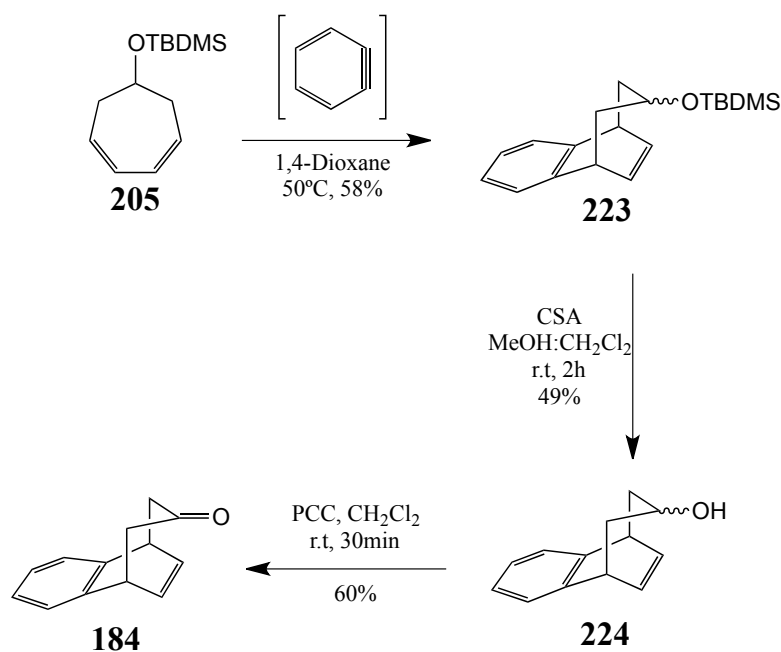


Scheme 42

Unfortunately, our desire to prepare a significant quantity of ketone **183** was not realised, as the synthetic route was found to be lengthy, low yielding and often, to some extent, capricious.

Whilst a range of new derivatives were prepared with various functional groups X and Y on the central carbon of the propano bridge, the number was severely limited not only by the availability of ketone **183**, but also by the chemical reactivity of the alkene  $\pi$ -clouds.

By way of contrast, synthetic studies in the propanonaphthalene series were relatively straightforward. The ketone intermediate **184** was prepared in six steps from cycloheptatriene, using the same diene **205** as an intermediate for trapping benzyne (Scheme 43).



Scheme 43

In order to allow for direct comparison with the parent diene system, an analogous range of derivatives was prepared as well as the cyanohydrin derivatives **239** and **240**. Although the propanonaphthalene derivatives were found to be far more robust than the analogous parent diene derivatives,

significant amounts of material were often lost when separating pure diastereoisomers by chromatography.

From a synthetic standpoint, the work has been, to some extent frustrating inasmuch as the chemical reactivity of both the parent diene and propanonaphthalene systems has precluded efforts to prepare many desirable compounds such as the fluorinated congeners and amine derivatives. There are however many methods for such functional group manipulations which, through lack of time, were not attempted and these may yield positive results in the future.

### **3.2 Conformational equilibria of the molecular balance systems**

Nevertheless, with viable, if not ideal, routes to both the parent diene and propanonaphthalene systems in hand, those compounds which could be prepared were studied in a range of solvents by dynamic NMR. A complete listing of these results together with those previously obtained for the propanoanthracene system as a comparison is supplied in the Appendix 11.

As always in any research programme new and unanticipated insights have been gained, with the strength of the “soft-soft” sulphur/ $\pi$  (arene or alkene) interaction and the cyano/ $\pi$  (arene) interaction being particularly noteworthy. Whilst it was certainly possible to explore the  $\pi$ -facial intramolecular hydrogen bond to a simple alkene using the parent diene framework, the question as to its strength relative to the much more studied O-H/ $\pi$  (arene) interaction remains to be fully answered, particularly in light of the emergence of the C-H/ $\pi$  (arene) interaction during our studies of the propanonaphthalene balance.

Throughout our work, it had always been of interest to compare the behaviour of non-covalent interactions in the solid state with that in solution, particularly as

database mining is a popular technique for the detection of non-covalent interactions. Unfortunately, the preparation of suitable crystals for X-Ray diffraction studies of both the parent diene and propanonaphthalene derivatives was found to be far from trivial.

Nevertheless, the results obtained have hopefully indicated that the conformationally restricted bicyclo[3.2.2] framework provides a very sensitive molecular balance for probing non-covalent intramolecular interactions of functional groups with  $\pi$ -systems as a function of solvent.

### **3.3 Future scope for extending the types of non-covalent $\pi$ -interactions investigated**

At this stage many opportunities for further study remain to be explored. Some areas which can be contemplated are outlined below.

#### **3.3.1 Investigation of other functional groups on the central carbon of the flexible bridge**

To offer a fuller comparative picture, it is of interest to prepare a wider range of functionalised derivatives within both the parent diene and propanonaphthalene series.

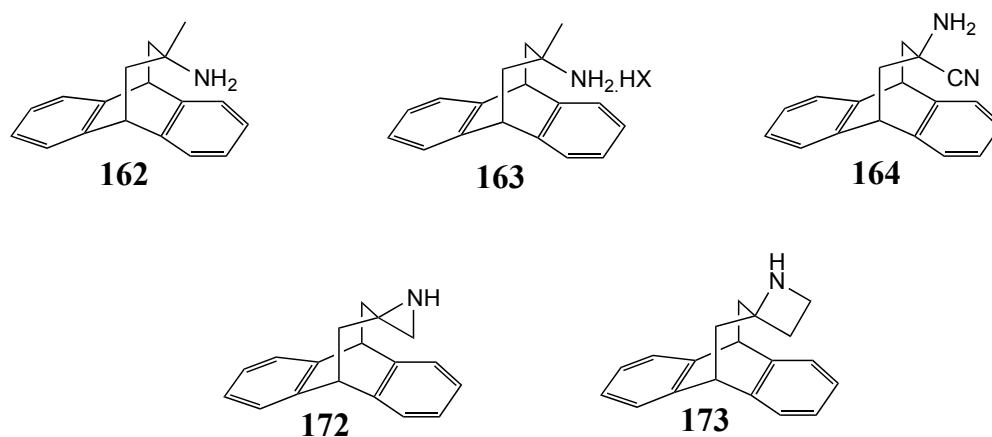


**Figure 116** Range of amine derivatives prepared in the propanoanthracene series

In the propanoanthracene series a range of amine derivatives were prepared, as shown in Figure 116. The preparation of a range of analogous parent diene and propanonaphthalene derivatives (Figure 117 and Figure 118) would allow us to compare olefinic and aromatic N-H/ $\pi$  interactions, and further probe cation- $\pi$  interactions. Such interactions are of interest as they commonly feature in biological systems.

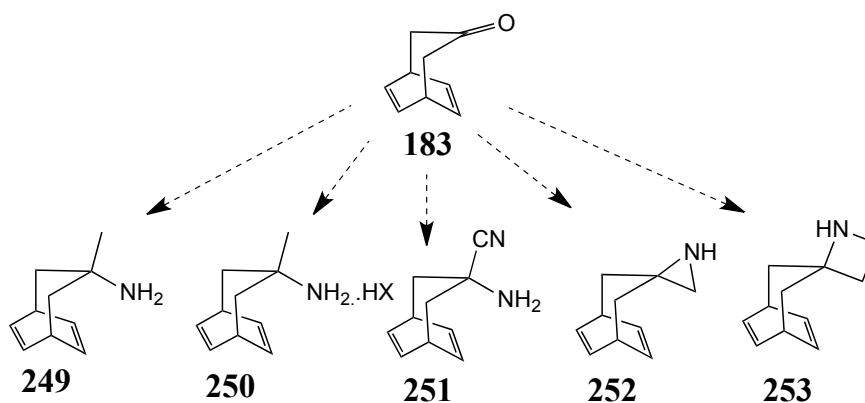


**Figure 117** Range of parent diene derivatives featuring an amine on the central carbon atom of the bridge

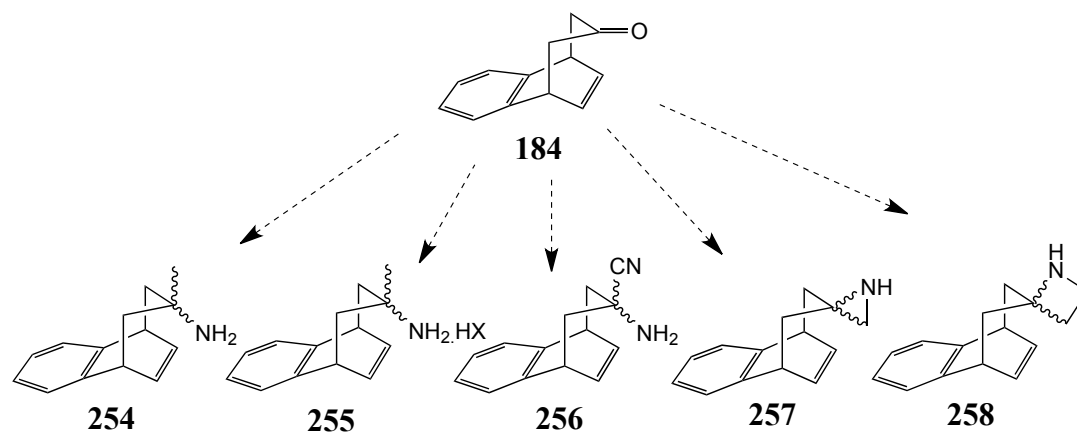


**Figure 118** Range of propanonaphthalene derivatives featuring an amine on the central carbon atom of the bridge

Continuing on from the exciting insights gained from the oxathiolane derivatives, it would be of interest to extend the range of sulphur substituted derivatives, as this would allow us to further probe the  $\text{S}/\pi$  interaction. Potential derivatives are shown in Figure 119 and Figure 120.

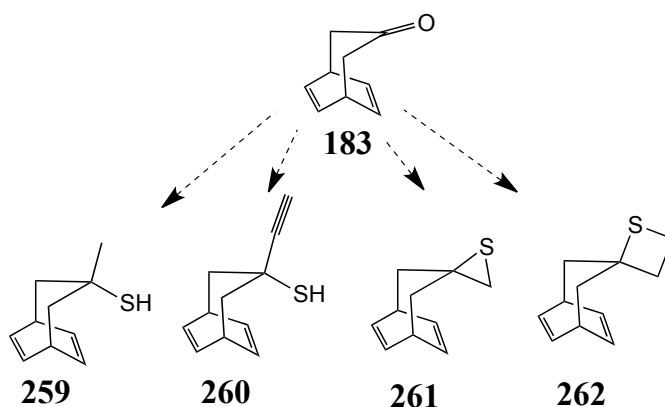


**Figure 119** Range of parent diene derivatives featuring a sulphur containing substituent on the central carbon atom of the bridge



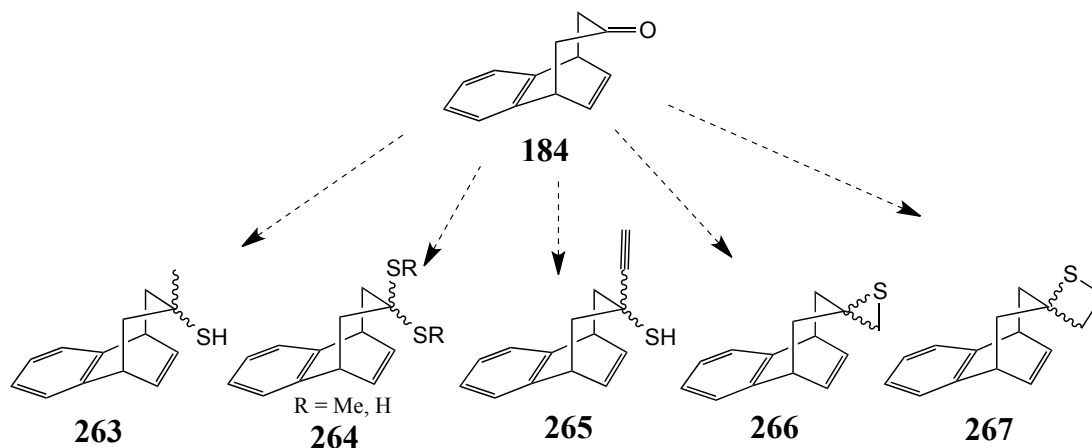


**Figure 120** Range of propanonaphthalene derivatives featuring a sulphur containing substituent on the central carbon atom of the bridge

### 3.3.2 Modification of the electron density of the $\pi$ system

In the longer term, a very exciting prospect for future study would be to explore the nature of functional group interactions with functionalised aromatics and with heteroaromatic systems. As non-covalent arene interactions are sensitive to the nature of the electron density of the aromatic scaffold, the interaction can be perturbed by modifying the electron density of the aromatic system. This can be achieved in the propanonaphthalene series by introducing powerful electron withdrawing or donating groups to the aromatic ring or by substituting the aromatic ring for a heteroaromatic ring. It would also be of interest to prepare a molecular balance system which features both an aromatic and a heteroaromatic ring such as **272**. Some potential frameworks are shown in Figure 121 by way of illustration.

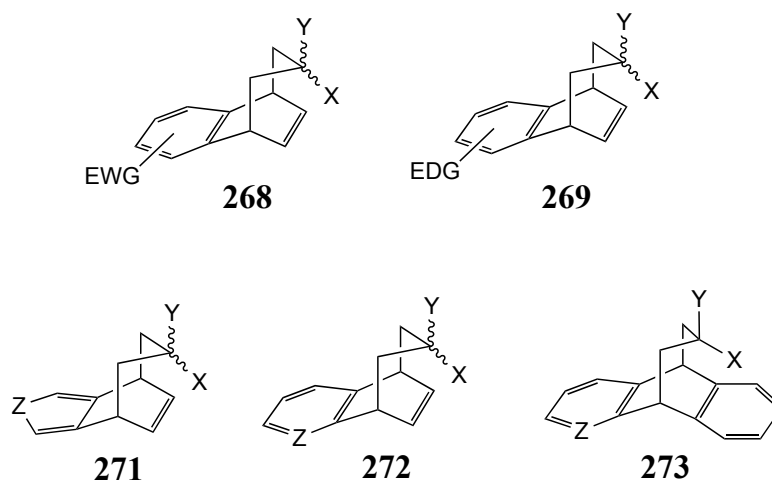


**Figure 121**

Clearly a vast amount of work remains to be done and hopefully this series of molecular balances will be taken up by other workers in the field.

---

# **CHAPTER 4**

## **EXPERIMENTAL**

## 4.1 General Information

All reactions using anhydrous solvents were carried out in oven-dried glassware under an atmosphere of nitrogen. Diethyl ether, tetrahydrofuran, toluene, acetonitrile and dichloromethane were used following purification from an anhydrous engineering zeolite drying apparatus. Methanol was distilled from magnesium turnings and iodine. Xylene was distilled from calcium hydride and stored over 4 Å molecular sieves. Diglyme was distilled from calcium hydride at reduced pressure and stored over 4 Å molecular sieves. DMSO was distilled from calcium hydride at reduced pressure and stored over 4 Å molecular sieves. Maleic anhydride was recrystallised from benzene or  $\text{CHCl}_3$ . Zinc dust was purified by washing with 1M aqueous HCl solution and oven dried. All other chemicals were used as supplied unless otherwise indicated.

Column chromatography was carried out using BDH (40-60  $\mu\text{m}$ ) silica gel and analytical thin layer chromatography was carried out using Merck Kieselgel aluminium-backed plates coated with silica gel. Components were visualized using combinations of ultra-violet lights, ceric ammonium molybdate, phosphomolybdic acid and potassium permanganate.

Melting points were determined using a Reichert Hotstage apparatus for all solids where possible and are quoted to the nearest  $^{\circ}\text{C}$  and are uncorrected. Recrystallisation solvents are recorded when this operation was performed.

Infrared spectra (IR) were recorded on a Perkin Elmer Spectrum 100 FT-IR spectrometer, and were recorded either neat or as a  $\text{CDCl}_3$  film. Absorption maxima are reported in wave-numbers ( $\text{cm}^{-1}$ ), using the following abbreviations; w (weak); m (medium); s, (strong); br (broad). Only selected absorbences are reported.

$^1\text{H}$  NMR spectra were recorded at 300MHz on a Bruker AMX300 spectrometer, at 400MHz on a Bruker AMX400 spectrometer, at 500MHz on a Bruker Avance DRX500 spectrometer, or at 600MHz on a Bruker Avance DRX600 spectrometer in the stated solvent using residual protic solvent  $\text{CHCl}_3$  ( $\delta = 7.26$

ppm, s) as the internal standards. The chemical shift ( $\delta$ ) of each peak is given relative to tetramethylsilane, where  $\delta$  TMS = 0 ppm. Spin multiplicities are indicated by the following symbols: s (singlet); d (doublet); t (triplet); q (quartet); qn (quintet); m (multiplet); or a combination of these. NMR data are reported as follows: number of protons, multiplicity, coupling constants ( $J$  values) recorded in Hertz. Variant temperature NMR experiments were carried out on a Bruker AMX400 spectrometer. 1D-NOE and 2D-noesy NMR experiments were carried out on a Bruker Avance DRX600 spectrometer.

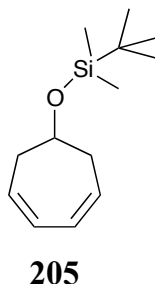
$^{13}\text{C}$  NMR spectra were recorded at 75 MHz on a Bruker AMX300 spectrometer, at 100 MHz on a Bruker AMX400 spectrometer, at 125 MHz on a Bruker Avance DRX500 spectrometer or at 150 MHz on a Bruker Avance DRX600 spectrometer in the stated solvent, using the central reference of  $\text{CDCl}_3$  ( $\delta$  = 77.0 ppm, t) as the internal standard. The chemical shift ( $\delta$ ) of each peak is given relative to the residual solvent peak and are reported to the nearest 0.1 ppm.

Mass spectra and accurate mass measurements were recorded on a VG ZAB SE instrument at the Univesity College London Chemistry Department either by Electron Impact (EI) or Chemical Ionisation (CI).

X-Ray crystal structures were determined using a Bruker-Nonius Kappa CCD diffractometer by Dr G. J. Tizzard at the UK National Crystallography Service.

## 4.2 Experimental Procedure

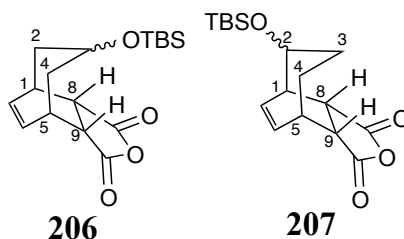
### *Tert*-butyl(cycloheptyloxy)dimethylsilane **205**



To a stirred solution of cyclohepta-3,5-dienol **193** (6.0 g, 54.45 mmol) in anhydrous  $\text{CH}_2\text{Cl}_2$  (55 mL) under an  $\text{N}_2$  atmosphere was added imidazole (9.45 g, 138.90 mmol) and *tert*-butyldimethylsilyl chloride (9.03 g, 59.92 mmol). After stirring overnight at room temperature the resulting mixture was poured into P.E. 40-60°C, washed with water and brine. The organic layer was dried over  $\text{Na}_2\text{SO}_4$ , filtered and concentrated under reduced pressure to afford the title compound **205** (11.97 g, 98%) as a colourless oil which was used without further purification.

**HRMS** found:  $\text{M}^+$  223.15184,  $\text{C}_{13}\text{H}_{23}\text{OSi}$  requires 223.15127; **EI-MS**,  $m/z$  (relative intensity), 223 ( $[\text{M}]^+$ , 21); **IR**  $\nu_{\text{max}}$  ( $\text{CDCl}_3$  film/ $\text{cm}^{-1}$ ) 2954 (w), 2929 (w), 2896 (w), 2857 (w), 1472 (w), 1462 (w), 1361 (w), 1252 (s), 1077 (s);  **$^1\text{H}$  NMR** (500 MHz,  $\text{CDCl}_3$ ) 5.91-5.88 (2H, m,  $\text{HC}=\text{C}$ ), 5.70-5.65 (2H, m,  $\text{HC}=\text{C}$ ), 4.22-4.20 (1H, m,  $\text{HC}-\text{O}$ ), 2.58-2.48 (4H, m,  $\text{CH}_2$ ), 0.90 (9H, s,  $\text{Si}-t\text{-Bu}$ ), 0.07 (6H, s,  $\text{Si}-\text{CH}_3$ );  **$^{13}\text{C}$  NMR** (125 MHz,  $\text{CDCl}_3$ ) 128.1 (CH), 126.0 (CH), 71.4 (CH), 41.0 ( $\text{CH}_2$ ), 26.0 ( $\text{CH}_2$ ), 25.9 ( $\text{CH}_3$ ), 18.3 ( $\text{CH}_3$ ), -4.7 ( $\text{C}_q$ )

3-(*tert*-butyl)dimethylsilyloxybicyclo[3.2.2]nona-6-ene-8,9-endo-dicarboxylic acid anhydride **206** and 2-(*tert*-butyl)dimethylsilyloxybicyclo[3.2.2]nona-6-ene-8,9-endo-dicarboxylic acid anhydride **207**



A mixture of protected cycloheptadienol **205** (4.48 g, 20 mmol), maleic anhydride (2.35 g, 24 mmol), hydroquinone (a few crystals) in anhydrous xylene (10 mL) was heated at reflux under a N<sub>2</sub> atmosphere for 24h. The mixture was cooled to room temperature, and filtered through celite and washed thoroughly with CH<sub>2</sub>Cl<sub>2</sub> (3 x 10 mL). The resulting filtrate was concentrated under reduced pressure. Column chromatography (silica gel, 5:1 P.E. 40-60 °C/Et<sub>2</sub>O) afforded the title compounds **206** (3.21 g, 50%) and **207** (1.79g, 28%) as white solids.

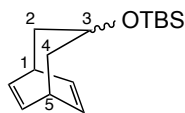
## 206

**R<sub>f</sub>** 0.43 (4:1 P.E. 40-60 °C/Et<sub>2</sub>O); **M.p.** 84 °C (Et<sub>2</sub>O); **HRMS** found: M<sup>+</sup> 323.16733, C<sub>17</sub>H<sub>27</sub>O<sub>4</sub>Si requires 323.16786; **CI-MS**, *m/z* (relative intensity), 323 ([M]<sup>+</sup>, 100); **IR** (CDCl<sub>3</sub> film/cm<sup>-1</sup>) 2936 (w), 2857 (w), 1862 (w), 1773 (s), 1471 (w), 1463 (w), 1386 (w), 1239 (w), 1216 (w); **<sup>1</sup>H NMR** (500 MHz, CDCl<sub>3</sub>) 6.20 (2H, dd, <sup>3</sup>*J* = 3.1 Hz, <sup>3</sup>*J* = 5.0 Hz, HC=C), 4.02 (1H, qn, <sup>3</sup>*J* = 4.9 Hz, H<sub>3</sub>), 3.78 (2H, s, H<sub>8</sub>, H<sub>9</sub>), 3.04 (2H, m, H<sub>1</sub>, H<sub>5</sub>), 1.93 (2H, ddd, <sup>3</sup>*J* = 3.5 Hz, <sup>3</sup>*J* = 1.0 Hz, <sup>2</sup>*J* = 14.5 Hz, H<sub>2</sub>, H<sub>4</sub>), 1.77 (2H, dt, <sup>3</sup>*J* = 4.7 Hz, <sup>2</sup>*J* = 14.5 Hz, H<sub>2</sub>, H<sub>4</sub>), 1.25 (9H, s, Si-*t*-Bu), 0.04 (6H, s, Si-CH<sub>3</sub>); **<sup>13</sup>C NMR** (125 MHz, CDCl<sub>3</sub>) 174.3 (C<sub>q</sub>), 133.3 (CH), 69.6 (CH), 46.4 (CH), 36.5 (CH<sub>2</sub>), 32.8 (CH), 22.7 (CH<sub>3</sub>), 18.0 (C<sub>q</sub>), -4.6 (CH<sub>3</sub>).

207

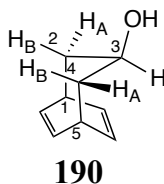
**R<sub>f</sub>** 0.33 (1:1 P.E. 40-60 °C:Et<sub>2</sub>O); **M.p.** 70 °C; **HRMS** found: M<sup>+</sup> 323.16715, C<sub>17</sub>H<sub>27</sub>O<sub>4</sub>Si requires 323.16786; **CI-MS**, *m/z* (relative intensity), 323 ([M]<sup>+</sup>, 99); **IR** ν<sub>max</sub> (CDCl<sub>3</sub> film/cm<sup>-1</sup>) 2930 (w), 2857 (w), 1866 (w), 1776 (s), 1471 (w), 1383 (w), 1252 (w); **<sup>1</sup>H NMR** (500 MHz, CDCl<sub>3</sub>) 6.17 (1H, d, <sup>3</sup>*J* = 9.6 Hz, HC=C), 6.07 (1H, dd, <sup>3</sup>*J* = 7.3 Hz, 9.7 Hz, HC=C), 3.45 (1H, dd, <sup>3</sup>*J* = 9.1 Hz, <sup>3</sup>*J* = 0.5 Hz, H<sub>2</sub>), 3.29 (1H, dd, <sup>3</sup>*J* = 2.0 Hz, <sup>3</sup>*J* = 9.1 Hz, H<sub>1</sub>), 3.09-3.05 (1H, m, H<sub>5</sub>), 1.82-1.61 (4H, m, H<sub>4</sub>, H<sub>3</sub>), 1.52-1.47 (2H, m, H<sub>8</sub>, H<sub>9</sub>), 0.93 (9H, s, Si-*t*-Bu), 0.15 (6H, s, Si-CH<sub>3</sub>); **<sup>13</sup>C NMR** (125 MHz, CDCl<sub>3</sub>) 174.0 (C<sub>q</sub>), 168.7 (C<sub>q</sub>), 139.5 (CH), 131.0 (CH), 51.2 (CH), 46.3 (CH), 44.8 (CH), 40.7 (CH<sub>2</sub>), 34.7 (CH), 26.2 (CH), 22.9 (CH<sub>3</sub>), 18.2 (C<sub>q</sub>), -5.1 (CH<sub>3</sub>).



Bicyclo[3.2.2]nona-6,8-dien-3-yloxy(*tert*-butyl)dimethylsilane **208****208**

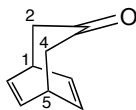
A mixture of bicyclic anhydride **206** (0.97 g, 3.00 mmol) and Bis(triphenylphosphine)dicarbonylnickel (0.96 g, 1.50 mmol) in anhydrous diglyme (3 mL) under an N<sub>2</sub> atmosphere, was slowly heated from 80 °C to 200 °C. The resulting brown mixture was heated at 200 °C for 48 h, the diglyme was then distilled off from the crude reaction mixture. The distillate was dissolved in CHCl<sub>3</sub> (20 mL), filtered through celite, washed thoroughly with CHCl<sub>3</sub> and concentrated under reduced pressure. Column chromatography (silica gel, 4:1 P.E. 40-60 °C/Et<sub>2</sub>O) afforded the title compound **208** (0.54 g, 72%) as a yellow oil.

**R<sub>f</sub>** 0.64 (1:1 P.E. 40-60 °C/Et<sub>2</sub>O); **HRMS** found: M<sup>+</sup> 251.18317, C<sub>15</sub>H<sub>27</sub>OSi requires 251.18312; **CI-MS**, *m/z* (relative intensity), 251 ([M]<sup>+</sup>, 34); **IR** ν<sub>max</sub> (CDCl<sub>3</sub> film/cm<sup>-1</sup>) 3043 (w), 2928 (w), 2857 (w), 1591 (w), 1472 (w), 1437 (w), 1374 (w), 1256 (w); **<sup>1</sup>H NMR** (500 MHz, CDCl<sub>3</sub>) 6.30 (2H, dd, <sup>3</sup>*J* = 3.1 Hz, <sup>3</sup>*J* = 4.6 Hz, HC=C), 6.14 (2H, dd, <sup>3</sup>*J* = 3.1 Hz, <sup>3</sup>*J* = 4.5 Hz, HC=C), 3.79-3.74 (1H, m, H<sub>3</sub>), 3.12-3.08 (2H, m, H<sub>1</sub>, H<sub>5</sub>), 1.90-1.85 (2H, m, H<sub>2</sub>, H<sub>4</sub>), 1.17-1.13 (2H, m, H<sub>2</sub>, H<sub>4</sub>), 0.84 (9H, s, Si-*t*-Bu), 0.01 (6H, s, Si-CH<sub>3</sub>); **<sup>13</sup>C NMR** (125 MHz, CDCl<sub>3</sub>) 136.4 (CH), 131.2 (CH), 70.6 (CH), 33.6 (CH<sub>2</sub>), 26.1 (CH), 22.6 (CH<sub>3</sub>) 18.2 (C<sub>q</sub>), -4.5 (CH<sub>3</sub>)



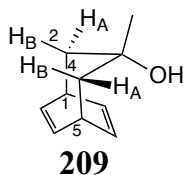
To a solution of compound **208** (0.60 g, 2.40 mmol) in MeOH:CH<sub>2</sub>Cl<sub>2</sub> (1:1, 24 mL) was added at once camphor sulphonic acid (0.12 g, 0.54 mmol). After 1 h the reaction was completed by TLC and was quenched by addition of KHCO<sub>3</sub> to avoid degradation. Water (20 mL) was added and the organic phases separated. The aqueous phase was extracted with CH<sub>2</sub>Cl<sub>2</sub> (3 x 50 mL). Organic phases were combined, dried over MgSO<sub>4</sub> and concentrated under reduced pressure. Purification by flash chromatography (3:2 P.E. 40-60 °C/Et<sub>2</sub>O) afforded the title compound **190** (0.21 g, 64%) as a white solid.

**R<sub>f</sub>** 0.16 (P.E. 40-60 °C/Et<sub>2</sub>O); **M.p.** 62 °C (Et<sub>2</sub>O); **HRMS** found: M<sup>+</sup> 137.09730, C<sub>9</sub>H<sub>13</sub>O requires 137.09664; **CI-MS**, *m/z* (relative intensity), 137 ([M]<sup>+</sup>, 19); **IR**  $\nu_{\text{max}}$  (CDCl<sub>3</sub> film/cm<sup>-1</sup>) 3415 (br), 2925 (s), 2852(s), 1734 (w), 1464 (w), 1378 (w), 1261 (w); **<sup>1</sup>H NMR** (600 MHz, CDCl<sub>3</sub>) 6.35 (2H, dd, <sup>3</sup>*J* = 3.9 Hz, <sup>3</sup>*J* = 4.5 Hz, HC=C), 6.18 (2H, dd, <sup>3</sup>*J* = 3.1 Hz, <sup>3</sup>*J* = 4.5 Hz, HC=C), 3.77 (1H, m, H<sub>3</sub>), 3.14 (2H, m, H<sub>1</sub>, H<sub>5</sub>), 2.03 (2H, apt dt, <sup>3</sup>*J*<sub>5,4A</sub> = <sup>3</sup>*J*<sub>1,2A</sub> = 6.5 Hz, *J* = 12.9 Hz, H<sub>2A</sub>, H<sub>4A</sub>), 1.18 (2H, ddd, <sup>3</sup>*J*<sub>5,4B</sub> = <sup>3</sup>*J*<sub>1,2B</sub> = 1.4 Hz, <sup>3</sup>*J*<sub>3,2B</sub> = <sup>3</sup>*J*<sub>3,4B</sub> = 9.6 Hz, <sup>2</sup>*J*<sub>2A,2B</sub> = <sup>2</sup>*J*<sub>4A,4B</sub> = 12.7 Hz, H<sub>2B</sub>, H<sub>4B</sub>); **<sup>13</sup>C NMR** (150 MHz, CDCl<sub>3</sub>) 135.6 (CH), 131.6 (CH), 70.2 (CH), 38.5 (CH<sub>2</sub>), 33.5 (CH).

Bicyclo[3.2.2]nona-6,8-dien-3-one **183****183**

Freshly prepared Jones reagent was added dropwise to a stirred solution of alcohol **190** (0.59 g, 4.33 mmol) in acetone (50 mL) in an ice bath at 0 °C, until the orange colour persisted. After 10 min of stirring at 0 °C methanol and ice were added to the solution. The aqueous layer was extracted with Et<sub>2</sub>O (3 x 25 mL) and the combined organic layers washed with water (50 mL) brine (50 mL), dried over MgSO<sub>4</sub> and concentrated under reduced pressure. Column chromatography (silica gel, 3:2 P.E. 40-60 °C/Et<sub>2</sub>O) afforded the title compound **183** (0.35 g, 60%) as a white semi-solid.

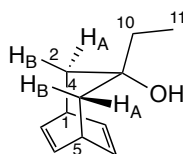
**R<sub>f</sub>** 0.20 (4:1 P.E. 40-60 °C/Et<sub>2</sub>O); **HRMS** found:  $M^+$  134.08032, C<sub>9</sub>H<sub>11</sub>O requires 134.08099; **CI-MS**,  $m/z$  (relative intensity), 135 ( $[M]^+$ , 99); **IR**  $\nu_{\max}$  (CDCl<sub>3</sub> film/cm<sup>-1</sup>) 3044 (w), 2933 (w), 1689 (s), 1612 (w), 1412 (w), 1376 (w), 1322 (w); **<sup>1</sup>H NMR** (500 MHz, CDCl<sub>3</sub>) 6.39 (4H, dd  $J = 3.2$  Hz, 4.4 Hz, HC=C), 3.33-3.27 (2H, m, H<sub>1</sub>, H<sub>5</sub>), 2.49 (4H, d,  $^3J_{5,4} = ^3J_{1,2} = 3.6$  Hz, H<sub>2</sub>, H<sub>4</sub>); **<sup>13</sup>C NMR** (125 MHz, CDCl<sub>3</sub>) 210.7 (C<sub>q</sub>), 134.8 (CH), 47.0 (CH<sub>2</sub>), 32.9 (CH).

3-Methylbicyclo[3.2.2]nona-6,8-dien-3-ol **209**

Cerium (III) chloride heptahydrate (0.74 g, 2.00 mmol) was ground in a mortar and pestle and quickly placed in a three-necked flask fitted with a nitrogen inlet adaptor and a dropping funnel. The flask was evacuated (0.1 mmHg) and heated to 140 °C without stirring for 1 h and then stirred for 1 h. The flask was cooled in an ice bath at 0 °C under N<sub>2</sub> and anhydrous THF (6 mL) was added in one portion with vigorous stirring. The suspension was stirred overnight at room temperature. The flask was then cooled to -78 °C under nitrogen and MeLi (1.6 M in Et<sub>2</sub>O, 1.24 mL, 2.00 mmol) was added dropwise and the yellow suspension was stirred for 1 h. A solution of ketone **183** (117 mg, 0.71 mmol) in anhydrous THF (6 mL) was added dropwise and the reaction mixture was stirred for 3 h, then warmed to 0°C. The mixture was poured into an aqueous HCl solution (2 M, 20 mL) and extracted with CH<sub>2</sub>Cl<sub>2</sub> (3 x 15 mL). The combined organic layers were washed with water (40 mL) brine (40 mL), dried over Na<sub>2</sub>SO<sub>4</sub> and concentrated under reduced pressure. Column chromatography (silica gel, 3:2 P.E. 40-60 °C/Et<sub>2</sub>O) afforded the title compound **209** (107 mg, 71%) as an off-white semi-solid.

**R<sub>f</sub>** 0.16 (4:1 P.E. 40-60 °C/Et<sub>2</sub>O); **HRMS** found: (M-H)<sup>+</sup> 149.09674, C<sub>10</sub>H<sub>13</sub>O (M-H) requires 149.09609; **EI-MS**, *m/z* (relative intensity), 149 ([M-H]<sup>+</sup>, 5); **IR**  $\nu_{\max}$  (CDCl<sub>3</sub> film/cm<sup>-1</sup>) 3569 (br, OH), 3041 (w), 2966 (w), 2928 (w), 1693 (w), 1456 (w), 1375 (w), 1312 (w); **<sup>1</sup>H NMR** (500 MHz, CDCl<sub>3</sub>) 5.54 (2H, dd, <sup>3</sup>*J* = 3.1 Hz, <sup>3</sup>*J* = 4.6 Hz, HC=C), 6.36 (2H, dd <sup>3</sup>*J* = 3.2 Hz, <sup>3</sup>*J* = 4.5 Hz, HC=C), 3.16-3.12 (2H, m, H<sub>1</sub>, H<sub>5</sub>), 2.49 (1H, s, OH), 1.92 (2H, ddd, <sup>4</sup>*J*<sub>2A,4A</sub> = 1.0 Hz, <sup>3</sup>*J*<sub>5,4A</sub> = <sup>3</sup>*J*<sub>1,2A</sub> = 6.5 Hz, <sup>2</sup>*J*<sub>4A,4B</sub> = <sup>2</sup>*J*<sub>2A,2B</sub> = 14.2 Hz, H<sub>2A</sub>, H<sub>4A</sub>), 1.60 (2H, dd <sup>3</sup>*J*<sub>5,4B</sub> = <sup>3</sup>*J*<sub>1,2B</sub> = 1.0 Hz, <sup>2</sup>*J*<sub>4A,4B</sub> = <sup>2</sup>*J*<sub>2A,2B</sub> = 14.2 Hz, H<sub>2B</sub>, H<sub>4B</sub>), 0.97 (3H, s, CH<sub>3</sub>); **<sup>13</sup>C NMR**

(125 MHz, CDCl<sub>3</sub>) 136.2 (CH), 133.9 (CH), 74.2 (C<sub>q</sub>), 47.0 (CH<sub>2</sub>), 40.0 (CH), 34.8 (CH<sub>3</sub>)

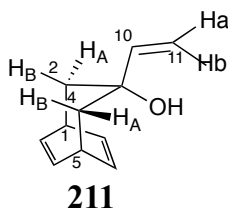
3-Ethylbicyclo[3.2.2]nona-6,8-dien-3-ol **210****210**

Cerium (III) chloride heptahydrate (0.40 g, 1.00 mmol) was ground in a mortar and pestle and quickly placed in a three-necked flask fitted with a nitrogen inlet adaptor and a dropping funnel. The flask was evacuated (0.1 mmHg) and heated to 140 °C without stirring for 1 h and then stirred for 1 h. The flask was cooled in an ice bath at 0 °C under N<sub>2</sub> and anhydrous THF (3 mL) was added in one portion with vigorous stirring. The suspension was stirred overnight at room temperature. The flask was cooled to 0°C under nitrogen and ethylmagnesium bromide (1.46 M in Et<sub>2</sub>O, 0.70 mL, 1.00 mmol) was added dropwise and the suspension was stirred for 1.5 h. A solution of ketone **183** (67 mg, 0.50 mmol) in anhydrous THF (3 mL) was added dropwise and the reaction mixture was stirred for 4 h at 0 °C. The mixture was poured into an aqueous HCl solution (2.0 M, 10 mL) and extracted with CH<sub>2</sub>Cl<sub>2</sub> (3 x 10 mL). The combined organic layers were washed with water (20 mL) brine (20 mL), dried over Na<sub>2</sub>SO<sub>4</sub> and concentrated under reduced pressure. Flash column chromatography (silica gel, 4:1 P.E. 40-60 °C/Et<sub>2</sub>O) afforded the title compound **210** (86 mg, 83%) as a pale yellow oil.

**R<sub>f</sub>** 0.21 (4:1 P.E. 40-60 °C/Et<sub>2</sub>O); **HRMS** found: (M-OH)<sup>+</sup> 147.11769, C<sub>11</sub>H<sub>15</sub> (M-OH) requires 147.11769; **CI-MS**, *m/z* (relative intensity), 148 ([M-OH]<sup>+</sup>, 42); **IR** ν<sub>max</sub> (CDCl<sub>3</sub> film/cm<sup>-1</sup>) 3575 (br, OH), 3041 (w), 2924 (w), 1461 (w), 1443 (w), 1376 (w), 1307 (w); **<sup>1</sup>H NMR** (600 MHz, CDCl<sub>3</sub>) 6.55 (2H, dd, <sup>3</sup>*J* = 3.2 Hz, <sup>3</sup>*J* = 4.2 Hz, HC=C), 6.37 (2H, dd, <sup>3</sup>*J* = 3.3 Hz, <sup>3</sup>*J* = 4.2 Hz, HC=C), 3.38 (1H, s, OH), 3.16-3.12 (2H, m, H<sub>1</sub>, H<sub>5</sub>), 1.86 (2H, dd, <sup>3</sup>*J*<sub>5,4A</sub> = <sup>3</sup>*J*<sub>1,2A</sub> = 6.4 Hz, <sup>2</sup>*J*<sub>2A,2B</sub> = <sup>2</sup>*J*<sub>4A,4B</sub> = 14.2 Hz, H<sub>2A</sub>, H<sub>4A</sub>), 1.57 (2H, dd, <sup>3</sup>*J*<sub>5,4B</sub> = <sup>3</sup>*J*<sub>1,2B</sub> = 1.0 Hz, <sup>2</sup>*J*<sub>2A,2B</sub> = <sup>2</sup>*J*<sub>4A,4B</sub> = 14.2 Hz, H<sub>2B</sub>, H<sub>4B</sub>), 1.23 (2H, q, <sup>3</sup>*J* = 7.5 Hz, H<sub>10</sub>), 0.80 (3H, t, <sup>3</sup>*J* = 7.5 Hz,

H<sub>11</sub>); <sup>13</sup>C NMR (150 MHz, CDCl<sub>3</sub>) 136.4 (CH), 135.9 (CH), 75.8 (C<sub>q</sub>), 41.5 (CH<sub>2</sub>), 38.5 (CH<sub>2</sub>), 34.7 (CH), 7.1 (CH<sub>3</sub>).

3-Vinylbicyclo[3.2.2]nona-6,8-dien-3-ol **211**

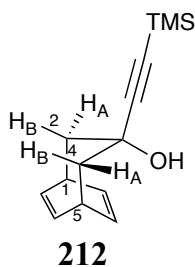


Cerium (III) chloride heptahydrate (0.40 g, 1.00 mmol) was ground in a mortar and pestle and quickly placed in a three-necked flask fitted with a nitrogen inlet adaptor and a dropping funnel. The flask was evacuated (0.1 mmHg) and heated to 140 °C without stirring for 1 h and then stirred for 1 h. The flask was cooled in an ice bath at 0 °C under N<sub>2</sub> and anhydrous THF (3 mL) was added in one portion with vigorous stirring. The suspension was stirred overnight at room temperature. The flask was cooled to -78 °C under nitrogen and vinylmagnesium bromide (1.0 M in THF, 1.00 mL, 1.00 mmol) was added dropwise and the suspension was stirred for 1.5 h. A solution of ketone **183** (67 mg, 0.50 mmol) in anhydrous THF (3 mL) was added dropwise and the reaction mixture was stirred for 4.5 h at -78 °C. The mixture warmed to room temperature, poured into an aqueous HCl solution (2 M, 10 mL) and extracted with CH<sub>2</sub>Cl<sub>2</sub> (3 x 10 mL). The combined organic layers were washed with water (20 mL) brine (20 mL), dried over Na<sub>2</sub>SO<sub>4</sub> and concentrated under reduced pressure. Column chromatography (silica gel, 4:1 P.E. 40-60 °C/Et<sub>2</sub>O) afforded the title compound **211** (54 mg, 67%) as a colourless oil.

**R<sub>f</sub>** 0.29 (4:1 P.E. 40-60 °C/Et<sub>2</sub>O); **HRMS** found: (M-OH)<sup>+</sup> 145.10069, C<sub>11</sub>H<sub>13</sub> (M-OH) requires 145.10118; **CI-MS**, *m/z* (relative intensity), 145 ([M-OH]<sup>+</sup>, 99); **IR** *v*<sub>max</sub> (CDCl<sub>3</sub> film/cm<sup>-1</sup>) 3387 (br, OH), 3041 (w), 2923 (s), 2853 (s), 1716 (w), 1639 (w), 1601 (w), 1448 (w), 1375 (w), 1260 (w), 1194 (w), 1081 (s);

**<sup>1</sup>H NMR** (600 MHz, CDCl<sub>3</sub>) 6.58 (2H, dd, <sup>3</sup>*J* = 3.1 Hz, <sup>3</sup>*J* = 4.6 Hz, HC=C), 6.39 (2H, dd, <sup>3</sup>*J* = 3.3 Hz, <sup>3</sup>*J* = 4.4 Hz, HC=C), 5.56 (1H, ddd, <sup>3</sup>*J* = 10.7 Hz, <sup>4</sup>*J* = 1.4 Hz, <sup>3</sup>*J* = 17.1 Hz, H<sub>10</sub>), 5.11 (1H, dd <sup>2</sup>*J* = 1.4 Hz, <sup>3</sup>*J* = 17.1 Hz, H<sub>11b</sub>), 4.88 (1H, dd, <sup>2</sup>*J* = 1.5 Hz, <sup>3</sup>*J* = 10.7 Hz, H<sub>11a</sub>), 3.52 (1H, s, OH), 3.18-3.14 (2H, m, H<sub>1</sub>, H<sub>5</sub>), 1.84 (2H, ddd, <sup>4</sup>*J*<sub>2A,4A</sub> = 1.0 Hz, <sup>3</sup>*J*<sub>5,4A</sub> = <sup>3</sup>*J*<sub>1,2A</sub> = 6.4 Hz, <sup>2</sup>*J*<sub>2A,2B</sub> = <sup>2</sup>*J*<sub>4A,4B</sub> = 14.3 Hz, H<sub>2A</sub>, H<sub>4A</sub>), 1.70 (2H, dd, <sup>3</sup>*J*<sub>5,4B</sub> = <sup>3</sup>*J*<sub>1,2B</sub> = 1.3 Hz, <sup>2</sup>*J*<sub>2A,2B</sub> = <sup>2</sup>*J*<sub>4A,4B</sub> = 14.3 Hz, H<sub>2B</sub>, H<sub>4B</sub>); **<sup>13</sup>C NMR** (150 MHz, CDCl<sub>3</sub>) 146.6 (CH), 136.5 (CH), 134.8 (CH), 111.0 (CH<sub>2</sub>), 76.15 (C<sub>q</sub>), 38.9 (CH<sub>2</sub>), 34.7 (CH).

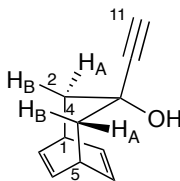


3-(Trimethylsilyl)ethynylbicyclo[3.2.2]nona-6,8-dien-3-ol **212**

Cerium (III) chloride heptahydrate (0.96 g, 2.50 mmol) was ground in a mortar and pestle and quickly placed in a three-necked flask fitted with a nitrogen inlet adaptor and a dropping funnel. The flask was evacuated (0.1 mmHg) and heated to 140 °C without stirring for 1 h and then stirred for 1 h. The flask was cooled in an ice bath under N<sub>2</sub> and anhydrous THF (12.5 mL) was added in one portion with vigorous stirring. The suspension was stirred overnight at room temperature. In a separate dry flask *n*-BuLi in hexanes (2.18 M, 1.17 mL, 2.50 mmol) was added dropwise to a solution of trimethylsilylacetylene (0.35 mL, 2.50 mmol) in anhydrous THF (3.5 mL) at 0 °C under N<sub>2</sub>. The yellow suspension was cooled to -78 °C and stirred for 30 min. Meanwhile, the suspension of cerium (III) chloride in THF was cooled to -78 °C before the dropwise addition of the organolithium solution *via* canular. The resulting mixture was stirred at -78 °C for 2 h and a solution of ketone **183** (67 mg, 0.50 mmol) in anhydrous THF (12.5 mL) was added dropwise. The resulting mixture was slowly warmed to 0 °C and stirred for 4 h, then warmed to room temperature and poured into a saturated aqueous NH<sub>4</sub>Cl solution (50 mL), filtered through celite and extracted with Et<sub>2</sub>O (3 x 25 mL). The combined organic layers were washed with brine (25 mL), dried over MgSO<sub>4</sub> and concentrated under reduced pressure. Flash column chromatography (silica gel, 9:1 P.E. 40-60 °C/Et<sub>2</sub>O) gave the title compound **212** (75 mg, 65%) as a white solid.

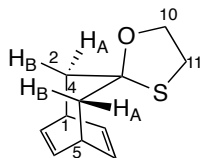
**R<sub>f</sub>** 0.16 (9:1 P.E. 40-60 °C/Et<sub>2</sub>O); **M.p.** 69 °C; **HRMS** found: M<sup>+</sup> 233.13511, C<sub>14</sub>H<sub>21</sub>OSi requires 233.13617; **CI-MS**, *m/z* (relative intensity), 233 ([M]<sup>+</sup>, 31);

**IR**  $\nu_{\max}$  (CDCl<sub>3</sub> film/cm<sup>-1</sup>) 3374 (br, OH), 2958 (w), 2928 (w), 2158 (w), 1632 (w), 1374 (w), 1324 (w), 1249 (w), 1089 (w), 1069 (w); **<sup>1</sup>H NMR** (600 MHz, CDCl<sub>3</sub>) 6.47 (2H, dd, <sup>3</sup>*J* = 3.0 Hz, <sup>3</sup>*J* = 4.5 Hz, HC=C), 6.34 (2H, dd, <sup>3</sup>*J* = 3.2 Hz, <sup>3</sup>*J* = 4.4 Hz, HC=C), 3.18-3.15 (2H, m, H<sub>1</sub>, H<sub>5</sub>), 2.97 (1H, s, OH), 2.09 (2H, dd, <sup>3</sup>*J*<sub>5,4B</sub> = <sup>3</sup>*J*<sub>1,2B</sub> = 3.1 Hz, <sup>2</sup>*J*<sub>2A,2B</sub> = <sup>2</sup>*J*<sub>4A,4B</sub> = 14.2 Hz, H<sub>2B</sub>, H<sub>4B</sub>), 1.99 (2H, dd, <sup>3</sup>*J*<sub>5,4A</sub> = <sup>3</sup>*J*<sub>1,2A</sub> = 4.6 Hz, <sup>2</sup>*J*<sub>2A,2B</sub> = <sup>2</sup>*J*<sub>4A,4B</sub> = 14.2 Hz, H<sub>2A</sub>, H<sub>4A</sub>), 0.13 (9H, s, Si(CH<sub>3</sub>)<sub>3</sub>); **<sup>13</sup>C NMR** (150 MHz, CDCl<sub>3</sub>) 136.2 (CH), 134.9 (CH), 111.7 (C<sub>q</sub>), 86.1 (C<sub>q</sub>), 71.4 (C<sub>q</sub>), 40.0 (CH<sub>2</sub>), 34.2 (CH), 0.04 (CH<sub>3</sub>)

3-Ethynylbicyclo[3.2.2]nona-6,8-dien-3-ol **213****211**

Potassium carbonate (75 mg, 0.54 mmol) was added to a stirred solution of tertiary alcohol **212** (63 mg, 0.27 mmol) in methanol (1 mL). After stirring for 1 h at room temperature, the resulting mixture was diluted with water (5 mL), extracted with  $\text{CH}_2\text{Cl}_2$  (3 x 10 mL). The combined organic layers were washed water (10 mL), brine (10 mL), dried over  $\text{Na}_2\text{SO}_4$  and concentrated under reduced pressure. Flash column chromatography (silica gel, 1:1 P.E. 40-60 °C/ $\text{Et}_2\text{O}$ ) gave the title compound **213** (34 mg, 80%) as a pale yellow semi-solid.

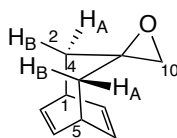
**R<sub>f</sub>** 0.12 (4:1 P.E. 40-60 °C/ $\text{Et}_2\text{O}$ ); **HRMS** found:  $\text{M}^+$  161.09741,  $\text{C}_{11}\text{H}_{13}\text{O}$  requires 161.09664; **CI-MS**,  $m/z$  (relative intensity), 161 ( $[\text{M}]^+$ , 9); **IR**  $\nu_{\text{max}}$  ( $\text{CDCl}_3$  film/ $\text{cm}^{-1}$ ) 3393 (br, OH), 3292 (w), 3042 (w), 2927 (w), 2159 (w), 1724 (w), 1635 (w), 1374 (W), 1322 (w), 1251 (w), 1229 (w), 1083 (w), 1079 (w); **<sup>1</sup>H NMR** (600 MHz,  $\text{CDCl}_3$ ) 6.49 (2H,  $^3J = 3.0$  Hz,  $^3J = 4.5$  Hz, HC=C), 6.37 (2H, dd,  $^3J = 3.2$  Hz,  $^3J = 4.4$  Hz, HC=C), 3.20-3.15 (2H, m, H<sub>1</sub>, H<sub>5</sub>), 3.05 (1H, s, OH), 2.41 (1H, s, H<sub>11</sub>), 2.10 (2H, dd,  $^3J_{5,4B} = ^3J_{1,2B} = 2.9$  Hz,  $^2J_{2A,2B} = ^2J_{4A,4B} = 14.1$  Hz, H<sub>2B</sub>, H<sub>4B</sub>), 2.05 (2H, dd,  $^3J_{5,4A} = ^3J_{1,2A} = 4.6$  Hz,  $^2J_{2A,2B} = ^2J_{4A,4B} = 14.1$  Hz, H<sub>2A</sub>, H<sub>4A</sub>); **<sup>13</sup>C NMR** (150 MHz,  $\text{CDCl}_3$ ) 136.2 (CH), 135.0 (CH), 89.8 (C<sub>q</sub>), 70.9 (C<sub>q</sub>), 70.4 (C<sub>q</sub>), 40.0 (CH<sub>2</sub>), 34.1 (CH)

Spiro[bicyclo[3.2.2]nona[6,8]diene-3,2'-[1,3]oxathiolane] **219****219**

Scandium (III) triflate (2 mg, 0.005 mmol) was added in one portion to a solution of ketone **183** (67 mg, 0.50 mmol), 2-mercaptoethanol (70  $\mu$ L, 1 mmol) in anhydrous  $\text{CH}_2\text{Cl}_2$  (5 mL) and the resulting solution stirred for 3 days at room temperature under an atmosphere of  $\text{N}_2$ . The reaction mixture was quenched with water (10 mL), extracted with  $\text{CH}_2\text{Cl}_2$  (3 x 10 mL). The combined organic layers were washed with aqueous NaOH (10%, 3 x 10 mL), water (3 x 10 mL), dried over  $\text{Na}_2\text{SO}_4$  and concentrated under reduced pressure. Flash column chromatography (silica gel, 4:1 P.E. 40-60  $^\circ\text{C}/\text{Et}_2\text{O}$ ) gave the title compound **219** (62 mg, 64%) as a colourless oil.

**R<sub>f</sub>** 0.51 (9:1 P.E. 40-60  $^\circ\text{C}/\text{Et}_2\text{O}$ ); **HRMS** found:  $\text{M}^+$  194.07510,  $\text{C}_{11}\text{H}_{11}\text{OS}$  requires 194.07510; **EI-MS**,  $m/z$  (relative intensity), 194 ( $[\text{M}]^+$ , 5); **IR**  $\nu_{\text{max}}$  ( $\text{CDCl}_3$  film/ $\text{cm}^{-1}$ ) 3042 (w), 2927 (w), 2868 (w), 1781 (w), 1608 (w), 1432 (w), 1374 (w), 1260 (w), 1073 (w), 1022 (w);  **$^1\text{H}$  NMR** (600 MHz,  $\text{CDCl}_3$ ) 6.38 (2H, dd,  $^3J = 3.3$  Hz,  $^3J = 4.2$  Hz, HC=C), 6.33 (2H, dd,  $^3J = 3.1$  Hz,  $^3J = 4.6$  Hz, HC=C), 4.02 (2H, t,  $^3J = 5.8$  Hz,  $\text{H}_{10}$ ), 3.21-3.17 (2H, m,  $\text{H}_1$ ,  $\text{H}_5$ ), 2.90 (2H, t,  $^3J = 5.8$  Hz,  $\text{H}_{11}$ ), 2.38 (2H, dd,  $^3J_{5,4A} = ^3J_{1,2A} = 6.2$  Hz,  $^2J_{2A,2B} = ^2J_{4A,4B} = 13.3$  Hz,  $\text{H}_{2A}$ ,  $\text{H}_{4A}$ ), 1.92 (2H, dd,  $^3J_{5,4B} = ^3J_{1,2B} = 1.5$  Hz,  $^2J_{2A,2B} = ^2J_{4A,4B} = 13.3$  Hz,  $\text{H}_{2B}$ ,  $\text{H}_{4B}$ );  **$^{13}\text{C}$  NMR** (150 MHz,  $\text{CDCl}_3$ ) 136.3 (CH), 134.4 (CH), 97.5 ( $\text{C}_q$ ), 68.9 ( $\text{CH}_2$ ), 43.1 ( $\text{CH}_2$ ), 33.8 ( $\text{CH}_2$ ), 27.1 (CH)

Attempted synthesis of Spiro[bicyclo[3.2.2]nona[6,8]diene-3,2'-oxirane] **218**

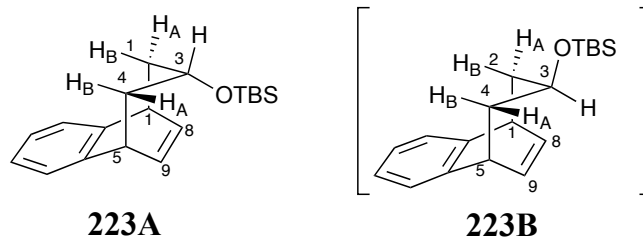


**218**

Sodium hydride (60% in mineral oil, 21 mg, 0.53 mmol) was added in one portion to a solution of tri-methylsulfoxonium iodide (0.12 g, 0.53 mmol) in anhydrous DMSO (1 mL) and the mixture stirred for 30 min at room temperature under N<sub>2</sub>. A solution of ketone **183** (67 mg, 0.50 mmol) in anhydrous DMSO (1 mL) was added dropwise and heated to 60 °C and stirred overnight. The reaction mixture was poured into ice and extracted with Et<sub>2</sub>O (3 x 5mL). The combined organic layers were washed water (10 mL), brine (10 mL), dried over MgSO<sub>4</sub> and concentrated under reduced pressure. Flash column chromatography (silica gel, 3:2 P.E. 40-60 °C/Et<sub>2</sub>O) afforded trace amounts of the title compound **218** as a white solid, which rapidly underwent decomposition.

**<sup>1</sup>H NMR** (600 MHz, CDCl<sub>3</sub>) 6.41 (2H, m, HC=C), 6.32 (2H, m, HC=C), 3.18-3.14 (2H, m, H<sub>1</sub>, H<sub>5</sub>), 2.32 (2H, s, H<sub>10</sub>), 1.77 (2H, dd, <sup>3</sup>J<sub>5,4A</sub> = <sup>3</sup>J<sub>1,2A</sub> = 4.0 Hz, <sup>2</sup>J<sub>2A,2B</sub> = <sup>2</sup>J<sub>4A,4B</sub> = 13.7 Hz, H<sub>2A</sub>, H<sub>4A</sub>), 1.62 (2H, dd, <sup>3</sup>J<sub>5,4B</sub> = <sup>3</sup>J<sub>1,2B</sub> = 3.7 Hz, <sup>2</sup>J<sub>2A,2B</sub> = <sup>2</sup>J<sub>4A,4B</sub> = 13.7 Hz, H<sub>2B</sub>, H<sub>4B</sub>)

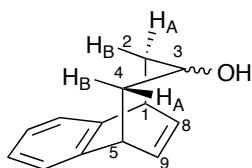
*Exo*- and *endo*-6,7-benzobicyclo[3.2.2]nona-6,8-dien-3-yloxy)(*tert*-butyl)dimethylsilane **223**



To a cold solution at 0 °C of anthranilic acid (2.08 g, 15.4 mmol) and trifluoroacetic acid (245 mg, 1.54 mmol) in THF (40 mL) in a PVC Erlenmeyer flask, isoamyl nitrite (1.53 g, 13.1 mmol) was added dropwise over a period of 1 min. After 30 min the red solution became a pale brown mixture which was filtered and washed with THF until washing were colorless, care was taken to ensure that the filter cake was not be allowed to become dry. The resulting pale brown solid was mixed with 1,2-dichloroethane (2 x 20 mL), diene **205** (2.63 g, 11.5 mmol) was added and the mixture heated to 50 °C for 3 h. The dark solution was cooled to room temperature and extracted with CH<sub>2</sub>Cl<sub>2</sub> (3 x mL). The combined organic layers were washed with water (10 mL), dried over MgSO<sub>4</sub> and concentrated under reduced pressure to obtain a yellow oil. Flash column chromatography (silica gel 10:1 P.E. 40-60 °C/Et<sub>2</sub>O) afforded the title compounds as a mixture which was used without further purification **223** (2.02 g, 43%) as a pale yellow solid. Major diastereomer **223A**, was purified by crystallization from cold Et<sub>2</sub>O to yield the product as yellow crystals.

**R<sub>f</sub>** 0.5 (10:1 P.E. 40-60 °C/Et<sub>2</sub>O); **M.p.** 72-73 °C (hexanes); **HRMS** found: M<sup>+</sup> 301.19876 C<sub>19</sub>H<sub>28</sub>OSi requires 301.19821, **CI-MS**, *m/z* = 301 ([M]<sup>+</sup>, 35); **IR** *v*<sub>max</sub> (solid/cm<sup>-1</sup>) 2952 (m), 2857 (m), 1470 (w), 1251 (m), 1057 (m), 892 (m), 836 (m), 776 (m), 717 (m); **<sup>1</sup>H NMR** (600 MHz, CDCl<sub>3</sub>) **223A**: 7.10 - 7.20 (4H, m, H<sub>Ar</sub>), 6.45 (2H, dd, <sup>3</sup>*J* = 4.6 Hz, <sup>3</sup>*J* = 3.0 Hz, HC=C), 3.56 (2H, dt, <sup>3</sup>*J* = 3.8 Hz, <sup>3</sup>*J* = 3.6 Hz, H<sub>1</sub>, H<sub>5</sub>), 3.12 (1H, tt, <sup>3</sup>*J* = 6.1 Hz, <sup>3</sup>*J* = 4.3 Hz, H<sub>3</sub>), 2.00 (2H, dd, <sup>2</sup>*J* = 12.2 Hz, <sup>3</sup>*J* = 7.1 Hz, H<sub>2</sub>, H<sub>4</sub>), 1.41 (2H, dd, <sup>2</sup>*J* = 12.3 Hz, <sup>3</sup>*J* = 10.7 Hz, H<sub>2</sub>, H<sub>4</sub>),

0.76 (9H, s, SiC(CH<sub>3</sub>)<sub>3</sub>), 0.15 (6H, s, Si(CH<sub>3</sub>)<sub>2</sub>); Mixture: 7.05 - 7.40 (4H, m, Ph<sup>major + minor</sup>), 6.47 (2H, dd, <sup>3</sup>J = 4.6, <sup>3</sup>J = 3.0, CH=CH<sup>major</sup>), 6.32 (0.3H, dd, <sup>3</sup>J = 4.6, <sup>3</sup>J = 3.0, CH=CH<sup>minor</sup>), 3.40 - 3.60 (2.9H, m, (H<sub>1</sub>, H<sub>5</sub>)<sup>major+minor</sup>), 3.10 - 3.20 (1.1H, m, H<sub>3</sub><sup>major+minor</sup>), 1.99 - 2.08 (2H, m, H<sub>2</sub><sup>major</sup>, H<sub>4</sub><sup>major</sup>), 1.82 - 1.95 (0.4H, m, H<sub>2</sub><sup>minor</sup>, H<sub>4</sub><sup>minor</sup>), 1.43 (2H, dd, J = 12.1, 10.7, H<sub>2</sub><sup>major</sup>, H<sub>4</sub><sup>major</sup>), 1.27 (0.5H, dd, J = 12.8, 9.9, H<sub>2</sub><sup>minor</sup>, H<sub>4</sub><sup>minor</sup>), 0.80 - 0.95 (1.35H, m, Si(CH<sub>3</sub>)<sub>3</sub><sup>minor</sup>), 0.78 (9H, s, Si(CH<sub>3</sub>)<sub>3</sub><sup>major</sup>), 0.00 - 0.25 (1H, m, Si(CH<sub>3</sub>)<sup>minor</sup>), -0.14 (6H, s, Si(CH<sub>3</sub>)<sup>major</sup>); <sup>13</sup>C NMR (150 MHz, CDCl<sub>3</sub>) 141.1 (C<sub>Ar</sub>), 136.0 (CH), 125.9 (CH), 125.0 (CH), 69.9 (CH), 38.4 (CH), 37.2 (CH<sub>2</sub>), 25.3 (CH<sub>3</sub>), 18.1 (C<sub>q</sub>), 4.7 (CH<sub>3</sub>).

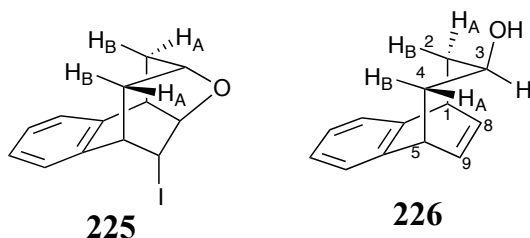
*Exo*- and *endo*-6,7-benzobicyclo[3.2.2]nona-6,8-dien-3-ol **224****224**

To a solution of compound **223** (19.0 g, 62.5 mmol) in MeOH:CH<sub>2</sub>Cl<sub>2</sub> (1:1, 180 mL) was added at once camphor sulphonic acid (0.12 g, 0.54 mmol). After 2 h the reaction was completed by TLC and was quenched by addition of KHCO<sub>3</sub> to avoid degradation. Water (100 mL) was added and the organic phases separated. The aqueous phase was extracted with CH<sub>2</sub>Cl<sub>2</sub> (3 x 50 mL). Organic phases were combined, dried over MgSO<sub>4</sub> and concentrated under reduced pressure. Flash column chromatography (silica gel, 1:1 P.E. 40-60 °C/Et<sub>2</sub>O) afforded the title compound **224** (11.0 g, 95%) as a pale yellow oil.

**R<sub>f</sub>** 0.44 (1:1 P.E. 40-60 °C/Et<sub>2</sub>O); **IR**  $\nu_{\text{max}}$  (solid/cm<sup>-1</sup>) 3381 (OH, m), 2925 (m), 2849 (m), 1457 (w), 1262 (m), 1098 (m), 1031 (m), 912 (m), 795 (m), 743 (s), 721 (w); **<sup>1</sup>H NMR** (600 MHz, CDCl<sub>3</sub>) 7.12 - 7.16 (4H, m, H<sub>Ar</sub>), 6.51 (2H, dd, <sup>3</sup>*J* = 4.6 Hz, <sup>3</sup>*J* = 3.0 Hz, H<sub>8</sub>, H<sub>9</sub>), 3.62 (2H, m, H<sub>1</sub>, H<sub>5</sub>), 3.20 (1H, m, H<sub>3</sub>), 2.17 (2H, apt dt, <sup>3</sup>*J*<sub>5,4A</sub> = <sup>3</sup>*J*<sub>1,2A</sub> = 6.5 Hz, *J* = 12.8 Hz, H<sub>2A</sub>, H<sub>4A</sub>), 1.43 (2H, ddd, <sup>3</sup>*J*<sub>5,4B</sub> = <sup>3</sup>*J*<sub>1,2B</sub> = 1.2 Hz, <sup>3</sup>*J*<sub>3,2B</sub> = <sup>3</sup>*J*<sub>3,4B</sub> = 10.5 Hz, <sup>2</sup>*J*<sub>2A,2B</sub> = <sup>2</sup>*J*<sub>4A,4B</sub> = 12.7 Hz, H<sub>2B</sub>, H<sub>4B</sub>); **<sup>13</sup>C NMR** (150 MHz, CDCl<sub>3</sub>) 141.2 (C<sub>Ar</sub>), 136.2 (CH), 126.0 (CH), 125.2 (CH), 69.3 (CH), 38.2 (CH), 36.8 (CH<sub>2</sub>).



4,5-Benzo-8-iodo-10-oxatricyclo[4.3.1.0<sup>3,9</sup>]nona-4-ene **225** and *exo*-6,7-benzobicyclo[3.2.2]nona-6,8-dien-3-ol **226**



To a solution of the secondary alcohol **224** (mixture of diastereoisomers) (97 mg, 0.52 mmol) in CH<sub>2</sub>Cl<sub>2</sub> (10 mL), pyridine (62 mg, 0.78 mmol) and iodine (132 mg, 0.52 mmol) were added. The dark brown solution was stirred for 2 h at room temperature and then quenched with a saturated solution of Na<sub>2</sub>SO<sub>3</sub> (10 mL) and extracted with CH<sub>2</sub>Cl<sub>2</sub> (3 x 10 mL). The combined organic layers were dried over MgSO<sub>4</sub>, filtered and concentrated under reduced pressure to yield a brown oil. Purification by flash column chromatography (silica gel, 1:1 P.E. 40-60 °C/Et<sub>2</sub>O to Et<sub>2</sub>O), afforded the iodo-ether **225** (30 mg, 0.10 mmol) and the secondary alcohol **226** (35 mg, 0.19 mmol) as colourless oils.

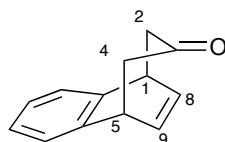
### 225

**R<sub>f</sub>** 0.67 (2:1 P.E. 40-60 °C/Et<sub>2</sub>O); **HRMS** found: (M)<sup>+</sup> 312.00094 C<sub>13</sub>H<sub>13</sub>OI requires 312.00056, **EI-MS**, *m/z* = 312 ([M]<sup>+</sup>, 5); **IR** *v*<sub>max</sub> (solid/cm<sup>-1</sup>) 3063 (w), 3022 (w), 2922 (s), 2853 (m), 1708 (m), 1600 (m), 1489 (m), 1456 (s), 1364 (m), 1324 (m), 1269 (m), 1233 (m), 1189 (m), 1149 (m), 1086 (m), 1057 (m), 1024 (s), 1004 (s), 980 (s), 967 (m), 926 (m); **<sup>1</sup>H NMR** (600 MHz, CDCl<sub>3</sub>) 7.24 (1H, d, <sup>3</sup>*J* = 6.0 Hz, H<sub>Ar</sub>), 7.15 - 7.23 (2H, m, H<sub>Ar</sub>), 7.08 (1H, d, <sup>3</sup>*J* = 6.0 Hz, H<sub>Ar</sub>), 4.96 (1H, dd, <sup>3</sup>*J* = 3.4 Hz, <sup>3</sup>*J* = 1.6 Hz, CH), 4.92 (1H, dt, *J* = 7.0, 1.9 Hz, CH), 4.54 (1H, t, <sup>3</sup>*J* = 5.3 Hz, CH), 3.64 (1H, dd, *J* = 9.7, 7.0 Hz, CH), 3.27 - 3.30 (1H, m, H<sub>5</sub>), 2.47 (1H, dtd, *J* = 13.7, 5.2, 1.7 Hz, CH<sub>2</sub>), 2.37 (1H, dddd, *J* = 11.7, 9.8, 5.9, 1.7 Hz, CH<sub>2</sub>), 1.99 (1H, d, <sup>3</sup>*J* = 13.7 Hz, CH<sub>2</sub>), 1.71 (1H, d, <sup>3</sup>*J* = 11.7 Hz, CH<sub>2</sub>); **<sup>13</sup>C NMR** (150 MHz, CDCl<sub>3</sub>) 142.8 (C<sub>Ar</sub>), 142.2 (C<sub>Ar</sub>), 127.9 (CH), 127.6 (CH), 126.1 (CH), 125.6 (CH), 80.1 (CH), 77.3 (CH), 76.5 (CH), 44.5 (CH), 42.9 (CH<sub>2</sub>), 41.4 (CH), 35.6 (CH<sub>2</sub>)

226

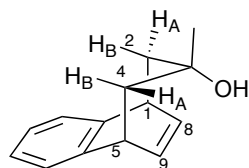
**R<sub>f</sub>** 0.44 (1:1 P.E. 40-60 °C/Et<sub>2</sub>O); **HRMS** found: (M)<sup>+</sup> 186.10414 C<sub>13</sub>H<sub>14</sub>O requires 186.10392, **EI-MS**,  $m/z$  = 186 ([M]<sup>+</sup>, 45); **IR**  $\nu_{\max}$  (solid/cm<sup>-1</sup>) 3351 (OH, m), 3040 (m), 2926 (s), 2856 (m), 1708 (m), 1485 (m), 1457 (m), 1030 (s) 718 (w); **<sup>1</sup>H NMR** (600 MHz, CDCl<sub>3</sub>) 7.1 - 7.30 (4H, m, H<sub>Ar</sub>), 6.36 (2H, dd, <sup>3</sup> $J$  = 4.5 Hz, <sup>3</sup> $J$  = 3.0 Hz, H<sub>8</sub>, H<sub>9</sub>), 3.84 (1H, m, H<sub>3</sub>), 3.62 – 3.68 (2H, m, H<sub>1</sub>, H<sub>5</sub>), 2.32 (2H, apt dt, <sup>3</sup> $J_{5,4A}$  = <sup>3</sup> $J_{1,2A}$  = 6.6 Hz,  $J$  = 12.2 Hz, H<sub>2A</sub>, H<sub>4A</sub>), 1.31 (2H, ddd, <sup>3</sup> $J_{5,4B}$  = <sup>3</sup> $J_{1,2B}$  = 1.6 Hz, <sup>3</sup> $J_{3,2B}$  = <sup>3</sup> $J_{3,4B}$  = 9.6 Hz, <sup>2</sup> $J_{2A,2B}$  = <sup>2</sup> $J_{4A,4B}$  = 12.2 Hz, H<sub>2B</sub>, H<sub>4B</sub>), 1.27 (1H, s, OH); **<sup>13</sup>C NMR** (150 MHz, CDCl<sub>3</sub>) 145.1 (C<sub>Ar</sub>), 132.0 (CH), 126.0 (CH), 125.2 (CH), 69.2 (CH), 38.8 (CH), 36.2 (CH<sub>2</sub>).



6,7-Benzobicyclo[3.2.2]nona-6,8-dien-3-one **184****184**

To a solution of secondary alcohol **224** (2.64 g, 14.2 mmol) in  $\text{CH}_2\text{Cl}_2$  (40 mL) a solution of PCC (6.12 g, 28.4 mmol) in  $\text{CH}_2\text{Cl}_2$  (40 mL) and NaOAc (1.16 g, 14.2 mmol) were added at once. After 1 h the reaction mixture turned black and was completed by TLC. The mixture was filtered through celite, the residual solid was washed with  $\text{CH}_2\text{Cl}_2$  (3 x 50 mL) and the solvent concentrated under reduced pressure to yield a black oil. Flash column chromatography (silica gel, 9:1 P.E. 40-60 °C/ $\text{Et}_2\text{O}$ ) afforded product **183** (1.95 g, 75%) as a white solid.

**R<sub>f</sub>** 0.86 (9:1 P.E. 40-60 °C/ $\text{Et}_2\text{O}$ ); **M.p** 84-85 °C (hexanes); **HRMS** found:  $\text{M}^+$  184.08794  $\text{C}_{13}\text{H}_{12}\text{O}$  requires 184.08826; **IR**  $\nu_{\text{max}}$  (solid/ $\text{cm}^{-1}$ ) 3038 (w), 2924 (w), 1682 (s), 1484 (w), 1458 (w), 1401 (w), 1362 (w), 1169 (w), 992 (w), 747 (s); **<sup>1</sup>H NMR** (600 MHz,  $\text{CDCl}_3$ ) 7.17 - 7.39 (4H, m,  $\text{H}_{\text{Ar}}$ ), 6.58 (2H, dd,  $^3J = 4.5$  Hz,  $^3J = 3.0$  Hz,  $\text{H}_8$ ,  $\text{H}_9$ ), 3.80 (2H, m,  $\text{H}_1$ ,  $\text{H}_5$ ), 2.73 (2H, dd,  $^3J = 3.7$  Hz,  $^2J = 17.9$  Hz,  $\text{H}_2$ ,  $\text{H}_4$ ), 2.63 (2H, dd,  $^3J = 3.7$  Hz,  $^2J = 17.9$  Hz,  $\text{H}_2$ ,  $\text{H}_4$ ); **<sup>13</sup>C NMR** (150 MHz,  $\text{CDCl}_3$ ) 210.1 ( $\text{C}_\text{q}$ ), 142.3 ( $\text{C}_{\text{Ar}}$ ), 134.9 (CH), 126.7 (CH), 125.6 (CH), 49.1 ( $\text{CH}_2$ ), 38.0 (CH).

*Endo*-3-methyl-6,7-benzobicyclo[3.2.2]nona-6,8-dien-3-ol **228****228**

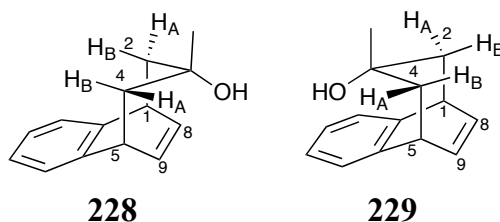
Cerium (III) chloride heptahydrate (0.74 g, 2.00 mmol) was ground in a mortar and pestle and quickly placed in a three-necked flask fitted with a nitrogen inlet adaptor and a dropping funnel. The flask was evacuated (0.1 mmHg) and heated to 140 °C without stirring for 1 h and then stirred for 1 h. The flask was cooled in an ice bath at 0 °C under N<sub>2</sub> and anhydrous THF (10 mL) was added in one portion with vigorous stirring. The suspension was stirred overnight at room temperature. The flask was cooled to -78 °C under nitrogen and methylmagnesium bromide (1.40 M in THF, 1.43 mL, 2.00 mmol) was added dropwise and the suspension was stirred for 1 h. A solution of ketone **184** (184 mg, 1.00 mmol) in anhydrous THF (10 mL) was added dropwise and the reaction mixture was stirred for 2 h at -78 °C and then slowly warmed to 0 °C and stirred for 3 h. The mixture was poured into an aqueous HCl solution (2.0 M, 20 mL), neutralized with aqueous NaHCO<sub>3</sub> and extracted with CH<sub>2</sub>Cl<sub>2</sub> (3 x 20 mL). The combined organic layers were washed with water (20 mL) brine (20 mL), dried over MgSO<sub>4</sub> and concentrated under reduced pressure. Column chromatography (silica gel, 20:1 P.E. 40-60 °C/Et<sub>2</sub>O) afforded the title compound **228** (108 mg, 54%) as a white solid.

**R<sub>f</sub>** 0.74 (2:1 P.E. 40-60 °C/Et<sub>2</sub>O); **M.p** 130 °C (hexanes); **HRMS** found: (M-OH)<sup>+</sup> 183.11730 C<sub>14</sub>H<sub>15</sub> (M-OH) requires 183.11738, **CI-MS**, *m/z* = 183 ([M-OH]<sup>+</sup>, 100); **IR** *v*<sub>max</sub> (solid/cm<sup>-1</sup>) 3587 (m), 3461 (w), 3040 (m), 2967 (w), 2924 (m), 1483 (w), 1458 (m), 1374 (m), 1311 (w), 1228 (w), 1113 (m), 1057 (m), 910 (m); **<sup>1</sup>H NMR** (600 MHz, CDCl<sub>3</sub>) 7.15-7.11 (4H, m, H<sub>Ar</sub>), 6.70 (2H, dd, <sup>3</sup>*J* = 3.2 Hz, <sup>3</sup>*J* = 4.7 Hz, H<sub>8</sub>, H<sub>9</sub>), 3.65-3.59 (2H, m, H<sub>1</sub>, H<sub>5</sub>), 2.02 (2H, ddd, <sup>4</sup>*J*<sub>2A,4A</sub> = 1.3

---

Hz,  $^3J_{5,4A} = ^3J_{1,2A} = 6.5$  Hz,  $^2J_{2A,2B} = ^2J_{4A,4B} = 14.0$  Hz, H<sub>2A</sub>, H<sub>4A</sub>), 1.71 (2H, dd,  $^3J_{5,4B} = ^3J_{1,2B} = 1.3$  Hz,  $^2J_{2A,2B} = ^2J_{4A,4B} = 14.0$  Hz, H<sub>2B</sub>, H<sub>4B</sub>), 0.90 (3H, s, CH<sub>3</sub>); **<sup>13</sup>C NMR** (150 MHz, CDCl<sub>3</sub>) 142.1 (C<sub>Ar</sub>), 135.7 (CH), 126.6 (CH), 126.3 (CH), 74.1 (C<sub>q</sub>), 41.7 (CH<sub>2</sub>), 39.2 (CH), 33.5 (CH<sub>3</sub>).

*Endo*- and *exo*-3-methyl-6,7-benzobicyclo[3.2.2]nona-6,8-dien-3-ol **228** and **229**



Cerium (III) chloride heptahydrate (0.88 g, 2.40 mmol) was ground in a mortar and pestle and quickly placed in a three-necked flask fitted with a nitrogen inlet adaptor and a dropping funnel. The flask was evacuated (0.1 mmHg) and heated to 140 °C without stirring for 1 h and then stirred for 1 h. The flask was cooled in an ice bath at 0 °C under N<sub>2</sub> and anhydrous THF (8 mL) was added in one portion with vigorous stirring. The suspension was stirred overnight at room temperature. The flask then was cooled to -78 °C under nitrogen and MeLi (1.6 M in Et<sub>2</sub>O, 1.50 mL, 2.40 mmol) was added dropwise and the yellow suspension was stirred for 1 h. A solution of ketone **184** (220 mg, 1.20 mmol) in anhydrous THF (8 mL) was added dropwise and the reaction mixture was warmed to 0 °C, then stirred for 4.5 h. The mixture was poured into an aqueous HCl solution (2.0 M, 25 mL) and extracted with CH<sub>2</sub>Cl<sub>2</sub> (3 x 20 mL). The combined organic layers were washed with water (40 mL) brine (40 mL), dried over Na<sub>2</sub>SO<sub>4</sub> and concentrated under reduced pressure. Column chromatography (silica gel, 4:1 P.E. 40-60 °C/Et<sub>2</sub>O) afforded the title compounds **228** (32 mg, 13%) and **229** (20 mg, 8%) as white solids.

#### *endo* **228**

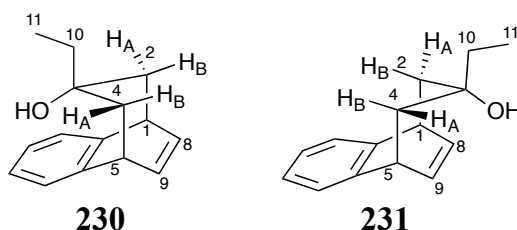
The spectroscopic data obtained was identical to what was previously described.

#### *exo* **229**

**R<sub>f</sub>** 0.26 (4:1 P.E. 40-60 °C/Et<sub>2</sub>O); **M.p.** 89 °C (hexanes);; **HRMS** found: (M)<sup>+</sup> 200.11907 C<sub>14</sub>H<sub>16</sub> O requires 200.11956, **EI-MS**, *m/z* = 200 ([M]<sup>+</sup>, 25); **IR** ν<sub>max</sub> (solid/cm<sup>-1</sup>) 3585 (w), 3452, (br, OH), 3041 (w), 2968 (w), 2922 (w), 1708 (w), 1483 (w), 1458 (w), 1374 (w), 1311 (w), 1228 (w), 1111 (w), 1057 (w); **<sup>1</sup>H**

**NMR** (600 MHz, CDCl<sub>3</sub>) 7.28-7.25 (2H, m, H<sub>Ar</sub>), 7.20-7.18 (2H, m, H<sub>Ar</sub>), 6.15 (2H, dd,  $^3J = 3.1$  Hz,  $^3J = 4.6$  Hz, H<sub>8</sub>, H<sub>9</sub>), 3.62-3.59 (2H, m, H<sub>1</sub>, H<sub>5</sub>), 2.02 (2H, ddd,  $^4J_{2A,4A} = 1.0$  Hz,  $^3J_{5,4A} = ^3J_{1,2A} = 6.7$  Hz,  $^2J_{2A,2B} = ^2J_{4A,4B} = 14.2$  Hz, H<sub>2A</sub>, H<sub>4A</sub>), 1.80 (2H, dd,  $^3J_{5,4B} = ^3J_{1,2B} = 0.9$  Hz,  $^2J_{2A,2B} = ^2J_{4A,4B} = 14.2$  Hz, H<sub>2B</sub>, H<sub>4B</sub>), 0.99 (3H, s, CH<sub>3</sub>); **<sup>13</sup>C NMR** (150 MHz, CDCl<sub>3</sub>) 145.1 (C<sub>Ar</sub>), 136.4 (CH), 125.9 (CH), 125.1 (CH), 73.1 (C<sub>q</sub>), 43.1 (CH<sub>2</sub>), 40.1 (CH), 32.8 (CH<sub>3</sub>).



*Exo*- and *endo*-3-ethyl-6,7-benzobicyclo[3.2.2]nona-6,8-dien-3-ol **230** and **231**

Cerium (III) chloride heptahydrate (0.40 g, 1.00 mmol) was ground in a mortar and pestle and quickly placed in a three-necked flask fitted with a nitrogen inlet adaptor and a dropping funnel. The flask was evacuated (0.1 mmHg) and heated to 140 °C without stirring for 1 h and then stirred for 1 h. The flask was cooled in an ice bath at 0 °C under N<sub>2</sub> and anhydrous THF (3 mL) was added in one portion with vigorous stirring. The suspension was stirred overnight at room temperature. The flask was then cooled to 0 °C under nitrogen, ethylmagnesium bromide (3.00 M in Et<sub>2</sub>O, 0.33 mL, 1.00 mmol) was added dropwise and the suspension was stirred for 1.5 h. A solution of ketone **184** (92 mg, 0.50 mmol) in anhydrous THF (3 mL) was added dropwise and the reaction mixture was stirred for 4 h at 0 °C. The mixture was poured into an aqueous HCl solution (2.0 M, 10 mL) and extracted with CH<sub>2</sub>Cl<sub>2</sub> (3 x 10 mL). The combined organic layers were washed with water (20 mL) brine (20 mL), dried over Na<sub>2</sub>SO<sub>4</sub> and concentrated under reduced pressure. Column chromatography (silica gel, 4:1 P.E. 40-60 °C/Et<sub>2</sub>O) afforded the title compounds **230** (79 mg, 74%) and **231** (26 mg, 24%) as colourless oils.

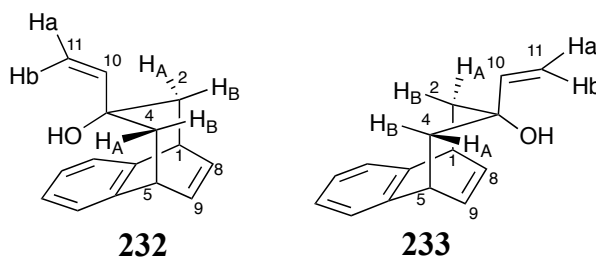
*Exo* **230**

**R<sub>f</sub>** 0.38 (4:1 P.E. 40-60 °C/Et<sub>2</sub>O); **HRMS** found: M<sup>+</sup> 214.13486, C<sub>15</sub>H<sub>18</sub>O requires 214.13521; **EI-MS**, *m/z* (relative intensity), 214 ([M<sup>+</sup>], 21); **IR** ν<sub>max</sub> (CDCl<sub>3</sub> film/cm<sup>-1</sup>) 3590 (w), 3465 (br, OH), 3040 (w), 2918 (w), 1639 (w), 1482 (w), 1458 (w), 1373 (w); **<sup>1</sup>H NMR** (600 MHz, CDCl<sub>3</sub>) 7.27-7.25 (2H, m, H<sub>Ar</sub>), 7.20-7.18 (2H, m, H<sub>Ar</sub>), 6.51 (2H, dd, <sup>3</sup>*J* = 3.1 Hz, <sup>3</sup>*J* = 4.6 Hz, H<sub>8</sub>, H<sub>9</sub>), 3.62-3.59 (2H, m, H<sub>1</sub>, H<sub>5</sub>), 1.96 (2H, ddd, <sup>4</sup>*J*<sub>2A,4A</sub> = 1.0 Hz, <sup>3</sup>*J*<sub>5,4A</sub> = <sup>3</sup>*J*<sub>1,2A</sub> = 6.8 Hz, <sup>2</sup>*J*<sub>2A,2B</sub> = <sup>2</sup>*J*<sub>4A,4B</sub> = 14.1 Hz, H<sub>2A</sub>, H<sub>4A</sub>), 1.76 (2H, dd, <sup>3</sup>*J*<sub>5,4B</sub> = <sup>3</sup>*J*<sub>1,2B</sub> = 1.0 Hz, <sup>2</sup>*J*<sub>2A,2B</sub> = <sup>2</sup>*J*<sub>4A,4B</sub>

= 14.1 Hz, H<sub>2B</sub>, H<sub>4B</sub>), 1.24 (2H, q,  $^3J = 7.5$  Hz, H<sub>10</sub>), 0.76 (3H, t,  $^3J = 7.5$  Hz, H<sub>11</sub>); **<sup>13</sup>C NMR** (150 MHz, CDCl<sub>3</sub>) 142.2 (C<sub>Ar</sub>), 135.7 (CH), 126.6 (CH), 126.2 (CH), 75.6 (C<sub>q</sub>), 40.2 (CH<sub>2</sub>), 39.1 (CH), 38.8 (CH<sub>2</sub>), 7.06 (CH<sub>3</sub>).

### Endo 230

**R<sub>f</sub>** 0.17 (4:1 P.E. 40-60 °C/Et<sub>2</sub>O); **HRMS** found: M<sup>+</sup> 214.13463, C<sub>15</sub>H<sub>18</sub>O requires 214.13521; **EI-MS**, *m/z* (relative intensity), 214 ([M<sup>+</sup>], 30); **IR** ν<sub>max</sub> (CDCl<sub>3</sub> film/cm<sup>-1</sup>) 3570 (w), 3466 (br, OH), 3039 (w), 2926 (w), 1484 (w), 1458 (w), 1374 (w), 1308 (w); **<sup>1</sup>H NMR** (600 MHz, CDCl<sub>3</sub>) 7.15-7.12 (4H, m, H<sub>Ar</sub>), 6.71 (2H, dd  $^3J = 3.1$  Hz,  $^3J = 1.5$  Hz, H<sub>8</sub>, H<sub>9</sub>), 3.67-3.64 (2H, m, H<sub>1</sub>, H<sub>5</sub>), 2.17 (2H, ddd,  $^4J_{2A,4A} = 1.2$  Hz,  $^3J_{5,4A} = ^3J_{1,2A} = 6.8$  Hz,  $^2J_{2A,2B} = ^2J_{4A,4B} = 14.3$  Hz, H<sub>2A</sub>, H<sub>4A</sub>), 1.66 (2H, dd,  $^3J_{5,4B} = ^3J_{1,2B} = 1.2$  Hz,  $^2J_{2A,2B} = ^2J_{4A,4B} = 14.3$  Hz, H<sub>2B</sub>, H<sub>4B</sub>), 1.17 (2H, q,  $^3J = 7.4$ , H<sub>10</sub>), 0.75 (3H, t,  $^3J = 7.4$ , H<sub>11</sub>); **<sup>13</sup>C NMR** (150 MHz, CDCl<sub>3</sub>) 145.3 (C<sub>Ar</sub>), 136.5 (CH), 125.8 (CH), 124.9 (CH), 74.6 (C<sub>q</sub>), 41.7 (CH<sub>2</sub>), 40.1 (CH), 38.2 (CH<sub>2</sub>), 7.02 (CH<sub>3</sub>).

*Exo*- and *endo*-3-vinyl-6,7-benzobicyclo[3.2.2]nona-6,8-dien-3-ol **232** and **233**

Cerium (III) chloride heptahydrate (0.40 g, 1.00 mmol) was ground in a mortar and pestle and quickly placed in a three-necked flask fitted with a nitrogen inlet adaptor and a dropping funnel. The flask was evacuated (0.1 mmHg) and heated to 140 °C without stirring for 1 h and then stirred for 1 h. The flask was cooled in an ice bath at 0 °C under N<sub>2</sub> and anhydrous THF (3 mL) was added in one portion with vigorous stirring. The suspension was stirred overnight at room temperature. The flask was cooled to -78 °C under nitrogen, vinylmagnesium bromide (1.00 M in THF, 1.00 mL, 1.00 mmol) was added dropwise and the suspension was stirred for 1.5 h. A solution of ketone **184** (92 mg, 0.50 mmol) in anhydrous THF (3 mL) was added dropwise and the reaction mixture was stirred for 4 h at -78 °C. The mixture was warmed to room temperature and poured into an aqueous HCl solution (2.0 M, 10 mL) and extracted with CH<sub>2</sub>Cl<sub>2</sub> (3 x 10 mL). The combined organic layers were washed with water (20 mL) brine (20 mL), dried over Na<sub>2</sub>SO<sub>4</sub> and concentrated under reduced pressure. Column chromatography (silica gel, 4:1 P.E. 40-60 °C/Et<sub>2</sub>O) afforded the title compounds **232** (55 mg, 52%) and **233** (16 mg, 15%) as white solids.

*Exo* **232**

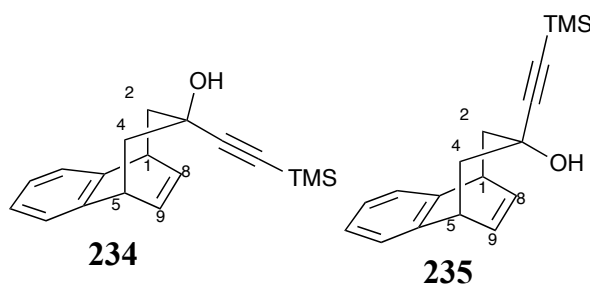
**R<sub>f</sub>** 0.35 (4:1 P.E. 40-60 °C/Et<sub>2</sub>O); **M.p.** 39°C; **IR**  $\nu_{\text{max}}$  (CDCl<sub>3</sub> film/cm<sup>-1</sup>) 3587 (w). 3480 (br, OH), 3041 (w), 2916 (w), 1641 (w), 1481 (w), 1458 (w), 1408 (w), 1220 (w), 1127 (w). **HRMS** found: M<sup>+</sup> 212.11946, C<sub>15</sub>H<sub>16</sub>O requires 212.11956; **EI-MS**, *m/z* (relative intensity), 212 ([M<sup>+</sup>], 20); **<sup>1</sup>H NMR** (600 MHz, CDCl<sub>3</sub>) 7.27-7.26 (2H, m, H<sub>Ar</sub>), 7.21-7.20 (2H, m, H<sub>Ar</sub>), 6.54 (2H, dd, <sup>3</sup>*J* = 3.2

Hz,  $^3J = 4.6$  Hz, H<sub>8</sub>, H<sub>9</sub>), 5.59 (1H, dd,  $^3J = 10.7$  Hz,  $^3J = 17.1$  Hz, H<sub>10</sub>), 5.05 (1H, dd,  $^2J = 1.3$  Hz,  $^3J = 17.1$  Hz, H<sub>11b</sub>), 4.86 (1H, dd,  $^2J = 1.3$  Hz,  $^3J = 10.6$  Hz, H<sub>11a</sub>), 3.64-3.61 (2H, m, H<sub>1</sub>, H<sub>5</sub>), 1.91-1.89 (2H, m, H<sub>2B</sub>, H<sub>4B</sub>), 0.89-0.82 (2H, m, H<sub>2A</sub>, H<sub>4A</sub>);  $^{13}\text{C}$  NMR (150 MHz, CDCl<sub>3</sub>) 146.6 (CH), 142.3 (C<sub>Ar</sub>), 135.9 (CH), 126.7 (CH), 126.2 (CH), 111.1 (CH<sub>2</sub>), 76.1 (C<sub>q</sub>), 40.5 (CH<sub>2</sub>), 39.1 (CH).

### Endo 233

**R<sub>f</sub>** 0.19 (4:1 P.E. 40-60 °C/Et<sub>2</sub>O); **M.p.** 80 °C; **HRMS** found: M<sup>+</sup> 212.11979, C<sub>15</sub>H<sub>16</sub>O requires 212.11956; **EI-MS**, *m/z* (relative intensity), 212 ([M<sup>+</sup>], 4); **IR**  $\nu_{\text{max}}$  (CDCl<sub>3</sub> film/cm<sup>-1</sup>) 3568 (w), 3442 (br, OH), 3040 (w), 2925 (w), 1694 (w), 1484 (w), 1458 (w), 1409 (w), 1228 (w), 1121 (w);  $^1\text{H}$  NMR (600 MHz, CDCl<sub>3</sub>) 7.28-7.26 (1H, m, H<sub>Ar</sub>), 7.21-7.19 (2H, m, H<sub>Ar</sub>), 7.16-7.13 (1H, m, H<sub>Ar</sub>), 6.54 (2H, dd,  $^3J = 3.1$  Hz,  $^3J = 4.6$  Hz, H<sub>8</sub>, H<sub>9</sub>), 5.40 (1H, ddd,  $^4J = 1.3$  Hz,  $^3J = 10.7$  Hz,  $^3J = 17.1$  Hz, H<sub>10</sub>), 5.08 (1H, dd,  $^2J = 1.5$  Hz,  $^3J = 17.1$  Hz, H<sub>11b</sub>), 4.82 (1H, dd,  $^2J = 1.5$  Hz,  $^3J = 10.7$  Hz, H<sub>11a</sub>), 3.68-3.65 (2H, m, H<sub>1</sub>, H<sub>5</sub>), 3.41 (1H, s, OH), 2.11 (2H, ddd,  $^4J_{2A,4A} = 1.2$  Hz,  $^3J_{5,4A} = ^3J_{1,2A} = 6.1$  Hz,  $^2J_{2A,2B} = ^2J_{4A,4B} = 14.0$ , H<sub>2A</sub>, H<sub>4A</sub>), 1.83 (2H, dd,  $^3J_{5,4B} = ^3J_{1,2B} = 1.5$  Hz,  $^2J_{2A,2B} = ^2J_{4A,4B} = 14.6$  Hz, H<sub>2B</sub>, H<sub>4B</sub>);  $^{13}\text{C}$  NMR (150 MHz, CDCl<sub>3</sub>) 146.0 (CH), 144.9 (C<sub>Ar</sub>), 136.7 (CH), 126.0 (CH), 125.1 (CH), 111.3 (CH<sub>2</sub>), 74.9 (C<sub>q</sub>), 41.9 (CH<sub>2</sub>), 40.0 (CH).

*Exo*- and *endo*-3-((Trimethylsilyl)ethynyl)-6,7-benzobicyclo[3.2.2]nona-6,8-dien-3-ol **234** and **235**



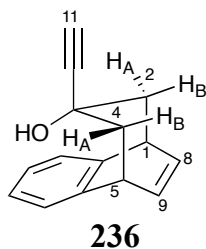
Cerium (III) chloride heptahydrate (0.75 g, 2.00 mmol) was ground in a mortar and pestle and quickly placed in a three-necked flask fitted with a nitrogen inlet adaptor and a dropping funnel. The flask was evacuated (0.1 mmHg) and heated to 140 °C without stirring for 1 h and then stirred for 1 h. The flask was cooled in an ice bath at 0 °C under N<sub>2</sub> and anhydrous THF (10 mL) was added in one portion with vigorous stirring. The suspension was stirred overnight at room temperature. In a separate dry flask *n*-BuLi in hexanes (2.00 M, 1.00 mL, 2.00 mmol) was added dropwise to a solution of trimethylsilylacetylene (0.28 mL, 2.00 mmol) in anhydrous THF (3 mL) at 0 °C under N<sub>2</sub>. The yellow suspension was cooled to -78 °C and stirred for 30 min. Meanwhile, the suspension of cerium (III) chloride in THF was cooled to -78°C before the dropwise addition of the organolithium solution *via* canular. The resulting mixture was stirred at -78 °C for 2 h and a solution of ketone **184** (180 mg, 1.00 mmol) in anhydrous THF (10 mL) was added dropwise. The resulting mixture was slowly warmed to 0 °C and stirred for 4 h, then warmed to room temperature and poured into a saturated aqueous NH<sub>4</sub>Cl solution (50 mL), filtered through celite and extracted with Et<sub>2</sub>O (3 x 25 mL). The combined organic layers were washed brine (25 mL), dried over MgSO<sub>4</sub> and concentrated under reduced pressure. Flash column chromatography (silica gel, 4:1 P.E. 40-60 °C/Et<sub>2</sub>O) gave the title compounds (**128** mg, 45%) and **235** (48 mg, 17%) as off-white solids.

*exo* **234**

**R<sub>f</sub>** 0.62 (4:1 P.E. 40-60 °C/Et<sub>2</sub>O); **M.p.** 63 °C (chloroform); **HRMS** found: M<sup>+</sup> 282.14325, C<sub>18</sub>H<sub>22</sub>OSi requires 282.14344; **EI-MS**, *m/z* (relative intensity), 282 ([M<sup>+</sup>], 10); **IR**  $\nu_{\max}$  (CDCl<sub>3</sub> film/cm<sup>-1</sup>) 3417 (br, OH), 3044 (w), 2956 (w), 2173 (w), 1485 (w), 1363 (w), 1320 (w), 1249 (w), 1082 (s); **<sup>1</sup>H NMR** (600 MHz, CDCl<sub>3</sub>) 7.15-7.23 (4H, m, H<sub>Ar</sub>), 6.50 (2H, dd, <sup>3</sup>*J* = 4.6 Hz, <sup>3</sup>*J* = 3.0 Hz, H<sub>8</sub>, H<sub>9</sub>), 3.63 (2H, m, H<sub>1</sub>, H<sub>5</sub>), 2.30 (2H, dd, <sup>3</sup>*J*<sub>5,4A</sub> = <sup>3</sup>*J*<sub>1,2A</sub> = 7.0 Hz, <sup>2</sup>*J*<sub>2A,2B</sub> = <sup>2</sup>*J*<sub>4A,4B</sub> = 14.3 Hz, H<sub>2</sub>, H<sub>4</sub>), 2.10 (2H, dd, <sup>3</sup>*J*<sub>5,4B</sub> = <sup>3</sup>*J*<sub>1,2B</sub> = 4.9 Hz, <sup>2</sup>*J*<sub>2A,2B</sub> = <sup>2</sup>*J*<sub>4A,4B</sub> = 14.3 Hz, H<sub>2</sub>, H<sub>4</sub>), 1.41 (1H, s, OH), 0.14 (9H, s, Si(CH<sub>3</sub>)<sub>3</sub>); **<sup>13</sup>C NMR** (150 MHz, CDCl<sub>3</sub>) 142.7 (C<sub>Ar</sub>), 134.9 (CH), 126.5 (CH), 125.8 (CH), 111.4 (C<sub>q</sub>), 86.5 (C<sub>q</sub>), 70.9 (C<sub>q</sub>), 41.9 (CH<sub>2</sub>), 38.9 (CH), 0.0 (CH<sub>3</sub>).

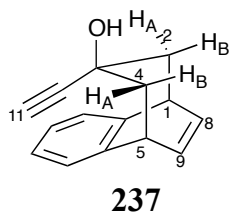
*endo* **235**

**R<sub>f</sub>** 0.43 (4:1 P.E. 40-60 °C/Et<sub>2</sub>O); **M.p.** 45 °C (chloroform); **HRMS** found: M<sup>+</sup> 282.14284, C<sub>18</sub>H<sub>22</sub>OSi requires 282.14344; **EI-MS**, *m/z* (relative intensity), 282 ([M<sup>+</sup>], 15); **IR**  $\nu_{\max}$  (CDCl<sub>3</sub> film/cm<sup>-1</sup>) 3400 (br, OH), 3042 (w), 2926 (w), 2168 (w), 1483 (w), 1459 (w), 1248 (w), 1094 (s); **<sup>1</sup>H NMR** (600 MHz, CDCl<sub>3</sub>) 7.18-7.11 (4H, m, H<sub>Ar</sub>), 6.59 (2H, dd <sup>3</sup>*J* = 4.7 Hz, <sup>3</sup>*J* = 3.1 Hz, H<sub>8</sub>, H<sub>9</sub>), 3.66 (2H, m, H<sub>1</sub>, H<sub>5</sub>), 2.57 (1H, s, OH), 2.28 (2H, dd, <sup>3</sup>*J*<sub>5,4A</sub> = <sup>3</sup>*J*<sub>1,2A</sub> = 4.9 Hz, <sup>2</sup>*J*<sub>2A,2B</sub> = <sup>2</sup>*J*<sub>4A,4B</sub> = 13.7 Hz, H<sub>2</sub>, H<sub>4</sub>), 2.08 (2H, dd, <sup>3</sup>*J*<sub>5,4B</sub> = <sup>3</sup>*J*<sub>1,2B</sub> = 3.2 Hz, <sup>2</sup>*J*<sub>2A,2B</sub> = <sup>2</sup>*J*<sub>4A,4B</sub> = 13.8 Hz, H<sub>2</sub>, H<sub>4</sub>), 0.01 (9H, s, Si(CH<sub>3</sub>)<sub>3</sub>); **<sup>13</sup>C NMR** (150 MHz, CDCl<sub>3</sub>) 142.5 (C<sub>Ar</sub>), 136.5 (CH), 126.1 (CH), 125.8 (CH), 110.1 (C<sub>q</sub>), 86.1 (C<sub>q</sub>), 70.2 (C<sub>q</sub>), 42.1 (CH<sub>2</sub>), 38.9 (CH), 0.0 (CH<sub>3</sub>).

*Exo*- 3-ethynyl-6,7-benzobicyclo[3.2.2]nona-6,8-dien-3-ol **236**

Potassium carbonate (120 mg, 0.84 mmol) was added to a stirred solution of tertiary alcohol **234** (120 mg, 0.42 mmol) in methanol (2 mL). After stirring for 2 h at room temperature, the resulting mixture was diluted with water (5 mL), extracted with CH<sub>2</sub>Cl<sub>2</sub> (3 x 10 mL). The combined organic layers were washed with water (10 mL), brine (10 mL), dried over Na<sub>2</sub>SO<sub>4</sub> and concentrated under reduced pressure. Flash column chromatography (silica gel, 4:1 P.E. 40-60 °C/Et<sub>2</sub>O) gave the title compound **236** (95 mg, 54%) as a white solid.

**R<sub>f</sub>** 0.25 (4:1 P.E. 40-60 °C/Et<sub>2</sub>O); **M.p.** 95 °C; **HRMS** found:  $M^+$  210.10426, C<sub>15</sub>H<sub>14</sub>O requires 210.10392; **EI-MS**,  $m/z$  (relative intensity), 210 ([M<sup>+</sup>], 12); **IR**  $\nu_{\max}$  (CDCl<sub>3</sub> film/cm<sup>-1</sup>) 3247 (s, OH), 3058 (w), 2946 (w), 1514 (w), 1484 (w), 1456 (w), 1364 (w), 1349 (w), 1080 (w), 1034 (s); **<sup>1</sup>H NMR** (600 MHz, CDCl<sub>3</sub>) 7.23 (2H, dd, <sup>3</sup> $J$  = 3.3 Hz, <sup>3</sup> $J$  = 5.4 Hz, H<sub>Ar</sub>), 7.19 (2H, dd, <sup>3</sup> $J$  = 3.3 Hz, <sup>3</sup> $J$  = 5.4 Hz, H<sub>Ar</sub>), 6.53 (2H, dd, <sup>3</sup> $J$  = 3.0 Hz, <sup>3</sup> $J$  = 4.6 Hz, H<sub>8</sub>, H<sub>9</sub>), 3.66-3.63 (2H, m, H<sub>1</sub>, H<sub>5</sub>), 2.43 (1H, s, OH), 2.31 (2H, dd, <sup>3</sup> $J_{5,4B}$  = <sup>3</sup> $J_{1,2B}$  = 2.8 Hz, <sup>2</sup> $J_{2A,2B}$  = <sup>2</sup> $J_{4A,4B}$  = 14.3 Hz, H<sub>2B</sub>, H<sub>4B</sub>), 2.16 (2H, dd, <sup>3</sup> $J_{5,4A}$  = <sup>3</sup> $J_{1,2A}$  = 5.0 Hz, <sup>2</sup> $J_{2A,2B}$  = <sup>2</sup> $J_{4A,4B}$  = 14.3 Hz, H<sub>2A</sub>, H<sub>4A</sub>), 1.40 (1H, s, H<sub>11</sub>); **<sup>13</sup>C NMR** (150 MHz, CDCl<sub>3</sub>) 142.5 (C<sub>Ar</sub>), 135.0 (CH), 126.6 (CH), 125.9 (CH), 89.5 (CH), 70.7 (CH), 70.6 (C<sub>q</sub>), 41.9 (CH<sub>2</sub>), 38.8 (CH).

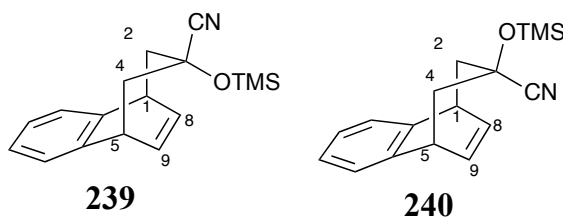
*Endo*- 3-ethynyl-6,7-benzobicyclo[3.2.2]nona-6,8-dien-3-ol **237**

Potassium carbonate (45 mg, 0.32 mmol) was added to a stirred solution of tertiary alcohol **235** (44 mg, 0.16 mmol) in methanol (2 mL). After stirring for 4 h at room temperature, the resulting mixture was diluted with water (5 mL), extracted with CH<sub>2</sub>Cl<sub>2</sub> (3 x 10 mL). The combined organic layers were washed water (10 mL), brine (10 mL), dried over Na<sub>2</sub>SO<sub>4</sub> and concentrated under reduced pressure. Flash column chromatography (silica gel, 4:1 P.E. 40-60 °C/Et<sub>2</sub>O) gave the title compound **237** (55 mg, 82%) as a white solid.

**R<sub>f</sub>** 0.66 (2:1 P.E. 40-60 °C/Et<sub>2</sub>O); **M.p.** 105-107 °C (chloroform); **HRMS** found: (M+H)<sup>+</sup> 211.11184, C<sub>15</sub>H<sub>15</sub>O requires 211.11229; **EI-MS**, *m/z* (relative intensity), 211 ([M+H]<sup>+</sup>, 5); **IR** *v*<sub>max</sub> (CDCl<sub>3</sub> film/cm<sup>-1</sup>) 3309 (s, OH), 3047 (w), 2932 (w), 1482 (w), 1458 (w), 1395 (w), 1260 (w), 1100 (w), 1082 (w), 1016 (s); **<sup>1</sup>H NMR** (600 MHz, CDCl<sub>3</sub>) 7.10-7.20 (4H, m, H<sub>Ar</sub>), 6.22 (2H, dd, <sup>3</sup>*J* = 4.5 Hz, <sup>3</sup>*J* = 3.1 Hz, H<sub>8</sub>, H<sub>9</sub>), 3.68 (2H, m, H<sub>1</sub>, H<sub>5</sub>), 2.70 (1H, s, OH), 2.27 (2H, d, <sup>3</sup>*J*<sub>5,4A</sub> = <sup>3</sup>*J*<sub>1,2A</sub> = 4.4 Hz, H<sub>2A</sub>, H<sub>4A</sub>), 2.15 (2H, d, <sup>3</sup>*J*<sub>5,4B</sub> = <sup>3</sup>*J*<sub>1,2B</sub> = 3.7 Hz, H<sub>2B</sub>, H<sub>4B</sub>), 2.07 (1H, s, H<sub>11</sub>); **<sup>13</sup>C NMR** (150 MHz, CDCl<sub>3</sub>) 142.7 (C<sub>Ar</sub>), 136.3.0 (CH), 126.0 (CH), 125.8 (CH), 88.2 (CH), 70.1 (CH), 69.9 (C<sub>q</sub>), 42.3 (CH<sub>2</sub>), 38.9 (CH).



*Endo*- and *exo*-3-cyano-6,7-benzobicyclo[3.2.2]nona-6,8-dien-3-hydroxytrimethylsilyl **239** and **240**



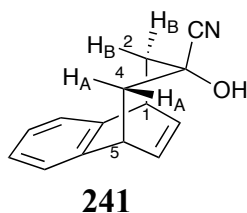
To a solution of bicyclic ketone **184** (552 mg, 3.00 mmol) in anhydrous  $\text{CH}_2\text{Cl}_2$  (15 mL) under a  $\text{N}_2$  atmosphere,  $\text{ZnI}_2$  (96 mg, 0.30 mmol) and trimethylsilylcyanide (0.83 mL, 6.60 mmol) were added. The resulting mixture was stirred for 4 h and concentrated under reduced pressure. The crude product was purified by flash column chromatography (silica gel, 1%  $\text{Et}_2\text{O}$  in hexanes) to afford the title compounds **239** (447 mg, 53%) and **240** (45 mg, 5%) as white solids.

#### *endo* **239**

**R<sub>f</sub>** 0.56 (9:1 P.E. 40-60 °C/ $\text{Et}_2\text{O}$ ); **HRMS** found:  $(\text{M})^+$  283.13807  $\text{C}_{17}\text{H}_{21}\text{NOSi}$   $(\text{M})^+$  requires 283.13869, **EI-MS**,  $m/z = 283$   $([\text{M}]^+, 45)$ ; **IR**  $\nu_{\text{max}}$  (solid/ $\text{cm}^{-1}$ ) 3046 (m), 2960 (m), 2162 (w), 1640 (w), 1485 (m), 1460 (m), 1362 (m), 1252 (s), 1096 (s), 1081 (s), 1033 (w), 1009 (w), 892 (s); **<sup>1</sup>H NMR** (600 MHz,  $\text{CDCl}_3$ ) 7.20-7.30 (4H, m,  $\text{H}_{\text{Ar}}$ ) 6.55 (2H, dd,  $^3J = 4.8$  Hz,  $^3J = 3.1$  Hz,  $\text{H}_8$ ,  $\text{H}_9$ ), 3.70 (2H, m,  $\text{H}_1$ ,  $\text{H}_5$ ), 2.50 (2H, dd,  $^2J = 14.8$  Hz,  $^3J = 7.1$  Hz,  $\text{H}_2$ ,  $\text{H}_4$ ), 1.81 (2H, dd,  $^2J = 14.8$  Hz,  $^3J = 0.9$  Hz,  $\text{H}_2$ ,  $\text{H}_4$ ), 0.15 (9H, s,  $\text{CH}_3$ ); **<sup>13</sup>C NMR** (150 MHz,  $\text{CDCl}_3$ ) 139.8 ( $\text{C}_{\text{Ar}}$ ), 127.1 (CH), 126.6 (CH), 121.7 (CN), 71.3 ( $\text{C}_q$ ), 41.0 ( $\text{CH}_2$ ), 37.7 (CH), 1.8 ( $\text{CH}_3$ ).

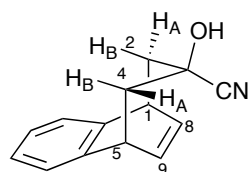
*exo* **240**

**R<sub>f</sub>** 0.50 (9:1 P.E. 40-60°C/Et<sub>2</sub>O); **M.p.**; **HRMS** found: (M)<sup>+</sup> 283.13881 C<sub>17</sub>H<sub>21</sub>NOSi (M)<sup>+</sup> requires 283.13869, **EI-MS**, *m/z* = 283 ([M]<sup>+</sup>, 75); **IR** *v*<sub>max</sub> (solid/cm<sup>-1</sup>) 3046 (w), 2955 (m), 1487 (m), 1459 (m), 1362 (w), 1302 (w), 1252 (s), 1170 (w), 1093 (s), 1069 (s), 1031 (m), 1017 (m), 886 (s), 872 (s), 845 (s), 755 (s), 724 (m), 687 (m); **<sup>1</sup>H NMR** (600 MHz, CDCl<sub>3</sub>) 7.10-7.20 (4H, m, CH<sub>Ar</sub>) 6.54 (2H, dd, <sup>3</sup>*J* = 2.9 Hz, <sup>3</sup>*J* = 4.6 Hz, H<sub>8</sub>, H<sub>9</sub>), 3.72 (2H, m, H<sub>1</sub>, H<sub>5</sub>), 2.63 (2H, dd, <sup>2</sup>*J* = 14.5 Hz, <sup>3</sup>*J* = 6.6 Hz, H<sub>2</sub>, H<sub>4</sub>), 1.71 (2H, dd, <sup>2</sup>*J* = 14.2 Hz, <sup>3</sup>*J* = 1.4 Hz, H<sub>2</sub>, H<sub>4</sub>), 0.15 (9H, s, CH<sub>3</sub>); **<sup>13</sup>C NMR** (150 MHz, CDCl<sub>3</sub>) 133.5 (C<sub>Ar</sub>), 126.2 (CH), 125.1 (CH), 124.5 (CN), 70.8 (C<sub>q</sub>), 41.1 (CH<sub>2</sub>), 38.3 (CH), 1.7 (CH<sub>3</sub>).

*Endo*-3-cyano-6,7-benzobicyclo[3.2.2]nona-6,8-dien-3-ol **241**

To a solution of bicyclic compound **239** (76 mg, 0.27 mmol) in THF (20 mL), 2M HCl (1 mL) was added at once. The colourless solution was stirred at room temperature for 30 min before CH<sub>2</sub>Cl<sub>2</sub> (20 mL) and water (20 mL) were added and the phases separated. The aqueous phase was washed with CH<sub>2</sub>Cl<sub>2</sub> (2 x 20 mL). The combined organic layers were dried over Na<sub>2</sub>SO<sub>4</sub> and concentrated under reduced pressure to obtain a white solid. Flash column chromatography (Hexanes then Et<sub>2</sub>O) afforded bicyclic alcohol **241** as a white solid (42 mg, 72%).

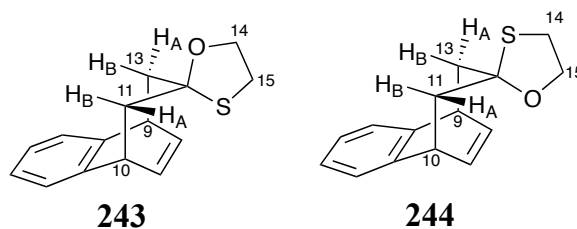
**R<sub>f</sub>** 0.5 (9:1 P.E. 40-60 °C/Et<sub>2</sub>O); **HRMS** found: (M)<sup>+</sup> 211.10014 C<sub>14</sub>H<sub>13</sub>NO (M)<sup>+</sup> requires 211.09917, **EI-MS**, *m/z* = 211 ([M]<sup>+</sup>, 30); **IR** *v*<sub>max</sub> (CDCl<sub>3</sub> film/cm<sup>-1</sup>) 3346 (s, OH), 3037 (w), 2949 (w), 2927 (w), 2858 (w), 2242 (CN, w), 1477 (w), 1459 (w), 1442 (w), 1418 (m), 1353 (w), 1269 (w), 1077 (m), 1052 (s), 1032 (w), 1002 (w), 791 (w), 764 (w), 748 (s); **<sup>1</sup>H NMR** (600 MHz, CDCl<sub>3</sub>) 7.20-7.30 (4H, m, H<sub>Ar</sub>), 6.60 (2H, dd, <sup>3</sup>*J* = 4.6 Hz, <sup>3</sup>*J* = 3.1 Hz, H<sub>8</sub>, H<sub>9</sub>), 3.74 (2H, m, H<sub>1</sub>, H<sub>5</sub>), 2.47 (2H, dd, <sup>3</sup>*J*<sub>5,4A</sub> = <sup>3</sup>*J*<sub>1,2A</sub> = 6.0 Hz, <sup>2</sup>*J*<sub>2A,2B</sub> = <sup>2</sup>*J*<sub>4A,4B</sub> = 13.7 Hz, H<sub>2A</sub>, H<sub>4A</sub>), 1.98 (2H, dd, <sup>3</sup>*J*<sub>5,4A</sub> = <sup>3</sup>*J*<sub>1,2A</sub> = 2.0 Hz, <sup>2</sup>*J*<sub>2A,2B</sub> = <sup>2</sup>*J*<sub>4A,4B</sub> = 13.8 Hz, H<sub>2B</sub>, H<sub>4B</sub>); **<sup>13</sup>C NMR** (150 MHz, CDCl<sub>3</sub>) 140.3 (C<sub>Ar</sub>) 136.3 (CH), 127.1 (CH), 126.4 (CH), 121.7 (CN), 70.2 (C<sub>q</sub>), 39.8 (CH<sub>2</sub>), 37.6 (CH).

*Exo*-3-cyano-6,7-benzobicyclo[3.2.2]nona-6,8-dien-3-ol **242****242**

To a solution of bicyclic compound **240** (36 mg, 0.13 mmol) in THF (20 mL), 2M HCl (1 mL) was added at once. The colourless solution was stirred at room temperature for 30 min before CH<sub>2</sub>Cl<sub>2</sub> (20 mL) and water (20 mL) were added and the phases separated. The aqueous phase was washed with CH<sub>2</sub>Cl<sub>2</sub> (2 x 20 mL). The combined organic layers were dried over Na<sub>2</sub>SO<sub>4</sub> and concentrated under reduced pressure to obtain a white solid. Flash column chromatography (Hexanes then Et<sub>2</sub>O) afforded bicyclic alcohol **242** as a white solid (4 mg, 15%).

**R<sub>f</sub>** 0.35 (9:1 P.E. 40-60 °C/Et<sub>2</sub>O); **HRMS** found: (M)<sup>+</sup> 211.09852 C<sub>14</sub>H<sub>13</sub>NO (M)<sup>+</sup> requires 211.09917, **EI-MS**, *m/z* = 211 ([M]<sup>+</sup>, 30); **IR** *v*<sub>max</sub> (CDCl<sub>3</sub> film/cm<sup>-1</sup>) 3397 (OH, m), 2948 (m), 2920 (m), 2845 (w), 1482 (w), 1459 (m), 1363 (w), 1260 (m), 1096 (m), 1064 (m), 1052 (m), 1029 (m), 799 (m); **<sup>1</sup>H NMR** (600 MHz, CDCl<sub>3</sub>) 7.15 - 7.25 (4H, m, H<sub>Ar</sub>), 6.58 (2H, dd, <sup>3</sup>*J* = 4.5 Hz, <sup>3</sup>*J* = 3.0 Hz, H<sub>8</sub>, H<sub>9</sub>), 3.74 (2H, m, H<sub>1</sub>, H<sub>5</sub>), 2.56 (2H, dd, <sup>3</sup>*J*<sub>5,4A</sub> = <sup>3</sup>*J*<sub>1,2A</sub> = 4.9 Hz, <sup>2</sup>*J*<sub>2A,2B</sub> = <sup>2</sup>*J*<sub>4A,4B</sub> = 14.3 Hz, H<sub>2A</sub>, H<sub>4A</sub>), 1.95 (2H, dd, <sup>3</sup>*J*<sub>5,4A</sub> = <sup>3</sup>*J*<sub>1,2A</sub> = 3.0 Hz, <sup>2</sup>*J*<sub>2A,2B</sub> = <sup>2</sup>*J*<sub>4A,4B</sub> = 14.2 Hz, H<sub>2B</sub>, H<sub>4B</sub>); **<sup>13</sup>C NMR** (150 MHz, CDCl<sub>3</sub>) 142.8 (C<sub>Ar</sub>), 134.2 (CH), 126.8 (CH), 125.6 (CH), 123.5 (CN), 70.4 (C<sub>q</sub>), 39.9 (CH<sub>2</sub>), 38.0 (CH).

*Exo*- and *endo*-spiro-6,7-benzobicyclo[3.2.2]nona-6,8-diene-3,2'-[1,3]oxathiolane] **243** and **244**



Scandium (III) triflate (8 mg, 0.02 mmol) was added in one portion to a solution of ketone **184** (368 mg, 2.00 mmol), 2-mercaptoethanol (0.28 mL, 4.00 mmol) in anhydrous CH<sub>2</sub>Cl<sub>2</sub> (20 mL) and the resulting solution stirred for 48 h at room temperature under an atmosphere of N<sub>2</sub>. The reaction mixture was quenched with water (20 mL), extracted with CH<sub>2</sub>Cl<sub>2</sub> (3 x 20 mL). The combined organic layers were washed with aqueous NaOH (10%, 3 x 20 mL), water (3 x 20 mL), dried over Na<sub>2</sub>SO<sub>4</sub> and concentrated under reduced pressure. Flash column chromatography (silica gel, 9:1 P.E. 40-60 °C/Et<sub>2</sub>O) gave the title compounds **243** (74 mg, 15%) and **244** (64 mg, 13%).

#### *exo* **243**

**R<sub>f</sub>** 0.33 (9:1 P.E. 40-60 °C/Et<sub>2</sub>O); **M.p.** 87 °C; **HRMS** found: M<sup>+</sup> 244.09084 C<sub>15</sub>H<sub>16</sub>OS requires 244.09163; **EI-MS**, *m/z* (relative intensity), 244 ([M<sup>+</sup>], 9); **IR** ν<sub>max</sub> (CDCl<sub>3</sub> film/cm<sup>-1</sup>) 3044 (w), 2938 (w), 2869 (w), 1485 (w), 1459 (w), 1362 (w), 1267 (w), 1223 (w), 1077 (w); **<sup>1</sup>H NMR** (600 MHz, CDCl<sub>3</sub>) 7.16-7.14 (2H, m, H<sub>Ar</sub>), 7.12-7.10 (2H, m, H<sub>Ar</sub>), 6.50 (2H, dd, <sup>3</sup>*J* = 3.1 Hz, <sup>3</sup>*J* = 4.7 Hz, H<sub>8</sub>, H<sub>9</sub>), 3.94 (2H, t, <sup>3</sup>*J* = 5.9 Hz, H<sub>11</sub>), 3.68-3.66 (2H, m, H<sub>1</sub>, H<sub>5</sub>), 2.90 (2H, t, <sup>3</sup>*J* = 5.9 Hz, H<sub>10</sub>), 2.57 (2H, dd, <sup>3</sup>*J*<sub>5,4A</sub> = <sup>3</sup>*J*<sub>1,2A</sub> = 6.1 Hz, <sup>2</sup>*J*<sub>2A,2B</sub> = <sup>2</sup>*J*<sub>4A,4B</sub> = 13.5 Hz, H<sub>2A</sub>, H<sub>4A</sub>), 2.05 (2H, dd, <sup>3</sup>*J*<sub>5,4B</sub> = <sup>3</sup>*J*<sub>1,2B</sub> = 2.2 Hz, <sup>2</sup>*J*<sub>2A,2B</sub> = <sup>2</sup>*J*<sub>4A,4B</sub> = 13.5 Hz, H<sub>2B</sub>, H<sub>4B</sub>); **<sup>13</sup>C NMR** (150 MHz, CDCl<sub>3</sub>) 144.9 (C<sub>Ar</sub>), 134.6 (CH), 125.8 (CH), 125.0 (CH), 96.6 (C<sub>q</sub>), 69.10 (CH<sub>2</sub>), 45.4 (CH<sub>2</sub>), 39.10 (CH), 33.8 (CH<sub>2</sub>).

*endo* **244**

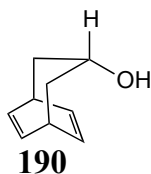
**R<sub>f</sub>** 0.67 (4:1 P.E. 40-60 °C/Et<sub>2</sub>O); **M.p.** 116 °C; **HRMS** found: M<sup>+</sup> 244.09135 C<sub>15</sub>H<sub>16</sub>OS requires 244.09163; **EI-MS**, *m/z* (relative intensity), 244 ([M<sup>+</sup>], 4); **IR**  $\nu_{\max}$  (CDCl<sub>3</sub> film/cm<sup>-1</sup>) 3043 (w), 2973 (w), 2941 (s), 2906 (w), 2863 (w), 1475 (w), 1456 (w), 1425 (w), 1359 (w), 1265 (w), 1156 (w), 1126 (w), 1079 (s); **<sup>1</sup>H NMR** (600 MHz, CDCl<sub>3</sub>) 7.26-7.18 (4H, m, H<sub>Ar</sub>), 6.55 (2H, dd, <sup>3</sup>*J* = 3.1 Hz, <sup>3</sup>*J* = 4.6 Hz, H<sub>8</sub>, H<sub>9</sub>), 3.98 (2H, t, <sup>3</sup>*J* = 5.8 Hz, H<sub>11</sub>), 3.69-3.67 (2H, m, H<sub>1</sub>, H<sub>5</sub>), 2.80 (2H, t, <sup>3</sup>*J* = 5.8 Hz, H<sub>10</sub>), 2.50 (2H, dd, <sup>3</sup>*J*<sub>5,4A</sub> = <sup>3</sup>*J*<sub>1,2A</sub> = 6.3 Hz, <sup>2</sup>*J*<sub>2A,2B</sub> = <sup>2</sup>*J*<sub>4A,4B</sub> = 13.7 Hz, H<sub>2A</sub>, H<sub>4A</sub>), 2.19 (2H, dd, <sup>3</sup>*J*<sub>5,4B</sub> = <sup>3</sup>*J*<sub>1,2B</sub> = 1.6 Hz, <sup>2</sup>*J*<sub>2A,2B</sub> = <sup>2</sup>*J*<sub>4A,4B</sub> = 13.7 Hz, H<sub>2B</sub>, H<sub>4B</sub>); **<sup>13</sup>C NMR** (150 MHz, CDCl<sub>3</sub>) 141.9 (C<sub>Ar</sub>), 136.0 (CH), 126.7 (CH), 126.1 (CH), 96.7 (C<sub>q</sub>), 68.9 (CH<sub>2</sub>), 43.9 (CH<sub>2</sub>), 38.6 (CH), 33.9 (CH<sub>2</sub>).

---

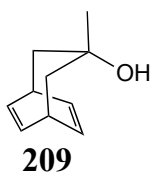
## **CHAPTER 5**

## **APPENDICES**

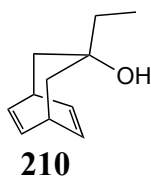
**Appendix 1** Population of the predominant conformer and experimental coupling constants for the parent diene derivatives in a range of solvents at 298 K



	CDCl <sub>3</sub>	C <sub>6</sub> D <sub>6</sub>	C <sub>6</sub> D <sub>5</sub> -CD <sub>3</sub>	CD <sub>3</sub> CN	CD <sub>3</sub> OD	Py- <i>d</i> <sub>5</sub>	DMSO	D <sub>2</sub> O
<b>Down</b>	H	H	-	H	H	H	H	H
<b><i>P<sub>A</sub></i></b>	99:01	99:01	-	100:0	67:33	76:24	100:0	100:0
<sup>3</sup> <i>J</i> <sub>5,4A</sub> (Hz)	6.6	6.6	-	6.6	4.9	5.5	6.4	7.4
<sup>3</sup> <i>J</i> <sub>5,4B</sub> (Hz)	1.3	1.3	-	1.1	3.1	2.7	0.9	0.8

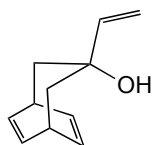


	CDCl <sub>3</sub>	C <sub>6</sub> D <sub>6</sub>	C <sub>6</sub> D <sub>5</sub> -CD <sub>3</sub>	CD <sub>3</sub> CN	CD <sub>3</sub> OD	Py- <i>d</i> <sub>5</sub>	DMSO	D <sub>2</sub> O
<b>Down</b>	OH	OH	OH	OH	OH	OH	OH	-
<b><i>P<sub>A</sub></i></b>	100:0	97:03	95:05	93:07	82:18	82:18	66:34	-
<sup>3</sup> <i>J</i> <sub>5,4A</sub>	6.7	6.4	6.2	6.2	5.6	5.6	4.7	-
<sup>3</sup> <i>J</i> <sub>5,4B</sub>	1.1	1.3	1.3	1.6	2.1	2.1	3.0	-



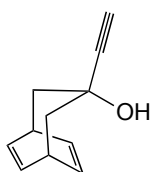
	CDCl <sub>3</sub>	C <sub>6</sub> D <sub>6</sub>	C <sub>6</sub> D <sub>5</sub> -CD <sub>3</sub>	CD <sub>3</sub> CN	CD <sub>3</sub> OD	Py- <i>d</i> <sub>5</sub>	DMSO	D <sub>2</sub> O
<b>Down</b>	OH	OH	-	OH	OH	OH	OH	OH
<b><i>P<sub>A</sub></i></b>	98:02	98:02	-	96:04	93:07	93:07	88:12	94:06
<sup>3</sup> <i>J</i> <sub>5,4A</sub>	6.5	6.5	-	6.4	6.2	5.4	4.6	6.3
<sup>3</sup> <i>J</i> <sub>5,4B</sub>	1.3	1.3	-	1.4	1.6	2.3	3.1	1.6





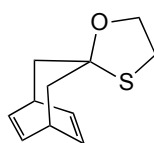
**211**

	CDCl <sub>3</sub>	C <sub>6</sub> D <sub>6</sub>	C <sub>6</sub> D <sub>5</sub> - CD <sub>3</sub>	CD <sub>3</sub> CN	CD <sub>3</sub> OD	Py- <i>d</i> <sub>5</sub>	DMSO	D <sub>2</sub> O
<b>Down</b>	OH	OH	OH	OH	OH	OH	OH	OH
<b><i>P<sub>A</sub></i></b>	97:03	97:03	94:06	79:21	84:16	79:21	64:36	79:21
<sup>3</sup> <i>J</i> <sub>5,4A</sub>	6.5	6.5	6.1	5.1	5.7	5.4	4.6	5.3
<sup>3</sup> <i>J</i> <sub>5,4B</sub>	1.4	1.4	1.4	2.0	2.0	2.3	3.1	2.6



**212**

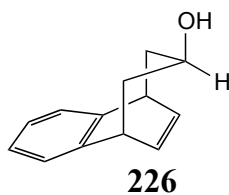
	CDCl <sub>3</sub>	C <sub>6</sub> D <sub>6</sub>	C <sub>6</sub> D <sub>5</sub> - CD <sub>3</sub>	CD <sub>3</sub> CN	CD <sub>3</sub> OD	Py- <i>d</i> <sub>5</sub>	DMSO	D <sub>2</sub> O
<b>Down</b>	OH	OH	-	OH	C≡CH	-	C≡CH	C≡CH
<b><i>P<sub>A</sub></i></b>	67:33	58:42	-	59:41	78:22	-	83:17	74:26
<sup>3</sup> <i>J</i> <sub>5,4A</sub>	4.7	4.4	-	4.4	5.5	-	5.7	5.3
<sup>3</sup> <i>J</i> <sub>5,4B</sub>	2.9	3.5	-	3.4	2.5	-	2.2	2.6



**219**

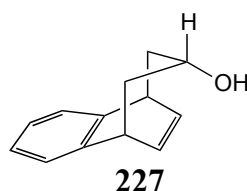
	CDCl <sub>3</sub>	C <sub>6</sub> D <sub>6</sub>	C <sub>6</sub> D <sub>5</sub> - CD <sub>3</sub>	CD <sub>3</sub> CN	CD <sub>3</sub> OD	Py- <i>d</i> <sub>5</sub>	DMSO	D <sub>2</sub> O
<b>Down</b>	-S-	-	-			-		
<b><i>P<sub>A</sub></i></b>	98:02	-	-			-		
<sup>3</sup> <i>J</i> <sub>5,4A</sub>	6.5	-	-			-		
<sup>3</sup> <i>J</i> <sub>5,4B</sub>	1.3	-	-			-		

**Appendix 2** Population of the predominant conformer and experimental coupling constants for the propanonaphthalene derivatives in a range of solvents at 298 K



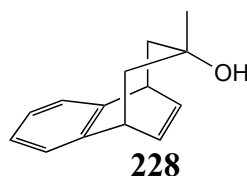
	CDCl <sub>3</sub>	C <sub>6</sub> D <sub>6</sub>	C <sub>6</sub> D <sub>5</sub> -CD <sub>3</sub>	CD <sub>3</sub> CN	CD <sub>3</sub> OD	Py- <i>d</i> <sub>5</sub>	DMSO	D <sub>2</sub> O
<b>Down</b>	H	H	H	H	H	H	H	H
<b><i>P<sub>A</sub></i></b>	100:0	85:15	100:0	100:0	100:0	100:0	100:0	100:0
<sup>3</sup> <i>J</i> <sub>5,4A</sub>	7.4	6.3	7.6	7.6	7.7	7.6	7.6	7.6
<sup>3</sup> <i>J</i> <sub>5,4B</sub>	0.9	1.8	0.9	1.1	1.0	1.0	0.9	0.9

N.B. Using the following boundary values  $J_S = 1.0$  Hz,  $J_L = 7.5$  Hz

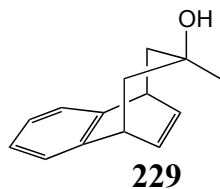


	CDCl <sub>3</sub>	C <sub>6</sub> D <sub>6</sub>	C <sub>6</sub> D <sub>5</sub> -CD <sub>3</sub>	CD <sub>3</sub> CN	CD <sub>3</sub> OD	Py- <i>d</i> <sub>5</sub>	DMSO	D <sub>2</sub> O
<b>Down</b>	H	H	H	H	H	H	H	H
<b><i>P<sub>A</sub></i></b>	88:12	96:04	99:01	99:01	95:05	100:0	99:01	98:02
<sup>3</sup> <i>J</i> <sub>5,4A</sub>	6.5	7.3	7.5	7.4	7.5	7.5	7.4	7.4
<sup>3</sup> <i>J</i> <sub>5,4B</sub>	1.2	1.3	1.1	1.1	1.0	1.0	1.0	1.1

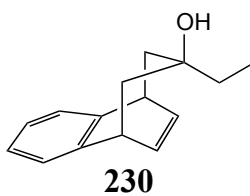
N.B. Using the following boundary values  $J_S = 1.0$  Hz,  $J_L = 7.5$  Hz



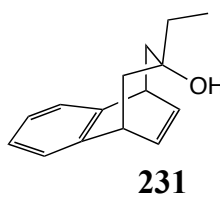
	CDCl <sub>3</sub>	C <sub>6</sub> D <sub>6</sub>	C <sub>6</sub> D <sub>5</sub> -CD <sub>3</sub>	CD <sub>3</sub> CN	CD <sub>3</sub> OD	Py- <i>d</i> <sub>5</sub>	DMSO	D <sub>2</sub> O
<b>Down</b>	OH	OH	-	OH	OH	OH	OH	OH
<b><i>P<sub>A</sub></i></b>	95:05	91:09	-	69:31	60:40	52:48	70:30	60:40
<sup>3</sup> <i>J</i> <sub>5,4A</sub>	6.5	6.3	-	4.5	4.5	4.1	5.2	4.6
<sup>3</sup> <i>J</i> <sub>5,4B</sub>	1.5	1.8	-	3.0	3.4	3.9	3.0	3.5



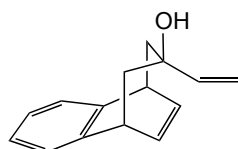
	CDCl <sub>3</sub>	C <sub>6</sub> D <sub>6</sub>	C <sub>6</sub> D <sub>5</sub> -CD <sub>3</sub>	CD <sub>3</sub> CN	CD <sub>3</sub> OD	Py- <i>d</i> <sub>5</sub>	DMSO	D <sub>2</sub> O
<b>Down</b>	OH	OH	OH	OH	OH	OH	OH	OH
<b><i>P<sub>A</sub></i></b>	95:05	99:01	99:01	95:05	86:14	85:15	77:23	88:12
<sup>3</sup> <i>J</i> <sub>5,4A</sub>	6.5	6.6	6.7	1.5	6.0	6.0	5.5	6.2
<sup>3</sup> <i>J</i> <sub>5,4B</sub>	1.5	1.2	1.3	6.4	2.0	2.1	2.5	2.0



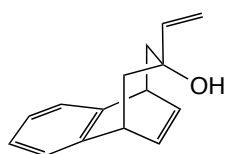
	CDCl <sub>3</sub>	C <sub>6</sub> D <sub>6</sub>	C <sub>6</sub> D <sub>5</sub> -CD <sub>3</sub>	CD <sub>3</sub> CN	CD <sub>3</sub> OD	Py- <i>d</i> <sub>5</sub>	DMSO	D <sub>2</sub> O
<b>Down</b>	OH	OH	-	OH	OH	OH	OH	OH
<b><i>P<sub>A</sub></i></b>	100:0	100:0	-	98:02	94:06	93:07	90:10	94:06
<sup>3</sup> <i>J</i> <sub>5,4A</sub>	6.7	6.8	-	6.7	6.3	6.3	6.2	6.4
<sup>3</sup> <i>J</i> <sub>5,4B</sub>	1.2	1.3	-	1.4	1.5	1.6	1.8	1.5



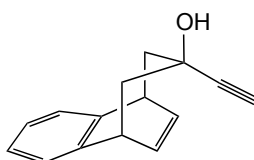
	CDCl <sub>3</sub>	C <sub>6</sub> D <sub>6</sub>	C <sub>6</sub> D <sub>5</sub> -CD <sub>3</sub>	CD <sub>3</sub> CN	CD <sub>3</sub> OD	Py- <i>d</i> <sub>5</sub>	DMSO	D <sub>2</sub> O
<b>Down</b>	OH	OH	-	OH	OH	OH	OH	-
<b><i>P<sub>A</sub></i></b>	99:01	98:02	-	87:13	67:33	74:26	54:46	-
<sup>3</sup> <i>J</i> <sub>5,4A</sub>	6.7	6.6	-	6.1	4.9	5.5	4.3	-
<sup>3</sup> <i>J</i> <sub>5,4B</sub>	1.3	1.4	-	2.1	3.0	2.9	3.8	-

**232**

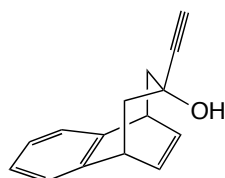
	CDCl <sub>3</sub>	C <sub>6</sub> D <sub>6</sub>	C <sub>6</sub> D <sub>5</sub> - CD <sub>3</sub>	CD <sub>3</sub> CN	CD <sub>3</sub> OD	Py- <i>d</i> <sub>5</sub>	DMSO	D <sub>2</sub> O
<b>Down</b>	OH	OH	-	OH	OH	OH	OH	-
<i>P<sub>A</sub></i>	87:13	99:01	-	93:07	88:12	85:15	81:19	-
<sup>3</sup> <i>J</i> <sub>5,4A</sub>	6.0	6.7	-	6.3	6.0	5.9	5.8	-
<sup>3</sup> <i>J</i> <sub>5,4B</sub>	1.9	1.3	-	1.6	1.9	2.0	2.3	-

**233**

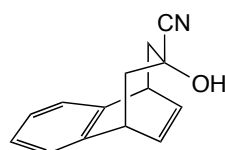
	CDCl <sub>3</sub>	C <sub>6</sub> D <sub>6</sub>	C <sub>6</sub> D <sub>5</sub> - CD <sub>3</sub>	CD <sub>3</sub> CN	CD <sub>3</sub> OD	Py- <i>d</i> <sub>5</sub>	DMSO	D <sub>2</sub> O
<b>Down</b>	OH	OH	-	OH	OH	OH	OH	-
<i>P<sub>A</sub></i>	92:08	91:09	-	70:30	60:40	51:49	56:44	-
<sup>3</sup> <i>J</i> <sub>5,4A</sub>	6.3	6.3	-	3.0	3.0	4.1	4.2	-
<sup>3</sup> <i>J</i> <sub>5,4B</sub>	1.7	1.9	-	5.2	4.1	4.0	3.5	-

**236**

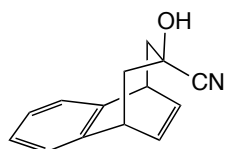
	CDCl <sub>3</sub>	C <sub>6</sub> D <sub>6</sub>	C <sub>6</sub> D <sub>5</sub> - CD <sub>3</sub>	CD <sub>3</sub> CN	CD <sub>3</sub> OD	Py- <i>d</i> <sub>5</sub>	DMSO	D <sub>2</sub> O
<b>Down</b>	OH	OH	OH	OH	C≡CH	C≡CH	C≡CH	-
<i>P<sub>A</sub></i>	72:28	63:37	64:36	53:47	66:34	74:26	71:29	-
<sup>3</sup> <i>J</i> <sub>5,4A</sub>	5.2	4.7	4.7	4.1	4.8	5.5	5.1	-
<sup>3</sup> <i>J</i> <sub>5,4B</sub>	2.8	3.3	3.1	3.8	3.1	2.9	2.9	-

**237**

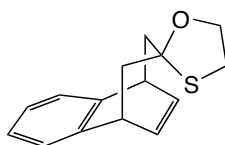
	CDCl <sub>3</sub>	C <sub>6</sub> D <sub>6</sub>	C <sub>6</sub> D <sub>5</sub> - CD <sub>3</sub>	CD <sub>3</sub> CN	CD <sub>3</sub> OD	Py- <i>d</i> <sub>5</sub>	DMSO	D <sub>2</sub> O
<b>Down</b>	C≡CH	C≡CH	-	C≡CH	C≡CH	C≡CH	C≡CH	C≡CH
<i>P<sub>A</sub></i>	56:44	68:32	-	84:16	94:06	93:07	94:06	98:02
<sup>3</sup> <i>J</i> <sub>5,4A</sub>	4.4	5.0	-	5.9	6.5	6.3	6.5	6.8
<sup>3</sup> <i>J</i> <sub>5,4B</sub>	3.1	3.0	-	2.1	1.7	1.6	1.7	1.5

**241**

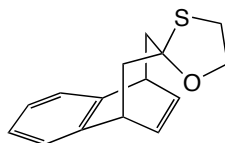
	CDCl <sub>3</sub>	C <sub>6</sub> D <sub>6</sub>	C <sub>6</sub> D <sub>5</sub> - CD <sub>3</sub>	CD <sub>3</sub> CN	CD <sub>3</sub> OD	Py- <i>d</i> <sub>5</sub>	DMSO	D <sub>2</sub> O
<b>Down</b>	CN	CN	-	CN	CN	CN	CN	-
<i>P<sub>A</sub></i>	85:15	86:14	-	100:0	100:0	100:0	100:0	-
<sup>3</sup> <i>J</i> <sub>5,4A</sub>	6.0	6.1	-	7.0	7.1	7.1	7.1	-
<sup>3</sup> <i>J</i> <sub>5,4B</sub>	2.2	2.1	-	1.2	1.1	1.2	1.1	-

**242**

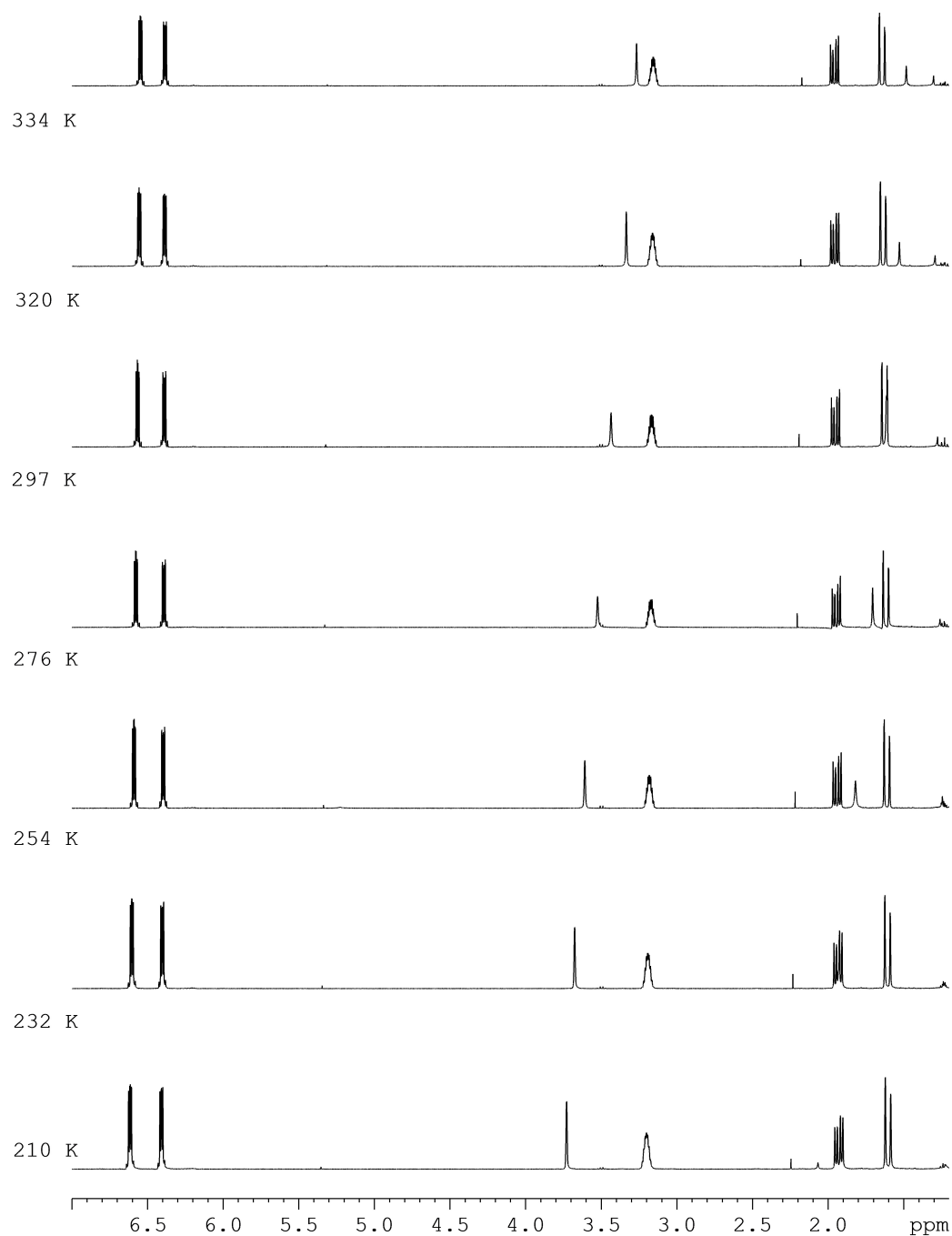
	CDCl <sub>3</sub>	C <sub>6</sub> D <sub>6</sub>	C <sub>6</sub> D <sub>5</sub> - CD <sub>3</sub>	CD <sub>3</sub> CN	CD <sub>3</sub> OD	Py- <i>d</i> <sub>5</sub>	DMSO	D <sub>2</sub> O
<b>Down</b>	CN	CN	-	CN	CN	CN	CN	-
<i>P<sub>A</sub></i>	66:34	78:12	-	91:09	97:03	-	99:01	-
<sup>3</sup> <i>J</i> <sub>5,4A</sub>	4.9	5.5	-	6.4	6.7	-	6.8	-
<sup>3</sup> <i>J</i> <sub>5,4B</sub>	3.1	2.4	-	1.9	1.6	-	1.4	-

**243**

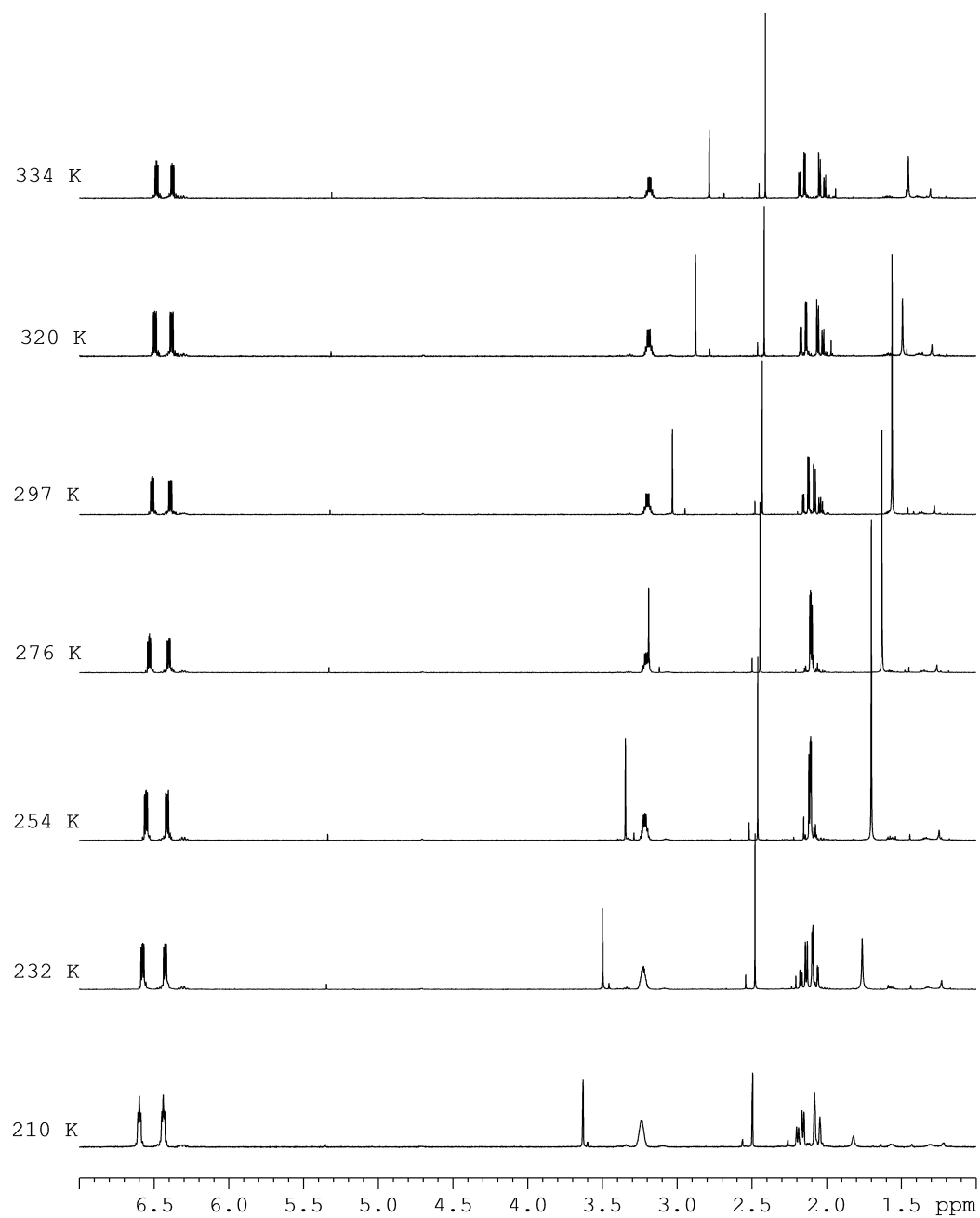
	CDCl <sub>3</sub>	C <sub>6</sub> D <sub>6</sub>	C <sub>6</sub> D <sub>5</sub> - CD <sub>3</sub>	CD <sub>3</sub> CN	CD <sub>3</sub> OD	Py- <i>d</i> <sub>5</sub>	DMSO	D <sub>2</sub> O
<b>Down</b>	S	S	-	S	S	S	S	-
<b><i>P<sub>A</sub></i></b>	85:15	86:14	-	76:24	84:16	83:17	85:15	-
<sup>3</sup> <i>J</i> <sub>5,4A</sub>	6.1	6.2	-	5.7	6.0	5.9	6.1	-
<sup>3</sup> <i>J</i> <sub>5,4B</sub>	2.2	2.2	-	2.8	2.3	2.3	2.2	-

**244**

	CDCl <sub>3</sub>	C <sub>6</sub> D <sub>6</sub>	C <sub>6</sub> D <sub>5</sub> - CD <sub>3</sub>	CD <sub>3</sub> CN	CD <sub>3</sub> OD	Py- <i>d</i> <sub>5</sub>	DMSO	D <sub>2</sub> O
<b>Down</b>	S	S	S	S	S	S	S	-
<b>Conformational ratio</b>	91:09	85:15	-	91:09	87:13	83:17	88:12	-
<sup>3</sup> <i>J</i> <sub>5,4A</sub>	6.4	6.0	-	6.4	6.2	5.9	6.3	-
<sup>3</sup> <i>J</i> <sub>5,4B</sub>	1.9	2.2	-	1.9	2.1	2.3	2.1	-

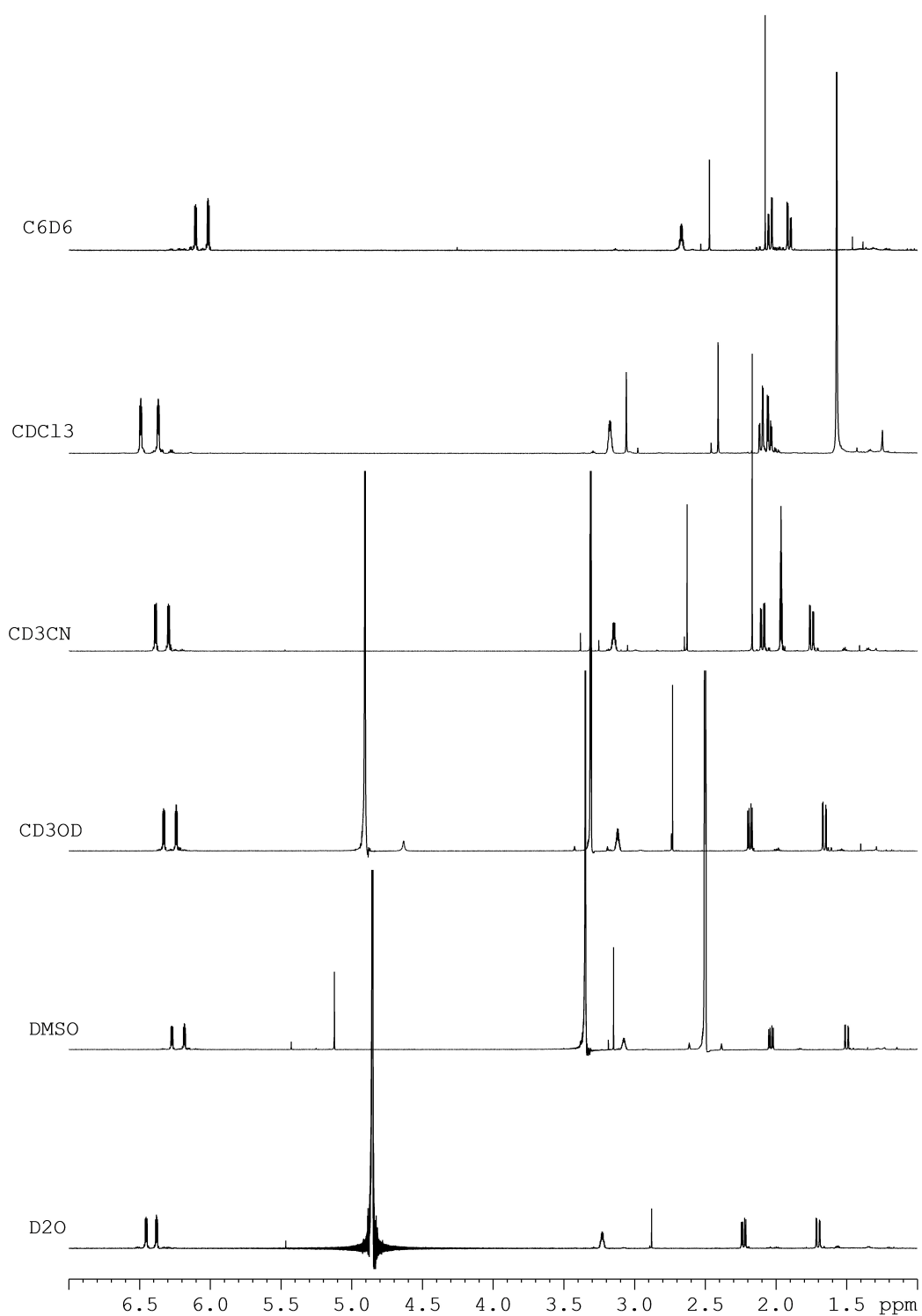
**Appendix 3**  $^1\text{H}$  NMR spectra of tertiary alcohol **209** in  $\text{CDCl}_3$  as a function of temperature

**Appendix 4**  $^1\text{H}$  NMR spectra of tertiary alcohol **212** in  $\text{CDCl}_3$  as a function of temperature

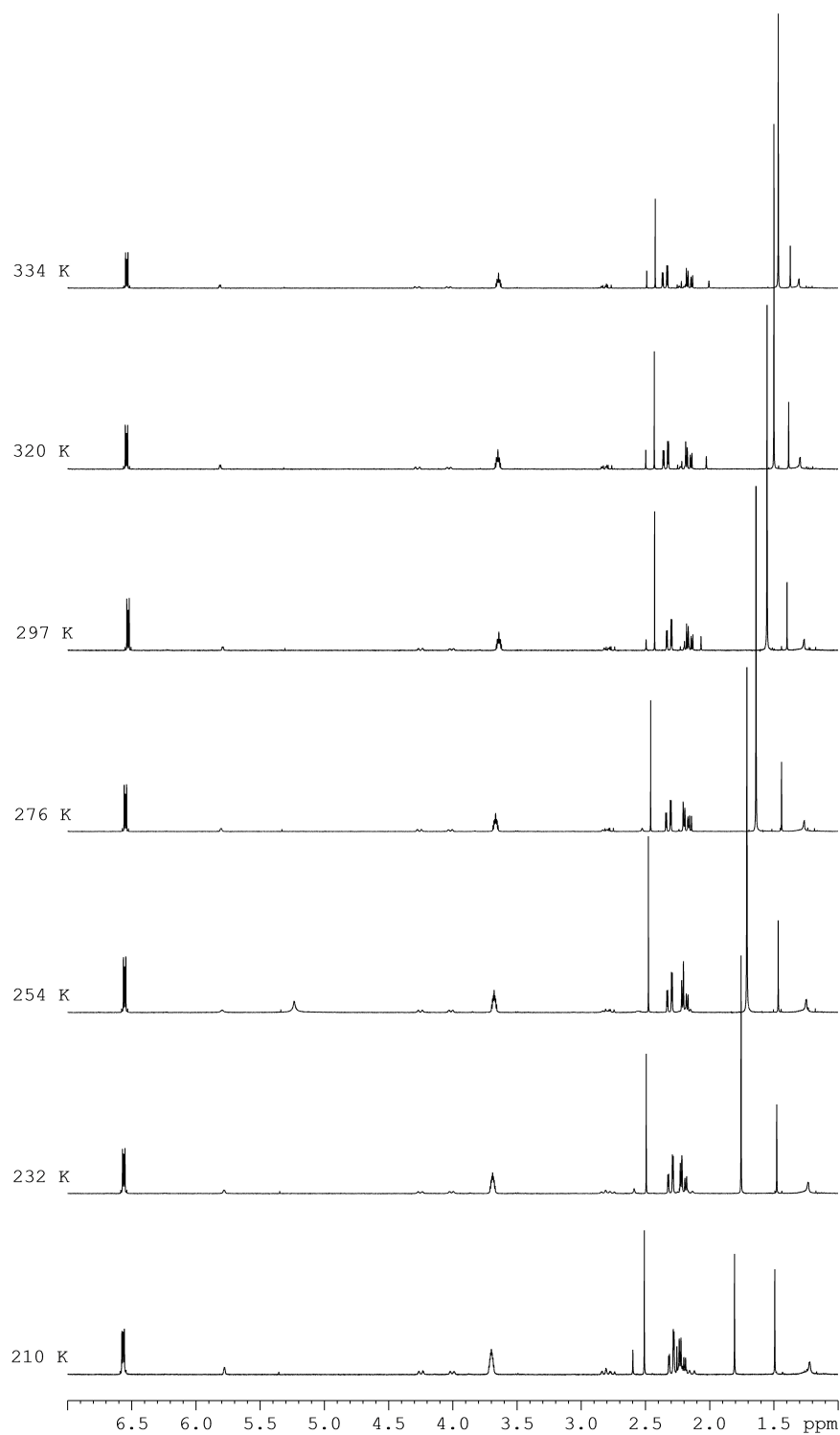




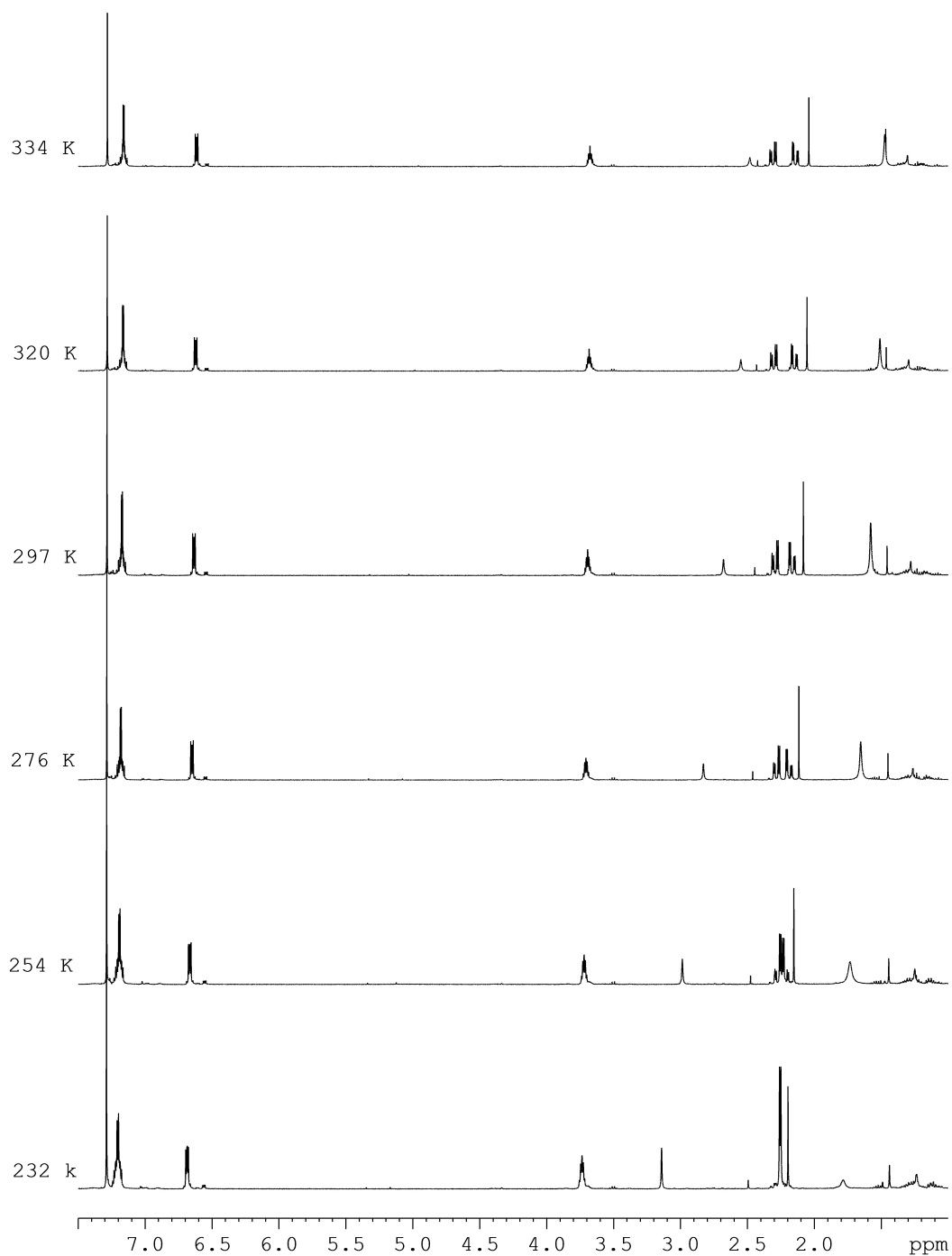
**Appendix 5**  $^1\text{H}$  NMR spectra of tertiary alcohol **212** at 298 K as a function of solvent

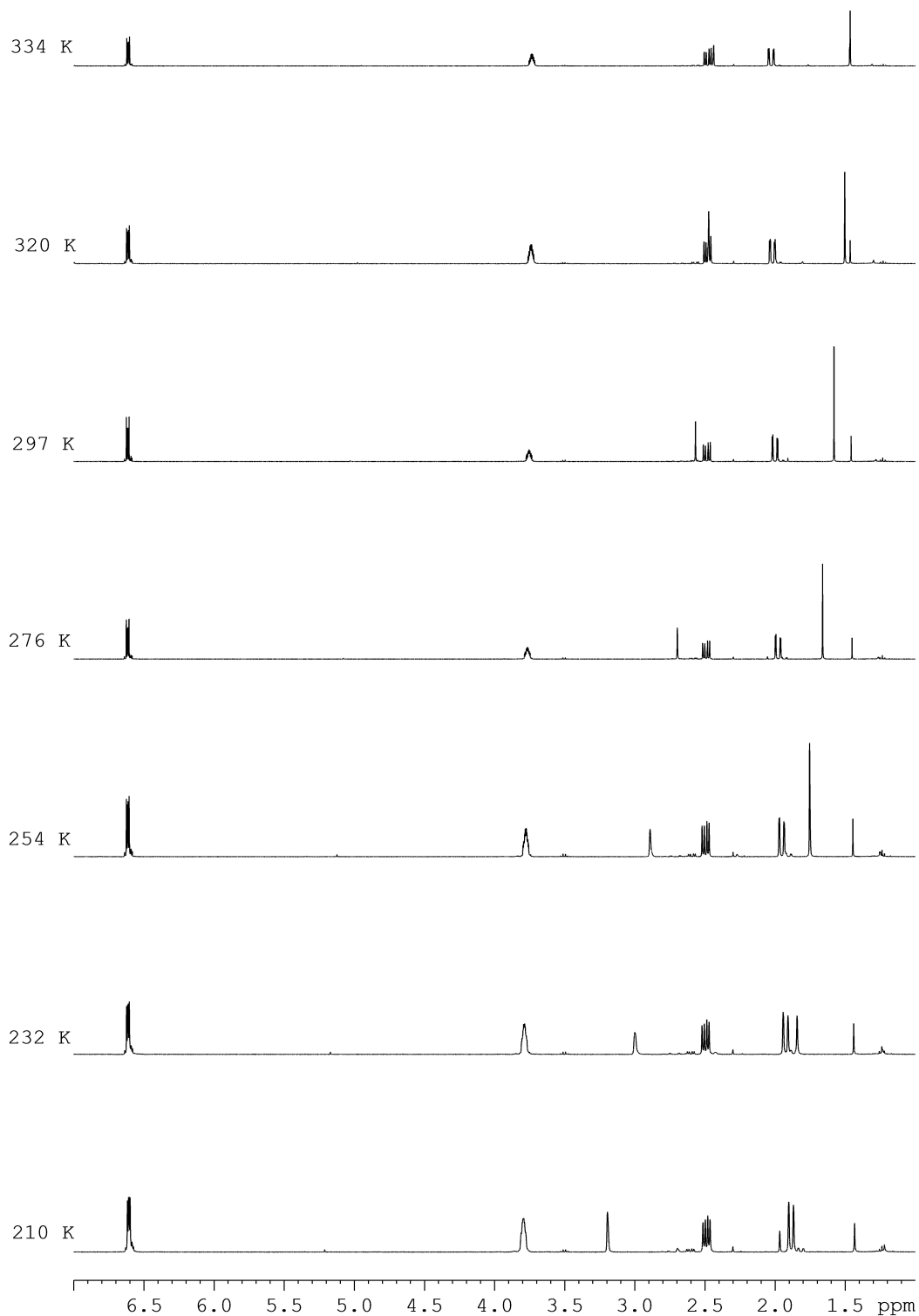


**Appendix 6**  $^1\text{H}$  NMR spectra of tertiary alcohol **236** in  $\text{CDCl}_3$  as a function of temperature

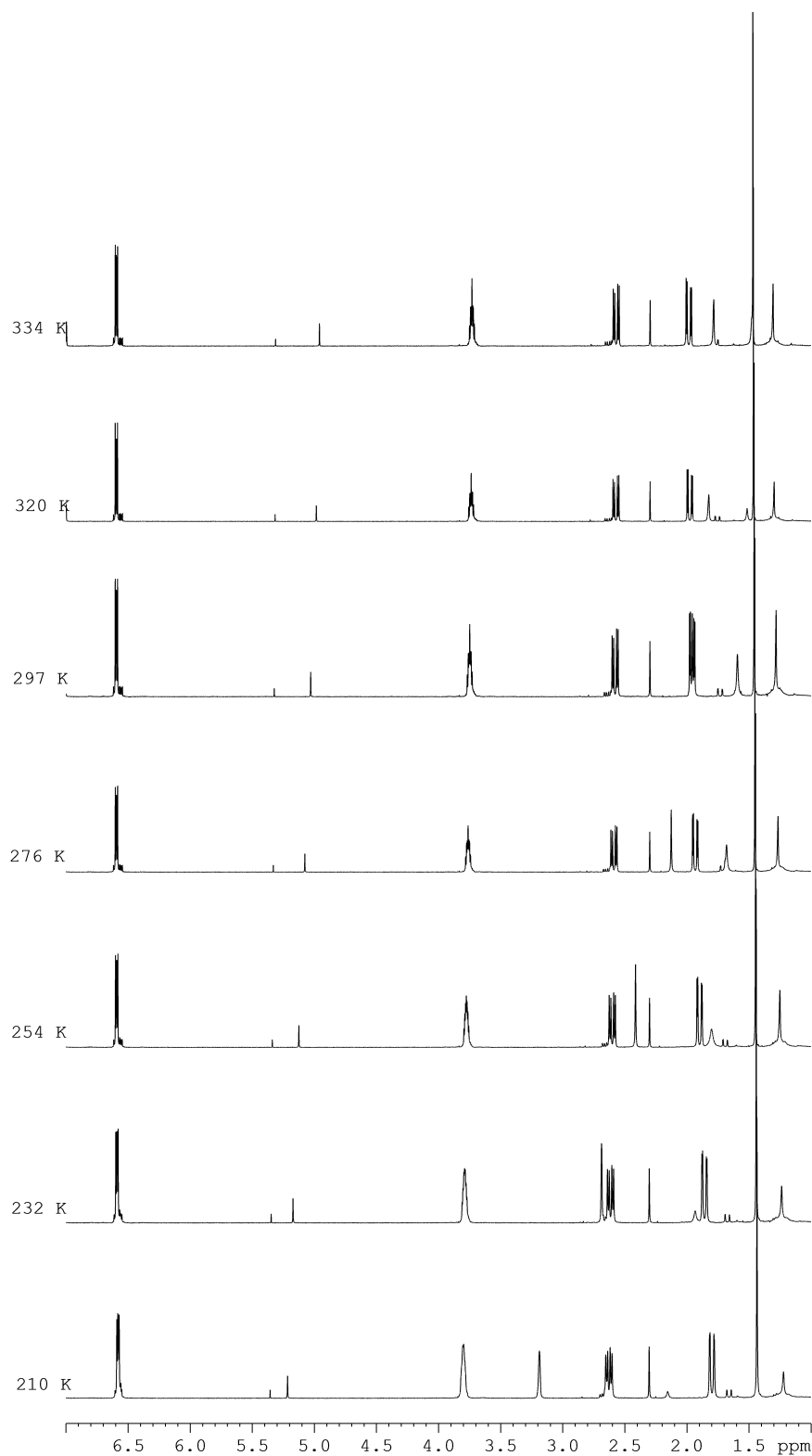


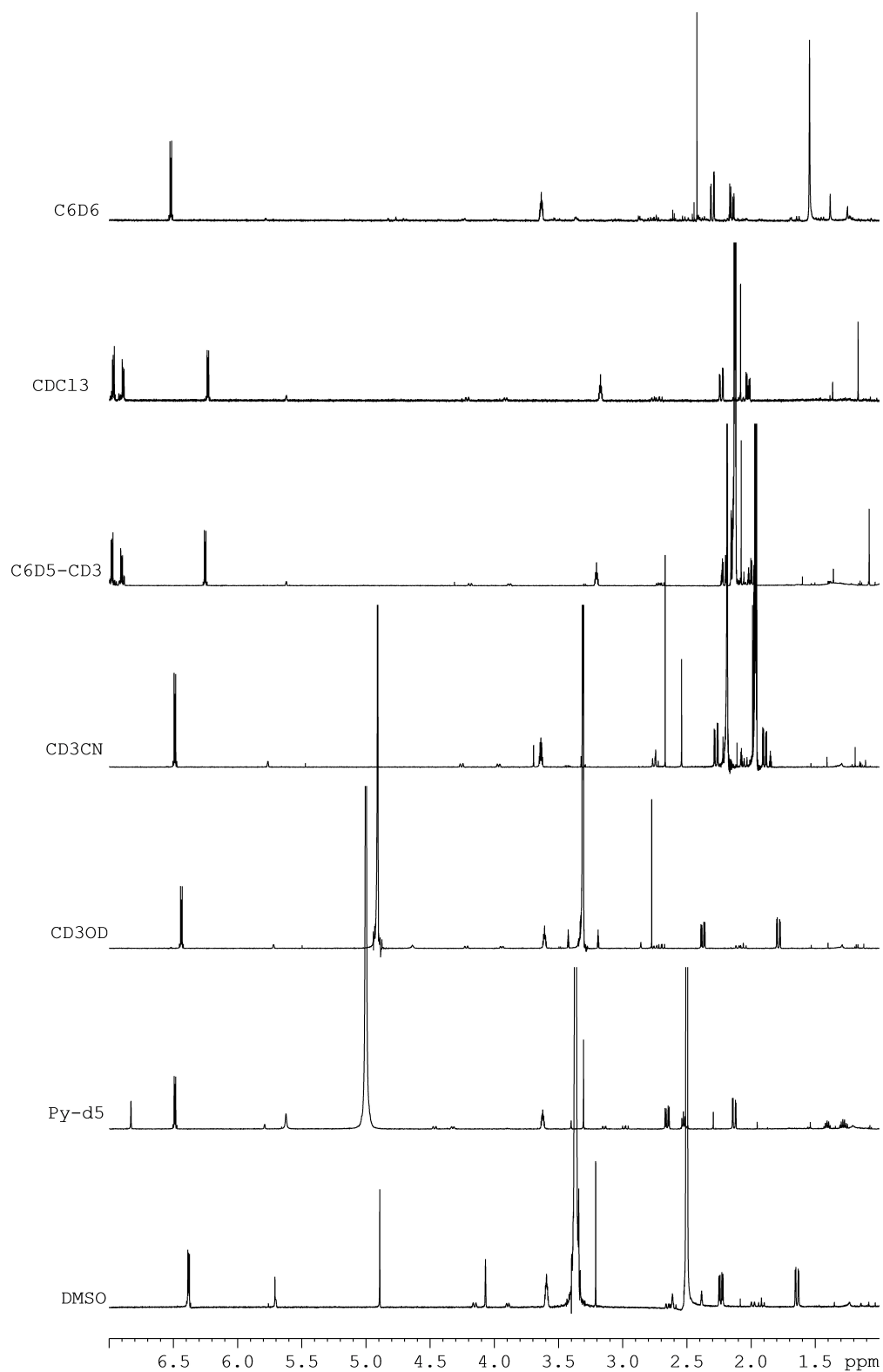
**Appendix 7**  $^1\text{H}$  NMR spectra of tertiary alcohol **237** in  $\text{CDCl}_3$  as a function of temperature



**Appendix 8**  $^1\text{H}$  NMR spectra of cyanohydrin **241** in  $\text{CDCl}_3$  as a function of temperature

**Appendix 9**  $^1\text{H}$  NMR spectra of cyanohydrin **242** in  $\text{CDCl}_3$  as a function of temperature



**Appendix 10**  $^1\text{H}$  NMR spectra of tertiary alcohol **236** at 298 K as a function of solvent

**Appendix 11** Conformational ratios and energy differences between conformers of the propanonaphthalene series in CDCl<sub>3</sub> at 298 K

	X-down	Y-up	$P_A$	$\Delta G^\circ$ kJmol <sup>-1</sup>
162	NH <sub>2</sub>	CH <sub>3</sub>	79:21	3.3
163	NH <sub>3</sub> Cl	CH <sub>3</sub>	~82:18	~3.7
164	CN	NH <sub>2</sub>	96:04	7.9
165	OH	CH <sub>3</sub>	94:06	6.8
166	H	F	91:09	5.6
167	F	CH <sub>3</sub>	96:04	7.9
168	OCH <sub>3</sub>	CH <sub>3</sub>	70:30	2.1
169	C≡CH	OH	52:48	0.2
170	-S-	-O-	77:23	3.0
171	-CH <sub>2</sub> -	-O-	89:11	5.2
172	-CH <sub>2</sub> -	-NH-	68:32	1.9
173	-CH <sub>2</sub> -	-NH-	61:39	1.1
174	-CH <sub>2</sub> -	-NH-	71:29	2.2
175	H	OH	93:07	6.4
176	OH	CHCH <sub>2</sub>	90:10	5.4
177	CN	OH	74:26	2.6
178	C≡CH	OCH <sub>3</sub>	74:26	2.6
179	-CH <sub>2</sub> -	-O-	50:50	0

**Appendix 12** Crystal structure and X-Ray data for **237**Crystal data and structure refinement details for **237**:

Empirical formula	C <sub>15</sub> H <sub>14</sub> O	
Formula weight	210.26	
Temperature	120(2) K	
Wavelength	0.71073 Å	
Crystal system	Tetragonal	
Space group	<i>P</i> -421 <i>c</i>	
Unit cell dimensions	<i>a</i> = 17.7479(4) Å	$\alpha = 90^\circ$
	<i>b</i> = 17.7479(4) Å	$\beta = 90^\circ$
	<i>c</i> = 7.02350(10) Å	$\gamma = 90^\circ$
Volume	2212.32(8) Å <sup>3</sup>	
<i>Z</i>	8	
Density (calculated)	1.263 Mg / m <sup>3</sup>	
Absorption coefficient	0.077 mm <sup>-1</sup>	
<i>F</i> (000)	896	
Crystal	Block; colourless	
Crystal size	0.60 × 0.20 × 0.20 mm <sup>3</sup>	
$\theta$ range for data collection	3.12 – 27.47°	
Index ranges	$-20 \leq h \leq 23, -23 \leq k \leq 22, -9 \leq l \leq 7$	
Reflections collected	14947	
Independent reflections	1448 [ <i>R</i> <sub>int</sub> = 0.0469]	
Completeness to $\theta = 27.47^\circ$	99.6 %	
Absorption correction	Semi-empirical from equivalents	
Max. and min. transmission	0.9847 and 0.9551	
Refinement method	Full-matrix least-squares on <i>F</i> <sup>2</sup>	



Data / restraints / parameters	1448 / 0 / 147
Goodness-of-fit on $F^2$	1.049
Final $R$ indices [ $F^2 > 2\sigma(F^2)$ ]	$RI = 0.0338$ , $wR2 = 0.0780$
$R$ indices (all data)	$RI = 0.0387$ , $wR2 = 0.0805$
Extinction coefficient	0.012(2)
Largest diff. peak and hole	0.183 and $-0.160 \text{ e } \text{\AA}^{-3}$

Atomic coordinates [ $\times 10^4$ ], equivalent isotropic displacement parameters [ $\text{\AA}^2 \times 10^3$ ] and site occupancy factors for **237**.  $U_{eq}$  is defined as one third of the trace of the orthogonalized  $U^{ij}$  tensor.

Atom	<i>x</i>	<i>y</i>	<i>z</i>	$U_{eq}$	<i>S.o.f.</i>
C1	2533(1)	423(1)	4887(2)	18(1)	1
C2	2744(1)	−140(1)	6151(3)	24(1)	1
C3	3456(1)	−457(1)	6030(3)	30(1)	1
C4	3957(1)	−209(1)	4662(3)	30(1)	1
C5	3755(1)	361(1)	3397(3)	24(1)	1
C6	3038(1)	677(1)	3496(2)	18(1)	1
C7	2750(1)	1281(1)	2153(3)	21(1)	1
C8	2321(1)	1858(1)	3294(3)	28(1)	1
C9	1838(1)	1621(1)	4591(3)	28(1)	1
C10	1756(1)	778(1)	4883(3)	23(1)	1
C11	1274(1)	442(1)	3239(3)	21(1)	1
C12	1680(1)	310(1)	1315(2)	17(1)	1
C13	2202(1)	952(1)	624(2)	19(1)	1
C14	2122(1)	−401(1)	1313(3)	18(1)	1
C15	2492(1)	−954(1)	1120(3)	25(1)	1
O1	1105(1)	217(1)	−136(2)	21(1)	1

Bond lengths [Å] and angles [°] for **237**:

C1–C2	1.388(2)	C12–C13	1.547(2)
C1–C6	1.400(2)	C13–H13A	0.9900
C1–C10	1.516(2)	C13–H13B	0.9900
C2–C3	1.386(3)	C14–C15	1.188(3)
C2–H2	0.9500	C15–H15	0.9500
C3–C4	1.382(3)	O1–H1	0.8400
C3–H3	0.9500		
C4–C5	1.393(3)	C2–C1–C6	120.40(16)
C4–H4	0.9500	C2–C1–C10	123.02(17)
C5–C6	1.393(2)	C6–C1–C10	116.56(16)
C5–H5	0.9500	C3–C2–C1	119.89(18)
C6–C7	1.517(2)	C3–C2–H2	120.1
C7–C8	1.507(3)	C1–C2–H2	120.1
C7–C13	1.561(2)	C4–C3–C2	120.03(18)
C7–H7	1.0000	C4–C3–H3	120.0
C8–C9	1.319(3)	C2–C3–H3	120.0
C8–H8	0.9500	C3–C4–C5	120.61(18)
C9–C10	1.518(3)	C3–C4–H4	119.7
C9–H9	0.9500	C5–C4–H4	119.7
C10–C11	1.555(2)	C6–C5–C4	119.72(19)
C10–H10	1.0000	C6–C5–H5	120.1
C11–C12	1.549(2)	C4–C5–H5	120.1
C11–H11A	0.9900		
C11–H11B	0.9900	C5–C6–C1	119.35(17)
C12–O1	1.452(2)	C5–C6–C7	124.17(17)
C12–C14	1.484(2)	C1–C6–C7	116.47(15)

C8–C7–C6	108.66(15)	O1–C12–C11	107.61(13)
C8–C7–C13	107.84(15)	C14–C12–C11	112.07(15)
C6–C7–C13	111.87(13)	C13–C12–C11	116.13(14)
C8–C7–H7	109.5	C12–C13–C7	115.65(14)
C6–C7–H7	109.5	C12–C13–H13A	108.4
C13–C7–H7	109.5	C7–C13–H13A	108.4
C9–C8–C7	118.56(17)	C12–C13–H13B	108.4
C9–C8–H8	120.7	C7–C13–H13B	108.4
C7–C8–H8	120.7	H13A–C13–H13B	107.4
C8–C9–C10	118.04(17)	C15–C14–C12	173.3(2)
C8–C9–H9	121.0	C14–C15–H15	180.0
C10–C9–H9	121.0	C12–O1–H1	109.5
C1–C10–C9	108.80(15)		
C1–C10–C11	110.05(14)		
C9–C10–C11	109.30(15)		
C1–C10–H10	109.6		
C9–C10–H10	109.6		
C11–C10–H10	109.6		
C12–C11–C10	116.74(14)		
C12–C11–H11A	108.1		
C10–C11–H11A	108.1		
C12–C11–H11B	108.1		
C10–C11–H11B	108.1		
H11A–C11–H11B	107.3		
O1–C12–C14	105.90(13)		
O1–C12–C13	106.55(13)		
C14–C12–C13	107.95(13)		

Anisotropic displacement parameters [ $\text{\AA}^2 \times 10^3$ ] for **237**. The anisotropic displacement factor exponent takes the form:  $-2\pi^2[h^2a^{*2}U^{11} + \dots + 2hk a^* b^* U^{12}]$ .

Atom	$U^{11}$	$U^{22}$	$U^{33}$	$U^{23}$	$U^{13}$	$U^{12}$
C1	18(1)	20(1)	15(1)	-5(1)	-2(1)	-2(1)
C2	31(1)	25(1)	17(1)	0(1)	-6(1)	-5(1)
C3	40(1)	21(1)	29(1)	-2(1)	-18(1)	2(1)
C4	24(1)	27(1)	40(1)	-14(1)	-13(1)	8(1)
C5	18(1)	29(1)	26(1)	-11(1)	1(1)	-3(1)
C6	19(1)	17(1)	17(1)	-5(1)	-2(1)	-2(1)
C7	25(1)	17(1)	21(1)	0(1)	-1(1)	-5(1)
C8	36(1)	17(1)	31(1)	-6(1)	-11(1)	3(1)
C9	28(1)	30(1)	26(1)	-12(1)	-8(1)	12(1)
C10	19(1)	35(1)	15(1)	-4(1)	2(1)	2(1)
C11	15(1)	29(1)	18(1)	-2(1)	0(1)	-1(1)
C12	18(1)	18(1)	14(1)	-1(1)	-3(1)	0(1)
C13	24(1)	16(1)	16(1)	2(1)	-2(1)	-1(1)
C14	18(1)	18(1)	17(1)	1(1)	-2(1)	-4(1)
C15	25(1)	20(1)	29(1)	-1(1)	-4(1)	1(1)
O1	22(1)	21(1)	20(1)	-1(1)	-7(1)	-1(1)

Hydrogen coordinates [ $\times 10^4$ ] and isotropic displacement parameters [ $\text{\AA}^2 \times 10^3$ ] for **237**:

Atom	<i>x</i>	<i>y</i>	<i>z</i>	<i>U<sub>eq</sub></i>	<i>S.o.f.</i>
H2	2400	−308	7098	29	1
H3	3599	−845	6888	36	1
H4	4444	−428	4583	36	1
H5	4105	533	2470	29	1
H7	3186	1529	1505	25	1
H8	2396	2382	3084	33	1
H9	1551	1968	5322	33	1
H10	1503	678	6129	27	1
H11A	1066	−46	3675	25	1
H11B	843	784	3011	25	1
H13A	1884	1367	134	23	1
H13B	2507	761	−454	23	1
H15	2787	−1396	966	30	1
H1	896	−205	−2	32	1

---

Torsion angles [°] for **237**:

---

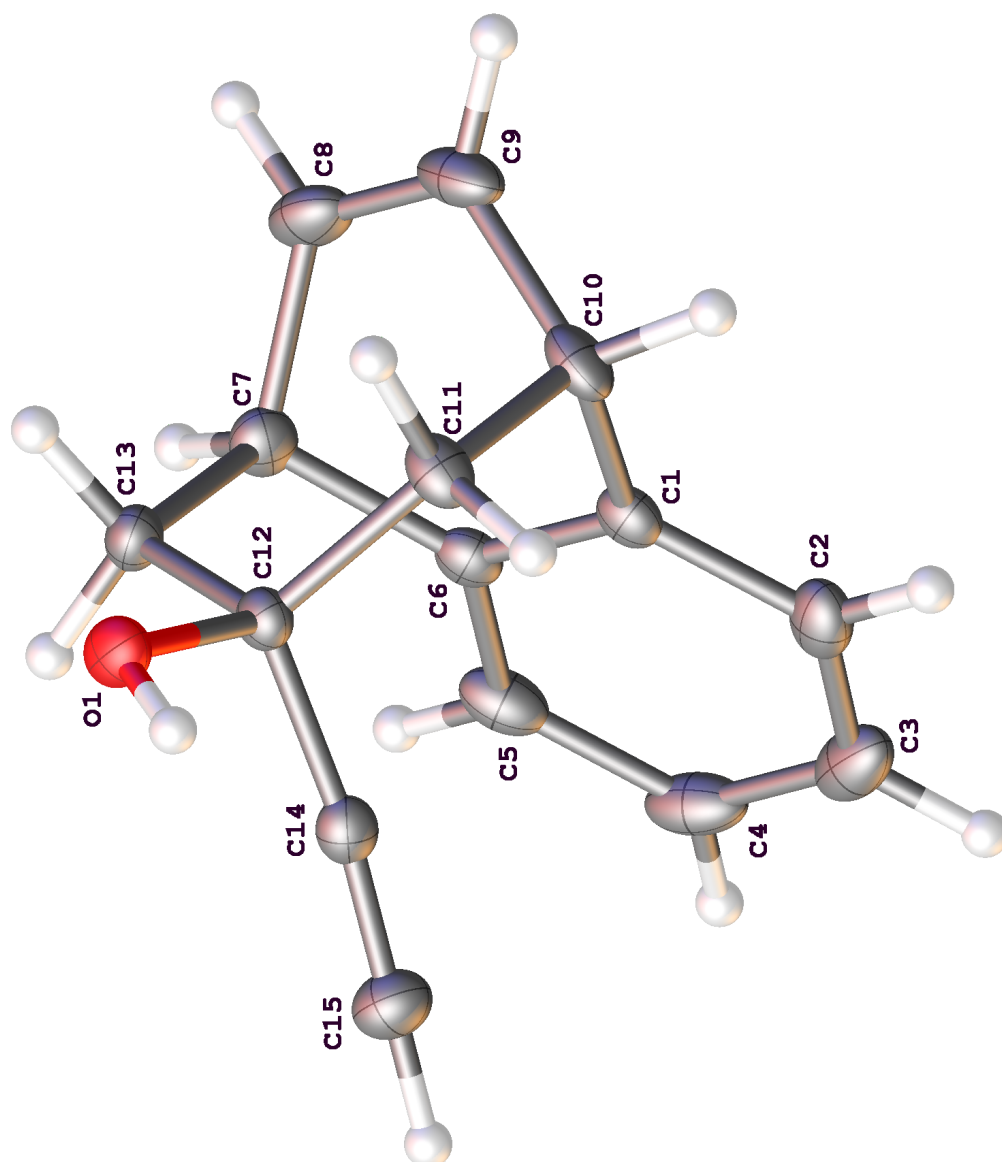
C6–C1–C2–C3	–0.5(3)
C10–C1–C2–C3	177.74(16)
C1–C2–C3–C4	0.5(3)
C2–C3–C4–C5	0.1(3)
C3–C4–C5–C6	–0.8(3)
C4–C5–C6–C1	0.8(3)
C4–C5–C6–C7	–177.95(16)
C2–C1–C6–C5	–0.2(2)
C10–C1–C6–C5	–178.50(15)
C2–C1–C6–C7	178.64(16)
C10–C1–C6–C7	0.3(2)
C5–C6–C7–C8	–138.00(17)
C1–C6–C7–C8	43.2(2)
C5–C6–C7–C13	103.1(2)
C1–C6–C7–C13	–75.72(19)
C6–C7–C8–C9	–44.9(2)
C13–C7–C8–C9	76.5(2)
C7–C8–C9–C10	1.2(3)
C2–C1–C10–C9	138.53(17)
C6–C1–C10–C9	–43.2(2)
C2–C1–C10–C11	–101.74(19)
C6–C1–C10–C11	76.52(19)
C8–C9–C10–C1	43.3(2)
C8–C9–C10–C11	–76.9(2)
C1–C10–C11–C12	–40.4(2)

C9–C10–C11–C12	79.0(2)
C10–C11–C12–O1	–163.24(14)
C10–C11–C12–C14	80.7(2)
C10–C11–C12–C13	–44.0(2)
O1–C12–C13–C7	166.21(14)
C14–C12–C13–C7	–80.41(19)
C11–C12–C13–C7	46.4(2)
C8–C7–C13–C12	–83.21(18)
C6–C7–C13–C12	36.2(2)
O1–C12–C14–C15	59.0(15)
C13–C12–C14–C15	–54.8(16)
C11–C12–C14–C15	176.0(15)

---

Symmetry transformations used to generate equivalent atoms:





## Appendix 13 Crystal Structure and X-Ray data for **241**

### Crystal data and structure refinement details for **241**

Empirical formula	$\text{C}_{14}\text{H}_{13}\text{NO}$		
Formula weight	211.25		
Temperature	120(2) K		
Wavelength	0.71073 Å		
Crystal system	Monoclinic		
Space group	$P21/c$		
Unit cell dimensions	$a = 21.1531(4)$ Å	$\alpha = 90^\circ$	
	$b = 6.94740(10)$ Å	$\beta$	=
	$111.8370(10)^\circ$	$c = 15.8281(3)$ Å	$\gamma = 90^\circ$
Volume	2159.18(7) Å <sup>3</sup>		
$Z$	8		
Density (calculated)	1.300 Mg / m <sup>3</sup>		
Absorption coefficient	0.082 mm <sup>-1</sup>		
$F(000)$	896		
Crystal	Block; colourless		
Crystal size	0.60 × 0.28 × 0.20 mm <sup>3</sup>		
$\theta$ range for data collection	2.93 – 27.48°		
Index ranges	$-27 \leq h \leq 25, -7 \leq k \leq 9, -20 \leq l \leq 20$		
Reflections collected	30097		
Independent reflections	4926 [ $R_{int} = 0.0484$ ]		
Completeness to $\theta = 27.48^\circ$	99.8 %		
Absorption correction	Semi-empirical from equivalents		
Max. and min. transmission	0.9838 and 0.9525		

Refinement method	Full-matrix least-squares on $F^2$
Data / restraints / parameters	4926 / 0 / 292
Goodness-of-fit on $F^2$	1.027
Final $R$ indices [ $F^2 > 2\sigma(F^2)$ ]	$RI = 0.0464$ , $wR2 = 0.1157$
$R$ indices (all data)	$RI = 0.0537$ , $wR2 = 0.1207$
Largest diff. peak and hole	0.377 and $-0.246 \text{ e } \text{\AA}^{-3}$

Atomic coordinates [ $\times 10^4$ ], equivalent isotropic displacement parameters [ $\text{\AA}^2 \times 10^3$ ] and site occupancy factors for **241**.  $U_{eq}$  is defined as one third of the trace of the orthogonalized  $U^{ij}$  tensor.

Atom	<i>x</i>	<i>y</i>	<i>z</i>	$U_{eq}$	<i>S.o.f.</i>
C1	1221(1)	1793(2)	8680(1)	16(1)	1
C2	1698(1)	3027(2)	8556(1)	19(1)	1
C3	1852(1)	2869(3)	7775(1)	22(1)	1
C4	1539(1)	1483(3)	7129(1)	22(1)	1
C5	1058(1)	250(3)	7244(1)	19(1)	1
C6	895(1)	412(2)	8020(1)	16(1)	1
C7	372(1)	−859(3)	8197(1)	18(1)	1
C8	−60(1)	399(3)	8558(1)	21(1)	1
C9	249(1)	1684(3)	9188(1)	22(1)	1
C10	1020(1)	1849(2)	9509(1)	18(1)	1
C11	1347(1)	145(2)	10164(1)	17(1)	1
C12	1364(1)	−1818(2)	9718(1)	17(1)	1
C13	718(1)	−2443(3)	8908(1)	17(1)	1
C14	1960(1)	−1852(2)	9416(1)	19(1)	1
N1	2436(1)	−1986(2)	9238(1)	27(1)	1
O1	1486(1)	−3317(2)	10378(1)	22(1)	1
C101	5914(1)	5667(2)	2846(1)	17(1)	1
C102	6123(1)	5604(3)	3790(1)	19(1)	1
C103	6644(1)	6816(3)	4324(1)	22(1)	1
C104	6952(1)	8092(3)	3922(1)	23(1)	1
C105	6746(1)	8146(2)	2976(1)	19(1)	1
C106	6231(1)	6934(2)	2440(1)	16(1)	1
C107	5984(1)	6888(2)	1409(1)	17(1)	1

C108	5210(1)	6833(3)	1027(1)	21(1)	1
C109	4905(1)	5656(3)	1412(1)	21(1)	1
C110	5346(1)	4426(3)	2204(1)	18(1)	1
C111	5636(1)	2714(3)	1826(1)	17(1)	1
C112	6263(1)	3174(2)	1583(1)	16(1)	1
C113	6254(1)	5082(2)	1072(1)	17(1)	1
C114	6885(1)	3126(2)	2442(1)	18(1)	1
N101	7373(1)	2950(2)	3072(1)	25(1)	1
O101	6323(1)	1587(2)	1046(1)	20(1)	1

Bond lengths [ $\text{\AA}$ ] and angles [ $^\circ$ ] for **241**

C1–C2	1.392(2)	C12–C13	1.548(2)
C1–C6	1.397(2)	C13–H13A	0.9900
C1–C10	1.523(2)	C13–H13B	0.9900
C2–C3	1.394(3)	C14–N1	1.148(2)
C2–H2	0.9500	O1–H1	0.8400
C3–C4	1.382(3)	C101–C102	1.393(3)
C3–H3	0.9500	C101–C106	1.401(2)
C4–C5	1.393(3)	C101–C110	1.520(2)
C4–H4	0.9500	C102–C103	1.395(3)
C5–C6	1.398(2)	C102–H102	0.9500
C5–H5	0.9500	C103–C104	1.387(3)
C6–C7	1.520(2)	C103–H103	0.9500
C7–C8	1.522(2)	C104–C105	1.395(3)
C7–C13	1.549(2)	C104–H104	0.9500
C7–H7	1.0000	C105–C106	1.389(2)
C8–C9	1.317(3)	C105–H105	0.9500
C8–H8	0.9500	C106–C107	1.518(2)
C9–C10	1.521(3)	C107–C108	1.520(3)
C9–H9	0.9500	C107–C113	1.553(2)
C10–C11	1.556(2)	C107–H107	1.0000
C10–H10	1.0000	C108–C109	1.323(3)
C11–C12	1.543(2)	C108–H108	0.9500
C11–H11A	0.9900	C109–C110	1.517(2)
C11–H11B	0.9900	C109–H109	0.9500
C12–O1	1.428(2)		
C12–C14	1.504(3)	C110–C111	1.556(2)

C110–H110	1.0000	C1–C6–C5	119.88(16)
C111–C112	1.545(2)	C1–C6–C7	116.82(15)
C111–H11C	0.9900	C5–C6–C7	123.30(16)
C111–H11D	0.9900	C6–C7–C8	108.44(14)
C112–O101	1.4269(19)	C6–C7–C13	111.51(14)
C112–C114	1.501(2)	C8–C7–C13	108.87(14)
C112–C113	1.549(2)	C6–C7–H7	109.3
C113–H11E	0.9900	C8–C7–H7	109.3
C113–H11F	0.9900	C13–C7–H7	109.3
C114–N101	1.144(2)	C9–C8–C7	118.29(16)
O101–H101	0.8400	C9–C8–H8	120.9
		C7–C8–H8	120.9
C2–C1–C6	119.96(16)	C8–C9–C10	118.27(16)
C2–C1–C10	123.70(16)	C8–C9–H9	120.9
C6–C1–C10	116.35(15)	C10–C9–H9	120.9
C1–C2–C3	119.78(17)	C9–C10–C1	108.53(15)
C1–C2–H2	120.1	C9–C10–C11	108.68(14)
C3–C2–H2	120.1	C1–C10–C11	111.00(13)
C4–C3–C2	120.39(17)	C9–C10–H10	109.5
C4–C3–H3	119.8	C1–C10–H10	109.5
C2–C3–H3	119.8	C11–C10–H10	109.5
C3–C4–C5	120.23(17)	C12–C11–C10	116.60(14)
C3–C4–H4	119.9	C12–C11–H11A	108.1
C5–C4–H4	119.9	C10–C11–H11A	108.1
C4–C5–C6	119.74(17)		
		C12–C11–H11B	108.1
C4–C5–H5	120.1	C10–C11–H11B	108.1
C6–C5–H5	120.1	H11A–C11–H11B	107.3

O1–C12–C14	106.04(14)	C106–C105–H105	120.0
O1–C12–C11	109.76(14)	C104–C105–H105	120.0
C14–C12–C11	108.98(14)	C105–C106–C101	120.14(16)
O1–C12–C13	105.36(13)	C105–C106–C107	123.24(16)
C14–C12–C13	108.52(14)	C101–C106–C107	116.62(15)
C11–C12–C13	117.56(14)	C106–C107–C108	108.52(15)
C12–C13–C7	115.81(14)	C106–C107–C113	111.27(14)
C12–C13–H13A	108.3	C108–C107–C113	108.78(14)
C7–C13–H13A	108.3	C106–C107–H107	109.4
C12–C13–H13B	108.3	C108–C107–H107	109.4
C7–C13–H13B	108.3	C113–C107–H107	109.4
H13A–C13–H13B	107.4	C109–C108–C107	118.02(16)
N1–C14–C12	174.6(2)	C109–C108–H108	121.0
C12–O1–H1	109.5	C107–C108–H108	121.0
C102–C101–C106	119.80(16)	C108–C109–C110	118.30(16)
C102–C101–C110	123.79(16)	C108–C109–H109	120.8
C106–C101–C110	116.41(15)	C110–C109–H109	120.8
C101–C102–C103	119.69(17)	C109–C110–C101	108.82(14)
C101–C102–H102	120.2	C109–C110–C111	108.76(14)
C103–C102–H102	120.2	C101–C110–C111	111.31(13)
C104–C103–C102	120.54(17)	C109–C110–H110	109.3
C104–C103–H103	119.7	C101–C110–H110	109.3
C102–C103–H103	119.7		
		C111–C110–H110	109.3
C103–C104–C105	119.86(17)	C112–C111–C110	115.85(14)
C103–C104–H104	120.1	C112–C111–H11C	108.3
C105–C104–H104	120.1	C110–C111–H11C	108.3
C106–C105–C104	119.97(17)	C112–C111–H11D	108.3



C110–C111–H11D	108.3
H11C–C111–H11D	107.4
O101–C112–C114	106.27(14)
O101–C112–C111	105.31(13)
C114–C112–C111	108.31(14)
O101–C112–C113	109.65(13)
C114–C112–C113	109.17(14)
C111–C112–C113	117.54(14)
C112–C113–C107	116.52(13)
C112–C113–H11E	108.2
C107–C113–H11E	108.2
C112–C113–H11F	108.2
C107–C113–H11F	108.2
H11E–C113–H11F	107.3
N101–C114–C112	174.35(19)
C112–O101–H101	109.5

Anisotropic displacement parameters [ $\text{\AA}^2 \times 10^3$ ] for **241**. The anisotropic displacement factor exponent takes the form:  $-2\pi^2[h^2a^{*2}U^{11} + \dots + 2hk a^* b^* U^{12}]$ .

Atom	$U^{11}$	$U^{22}$	$U^{33}$	$U^{23}$	$U^{13}$	$U^{12}$
C1	15(1)	15(1)	15(1)	1(1)	4(1)	4(1)
C2	19(1)	15(1)	21(1)	0(1)	4(1)	-1(1)
C3	18(1)	23(1)	25(1)	3(1)	10(1)	-4(1)
C4	23(1)	25(1)	21(1)	3(1)	12(1)	1(1)
C5	21(1)	19(1)	18(1)	-2(1)	7(1)	-1(1)
C6	14(1)	14(1)	16(1)	2(1)	4(1)	1(1)
C7	16(1)	21(1)	15(1)	-2(1)	5(1)	-4(1)
C8	16(1)	29(1)	21(1)	9(1)	9(1)	5(1)
C9	23(1)	24(1)	21(1)	7(1)	12(1)	9(1)
C10	22(1)	15(1)	16(1)	-1(1)	7(1)	2(1)
C11	19(1)	17(1)	14(1)	-2(1)	6(1)	0(1)
C12	17(1)	15(1)	18(1)	2(1)	6(1)	1(1)
C13	17(1)	15(1)	18(1)	-2(1)	7(1)	-4(1)
C14	19(1)	15(1)	21(1)	-3(1)	5(1)	-1(1)
N1	23(1)	27(1)	34(1)	-5(1)	13(1)	1(1)
O1	26(1)	17(1)	19(1)	5(1)	3(1)	-2(1)
C101	16(1)	16(1)	18(1)	-1(1)	7(1)	2(1)
C102	23(1)	19(1)	18(1)	0(1)	9(1)	2(1)
C103	24(1)	24(1)	16(1)	-2(1)	4(1)	4(1)
C104	20(1)	20(1)	25(1)	-6(1)	4(1)	0(1)
C105	18(1)	16(1)	25(1)	-1(1)	9(1)	1(1)
C106	16(1)	14(1)	17(1)	-1(1)	6(1)	3(1)
C107	20(1)	14(1)	17(1)	2(1)	7(1)	0(1)

C108	22(1)	21(1)	16(1)	−1(1)	3(1)	6(1)
C109	16(1)	28(1)	18(1)	−4(1)	5(1)	2(1)
C110	16(1)	20(1)	18(1)	−2(1)	8(1)	−3(1)
C111	16(1)	18(1)	18(1)	−2(1)	7(1)	−6(1)
C112	17(1)	15(1)	16(1)	−3(1)	6(1)	−2(1)
C113	18(1)	17(1)	17(1)	0(1)	8(1)	−2(1)
C114	19(1)	14(1)	21(1)	0(1)	9(1)	−2(1)
N101	22(1)	24(1)	25(1)	0(1)	4(1)	−1(1)
O101	21(1)	17(1)	26(1)	−6(1)	12(1)	−2(1)

Hydrogen coordinates [ $\times 10^4$ ] and isotropic displacement parameters [ $\text{\AA}^2 \times 10^3$ ] for **241**

Atom	<i>x</i>	<i>y</i>	<i>z</i>	<i>U</i> <sub>eq</sub>	<i>S.o.f.</i>
H2	1918	3973	9002	23	1
H3	2174	3719	7688	26	1
H4	1652	1371	6603	26	1
H5	841	−698	6797	23	1
H7	74	−1475	7614	21	1
H8	−541	260	8335	26	1
H9	−2	2487	9435	26	1
H10	1171	3095	9839	21	1
H11A	1820	506	10546	20	1
H11B	1094	−17	10576	20	1
H13A	382	−2934	9153	20	1
H13B	842	−3524	8592	20	1
H1	1810	−3000	10856	34	1
H102	5911	4740	4070	23	1
H103	6789	6767	4968	27	1
H104	7301	8927	4290	27	1
H105	6959	9011	2699	23	1
H107	6142	8074	1188	20	1
H108	4953	7621	526	25	1
H109	4422	5583	1198	25	1
H110	5062	3913	2537	21	1
H11C	5761	1670	2284	20	1
H11D	5270	2218	1274	20	1
H11E	5971	4886	420	20	1

H11F	6724	5353	1113	20	1
H101	6681	1704	937	30	1

Torsion angles [°] for **241**

---

C6–C1–C2–C3	–0.4(3)
C10–C1–C2–C3	179.82(16)
C1–C2–C3–C4	–0.6(3)
C2–C3–C4–C5	1.0(3)
C3–C4–C5–C6	–0.3(3)
C2–C1–C6–C5	1.1(2)
C10–C1–C6–C5	–179.13(15)
C2–C1–C6–C7	–179.01(15)
C10–C1–C6–C7	0.8(2)
C4–C5–C6–C1	–0.7(3)
C4–C5–C6–C7	179.39(16)
C1–C6–C7–C8	43.0(2)
C5–C6–C7–C8	–137.14(17)
C1–C6–C7–C13	–76.90(19)
C5–C6–C7–C13	103.01(19)
C6–C7–C8–C9	–44.6(2)
C13–C7–C8–C9	76.9(2)
C7–C8–C9–C10	0.7(2)
C8–C9–C10–C1	44.0(2)
C8–C9–C10–C11	–76.8(2)
C2–C1–C10–C9	135.84(17)
C6–C1–C10–C9	–43.94(19)
C2–C1–C10–C11	–104.78(18)
C6–C1–C10–C11	75.44(19)
C9–C10–C11–C12	79.30(18)
C1–C10–C11–C12	–40.0(2)

---

C10–C11–C12–O1	–163.06(14)
C10–C11–C12–C14	81.22(18)
C10–C11–C12–C13	–42.7(2)
O1–C12–C13–C7	165.71(14)
C14–C12–C13–C7	–81.08(18)
C11–C12–C13–C7	43.1(2)
C6–C7–C13–C12	39.3(2)
C8–C7–C13–C12	–80.28(18)
O1–C12–C14–N1	–6(2)
C11–C12–C14–N1	112(2)
C13–C12–C14–N1	–119(2)
C106–C101–C102–C103	0.5(3)
C110–C101–C102–C103	–179.24(16)
C101–C102–C103–C104	0.5(3)
C102–C103–C104–C105	–1.0(3)
C103–C104–C105–C106	0.5(3)
C104–C105–C106–C101	0.5(3)
C104–C105–C106–C107	–179.31(16)
C102–C101–C106–C105	–1.0(2)
C110–C101–C106–C105	178.79(15)
C102–C101–C106–C107	178.81(15)
C110–C101–C106–C107	–1.4(2)
C105–C106–C107–C108	–135.77(17)
C101–C106–C107–C108	44.4(2)
C105–C106–C107–C113	104.58(18)
C101–C106–C107–C113	–75.22(19)
C106–C107–C108–C109	–44.2(2)
C113–C107–C108–C109	77.0(2)

---

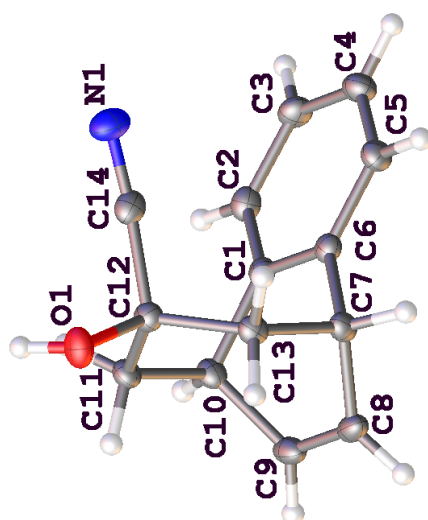
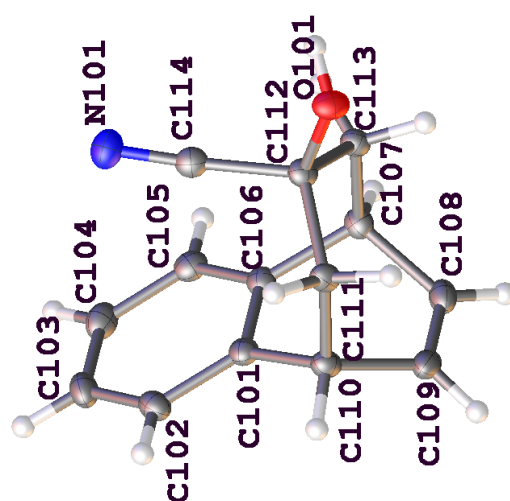
C107–C108–C109–C110	–0.5(2)
C108–C109–C110–C101	44.4(2)
C108–C109–C110–C111	–77.0(2)
C102–C101–C110–C109	137.22(17)
C106–C101–C110–C109	–42.5(2)
C102–C101–C110–C111	–102.94(19)
C106–C101–C110–C111	77.29(19)
C109–C110–C111–C112	80.38(18)
C101–C110–C111–C112	–39.5(2)
C110–C111–C112–O101	–165.37(14)
C110–C111–C112–C114	81.27(18)
C110–C111–C112–C113	–43.0(2)
O101–C112–C113–C107	162.77(14)
C114–C112–C113–C107	–81.19(18)
C111–C112–C113–C107	42.6(2)
C106–C107–C113–C112	40.1(2)
C108–C107–C113–C112	–79.43(18)
O101–C112–C114–N101	–5(2)
C111–C112–C114–N101	107.7(19)
C113–C112–C114–N101	–123.2(19)

---

Symmetry transformations used to generate equivalent atoms:

---





---

## **CHAPTER 6**

## **REFERENCES**

- 
- (1) Burley, S. K.; Petsko, G. A., *Science*, **1985**, 229, 23.
  - (2) Burley, S. K.; Petsko, G. A. *Adv. Protein Chem.*, **1988**, 39, 125.
  - (3) Hunter, C., *Chem. Soc. Rev.*, **1994**, 23, 101-109.
  - (4) Schneider, H. J., *Angew. Chem. Int. Ed.*, **2009**, 48, 3924.
  - (5) Schneider, H. J., *Angew. Chem. Int. Ed. Engl.*, **1991**, 30, 1417.
  - (6) Meyer, E. A.; Castellano, R. K.; Diederich, F., *Angew. Chem. Int. Ed.*, **2003**, 42, 1210.
  - (7) Karlstrom, G.; Linse, P.; Wallqvist, A.; Jonssonf, B., *J. Am. Chem. Soc.*, **1983**, 105, 3777.
  - (8) Burley, S. K.; Petsko, G. A., *J. Am. Chem. Soc* **1986**, 108, 7995.
  - (9) Felker, P. M.; Maxton, P. M.; Schaeffer, M. W. *Chem. Rev.*, **1994**, 94, 1787.
  - (10) Sinnokrot, M. O.; Sherrill, C. D., *J. Phys. Chem. A*, **2006**, 110, 10656.
  - (11) Janda, K. C.; Hemminger, C.; Winn, J. S.; Novick, S. E.; Harris, S. J., *J. Chem. Phys.*, **1975**, 63, 1419.
  - (12) Steed, J. M.; Dixon, T. A.; Klemperer, W., *J. Chem. Phys.*, **1979**, 40, 4940.
  - (13) Sun, S.; Bernstein, E. R. *J. Phys. Chem.*, **1996**, 100, 13348.
  - (14) a) Vrbancich, J.; Ritchie, G. L. D., *J. Chem. Soc., Faraday Trans. 2*, **1980**, 76, 648; b) Pawliszyn, J.; Szczesniak, M. M.; Scheiner, S., *J. Phys. Chem.*, **1984**, 88, 1726.
  - (15) Price, S.L.; Stone, A.J.J., *J. Chem. Phys.*, **1987**, 86, 2859.
  - (16) Jorgensen, W. L.; Severance, D. L., *J. Am. Chem. Soc.*, **1990**, 112, 4768.
  - (17) Linse, P., *J. Am. Chem. Soc.*, **1992**, 114, 4366.
  - (18) Jaffe, R. L.; Smith, G. D., *J. Chem. Phys.*, **1996**, 105, 2780.
  - (19) a) Carsky, P.; Selzle, H. L.; Schlag, E. W., *Chem. Phys.*, **1988**, 125, 165; b) Selzle, H. L.; Neusser, H. J.; Ernstberger, B; Krause, H; Schlag, E. W., *J. Phys. Chem.*, **1989**, 93, 7535.
  - (20) a) Hobza, P.; Selzle, H. L.; Schlag, E. W. *J. Chem. Phys.* **1990**, 93, 5893; b) Hobza, P.; Selzle, H. L.; Schlag, E. W., *J. Chem. Phys.*, **1991**, 95, 391.

- 
- (21) Hobza, P.; Selzle, H. L.; Schlag, E. W., *J. Phys. Chem.*, **1993**, 97, 3937.
- (22) Jaffe, R. L.; Smith, G. D., *J. Phys. Chem.*, **1996**, 100, 9624.
- (23) Tsuzuki, S.; Honda, K.; Azumi, R., *J. Am. Chem. Soc.*, **2002**, 124, 12200.
- (24) Hunter, C. A.; Sanders, J. K. M., *J. Am. Chem. Soc.*, **1990**, 112, 5525.
- (25) Hunter, C. A.; Sanders, J. K. M.; Stone, A. J., *Chem. Phys.*, **1989**, 133, 395.
- (26) Hunter, C. A.; Leighton, P.; Sanders, J. K. M., *J. Chem. Soc., Perkin Trans. 1*, **1989**, 547.
- (27) Anderson, H. L.; Hunter, C. A.; Meah, M. N.; Sanders, J. K. M., *J. Am. Chem. Soc.*, **1990**, 112, 5780.
- (28) Hunter, C. A.; Meah, M. N.; Sanders, J. K. M., *J. Am. Chem. Soc.*, **1990**, 112, 5773.
- (29) Hunter, C.; Lawson, K.; Perkins, J., *J. Chem. Soc., Perkin Trans. 2*, **2001**, 651.
- (30) Ahmad, A.; Singh, N., *Can. J. Anal. Sci. Spectros.*, **2009**, 54, 12.
- (31) Hunter, C. A., *Angew. Chem. Int. Ed. Engl.*, **1993**, 32, 1584.
- (32) Hunter, C. A., *Angew. Chem. Int. Ed.*, **2004**, 43, 5310.
- (33) Wheeler, S. E.; Houk, K. N., *J. Am. Chem. Soc.*, **2008**, 130, 10854.
- (34) Wheeler, S. E.; Houk, K.; Mcneil, A. J.; Muller, P.; Swager, T. M., *J. Am. Chem. Soc.* **2010**, 132, 3304.
- (35) Wheeler, S. E.; Houk, K. N., *Mol. Phys.*, **2009**, 107, 749.
- (36) Gung, B. W.; Xue, X.; Reich, H. J., *J. Org. Chem.*, **2005**, 70, 3641.
- (37) Cockroft, S. L.; Hunter, C. A.; Lawson, K. R.; Perkins, J.; Urch, C. J., *J. Am. Chem. Soc.*, **2005**, 127, 8594.
- (38) Kodama, Y.; Nishihata, K.; Nishio, M., *Tetrahedron Lett.*, **1977**, 2105.
- (39) a) Nishio, M.; Hirota, M., *Tetrahedron*, **1989**, 45, 7201; b) Nishio, M.; Umezawa, Y.; Hirota, M.; Takeuchi, Y., *Tetrahedron* **1995**, 51, 8665.

- 
- (40) Nishio, M.; Umezawa, Y.; Hirota, M., *The C-H/ $\pi$  interaction*, Wiley-VCH, New York, **1998**.
- (41) Nishio, M.; Umezawa, Y.; Honda, K.; Tsuboyama, S.; Suezawa, H., *CrystEngComm* **2009**, *11*, 1757.
- (42) Takahashi, O.; Kohno, Y.; Nishio, M., *Chem. Rev.*, **2010**, *110*, 6049.
- (43) Steiner, T., *Angew. Chem. Int. Ed. Engl.*, **2002**, *48*.
- (44) Umezawa, Y.; Nishio, M., *Bioorg. Med. Chem.*, **1998**, *6*, 2507.
- (45) Umezawa, Y.; Tsuboyama, S.; Takahshi, H.; Uzawa, J.; Nishio, M., *Tetrahedron*, **1999**, *55*, 10047.
- (46) Suezawa, H.; Yoshida, T.; Umezawa, Y.; Tsuboyama, S.; Nishio, M., *Eur. J. Inorg. Chem*, **2002**, *12*, 3148.
- (47) Sakaki, S.; Kato, K.; Miyazaki, T.; Musashi, Y.; Ohkubo, K.; Ihara, H.; Hirayama, C., *J. Chem. Soc., Faraday Trans. 2* **1993**, *89*, 659.
- (48) Gung, B. W.; Fouch, R. A.; Zhu, Z., *J. Am. Chem. Soc.*, **1995**, *117*, 1783.
- (49) Tsuzuki, S.; Honda, K.; Uchimaru, T.; Mikami, M.; Tanabe, K., *J. Phys. Chem. A*, **1999**, *103*, 8265.
- (50) Hirota, M.; Sakaibara, K.; Suezawa, H.; Yuzuri, T.; Ankai, E.; Nishio, M., *J. Phys. Org. Chem.*, **2000**, *13*, 620.
- (51) Sinnokrot, O.; Sherrill, C. D., *J. Am. Chem. Soc.*, **2004**, *126*, 7690.
- (52) Manojkumar, T. K.; Choi, H. S.; Hong, B. H.; Tarakeshwar, P.; Kim, K. S., *J. Chem. Phys.*, **2004**, *121*, 841.
- (53) a) Fujii, A.; Tsuzuki, S., *PCCP*, **2008**, *10*, 2584; b) Fujii, A.; Shibasaki, K.; Kazama, T.; Itaya, R.; Mikami, N.; Tsuzuki, S., *PCCP*, **2008**, *10*, 2836.
- (54) Fujii, A.; Morita, S.; Miyazaki, M.; Ebata, T.; Mikami, N., *J. Phys. Chem. A*, **2004**, *108*, 2652.
- (55) Suezawa, H.; Hashimoto, T.; Tsuchinaga, K.; Yoshida, T.; Yuzuri, T.; Sakakibara, K.; Nishio, M., *J. Chem. Soc., Perkin Trans. 2*, **2000**, 1243.

- 
- (56) Takahashi, O.; Kohno, Y.; Saito, K.; Nishio, M., *Chem. Eur. J.* **2003**, *9*, 756.
- (57) Weiss, H.C.; Bläser, D.; Boese, R.; Doughan, B. M.; Haley, M. M., *Chem. Commun.*, **1997**, 1703.
- (58) Levitt, M.; Perutz, M. F., *J. Mol. Biol.*, **1988**, *201*, 751.
- (59) Toth, G.; Kover, K. E.; Murphy, R. F.; Lovas, S., *J. Phys. Chem. B*, **2004**, *108*, 9287.
- (60) Wlodawer, A.; Walter, J.; Huber, R.; Sjolín, L., *J. Mol. Biol.*, **1984**, *180*, 301.
- (61) Josien, M. L.; Dizabo, P.; Castinel, C., *Bull. Soc. Chim. Fr.*, **1957**, 1957.
- (62) Josien, M. L.; Sourisseau, G., *Bull. Soc. Chim. Fr.*, **1955**, 178.
- (63) Ōki, M.; Iwamura, H., *J. Am. Chem. Soc.* **1967**, *89*, 576.
- (64) Yoshida, Z.; Osawa, E., *J. Am. Chem. Soc.* **1965**, *87*, 1467.
- (65) Korenaga, T.; Tanaka, H.; Ema, T.; Sakai, T., *J. Fluorine Chem.*, **2003**, *122*, 201.
- (66) Flocco, M. M.; Mowbray, S. L., *J. Mol. Biol.*, **1994**, *235*, 709.
- (67) Ueji, S.; Nakatsu, K.; Yoshida, H.; Kinoshita, K., *Tetrahedron Lett.*, **1982**, *23*, 1173.
- (68) Rodham, D. A.; Suzuki, S.; Suenram, R. D.; Lovas, F. J.; Dasgupta, S.; Goddard III, W. A.; Blake, G. A., *Nature*, **1993**, *362*, 735.
- (69) Suzuki, S.; Green, P. G.; R.E., B.; Dasgupta, S.; Goddard III, W. A.; Blake, G. A., *Science*, **1992**, *257*, 942.
- (70) Tsuzuki, S.; Honda, K.; Uchimar, T.; Mikami, M.; Tanabe, K., *J. Am. Chem. Soc.*, **2000**, *122*, 11450.
- (71) Roelens, S.; Torriti, R., *J. Am. Chem. Soc.*, **1998**, *120*, 12443.
- (72) Scrutton, N. S.; Raine, A. R. C., *Biochem. J.*, **1996**, *319*, 1.
- (73) Kryger, G.; Silman, I.; Sussman, J. L., *J. Physiol.*, **1998**, *92*, 191.
- (74) Kryger, G.; Silman, I.; Sussman, J. L., *Structure*, **1999**, *7*, 297.
- (75) Shepodd, T. J.; Petti, M. A.; Dougherty, D. A., *Tetrahedron*, **1988**, *12*, 1983.

- 
- (76) Ma, J. C.; Dougherty, D. A., *Chem. Rev.*, **1997**, *97*, 1303.
- (77) Kebarle, P.; Nishizawa, K.; Sunner, J., *J. Phys. Chem.*, **1981**, *85*, 1814.
- (78) Meotner, M.; Deakyne, C. A., *J. Am. Chem. Soc.*, **1985**, *107*, 469.
- (79) Meotner, M.; Deakyne, C. A., *J. Am. Chem. Soc.*, **1985**, *107*, 474.
- (80) Dougherty, D. A.; Kumpf, R. A., *Science*, **1993**, *261*, 1708.
- (81) Mecozzi, S.; West, A. P. J.; Dougherty, D. A., *J. Am. Chem. Soc.*, **1996**, *118*, 2307.
- (82) Caldwell, J. W.; Kollman, P. A., *J. Am. Chem. Soc.*, **1995**, *117*, 4177.
- (83) Faust, R.; Vollhardt, K. P. C., *Chem. Soc., Chem. Commun.*, **1993**, 1471.
- (84) Cioslowski, J.; Lin, Q. J., *J. Am. Chem. Soc.*, **1995**, *117*, 2553.
- (85) Shepodd, T. J.; Petti, M. A.; Dougherty, D. A., *J. Am. Chem. Soc.*, **1986**, *108*, 6085.
- (86) Shepodd, T. J.; Petti, M. A.; Dougherty, D. A., *J. Am. Chem. Soc.*, **1988**, *110*, 1983.
- (87) Petti, M. A.; Shepodd, T. J.; Barrans, J. R. E.; Dougherty, D. A., *J. Am. Chem. Soc.*, **1988**, *110*, 6825.
- (88) Kearney, P. C.; Mizoue, L. S.; Kumpf, R. A.; Forman, J. E.; McCurdy, A.; Dougherty, D. A., *J. Am. Chem. Soc.*, **1993**, *115*, 9907.
- (89) Forman, J. E.; Barrans, J. R. E.; Dougherty, D. A., *J. Am. Chem. Soc.*, **1995**, *117*, 9213.
- (90) Stauffer, D. A.; Dougherty, D. A.; Barrans, J. R. E., *J. Org. Chem.*, **1990**, *55*, 2762.
- (91) Stauffer, D. A.; Dougherty, D. A., *Tetrahedron Lett.*, **1988**, *29*, 6039.
- (92) Mati, I. K.; Cockroft, S. L., *Chem. Soc. Rev.*, **2010**, *39*, 4195.
- (93) Paliwal, S.; Geib, S.; Wilcox, C. S., *J. Am. Chem. Soc.*, **1994**, *116*, 4497.
- (94) Kim, E.; Paliwal, S.; Wilcox, C. S., *J. Am. Chem. Soc.*, **1998**, *120*, 11192.
- (95) Fischer, F. R.; Schweizer, W. B.; Diederich, F., *Chem. Commun.*, **2008**, 4031.
- (96) Ren, T.; Kin, Y.; Kim, K. S., *J. Biomol. Struct. Dyn.*, **1997**, *15*, 401.

- 
- (97) Hof, F.; Scofield, D. M.; Schweizer, W. B.; Diederich, F., *Angew. Chem. Int. Ed.*, **2004**, *43*, 5056.
- (98) Cockroft, S. L.; Hunter, C. A., *Chem. Commun.*, **2006**, 3806.
- (99) Cockroft, S. L.; Hunter, C. A., *Chem. Commun.* **2009**, 3961.
- (100) Fischer, F. R.; Schweizer, W. B.; Diederich, F., *Angew. Chem. Int. Ed.*, **2007**, *46*, 8270.
- (101) Hof, F.; Scofield, D. M.; Schweizer, W. B.; Diederich, F., *Angew. Chem. Int. Ed.*, **2004**, *43*, 5056.
- (102) Bhayana, B.; Wilcox, C. S., *Angew. Chem. Int. Ed.*, **2007**, *46*, 6833.
- (103) Cozzi, F.; Cinquini, M.; Annunziata, R.; Siegel, J. S.; Dwyer, T., *J. Am. Chem. Soc.*, **1992**, *114*, 5729.
- (104) Cozzi, F.; Cinquini, M.; Annunziata, R.; Siegel, J. S., *J. Am. Chem. Soc.*, **1993**, *115*, 5330.
- (105) Cozzi, F.; Ponzini, F.; Annunziata, R.; Cinquini, M.; Siegel, J. S., *Angew. Chem. Int. Ed. Engl.*, **1995**, *34*, 1019.
- (106) Cozzi, F.; Siegel, J. S., *Pure Appl. Chem.*, **1995**, *67*, 683.
- (107) Cozzi, F.; Annunziata, R.; Benaglia, M.; Estrada, J.; Baldrige, K. K.; Siegel, J. S.; Aguire, G.; Sritana-Anant, Y., *PCCP*, **2008**, *10*, 2686.
- (108) Cozzi, F.; Annunziata, R.; Benaglia, M.; Cinquini, M.; Raimondi, L.; Baldrige, K. K.; Siegel, J. S., *Org. Biomol. Chem.*, **2003**, *1*, 157.
- (109) Zoltewicz, J. A.; Maier, N. M.; Fabian, W. M. F., *J. Org. Chem.*, **1996**, *61*, 7018.
- (110) Zoltewicz, J. A.; Maier, N. M.; Lavieri, S.; Ghiviriga, I.; Abboud Walter, M.; Khalil, A., *J. Org. Chem.*, **1997**, *53*, 5379.
- (111) Zoltewicz, J. A.; Maier, N., *J. Org. Chem.*, **1997**, *53*, 3215.
- (112) Zoltewicz, J. A.; Maier, N. M.; Lavieri, S.; Ghiviriga, I.; Abboud, K. A., *Tetrahedron*, **1997**, *53*, 5379.
- (113) Lavieri, S.; Zoltewicz, J. A., *J. Org. Chem.*, **2001**, 7227.



- 
- (114) Rashkin, M. J.; Waters, M. L., *J. Am. Chem. Soc.*, **2002**, *124*, 1860.
- (115) Rashkin, M. J.; Hughes, R. M.; Calloway, N. T.; Waters, M. L., *J. Am. Chem. Soc.*, **2004**, *126*, 13320.
- (116) Newcomb, L. F.; Gellman, S. H., *J. Am. Chem. Soc.*, **1994**, *116*, 4993.
- (117) Gardner, R. R.; Christianson, L. A.; Gellman, S. H., *J. Am. Chem. Soc.*, **1997**, *119*, 5041.
- (118) Gardner, R. R.; McKay, S. L.; Gellman, S. H., *Org. Lett.*, **2000**, *2*, 2335.
- (119) McKay, S. L.; Haptonstall, B.; Gellman, S. H., *J. Am. Chem. Soc.*, **2001**, *123*, 1244.
- (120) Ōki, M., *Acc. Chem. Res.*, **1990**, *23*, 351.
- (121) Gung, B.; Xue, X., *J. Org. Chem.*, **2005**, *70*, 7232.
- (122) Gung, B. W.; Patel, M.; Xue, X., *J. Org. Chem.*, **2005**, *70*, 10532.
- (123) Gung, B. W.; Wekesa, F.; Barnes, C. L., *J. Org. Chem.*, **2008**, *73*, 1803.
- (124) Annunziata, R.; Benaglia, M.; Cozzi, F.; Mazzanti, A., *Chem. Eur. J.*, **2009**, *15*, 4373.
- (125) Benaglia, M.; Cozzi, F.; Mancinelli, M.; Mazzanti, A., *Chem. Eur. J.*, **2010**, 7456.
- (126) Gung, B. W.; Zou, Y.; Xu, Z.; Amicangelo, J. C.; Irwin, D. G., *J. Org. Chem.*, **2008**, *73*, 689.
- (127) Cornago, P.; Claramunt, R. M.; Bouissane, L., *Tetrahedron*, **2008**, *64*, 3667.
- (128) Ramaiah, D.; Neelakandan, P. P.; Nair, A. K.; Avirah, R. R., *Chem. Soc. Rev.*, **2010**, *39*, 4158.
- (129) Kamieth, M.; Klärner, F.-G.; Diederich, F., *Angew. Chem. Int. Ed.*, **1998**, *37*, 3303.
- (130) Klärner, F.-G.; Burkert, U.; Kamieth, M.; Boese, R.; Benet-Buchholz, J., *Chem. Eur. J.*, **1999**, *5*, 1700.
- (131) a) Klärner, F.-G.; Kahlert, B.; Boese, R.; Bläser, D.; Juris, A.; Marchioni, F., *Chem. Eur. J.*, **2005**, *11*, 3363; b) Klärner, F.-G.; Kahlert, B., *Acc. Chem. Res.*, **2003**, *36*, 919.
- (132) a) Di Cera, E., *Chem. Rev.*, **1998**, *98*, 1563; b) Schreiber, G., *Biomol. Sens.*, **2002**, 19.

- (133) a) Cockroft, S. L.; Hunter, C. A., *Chem. Soc. Rev.*, **2007**, 36, 172; b) Cockroft, S. L.; Perkins, J.; Zonta, C.; Adams, H.; Spey, S. E.; Low, C. M. R.; Vinter, J. G.; Lawson, K. R.; Urch, C. J.; Hunter, C. A., *Org. Biomol. Chem.*, **2007**, 5, 1062; c) Bisson, A. P.; Carver, F. J.; Hunter, C. A.; Waltho, J. P., *J. Am. Chem. Soc.*, **1994**, 116, 10292; d) Carver, F. J.; Hunter, C. A.; Jones, P. S.; Livingstone, J. F.; Seward, E. M.; Tiger, P., *Chem. Eur. J.*, **2001**, 7, 4854.
- (134) Nishio, M., *Tetrahedron*, **2005**, 61, 6923.
- (135) a) Kobayashi, Y.; Kurasawa, T.; Kinbara, K.; Saigo, K., *J. Org. Chem.*, **2004**, 69, 7436; b) Sodupe, M.; Rios, R.; Branchadell, V.; Nicholas, T.; Oliva, A.; Dannenberg, J. J., *J. Am. Chem. Soc.*, **1997**, 119, 4232; c) Kobuke, Y.; Fueno, T.; Furukawa, J., *J. Am. Chem. Soc.*, **1970**, 92, 6548; d) Mataka, S.; Ma, J.; Thiemann, T.; Rudzinski, J. M.; Tsuzuki, H.; Sawada, T.; Tashiro, M., *Tetrahedron*, **1997**, 53, 885.
- (136) a) Malkov, A. V.; Mariani, A.; MacDougall, K. N.; Kocovsky, P., *Org. Lett.*, **2004**, 69, 2253; b) Yamada, I.; Noyori, R., *Org. Lett.*, **2001**, 2, 3425; c) Yamakawa, M.; Yamada, I.; Noyori, R., *Angew. Chem., Int. Ed.*, **2001**, 40, 2818; d) Becker, H.; Hou, P.-T.; Kolb, H. C.; Loren, S.; Norrby, P.-O.; Sharpless, K. B., *Tetrahedron Lett.*, **1994**, 35, 7315.
- (137) a) Honda, K.; Nakanishi, F.; Feeder, N., *J. Am. Chem. Soc.*, **1999**, 121, 8246; b) Honda, K.; Nakanishi, F.; Lee, S.-A.; Mikami, M.; Tsuzuki, S.; Yamamoto, T.; Feeder, N., *Mol. Cryst. Liq. Cryst.*, **2001**, 356, 413; c) Sakamoto, M.; Takahashi, M.; Fujita, T.; Watanabe, S.; Nishio, T.; Iida, I.; Aoyama, H., *J. Org. Chem.*, **1997**, 62, 6298; d) Obata, T.; Shimo, T.; Yasutake, M.; Shinmyozu, T.; Kawaminami, M.; Yoshida, R.; Somekawa, K., *Tetrahedron*, **2001**, 57, 1531.
- (138) a) Nakamura, M.; Okawa, H.; Inazu, T.; Kida, S., *Bull. Chem. Soc. Jpn.*, **1982**, 55, 2400; b) Okawa, H.; Ueda, K.; Kida, S., *Inorg. Chem.*, **1982**, 21, 1594; c) Yamanari, K.; Dogi, S.; Okubo, K.; Fujihara, T.; Fuyuhiko, A.; Kaizaki, S., *Bull. Chem. Soc. Jpn.*, **1994**, 67, 3004; d) Kojima, T.; Miyazaki, S.; Hayashi, K.; Shimazaki, Y.; Tani, F.; Naruta, Y.; Matsuda, Y., *Chem. Eur. J.*, **2004**, 10, 6402; e) Brunner, H.; Aglifoglio, G.; Bernal, I.; Creswick, M. W., *Angew. Chem., Int. Ed. Engl.*, **1980**, 19, 647.
- (139) Yamada, S.; Morita, C., *J. Am. Chem. Soc.*, **2002**, 124, 8184.
- (140) Ujaque, G.; Lee, P. S.; Houk, K.; Hentemann, M. F.; Danishefsky, S. J., *Chem. Eur. J.*, **2002**, 8, 3423.
- (141) Tarakeshwar, P.; Choi, H. S.; Kim, K. S., *J. Am. Chem. Soc.*, **2001**, 123, 3323.

- 
- (142) Baker, A. J.; Chalmers, A. M.; Flood, W. W.; MacNicol, D. D.; Penrose, A. B.; Raphael, R. A., *J. Chem. Soc. Chem. Commun.*, **1970**, 166.
- (143) a) Schmid, H.; Frater, G., *Helv. Chim. Acta*, **1967**, *1*, 255; b) Waespe, H.-R.; Heimgartner, H.; Schmid, H.; Hansen, H.-J.; Paul, H.; Fischer, H., *Helv. Chim. Acta*, **1978**, *61*, 401.
- (144) Baker, A. W.; Shulgin, A., *Spectrochim. Acta.*, **1964**, *20*, 153.
- (145) Baker, A. W.; Shulgin, A. T., *J. Am. Chem. Soc.*, **1958**, *80*, 5358.
- (146) Ōki, M.; Iwamura, H., *Bull. Chem. Soc. Jpn.*, **1960**, *33*, 717.
- (147) Schaefer, T.; Sebastian, R.; Wildman, T. A., *Can. J. Chem.*, **1979**, *57*, 3005.
- (148) Kim, K. S.; Hsu, S. C.; Li, S.; Bernstein, E. R., *J. Chem. Phys.*, **1991**, *95*, 3290.
- (149) Berdyshev, D. V.; Glazunov, V. D.; Novikov, V. L., *J. Appl. Spectrosc.*, **2009**, *76*, 630.
- (150) Bosch-Montalvá, M. T.; Domingo, L. R.; Jiménez, M. C.; Miranda, M. A.; Tormos, R., *J. Chem. Soc., Perkin Trans. 2*, **1998**, 2175.
- (151) Leo, E. A.; Tormos, R.; Monti, S.; Domingo, L. R.; Miranda, M. A., *J. Phys. Chem. A*, **2005**, *109*, 1758.
- (152) a) Rademacher, P.; Khelashvili, L.; Kowski, K., *Org. Biomol. Chem.*, **2005**, *3*, 2620; b) Rademacher, P.; Khelashvili, L., *Mendeleev Commun.*, **2004**, *14*, 286.
- (153) Chow, Y. L.; Zhou, X.-M.; Gaitan, T. J.; Wu, Z.-Z., *J. Am. Chem. Soc.*, **1989**, *111*, 3813.
- (154) Tsuzuki, S.; Honda, K.; Uchimaru, T.; Mikami, M., *J. Phys. Chem. A*, **1999**, *103*, 8265.
- (155) Takagi, T.; Tananka, A.; Matsuo, S.; Maezaki, H.; Tani, M.; Fujiwara, H.; Sasaki, Y., *J. Chem. Soc., Perkin Trans. 2*, **1987**, 1015.
- (156) Tsuzuki, S.; Houjou, H.; Nagawa, Y.; Hiratani, K., *J. Chem. Soc., Perkin Trans. 2*, **2001**, 1951.
- (157) Linares, M.; Pellegatti, A.; Roussel, C., *J. Mol. Struct. THEOCHEM*, **2004**, *680*, 169.
- (158) Fraser, G. T.; Xu, L.-H.; Suenram, R. D.; Lugez, L. J., *J. Chem. Phys.*, **2000**, *112*, 6209.
- (159) M. Nic, PhD Thesis, University of London, **1995**.

- 
- (160) J. Moïse, PhD Thesis, University of London, **2006**.
- (161) Motherwell, W. B.; Moïse, J.; Aliev, A. E.; Nič, M.; Coles, S. J.; Horton, P. N.; Hursthouse, M. B.; Chessari, G.; Hunter, C. A.; Vinter, J. G. *Angew. Chem. Int. Ed.*, **2007**, *46*, 7823.
- (162) Motherwell, W. B.; Moïse, J.; Aliev, A. E.; Nič, M.; Courtier-Murias, D.; Tocher, D. A., *PCCP*, **2009**, *11*, 97.
- (163) Hill, A. E.; Hoffmann, H. M. R., *J. Am. Chem. Soc.*, **1974**, *96*, 4597.
- (164) Hill, A. E.; Hoffman H. M. R., *Angew. Chem. Int. Ed. Engl.*, **1974**, *13*, 136.
- (165) Takakis, I. M.; Agosta, W. C.; *J. Org. Chem.*, **1978**, *43*, 1952.
- (166) Radlick, P., *J. Org. Chem.*, **1964**, *29*, 960.
- (167) Dahnke, K. R.; Paquette, L. A.; *Org. Synth.*, **1998**, *9*, 396.
- (168) a) Parham, W. E.; Soeder, R. W.; Dodson, R. M., *J. Am. Chem. Soc.*, **1962**, *84*, 1755; b) Parham, W. E.; Soeder, R. W.; Throckmorton, J. R.; Kuncl, K.; Dodson, R. M., *J. Am. Chem. Soc.*, **1965**, *87*, 321.
- (169) Kahsman, Y.; Awerbouch, O., *Tetrahedron*, **1970**, *26*, 4213.
- (170) Fleming, I.; Bishop, M. J.; *J. Chem. Soc. C.*, **1970**, *18*, 2524.
- (171) Johnson, C. R.; Golebiowski, A.; Steensma, D. H., *J. Am. Chem. Soc.*, **1992**, *114*, 9414.
- (172) a) De Lucchi, O.; Modena, G., *Tetrahedron*, **1984**, *40*, 2585; b) De Lucchi, O.; Modena, G., *J. Chem. Soc., Chem. Commun.*, **1982**, 914; c) De Lucchi, O.; Modena, G., *Tetrahedron Lett.*, **1983**, *24*, 1653; d) De Lucchi, O.; Modena, G.; Lucchini, V.; Pasquato, L., *J. Org. Chem.*, **1984**, *49*, 596.
- (173) Paquette, L. A.; Waykole, L., *Org. Synth.*, **1993**, *8*, 281.
- (174) a) Magee, T. V.; Stork, G.; Fludzinski, P., *Tetrahedron Lett.*, **1995**, *36*, 7607; b) Eguchi, S.; Ishiura, K.; Noda, T.; Sasaki, T., *J. Org. Chem.*, **1987**, *52*, 496.
- (175) Trost, B. M.; Chen, F., *Tetrahedron Lett.*, **1971**, 2603.

- (176) a) Wiesner, K.; Ho, P.; Jain, R. C.; Lee, S. F.; Oida, S.; Philipp, A., *Can. J. Chem.*, **1973**, *51*, 1448; b) Dauben, W.G.; Rivers, G. T.; Twieg, R. J.; Zimmerman, W.T., *J. Org. Chem.*, **1976**, *41*, 887.
- (177) Ratcliffe, R.; Rodehorst, R., *J. Org. Chem.*, **1970**, *35*, 4000.
- (178) a) Hatano, M.; Ishihara, K., *Synthesis*, **2008**, *11*, 1647; b) Imamoto, T., *Comprehensive Organic Synthesis. Selectivity, Strategy and Efficiency in Modern Organic Chemistry. Volume 1: Additions to C-X  $\pi$ -bonds. Part I*; Trost, B. M.; Fleming, I.; Schreiber, S. L.; Eds. Pergamon Press. Oxford, **1991**; pp231.
- (179) Imamoto, T.; Sugiura, Y.; Takiyama, N., *Tetrahedron Lett.*, **1984**, *25*, 4233.
- (180) Imamoto, T.; Takiyama, N.; Nakamura, K., *Tetrahedron Lett.*, **1985**, *26*, 4763.
- (181) a) Imamoto, T.; Kusumoto, T.; Tawarayama, Y.; Sugiura, Y.; Mita, T.; Hatanaka, Y.; Yokoyama, M., *J. Org. Chem.*, **1984**, *49*, 3904; b) Liu, H-J.; Shia, K-S.; Shang, X.; Zhu, B-Y., *Tetrahedron*, **1999**, *55*, 3803; c) Wang, Y.; Li, J.; Wu, Y.; Huang, Y.; Shi, L.; Yang, J., *Tetrahedron Lett.*, **1996**, *38*, 4583.
- (182) Vacher, B.; Bonnaud, B.; Funes, P.; Jubault, N.; Koek, W.; Assié, M-B.; Cosi, C.; Kleven, M., *J. Med. Chem.*, **1999**, *42*, 1648.
- (183) Karimi, B.; Ma'mani, L., *Synthesis*, **2003**, *16*, 2503.
- (184) Pellissier, H.; Santelli, M., *Tetrahedron*, **2003**, *59*, 701.
- (185) a) Logullo, F. M.; Seitz, A. H.; Friedman, L., *Org. Synth.*, **1973**, *5*, 54; b) Ciabattini, J.; Crowley, J. E.; Kende, A. S., *J. Am. Chem. Soc.*, **1967**, *89*, 2778.
- (186) Henderson, J. L.; Edwards, A. S.; Greaney, M. F., *J. Am. Chem. Soc.*, **2006**, *128*, 7426.
- (187) Corey, E. J.; William Suggs, J., *Tetrahedron Lett.*, **1975**, 2647.
- (188) Cordi, A. A.; Berque-Bestel, I.; Persigand, T.; Lacoste, J-M.; Newman-Tancredi, A.; Audinot, V.; Millan, M. J., *J. Med. Chem.*, **2001**, *44*, 787.
- (189) Neuhaus, D.; Williamson, M. P.; *The Nuclear Overhauser Effect in Structural and Conformational Analysis*, 2nd Edition, Wiley-VCH, **2000**.
- (190) Salonen, L. M.; Ellermann, M.; Diederich, F., *Angew. Chem. Int. Ed.*, **2011**, *50*, 4808.